Development of Particulate and Hazardous Emission Factors for Electric Arc Welding (AP-42, Section 12.19)

Revised Final Report

For U.S. Environmental Protection Agency
Office of Air Quality Planning and Standards
Emission Inventory Branch

EPA Contract No. 68-D2-0159
Work Assignment No. I-02

MRI Project No. 4601-02
May 20, 1994

This document is printed on recycled paper.

Development of Particulate and Hazardous Emission Factors for Electric Arc Welding (AP-42, Section 12.19)

Revised Final Report

For U.S. Environmental Protection Agency
Office of Air Quality Planning and Standards
Emission Inventory Branch
Research Triangle Park, NC 27711

Attn: Mr. Ron Meyers

EPA Contract No. 68-D2-0159
Work Assignment No. I-02

MRI Project No. 4601-02
May 20, 1994

NOTICE

This document is intended for internal Agency use only. Mention of trade names or commercial products does not constitute endorsement or recommendation for use.

PREFACE

This report was prepared for the Office of Air Quality Planning and Standards (OAQPS), U.S. Environmental Protection Agency (EPA), under EPA Contract No. 68-D2-0159, Work Assignment No. I-02. Mr. Dennis Shipman and Mr. Ron Meyers were the requestors of the work. The report was prepared by Mr. Lance Henning with assistance from Mr. John Kinsey.

MIDWEST RESEARCH INSTITUTE

Roy Neulicht
Program Manager
Environmental Engineering Department

Approved:

Charles F. Holt, Director
Engineering and Environmental
Technology Department

May 20, 1994

CONTENTS

FIGURES

TABLES

SECTION 1

INTRODUCTION

The document *Compilation of Air Pollutant Emissions Factors* (AP-42) has been published by the U.S. Environmental Protection Agency (EPA) since 1972. Supplements to the AP-42 are issued to add new emission source categories and to update existing emission factors. The EPA also routinely updates AP-42 in response to the needs of Federal, state, and local air pollution control programs and industry.

An emission factor relates the quantity (weight) of pollutants emitted to a unit of source activity. Emission factors reported in AP-42 are used to:

1. Estimate areawide emissions.

2. Estimate emissions for a specific facility.

3. Evaluate emissions relative to ambient air quality.

This report provides background information from test reports and other information to support preparation of a new AP-42 section for Electric Arc Welding. The information in the proposed AP-42 section is based on a review of the available literature for particulate phase air pollutants produced by welding operations. Gas phase pollutants were not included in the scope of the current work assignment.

This report contains five sections. Following the introduction, Section 2 describes welding equipment, practices, and allied processes. Section 3 describes data collection and rating procedures, and Section 4 describes the emission factor development. Section 5 presents the proposed AP-42 section.

SECTION 2

INDUSTRY AND PROCESS DESCRIPTION

2.1 INDUSTRY CHARACTERIZATION[1,2,3,4,5]

Welding operations are common, but not exclusive, to manufacturing and construction industries. Since welding is not usually considered an industry itself, but a process within an industry, few statistics or trends are recorded for welding operations. Manufacturers report the number of consumable electrodes sold for arc welding, the most often used welding process. The percentage of consumable electrodes purchased in 1991 were distributed as follows:

- Shielded Metal Arc Welding (SMAW)—45%
- Gas Metal Arc Welding (GMAW)—34%
- Flux Cored Arc Welding (FCAW)—17%
- Submerged Arc Welding (SAW)—4%

As shown above, SMAW is the most commonly used form of arc welding.

Limited survey data are available for the various welding processes. Data presented in Tables 2-1 through 2-3 are for welding operations in two shipyards and for one manufacturer of pressure vessels. These data are based only on availability and, therefore, do not necessarily represent the normal distribution of welding operations across all industry types. Tables 2-1 to 2-3 are only intended to show typical utilization by the different organizations surveyed.

TABLE 2-1. WELDING PROCESSES FOR ONE BRITISH SHIPYARD[2]

Welding process	Percentage utilization
Shielded metal arc welding (SMAW)	68.1
Gas tungsten arc welding (GTAW)	13.6
Gas metal arc welding (GMAW)	12.3
Submerged arc welding (SAW)	3.4
Oxyfuel welding	1.3
Atomic hydrogen welding	0.8
Spot welding	0.4
Stub welding	0.2

TABLE 2-2. WELDING PROCESSES FOR ONE MANUFACTURER OF PRESSURE VESSELS[3]

Welding process	Percentage utilization
Shielded metal arc welding (SMAW)	50
Submerged arc welding (SAW)	25
Flux cored arc welding (FCAW)	20
Gas metal arc welding (GMAW) and gas tungsten arc welding (GTAW)	5

TABLE 2-3. WELDING PROCESSES FOR ONE CALIFORNIA SHIPYARD[4]

Welding process	Percentage utilization
Flux cored arc welding (FCAW)	53.1
Gas tungsten arc welding (GTAW)	27.2
Shielded metal arc welding (SMAW)	17.6
Gas metal arc welding (GMAW)	0.9
Submerged arc welding (SAW)	0.8
Pulse arc welding	0.3
Brazing	0.1

Welding operations continued to grow in the 1980s in value of sales. Sales of all welding apparatus, including electrodes, arc welding machines, and gas welding equipment, grew from 1.6 billion dollars in 1982 to 1.9 billion dollars in 1987, as reported in the 1987 Census of Manufactures.

2.2 PROCESS DESCRIPTION[6,7]

There are more than 80 different types of welding operations, including brazing, thermal cutting, and gauging, in commercial use. Figure 2-1 shows a diagram of the major types of welding and the relationship between major variations of each process.

By definition, welding is the process joining of two metal parts by melting the parts at the joint and filling the space with molten metal. In welding and similar operations, such as brazing, thermal cutting, and gauging, the most frequently used method for generating heat is obtained either from an electric arc or a gas-oxygen flame. The most commonly used processes are described below.

2.2.1 Arc Welding[6,8,9]

Electric arc welding, the most frequently used process, includes many different variations that involve various types of electrodes, fluxes, shielding gases, and types of equipment. Electric arc welding can be divided into processes using nonconsumable electrodes and consumable electrodes.

In electric arc welding, a flow of electricity across the gap from the tip of the welding electrode to the base metal creates the heat needed for melting and joining the metal parts. The electric current melts both the electrode and the base metal at the joint to form a molten pool, which solidifies upon cooling. A description of each major type of electric arc welding process is provided below.

Welding Process
Resistance Welding (3-09-041)
Brazing (3-09-042)
Soldering (3-09-043)
Arc Welding (3-09-050)
Oxyfuel Welding (3-09-044)
Thermal Spraying (3-09-045)
Thermal Cutting
Others
Oxyfuel Cutting (3-09-046)
Arc Cutting (3-09-047)
Others
Consumable Electrode
Non-consumable Electrode
Shielded Metal Arc Welding (SMAW) (3-09-051)
Gas Metal Arc Welding (GMAW) (3-09-052)
Flux Cored Arc Welding (FCAW) (3-09-051)
Submerged Arc Welding (SAW) (3-09-054)
Electrogas Welding (EGW) (3-09-055)
Electrostag Welding (ESW) (3-09-056)
Others
Gas Tungsten Arc Welding (GTAW) (3-09-058)
Plasma Arc Welding (PAW) (3-09-059)

2.2.1.1 Gas Tungsten Arc Welding[7,9,10]—

Gas tungsten arc welding (GTAW) uses a nonconsumable tungsten electrode that creates an arc between the electrode and the weld pool. An inert shielding gas is used in the process at no applied pressure. Argon is most commonly used as the shielding gas, and the process may be employed with or without the addition of filler metal. An illustration of the gas tungsten arc welding process, also referred to as nonconsumable electrode welding, and tungsten inert gas (TIG) welding is shown in Figure 2-2.

Advantages of GTAW include its versatility, low equipment costs, control, and weld quality. It is widely used for the welding of light gauge stainless steel and aluminum and root passes in pipe butt joints. The GTAW process can easily be set up as an automated process.

Another positive attribute of GTAW is the very low fume formation rate (FFR). The filler wire is fed and melted into the weld pool allowing a lower FFR. This procedure is different from other processes that require the fill material to pass through the arc. Since filler is fed directly to the weld pool, operating variables have little effect on the FFR.

Disadvantages of GTAW are its low speed and deposition rate which utilizes hot or cold wire feed and high heat input efficiency. By using shielding gas, these problems can be overcome. The GTAW weld zone is also difficult to shield properly in drafty environments.

2.2.1.2 Plasma Arc Welding[8,10]—

Plasma arc welding (PAW) is a process that fuses workpiece metals by heat from an arc between the electrode and the workpiece or from an arc between the electrode and the constricting nozzle. The ionization of the gas issuing from the torch produces plasma. An auxiliary shielding gas made of a single inert gas or a mixture of inert gases generally supplements the plasma. The process may be used with or without a filler metal; pressure is not applied in the system. Figure 2-3 shows the PAW torch and process.

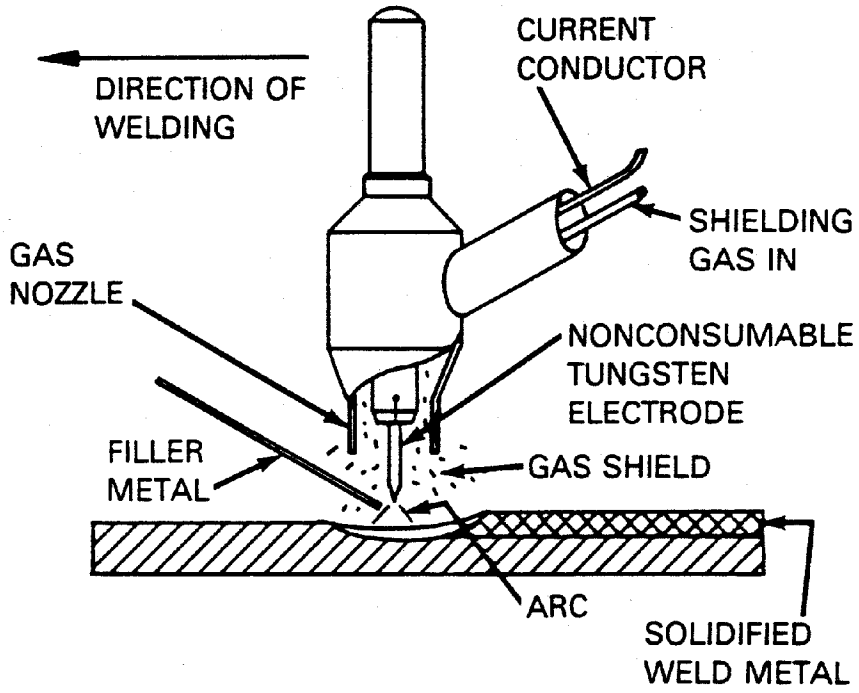

Figure 2-2. Gas tungsten arc welding (GTAW) operation.[10]

(Figure reprinted with permission of the American Welding Society.)

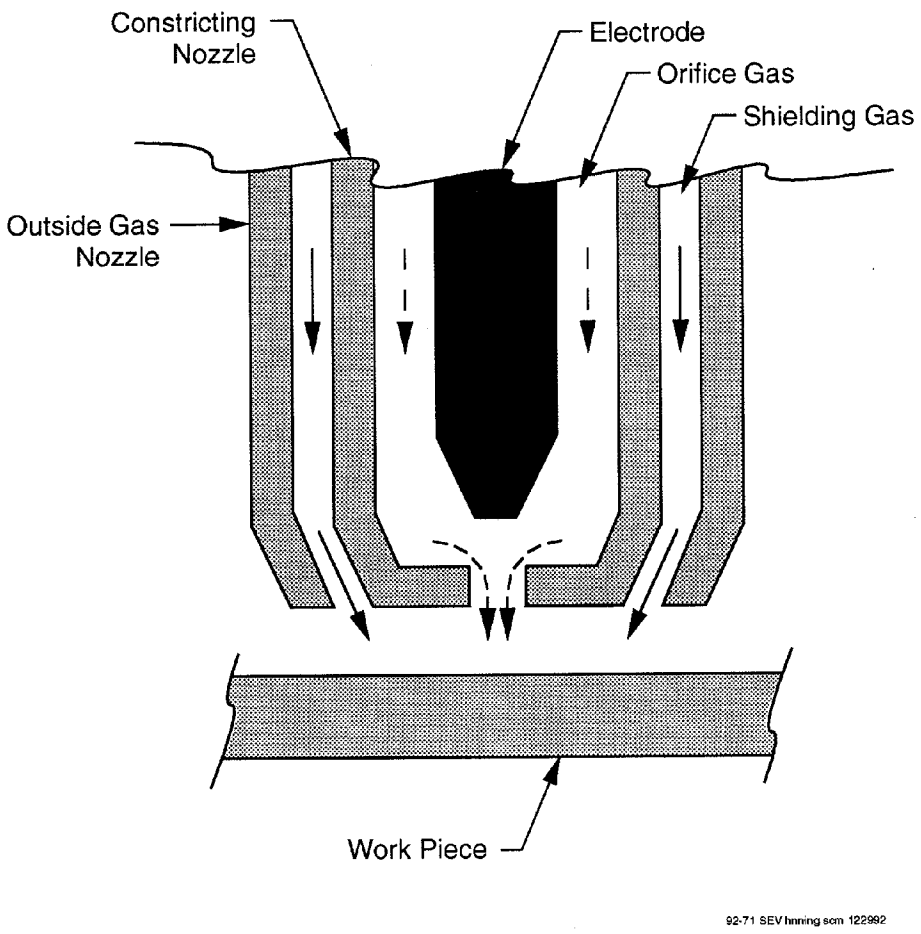

Figure 2-3. Diagram of a plasma arc welding (PAW).[10]

As in GTAW, plasma arc welding makes use of a nonconsumable electrode. A chamber surrounds the electrode on the PAW torch. The chamber fills with gas that is heated by the arc to a temperature where the gas ionizes and conducts electricity. This ionized gas, referred to as plasma, exits from the nozzle at a approximate temperature of 16,700°C (30,000°F).

Plasma arc welding has the ability to join most types of metals in the majority of welding positions. A workpiece welded by PAW has a smaller heat-affected zone than GTAW. PAW also operates with better directional control of the arc than GTAW. Compared to other welding processes, PAW uses a lower current to produce a given weld, and there is less shrinkage to the welded area.

The major disadvantage of plasma arc welding is the high equipment expense. PAW involves more extensive operator training, more complex welding procedures, and more process control variables, as compared to GTAW. Due to the higher temperatures used in the process, PAW has the disadvantage of higher noise levels and higher ozone production than other processes.

2.2.1.3 Shielded Metal Arc Welding[10]—

Shielded metal arc welding (SMAW) is the most widely used electric arc welding process and the first type to use consumable electrodes. The process also is referred to as manual metal arc welding (MMAW). Shielded metal arc welding uses heat that is produced by an electric arc to melt the metals. The electric arc is maintained between the welding joint at the surface of the base metal and the tip of the covered welding electrode (Figure 2-4).

During operation, the core rod conducts electric current to produce the arc and provides filler metal for the joint. The core of the covered electrode consists of either a solid metal rod of drawn or cast material or a solid metal rod fabricated by encasing metal powders in a metallic sheath. The electrode covering provides stability to the arc and protects the molten metal by the creation of shielding gases from the vaporization of the electrode cover.

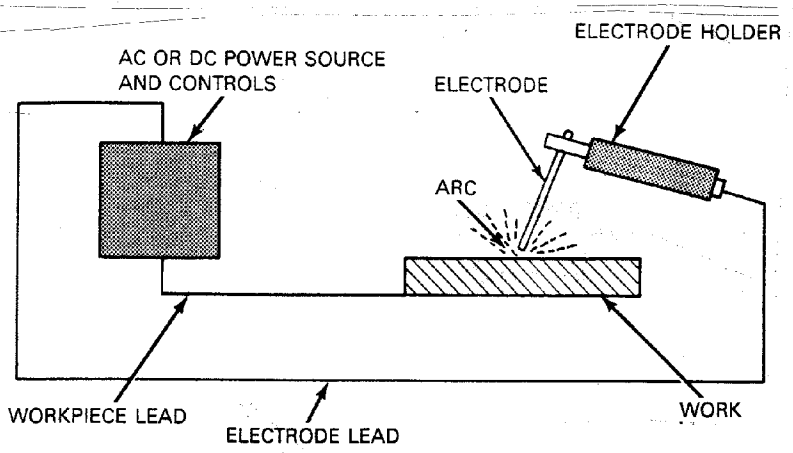

2-4a. Basic SMAW apparatus.

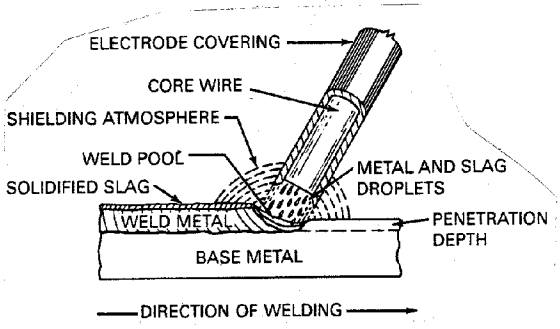

2-4b. Detail of SMAW process.

Figure 2-4. Diagram of the shielded metal arc welding (SMAW).[10]

(Both figures reprinted with permission of the American Welding Society.)

The arc characteristics of the electrode and the mechanical properties, chemical composition, and metallurgical structure of the weld are influenced by the type of shielding used, along with other ingredients within the covering and core wire. Each type of electrode used in SMAW has a different type of electrode covering, depending on the application.

The advantages of the SMAW process include its simplicity, low cost, portability, and the fact that a shielding gas is not needed. One restriction of SMAW is that the deposition cycle is normally less than for processes using continuous electrodes.

2.2.1.4 Gas Metal Arc Welding[10]—

Gas metal arc welding (GMAW) is a consumable electrode welding process that produces an arc between the weld pool and a continuously supplied filler metal. An externally supplied gas is used to shield the arc (Figure 2-5). GMAW originally was referred to as metal inert gas (MIG) welding because it used an inert gas for shielding. Although it still is sometimes called MIG welding, developments have led to the use of both inert and reactive gases.

A variation of the GMAW process, referred to as metal cored electrodes, uses a tubular electrode filled mostly with metallic powders forms. These types of electrodes must use a gas shield to prevent contamination of the molten weld by the atmosphere. The American Welding Society (AWS) considers metal cored electrodes a part of GMAW, although metal cored electrodes are grouped with flux cored electrodes by foreign welding associations.

Advantages of GMAW include its ability to be operated in semiautomatic, machine, or automatic modes. It is the only consumable process that can weld all commercially important metals, such as carbon steel, high-strength low alloy steel, stainless steel, nickel alloys, titanium, aluminum, and copper. A weld can be performed in all positions with the proper choice of electrode, shielding gas, and welding variables. Compared with shielded metal arc welding (SMAW), the deposition rates and welding rates are higher for GMAW. Also, the continuous electrode feed makes long welds possible without stops and starts. On the downside, the equipment for GMAW is more complex, more expensive, and less portable than the SMAW process.

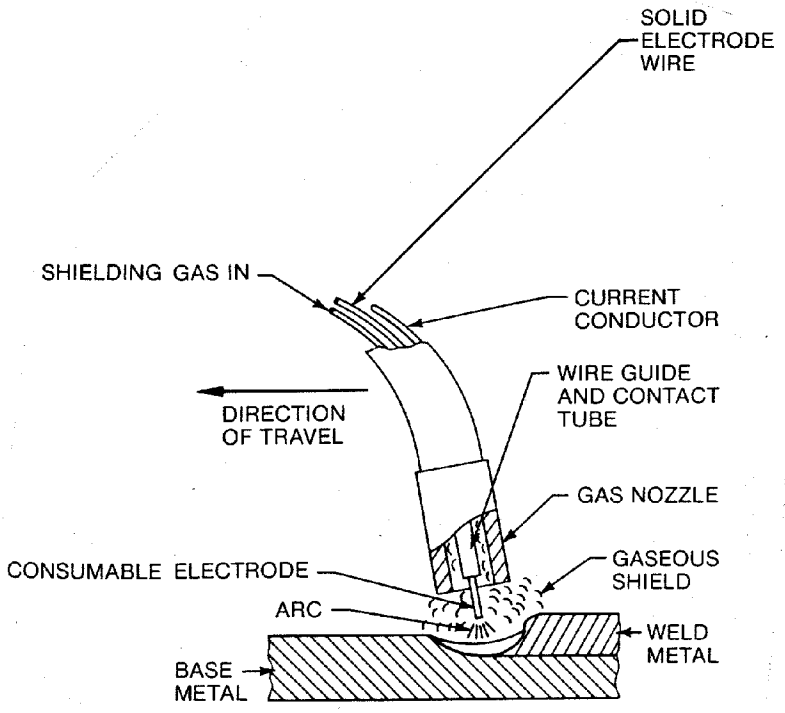

Figure 2-5. Gas metal arc welding (GMAW) process.[10]

(Figure reprinted with permission of the American Welding Society.)

2.2.1.5 Flux Cored Arc Welding[10]—

Flux cored arc welding (FCAW) is a consumable electrode welding process that uses shielding from flux contained within the tubular electrode. The heat-generating arc for FCAW operates between a continuous filler metal electrode and the weld pool. Additional shielding may or may not be supplied by an external gas, and the process is used without the application of gas pressure.

The flux cored electrode consists of a metal sheath surrounding a core of various powdered materials. The FCAW process is unique in its method of enclosing the fluxing ingredients within the continuously fed electrode. The electrode core material produces a slag cover on the face of the weld bead during the welding process.

The two major process variations of FCAW protect the weld pool from contamination by the atmosphere with different methods. The first method, called self-shielded FCAW, protects the welding pool by the break down and vaporization of the flux core through the heat of the arc (Figure 2-6). The second FCAW variation uses a shielding gas to protect the welding pool, in addition to protecting the vaporized flux core (Figure 2-7).

Compared to SMAW, the FCAW process provides a high-quality weld metal at lower cost and with less effort by the welder. The process allows for more versatility than submerged arc welding and proves to be more forgiving than gas metal arc welding. On the negative side, the equipment and electrodes for FCAW are more expensive than SMAW, and the slag covering produced must be removed.

2.2.1.6 Submerged Arc Welding[9,10]—

Submerged arc welding (SAW) produces an arc between a bare metal electrode and the work contained in a blanket of granular fusible flux (Figures 2-8 and 2-9). The flux submerges the arc and welding pool. Generally, the electrode serves as the filler material, although a welding rod or metal granules may be added.

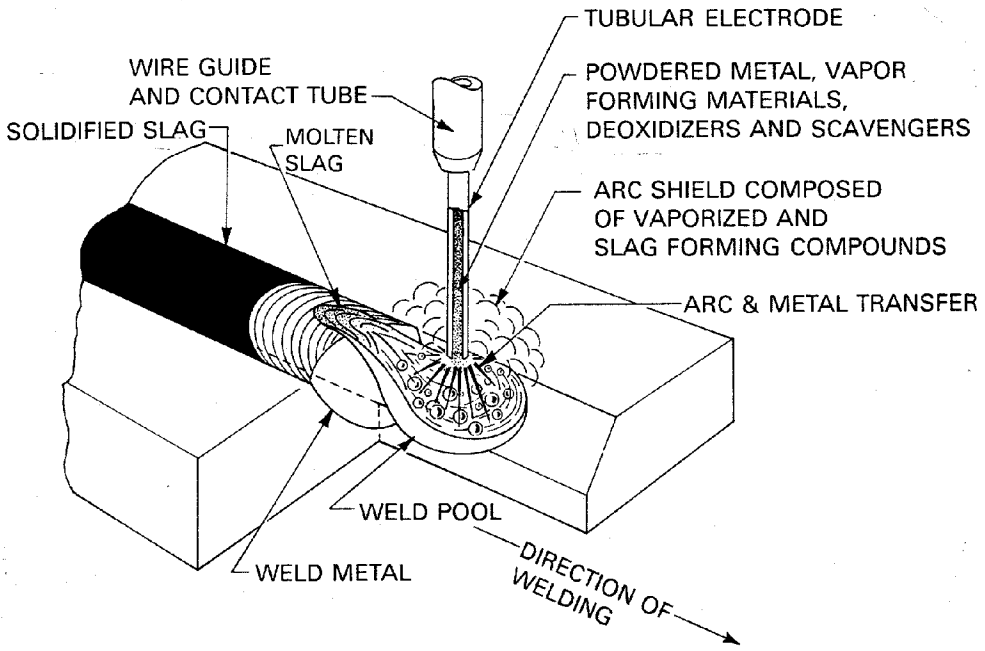

Figure 2-6. Shelf-shielded flux cored arc welding (FCAW).[10]

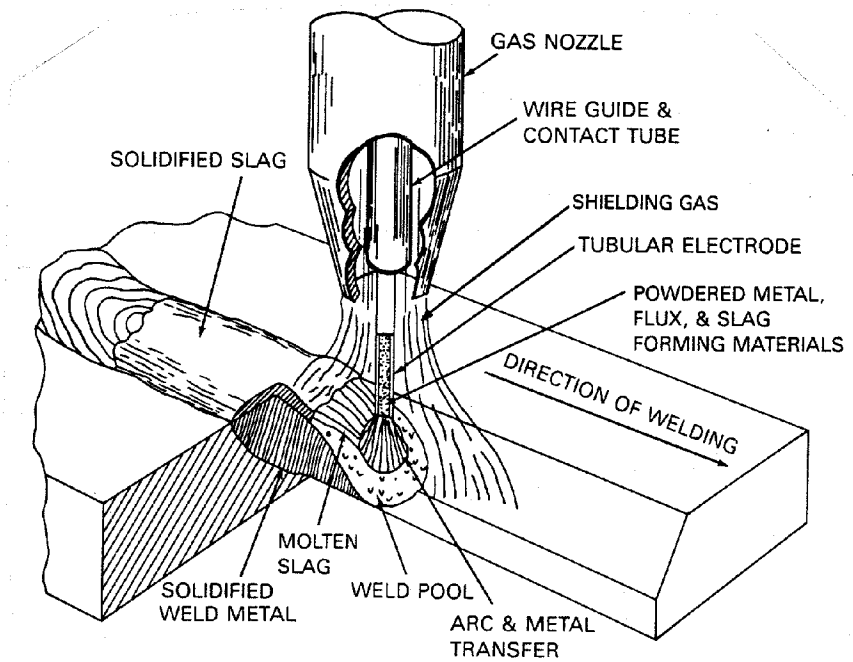

Figure 2-7. Gas-shielded flux cored arc welding (FCAW).[10]

(Both figures reprinted with permission of the America Welding Society.)

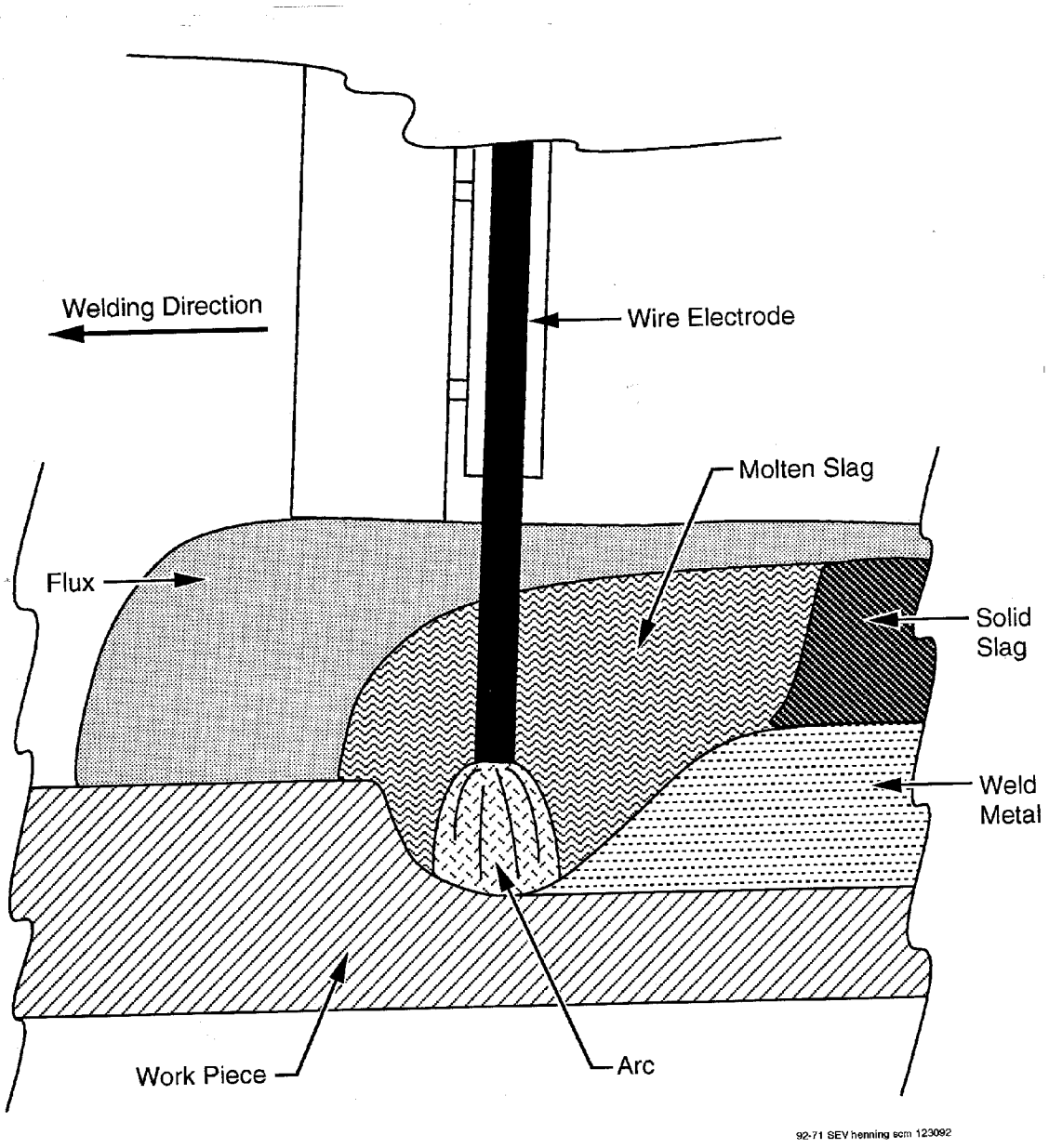

Figure 2-8. General submerged arc welding (SAW) process.[9]

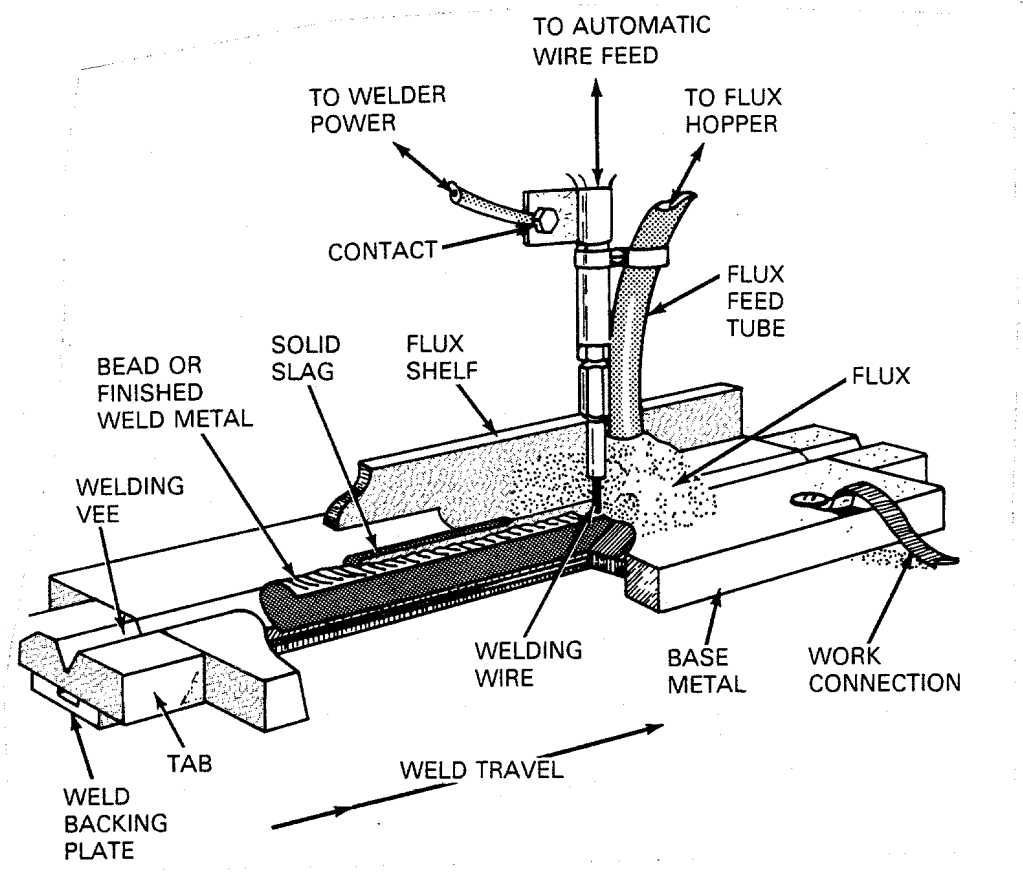

Figure 2-9. Schematic view of automated submerged arc welding (SAW).[10]

(Figure reprinted with permission of the America Welding Society.)

The flux covering the arc in submerged arc welding is an important factor in the process. The flux's role influences the stability of the arc and the mechanical and chemical properties of the final weld deposit. The quality of the weld is dependent on the handling and care of the flux.

Medium and heavy fabrication industries use the SAW process for fillet and main butt joints in pipe, cylinders, pressure vessels, columns, and beams. Generally, the welding head is fully automatic and mounted on a manipulator or carriage; however, for fillet welding hand held torches are available. Although SAW is limited to the downhand and horizontal positions, these positions can be utilized by informed design and job positioning. The process is also restricted by the high proportion of time needed to align the torch with the joint.

Since the arc operates in a cavity under the flux, the FFR of this process is extremely low. Hence, changes in operating variables have little effect on the rate of the fume formation if the flux cover is adequate.

2.2.1.7 Electrogas Welding[10]—

Electrogas welding (EGW) is a vertical welding process that uses an arc between a continuous filler metal electrode and the weld pool. The process is performed vertically with a backing to confine the welding pool (Figure 2-10). The method can either use an externally supplied shielding gas or be used without a shielding gas.

Electrogas welding is performed by an automated machine. The joint, a square-groove or single-V groove, is positioned vertically. The weld is made continuously in one pass and cannot be repositioned once the welding process has started. Electrogas welding is quiet with little splatter and results in a high quality weld deposit. In thicker materials or on vertical materials, EGW has a cost advantage over conventional joining methods, such as submerged arc welding and flux arc welding.

2.2.1.8 Electroslag Welding[10]—

Electroslag welding (ESW) is a process that produces molten slag that melts the surfaces of the workpieces to be welded and the filler metal. The slag shields the

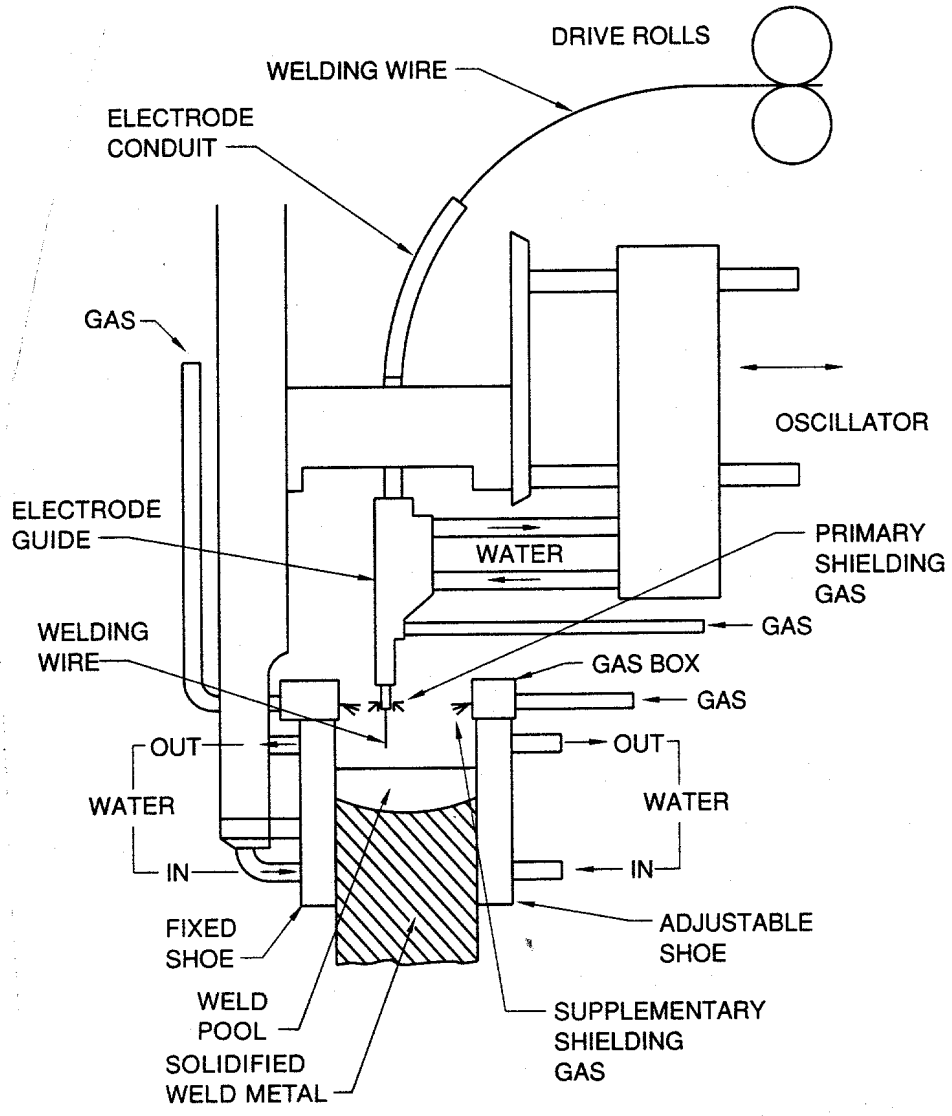

Figure 2-10. Electrogas welding (EGW) with a solid electrode.

(Figure reprinted with permission of the American Welding Society.)

weld pool from contaminants. The weld pool and slag move along the full width of the joint as welding progresses.

The process starts with an arc, generally in a sump below the joint, that heats a granulated flux and melts it to form the slag. The slag, which extinguishes the arc, remains molten by its resistance to electric current passing between the workpieces and the electrode. The molten slag generates enough resistance to fuse the welding electrode and the edges of the workpiece. The surface temperature of the welding bath runs near 1650°C (3000°F), while the interior of the molten bath is approximately 1925°C (3500°F). Just below the molten slag, the work-base metals and the electrode collect and form the weld by slowly solidifying. As shown in Figures 2-11 and 2-12, the process solidifies from the bottom up, following the upward moving welding process.

Since electroslag welding is the predecessor to electrogas welding, there are many similarities in processes and advantages. The electroslag welding process is a continuous welding process performed by machine. Once the process has started, it is performed to completion. The process results in a high-quality weld deposit and has no angular distortion of the base metal plates. It is also quiet, spatter-free, and has the ability to weld very thick sections in one pass.

2.2.2 Oxyfuel Gas Welding[6,10]

The second major type of welding process, oxyfuel welding, uses combustible gases to heat and melt the base metal without a welding electrode. Welding rods are only used when extra metal is needed as a filler for the joint to make a complete bond. The consumable rods are close in composition to the base metals, and the rod composition varies with application.

One advantage of oxyfuel welding is the greater control a welder can obtain over heat input and temperature, independent of the addition of filler metal. The welding equipment is inexpensive, generally portable, and versatile, allowing it to be used in a variety of operations such as bonding, preheating, surfacing, and brazing.

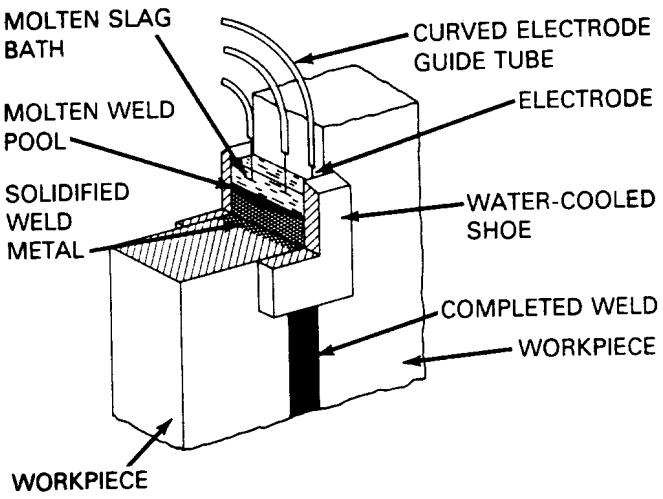

Figure 2-11. Nonconsumable guide (three electrode) method of electroslag welding (ESW).[10]

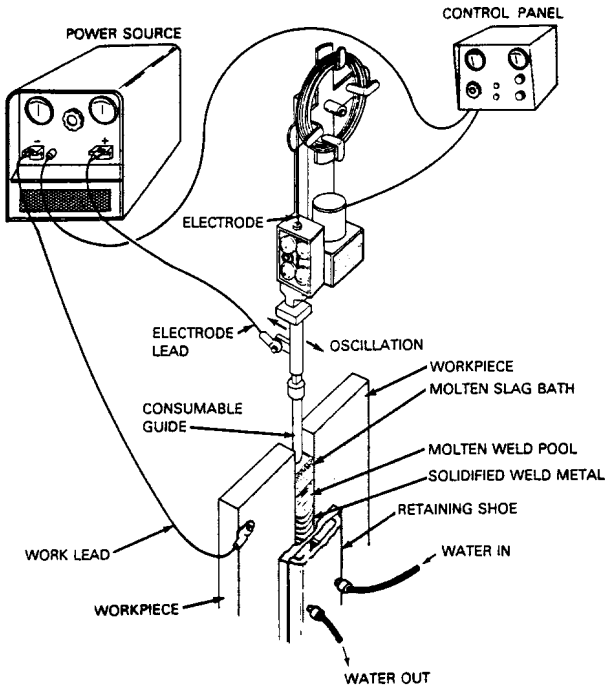

Figure 2-12. Consumable guide method of electroslag welding (ESW).[10]

(Both figures reprinted with permission of the American Welding Society.)

2.2.3 Resistance Welding[6]

In resistance welding, pieces of metal are pressed together while a electric current is passed through them. At this contact point, the resistance is sufficient to increase the temperature and melt the base metals.

2.2.4 Brazing[6,10]

In brazing, metals are heated and joined together by a molten filler metal at temperatures exceeding 450°C (840°F). The filler metal used in brazing may take on one of many forms including wire, foil, filings, slugs, powder, paste, or tape. To prevent atmospheric contamination, a flux must be used.

One advantage of brazing is that it is relatively economical when done in large batches. The joint can also be taken apart at a later time. Another important advantage of brazing is that dissimilar metals can be joined because the base metals are not melted. A disadvantage is that a highly skilled technician must perform the operation.

2.2.5 Soldering[10]

Soldering is similar to brazing. The main difference between the two processes is that soldering uses a filler metal in a liquid state below 450°C (840°F), and brazing uses temperatures over 450°C (840°F). The filler metal is held in the joint or drawn into the joint by capillary action.

One advantage of soldering is that the low temperatures of the process have minimum effect on base-metal properties. In addition, the low temperatures require low energy and allow precise control of the process. Many different methods of heating allow flexibility in design and manufacturing procedures.

2.2.6 Oxyfuel Cutting[10]

In oxyfuel gas cutting (OFC), metal is severed or removed at high temperatures by a chemical reaction with oxygen. The necessary heat is generated by a flame that is produced by burning a gaseous fuel in oxygen. Chemical fluxes or metal powders can

be added to aid in cutting oxidation-resistant metals. Figures 2-13 and 2-14 show typical cutting torches used in OFC.

Although the process has been called various other names, such as burning, flame cutting, and flame machining, the cutting process is performed by the oxygen stream. The oxygen-fuel gas flame raises the base metal to the acceptable preheat temperature range and maintains the cutting operation.

An advantage of the OFC torch is its versatility. Generally, it is portable, able to cut plates up to 2 m (7 ft) thick, and is capable of cutting straight edges and curved shapes. In addition, the cutting direction can be changed continuously throughout the operation.

2.2.7 Arc Cutting[10]

Arc cutting (AC) includes a group of thermal cutting processes that use the heat of an arc between an electrode and the workpiece to sever or remove metal. Generally, arc cutting is used with nonferrous metals, stainless steel, or steels with high chromium or tungsten content.

Arc cutting covers a list of processes that include:

- **!** Plasma Arc Cutting (PAC)
- **!** Air Carbon Arc Cutting (CAC-A)
- **!** Shielded Metal Arc Cutting (SMAC)
- **!** Gas Metal Arc Cutting (GMAC)
- **!** Gas Tungsten Arc Cutting (GTAC)
- **!** Oxygen Arc Cutting (AOC)
- **!** Carbon Arc Cutting (CAC)

Plasma arc cutting and air carbon arc cutting are more commonly used than the other processes listed.

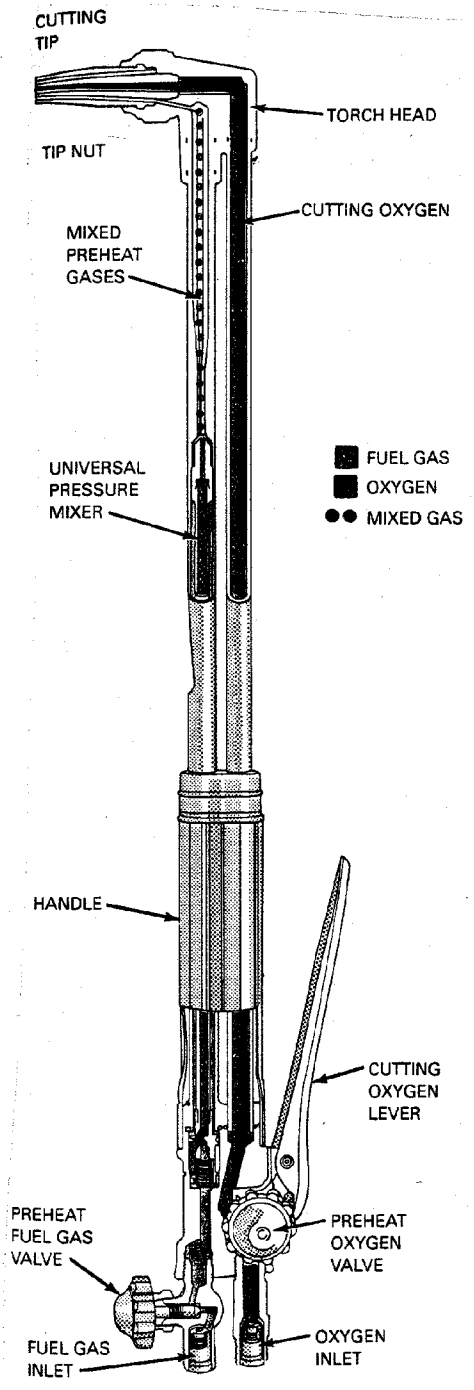

Figure 2-13. Typical premixing-type cutting torch.[10]

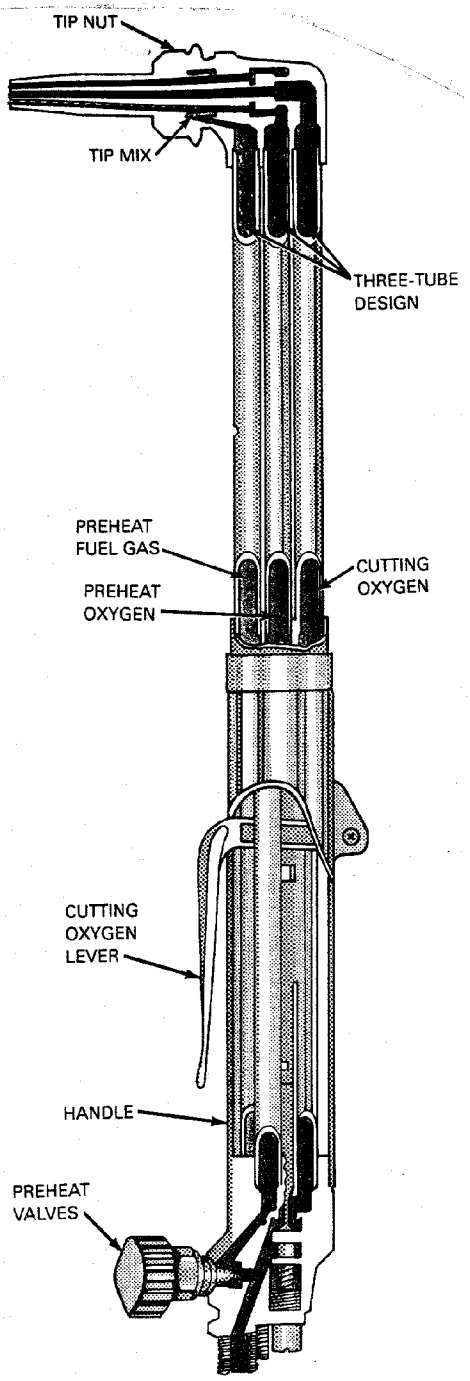

Figure 2-14. Typical tip mix cutting torch.[10]

(Both figures reprinted with permission of the America Welding Society.)

2.3 AIR POLLUTANT EMISSIONS[6,9,15,16,17,18]

The main pollutants of concern during welding operations are particulate matter and particulate phase hazardous air pollutants. Only electric arc welding generates pollutants in quantities of major concern. Resistance welding using certain materials also may generate hazardous pollutants. Due to the lower temperatures of the other welding processes, fewer fumes are released.

The quantity of emissions released depends largely on the type of welding process used and its operating conditions. Figures 2-15 and 2-16 show the variations in FFR for different processes according to the type of electrode and applied current, respectively.[9,15] Depending on the choice of electrode and its diameter and composition, emissions are reduced or increased. The workpiece composition also affects the quantity of fume released. Coatings on the workpiece generate organic and metallic fumes (e.g., galvanized coatings, cleaners, oils, paints, etc.), depending on the particular application. Operating conditions that influence fume emissions include travel speed, voltage, current, arc length, polarity, welding position, electrode angle, and deposition rate.

The welding fume is formed by the vaporization and recondensation of metallic elements upon cooling in ambient air. As such, the particulate matter produced is generally submicron in size with approximately 50% to 75% of the particles having diameters in the range of 0.4 to 0.8 μm.[18] The amount of the emissions generated can vary substantially from process to process. Essentially no fume is generated by submerged arc welding, and nearly 80 g fume/kg electrode is produced by flux cored arc welding operating at high current.[9,15]

The elemental composition of the fume varies with the electrode and workpiece composition. Hazardous metals listed in the 1990 Clean Air Act Amendments, which have been detected in welding fume, include manganese, nickel, chromium, cobalt, and lead. Manganese is present at detectable levels in most welding processes. The other metals are found at lower quantities. Again, the amount of hazardous metal emissions depends largely on the process, electrode, workpiece, and operating conditions used.

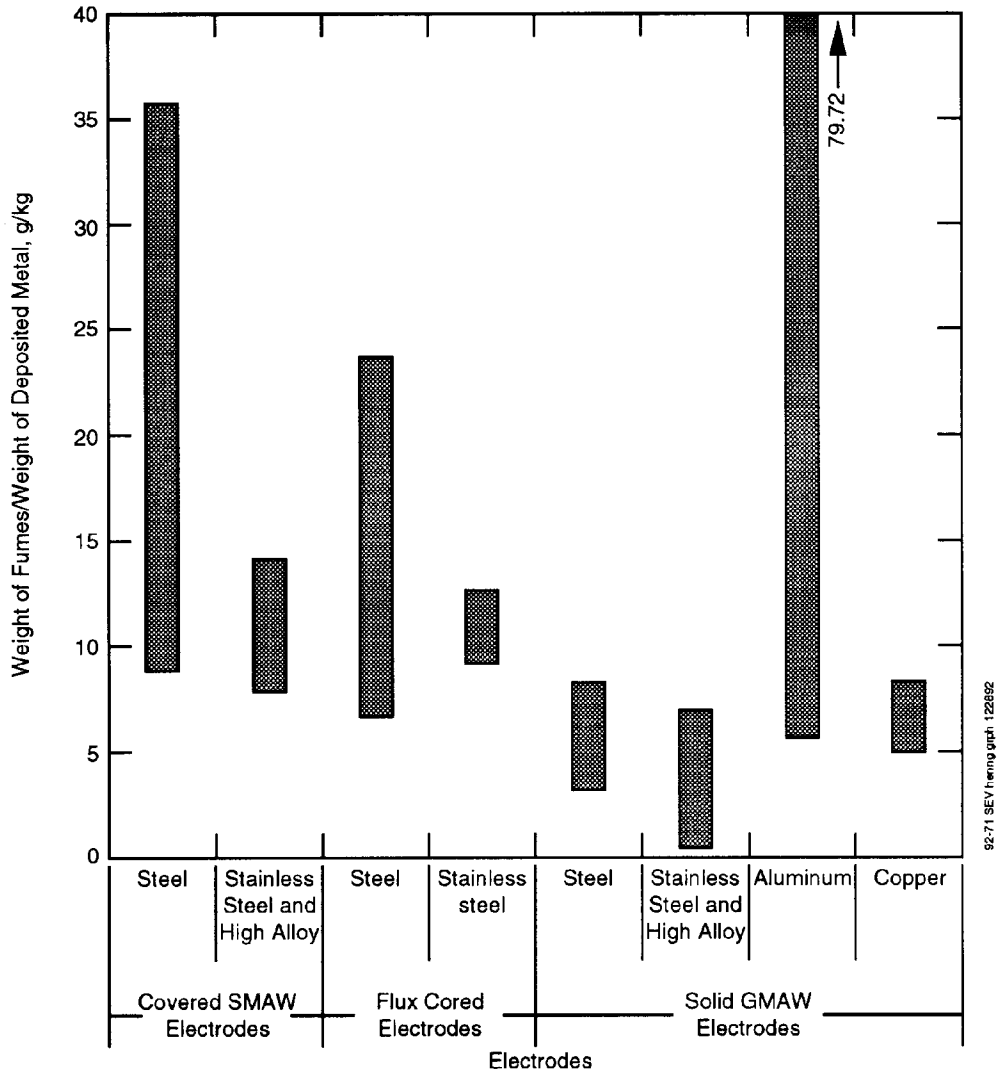

Figure 2-15. Particulate emissions from various arc welding processes according to type of electrode.[15]

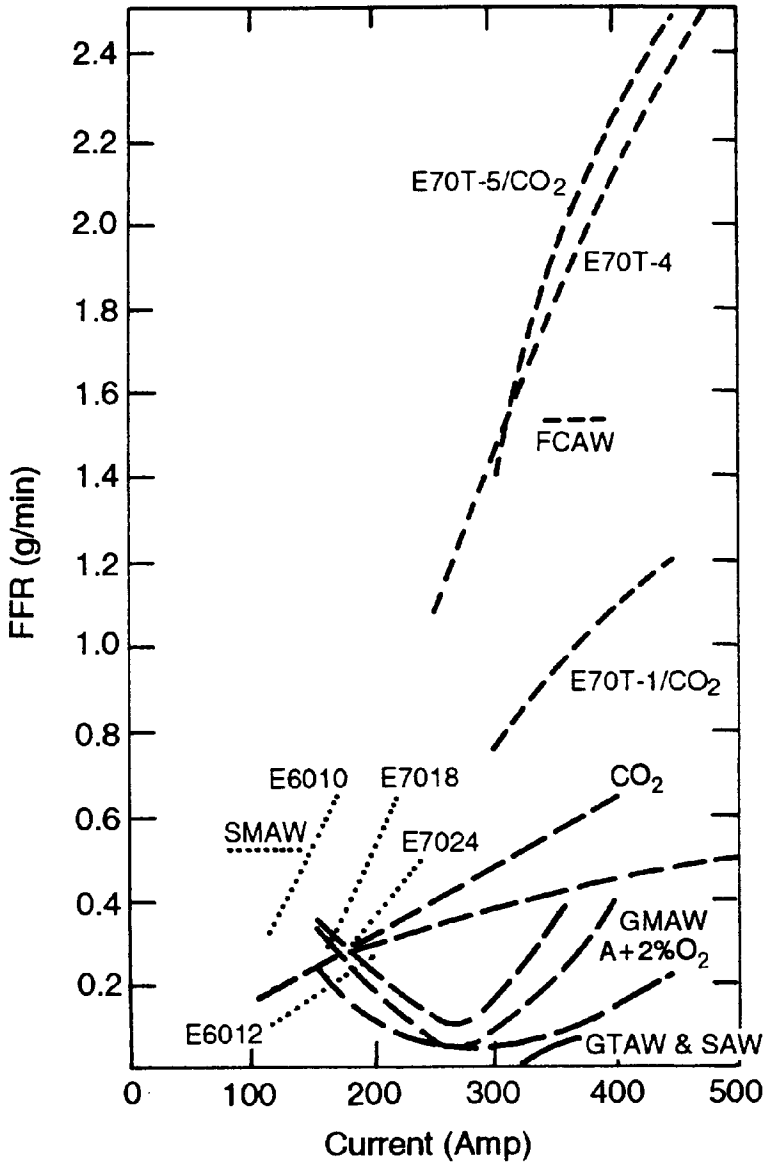

Figure 2-16. Particulate emissions from various arc welding processes by applied current.[9]

While gas phase pollutants are generated during welding operations, little information is available on the gases produced. Known gaseous pollutants (including "greenhouse" gases) released in some welding processes include CO_2, CO, NO_x, and O_3. Also, many of the gases produced are not considered hazardous pollutants, but only simple asphyxiants.

2.4 CONTROLS[6]

Welding operations are diverse and dynamic, making the use of controls difficult. Many site and operator variables play important roles in the amount of fume produced. The following describes some of the controls and steps used to reduce welding fume emissions.

2.4.1 Process Controls[6,9,13,14,15,16]

The amount of fume generated must be considered when deciding upon a particular welding process. Results of the two source tests graphed previously in Figures 2-15 and 2-16 show that different welding methods generate different amounts of fume. Whenever specifications and conditions allow, the process generating lesser fume should be chosen. In general, SAW has the lowest fume emission and FCAW has the highest fume emission.

Other process controls should be used as applicable. When permitted, a base metal workpiece should be selected that produces less fume and allows a low fume emitting process to be used. The type of electrode and, if necessary, the type of shielding gas should be given consideration in the control of emissions. Figure 2-16 shows that there are not only variations in fume emissions between processes, but between different electrode types within the same process. The same holds true for different shielding gases. A CO_2 shielding gas usually will have a higher emission than an inert gas such as argon.

2.4.2 Operating Variables[6,9,13,14,15,16]

The proper current, arc voltage, arc length, travel speed, and welding electrode angle should be selected to reduce fume emissions. The skilled welder pays close attention to all these variables to ensure low fume emissions and good weld quality.

Figure 2-16 shows that an increase in current tends to increase the amount of fume generated. The operator should select the lowest recommended current and voltage that will provide quality welds. By maintaining the welding angle close to perpendicular, the voltage can be reduced, which will likewise reduce the fume emission.

2.4.3 Capture and Collection[6,11,12,13,15,16,19]

Except for manual welding, welding fume normally is captured by forced air removal from the building or shop area. A forced air booth or room may be a good option in an automated welding process.

Manual welding uses portable ducts or hoods for emissions capture. For small items and repetitive work, small booths equipped with hoods or stationary ducts satisfactorily remove the fume. For large or random work, portable or flexible ducts are used. Figure 2-17 shows a typical flexible duct fume capture system and its appropriate placement. The portable ducts are moved to the welding location in the shop and later moved to another welding operation as needed.

Side baffles or flanges on the hood or duct inlet have been found to assist in the capture of a larger quantity of fume. It is important that all hoods or duct inlets be placed as close to the welding as possible. Generally, a placement distance of 6 to 12 in is recommended.[19]

Another method used to capture the fume is torch fume extraction. The extracting duct, mounted on the torch, removes the fume directly from the work area (Figure 2-18). Care must be observed so as not to also extract the shielding gas.

Once the fume has been captured, it is delivered to some type of collector. Typically, the particulate is removed with a high efficiency filter or electrostatic precipitator (ESP) and then the organic gases are removed by adsorption on activated carbon. Particulate scrubbers, which provide another technique to remove welding fumes, are generally less efficient.

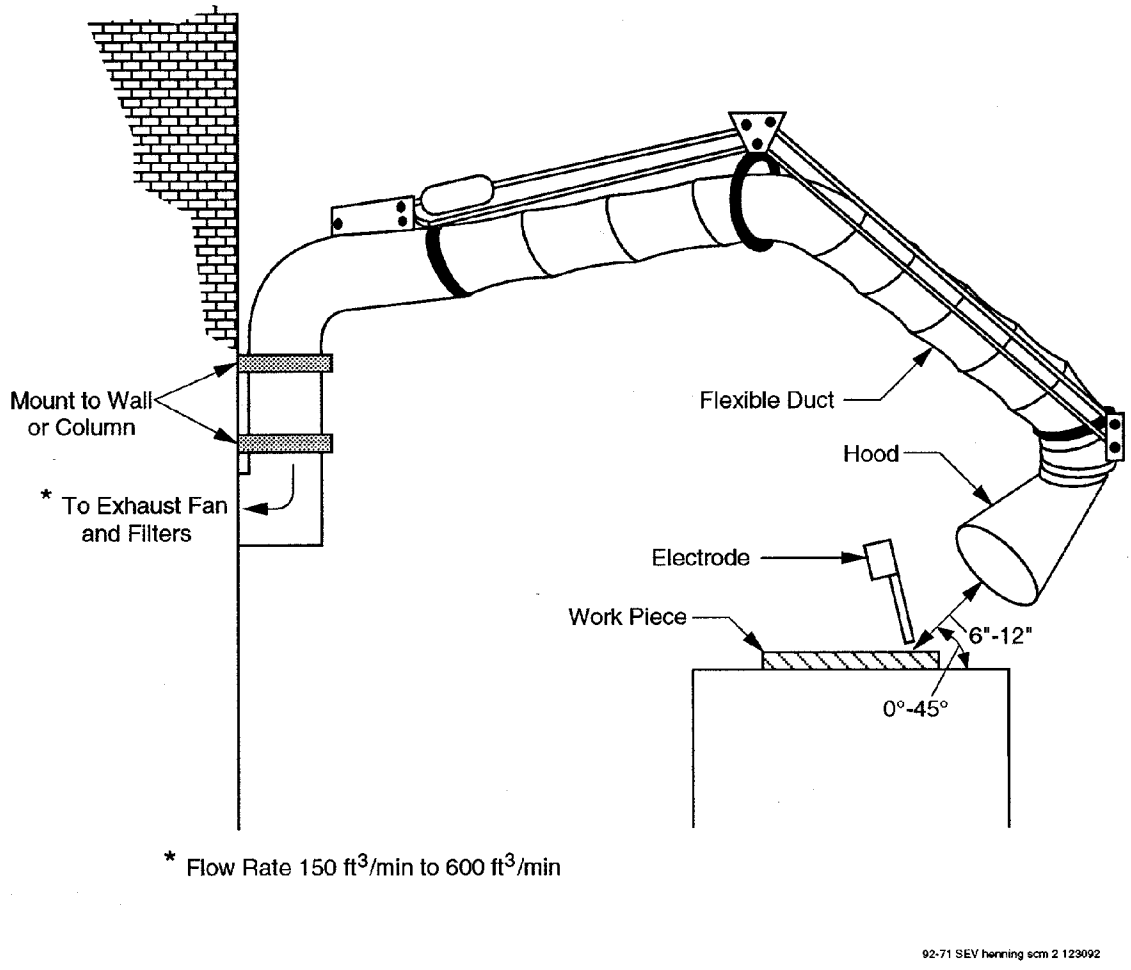

Figure 2-17. Flexible duct from capture system.[18]

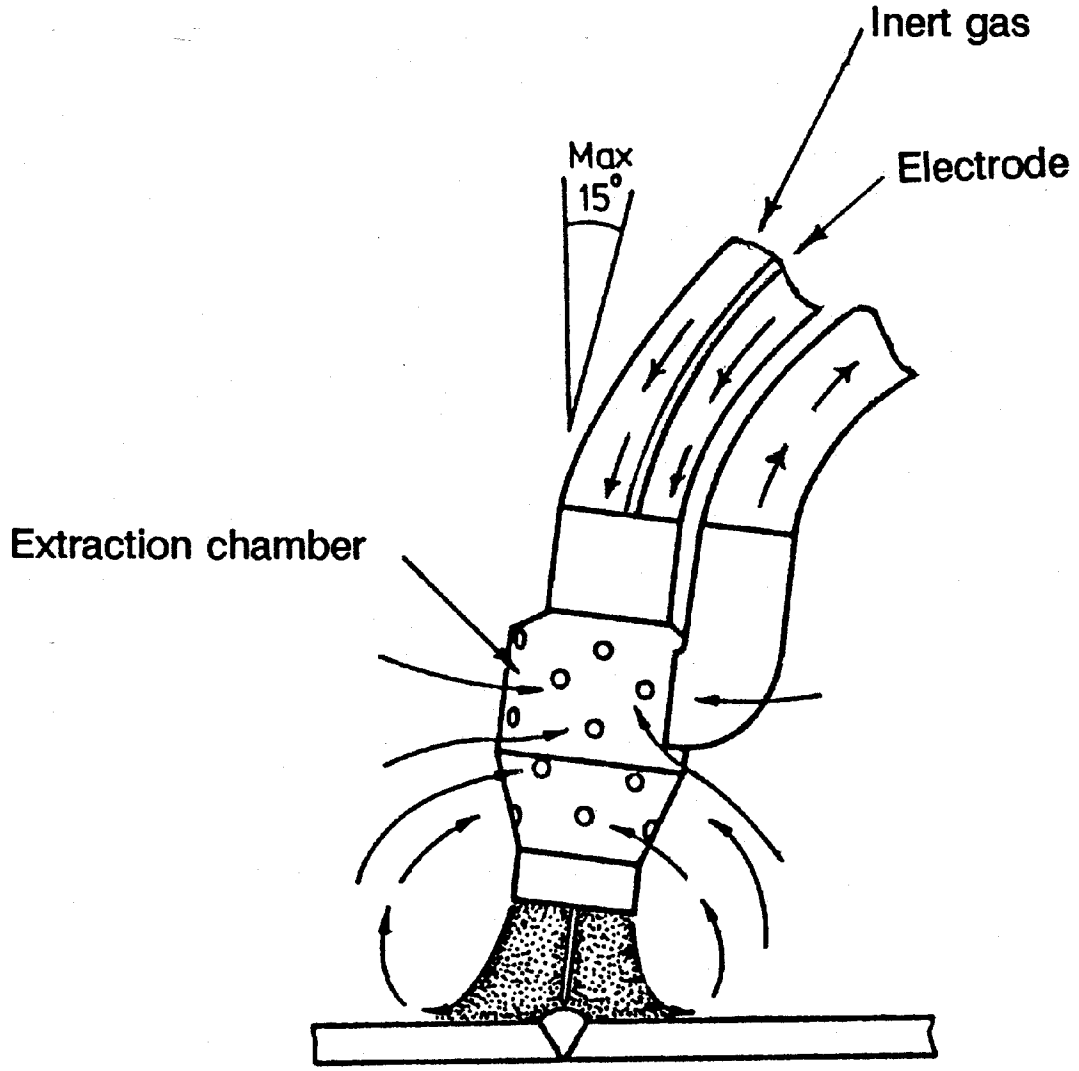

Figure 2-18. Torch fume extractor.[7]

2.4.4 Cleanup[6]

When cleaning up a welding area, no potentially toxic materials should be swept up dry or blown off the surface. Instead, these materials are cleaned up by wet mopping or by vacuum pickup. This procedure is considered a safety item, but it also helps reduce potential fugitive emissions.

2.4.5 Work Awareness[6]

All of the practices discussed in the previous subsections should be passed on to the welder. The welder should be informed of operating techniques and all procedures that reduce welding fumes. The training should describe how tasks are properly performed, how work practices reduce fumes, and how these practices will benefit the welder. Although much of this knowledge is acquired in safety training and is monitored as good safety practices, it applies to good environmental practices as well. While the previously discussed controls help reduce fumes, a skilled, aware welder, following proper procedures and techniques, can reduce fumes by up to a factor of 6.[6]

REFERENCES FOR SECTION 2

1. Telephone conversation between Rosalie Brosilow, Editor, *Welding Design and Fabrication Magazine*, Penton Publishing, Cleveland, Ohio, and Lance Henning, Midwest Research Institute, Kansas City, Missouri, October 16, 1992.

2. G. H. G. McMillan, "The Health of Welders in Naval Dockyards: Final Summary Report," *J. Roy. Nav. Med. Serv.*, **69**:125-131, 1983.

3. CBI Services Inc., Kankakee, Illinois, Welding Engineer, by phone.

4. National Steel and Shipbuilding Co., San Diego, California, Dan Buell, by letter.

5. *Census of Manufactures, Industry Series*, U.S. Department of Commerce, Bureau of Census, Washington, D.C., March 1990.

6. National Institute for Occupational Safety and Health, *Criteria for a Recommended Standard Welding, Brazing, and Thermal Cutting*, Publication No. 88-110, U.S. Department of Health and Human Services, Cincinnati, Ohio, April 1988.

7. M. E. Reinders, *Handbook of Emission Factors, Part 2, Industrial Sources*, Government Publishing Office, The Hague, Netherlands, 1984.

8. N. Jenkins et al., *Welding Fume, Sources*Characteristics*Control*, Volumes 1-3, The Welding Institute, Abington Hall, Cambridge, England, 1981.

9. K. Houghton and P. Kuebler, "Consider a Low Fume Process for Higher Productivity," Paper 21 in *Proceedings, Joint Australasian Welding and Testing Conference*, Australian Welding Institute and Australian Institute for Nondestructive Testing, Perth, 1984.

10. *Welding Handbook, Welding Processes, Volume 2, Eighth Edition*, American Welding Society, Miami, Florida, 1991.

11. L. Bauer, "How to Select Exhaust Equipment," *Welding Design and Fabrication*, 64:7, 27-31, July 1991.

12. G. C. Barnes, "Control of Fumes in the Welding Environment," *Svetsaren*, 1:16-18, 1990.

13. C. N. Gray and P. J. Hewitt, "Control of Particulate Emissions from Electric-Arc Welding by Process Modification," *Ann. Occupy. Hyg.*, 25:4, 431-438, 1982.

14. I. W. Head and S. J. Silk, "Integral Fume Extraction in MIG/CO_2 Welding," *Metal Construction*, 11:12, 633-638, December 1979.

15. R. M. Evans et al., *Fumes and Gases in the Welding Environment*, American Welding Society, Miami, Florida, 1979.

16. R. F. Heile and D. C. Hill, "Particulate Fume Generation in Arc Welding Processes," *Welding Journal*, 54:7, 201s-210s, July 1975.

17. Y. Sugiyama et al., "Fumes and Gases Generated in Inert Gas Metal Arc Welding of Aluminum and Hg Alloys," in Proceeding of the *Colloquium on Aluminum and Its Alloys in Welded Construction*, Porto, Portugal, September 8, 1981.

18. E. J. Fasiska, et al., *Characterization of Arc Welding Fume*, American Welding Society, Miami, Florida, February 1983.

19. L. Baver, "How to Select Exhaust Equipment," *Welding Design and Fabrication*, 64:7, 27-31, July 1991.

SECTION 3

GENERAL DATA REVIEW AND ANALYSIS

3.1 LITERATURE SEARCH AND SCREENING[1]

The first step of this investigation was an extensive search of the available literature relating to the fume emissions associated with welding and allied processes. This search included data contained in the open literature (e.g., National Technical Information Service); source test reports and background documents located in the files of the EPA's Office of Air Quality Planning and Standards (OAQPS); data base searches (e.g., SPECIATE); and MRI's own files (Kansas City and North Carolina). The search was thorough but not exhaustive.

To reduce the large amount of literature collected to a final group of references, the following general criteria were used:

1. Emissions data must be from a primary reference:

    a. Source testing must be from a referenced study that does not reiterate information from previous studies.

    b. The document must constitute the original source (or publication) of the test data.

2. The report must contain sufficient data to evaluate the testing procedures and source operating conditions.

The above criteria were followed except in very limited cases where the inclusion of such information was felt to substantially expand the data base and improve the resulting candidate emission factors.

A final set of reference materials was compiled after a thorough review of the pertinent reports, documents, and information according to the above criteria. This set of documents was further analyzed to derive candidate emission factors for welding operations.

3.2 DATA QUALITY RATING SYSTEM[1]

As part of MRI's analysis, the final set of reference documents was evaluated as to the quantity and quality of data. The following data were always excluded from consideration:

1. Test series averages reported in units that cannot be converted to the selected reporting units.

2. Test series representing incompatible test methods.

3. Test series in which the control device (or equipment) is not specified.

4. Test series in which the welding process is not clearly identified and described.

5. Test series in which it is not clear whether the emissions were measured before or after the control device.

If there was no reason to exclude a particular data set, each was assigned a rating as to its quality. The rating system used was that specified by the EPA's Office of Air Quality Planning and Standards (OAQPS) for the preparation of AP-42 Sections.[1] The data were rated as follows:

A—Multiple tests performed on the same source using sound methodology and reported in enough detail for adequate validation. These tests do not necessarily have

to conform to the methodology specified by EPA reference test methods, although such were certainly used as a guide.

B—Tests that are performed by a generally sound methodology, but they lack enough detail for adequate validation.

C—Tests that are based on an untested or new methodology or that lack a significant amount of background data.

D—Tests that are based on a generally unacceptable method, but the method may provide an order-of-magnitude value for the source.

The following criteria were used to evaluate source test reports for sound methodology and adequate detail:

1. Source operation. The manner in which the source was operated is well documented in the report. The source was operating within typical parameters during the test.

2. Sampling procedures. The sampling procedures conformed to a generally accepted methodology. If actual procedures deviated from accepted methods, the deviations were well documented.

3. Sampling and process data. Adequate sampling and process data were documented in the report. Many variations may be unnoticed and occur without warning during testing. Such variations can induce wide deviations in sampling results. If a large spread between test results cannot be explained by information contained in the test report, the data are suspect and were given a lower rating.

4. Analysis and calculations. The test reports contain original raw data sheets. The nomenclature and equations used were compared to those specified by EPA (if any) to establish equivalency. The depth of review of the calculations was dictated by the reviewer's confidence in the ability and conscientiousness of the tester, which in turn was based on factors

such as consistency of results and completeness of other areas of the test report.

3.3 EMISSION FACTOR QUALITY RATING SYSTEM[1]

The quality of the emission factors developed from analysis of the test data was rated utilizing the following general criteria:

A—Excellent: Developed only from A-rated test data taken from many randomly chosen operations or facilities in the industry population. The source category* is specific enough so that variability within the source category population may be minimized.

B-Above average: Developed only from A-rated test data from a reasonable number of operations or facilities. Although no specific bias is evident, it is not clear if the operations or facilities tested represent a random sample. As in the A-rating, the source category is specific enough so that variability within the source category population may be minimized.

C—Average: Developed only from A- and B-rated test data from a reasonable number of operations or facilities. Although no specific bias is evident, it is not clear if the operations or facilities tested represent a random sample. As in the A-rating, the source category is specific enough so that variability within the source category population may be minimized.

D—Below average: Developed only from A- and B-rated test data from a small number of operations or facilities, and there is reason to suspect that these operations or facilities do not represent a random sample. There also may be evidence of variability within the source category population. Limitations on the use of the emission factor are footnoted in the emission factor table.

E—Poor: Developed from C- and D-rated test data, and there is reason to suspect that the operations or facilities tested do not represent a random sample.

---

* Source category: A category in the emission factor table for which an emission factor has been calculated (generally a single-type of process equipment or operation).

There also may be evidence of variability within the source category population. Limitations on the use of these factors are always footnoted.

The use of the above criteria is somewhat subjective depending to a large extent on the individual reviewer. Details of how each candidate emission factor was rated are provided in Section 4.4.

3.4 EMISSION TEST METHODS

A number of different methods have been developed over the past 20 plus years for the quantification and characterization of welding fume. In general, these methods involve the total enclosure of the welding operation by means of either a small, laboratory-scale chamber or through the use of temporary barriers. A flow of air is then introduced through the enclosure and the emissions are collected on a filter for subsequent gravimetric and chemical analyses. Operating variables also are characterized during testing to determine the FFR, usually in terms of mass of fume/ mass of electrode consumed.

In the United States, the American National Standards Institute/American Welding Society (ANSI/AWS) test procedure is generally recognized as the most accepted method for testing welding fumes.[2] While there has not been an agreed-on standard method internationally, the ANSI/AWS test procedure is similar to many other test methods. The different test methods used to collect emissions data on welding fume that were considered during the development of the candidate emission factors for this source are described in the following subsections.

3.4.1 ANSI/AWS F1.2-85[2]

The conical test chamber, shown in Figures 3-1 and 3-2, is utilized in the ANSI/AWS Method F1.2-85. The chamber contains two hand holes for access and a sighting window, equipped with shaded lens, is located in the center. An air gap of ½ in to ¾ in is maintained, and leveling bolts allow air to enter the bottom of the apparatus. The fumes are collected at the top of the unit by the filter and its supports for later analysis. The filter is generally made of cellulose fiber. A pressure drop gage and a constant flow rate pump are mounted on the top of the chamber.

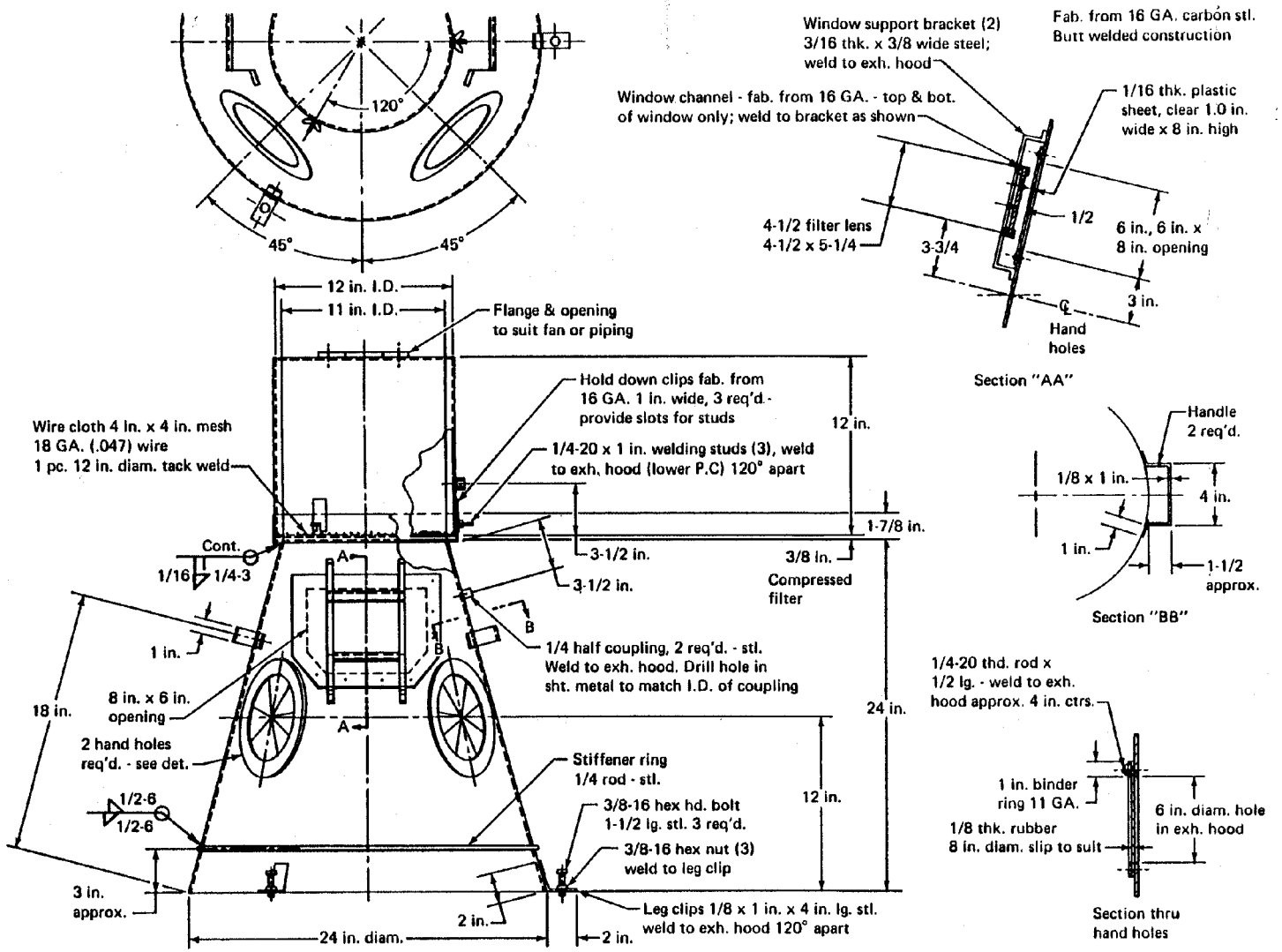

Figure 3-1. Details of ANSI/AWS test chamber.[2]

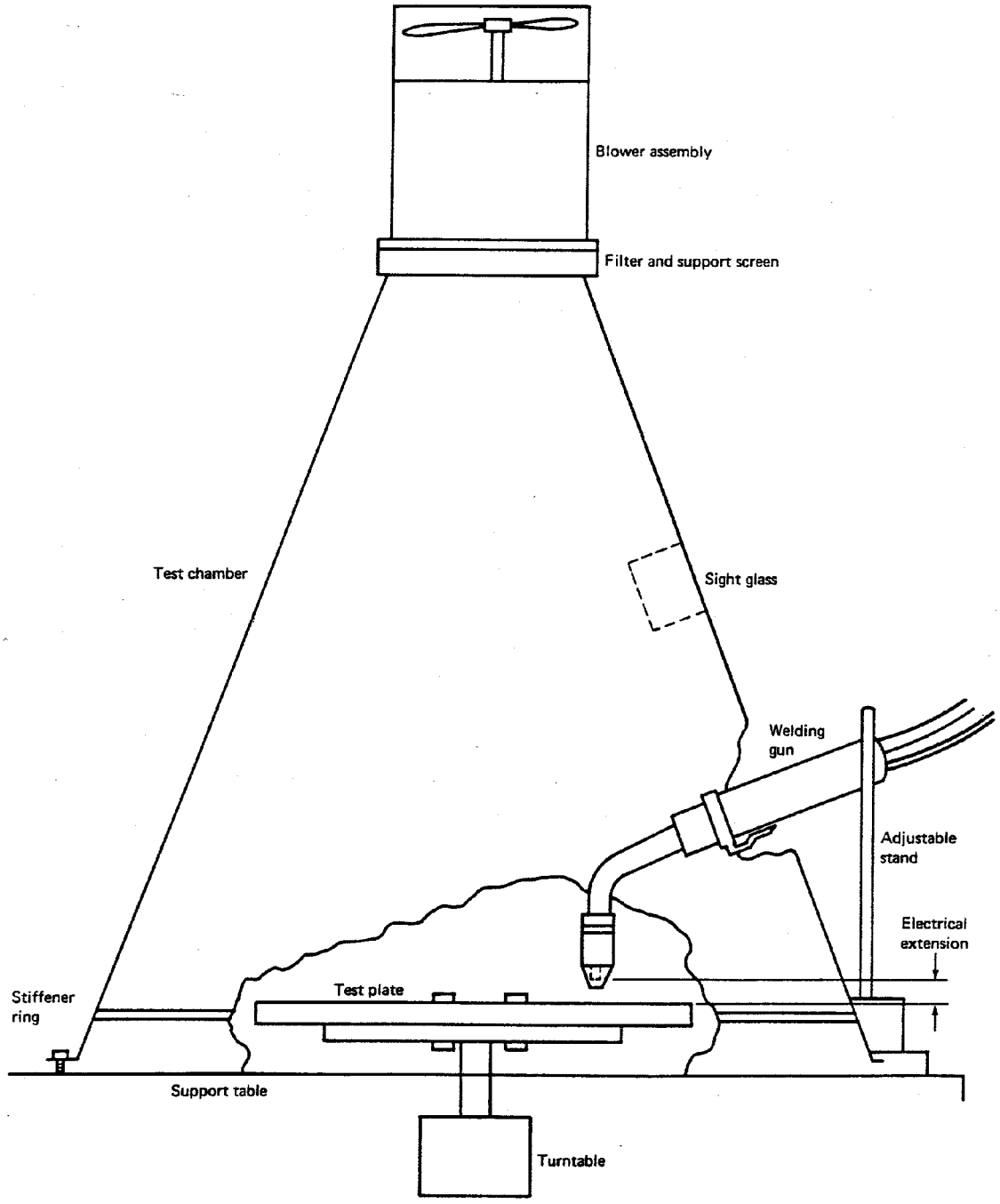

Figure 3-2. Cut-away view of ANSI/AWS test chamber.[2]

The ANSI/AWS chamber may be used for testing either automatic, semiautomatic, or manual processes. For the automatic process, plate movement on a turntable is suggested. The torch is mounted through one of the hand holes.

3.4.2 Swedish Fume Box[4]

The Swedish Fume Box test method was developed by Swedish electrode manufacturers and became a standard in Sweden in 1976. The method has been used in testing at four different research laboratories. Several other methods used to test fume formation rates are modified versions of the Swedish Fume Box or are similar in design and method.

Through the slot in the front of the fume box (Figure 3-3), the welder places a horizontal-vertical fillet, using the maximum recommended current for the electrode. An extractor pump draws the emitted fume and the air in the chamber up the outlet duct to be collected on 240-mm diameter filter paper. The total fume emitted from the welding process is collected on the filter. The fume emission rate can be calculated by the net fume weight collected and the welding time.

3.4.3 Battelle Fume Collection Chamber[5,6]

The Battelle fume collection chamber (Figures 3-4a and 3-4b) occupies a volume of approximately 33 ft^3 (0.93 m^3). The sheet metal chamber tapers inward at the upper portion of the chamber with the filter and holder located at the top. An exhaust blower removes the fumes from the chamber. The chamber can be sealed to prevent loss of fumes during sampling .

During testing, the welder operates the torch that is mounted on a stationary stand. The workpiece is placed on a variable speed turntable. A prefilter and an absolute filter are used to collect the total fumes. The prefilter is made from two layers of glass fiber insulation, and the absolute filter is a glass fiber absolute (i.e., HEPA) filter.

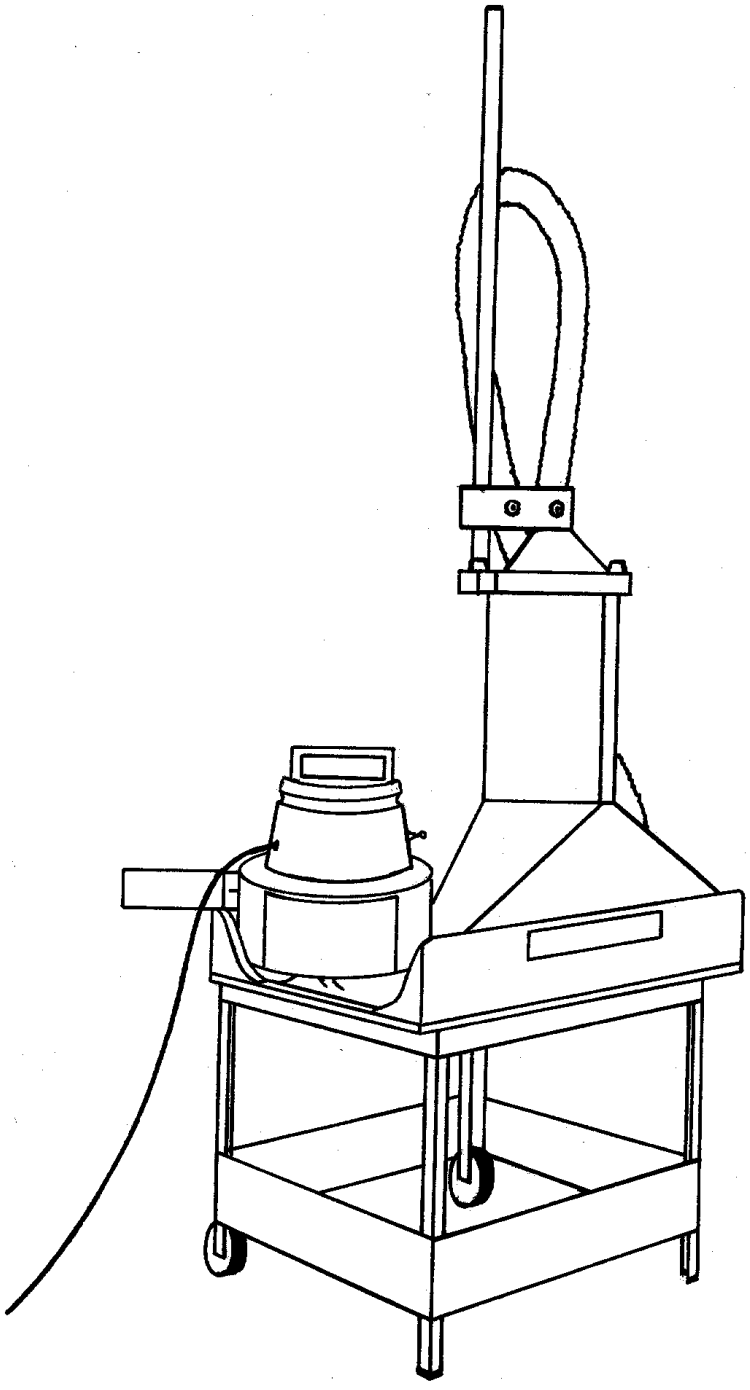

Figure 3-3. Illustration of Swedish fume box.[4]

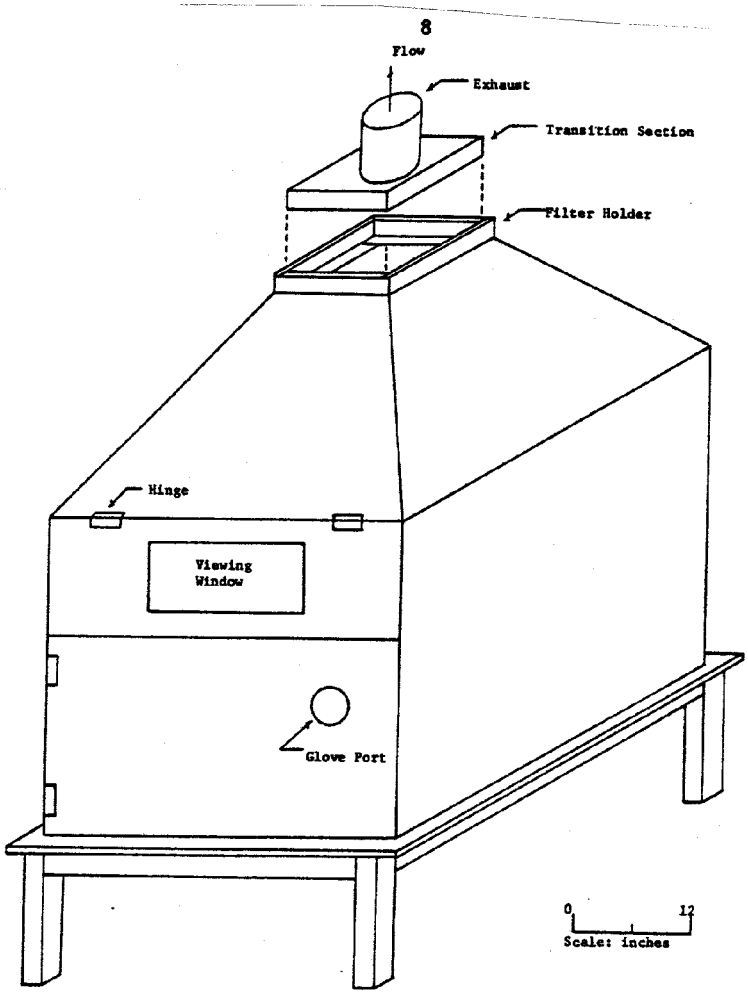

Figure 3-4a. Illustration of Battelle welding chamber.[6]

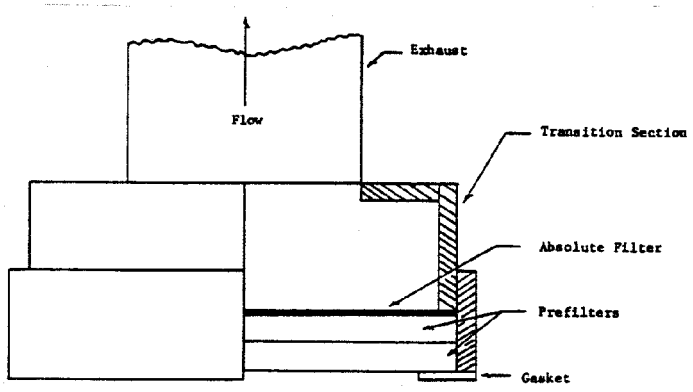

Figure 3-4b. Filter holder assembly used with Battelle welding chamber.[6]

3.4.4 Press/Florian Fume Chamber[7]

The Press/Florian fume capture chamber (Figure 3-5) stands 2 m x 2 m x 2 m high plus the fume hood. The welding, which is carried out automatically within the chamber, is performed with disks on a rotary table and a stationary welding torch. The fume extraction is carried out isokinetically to provide a representative sample of solid particles.

3.4.5 Welding Institute Fume Box[8,9,10]

The Welding Institute (Great Britain) fume box consists of a hollow cone placed on a box at table height. Air enters through an opening in the front of the box. Specified welding conditions are followed as the weld is performed on a vertical plate. A pump pulls the particulate fume that is emitted during welding up the cone where it is collected on a large diameter filter. Sampling continues until the chamber has cleared of the fume.

3.4.6 High Intensity Fume Collector[11]

The High Intensity Fume Collector (Figure 3-6) was designed by the Australian Welding Research Association. It is a modified version of the Swedish Fume Box. In this case, however, a felt made from polyester fibers is used for the filter, which is augmented electrostatically to improve collection efficiency. The filter was later analyzed to determine the fume formulation rate from the welding process tested.

3.4.7 Japanese Method[3,4]

Tests have been made by Japanese investigators using a total sampling technique similar to the Swedish method. The Japanese standard method for this determination is JIS Z 3930-1979, "Method of Measuring Total Amount of Weld Fumes Generated by Covered Electrodes."

3.4.8 BOC Fume Chamber[12]

The BOC Fume was designed at BOC Limited to remove all generated fume particulate without disrupting the shielding gas. The test chamber (Figure 3-7) is nearly 350 mm square, with a height of 550 mm and a collection face 100 mm in diameter.

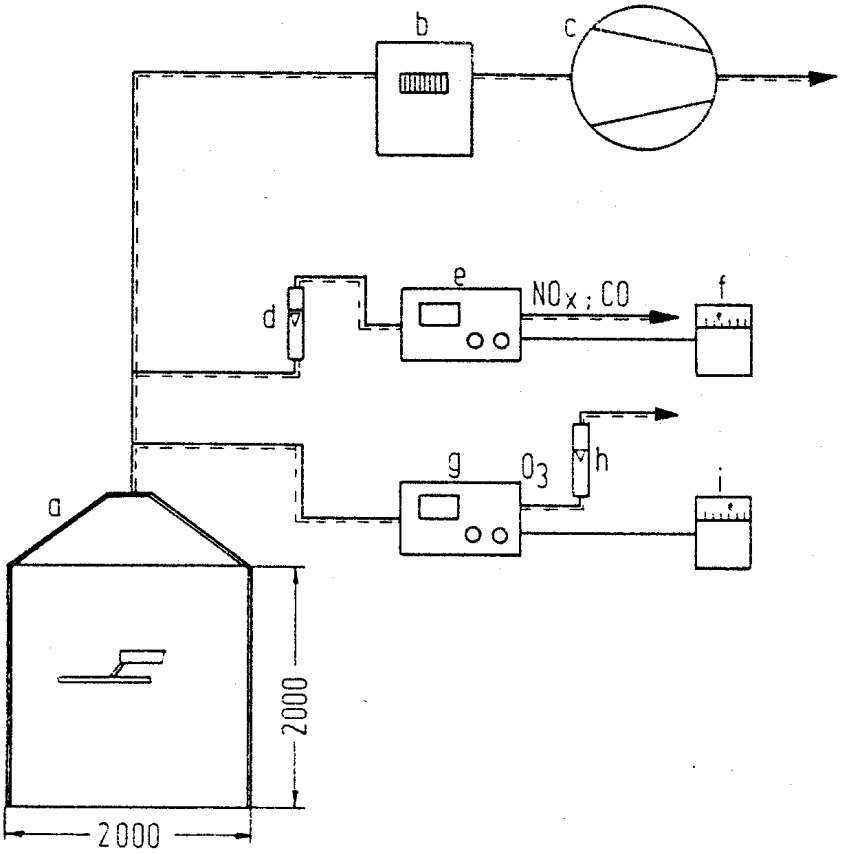

a) Measuring chamber
b) Gas meter (main stream of exhaust air)
c) Fan (main stream of exhaust air)
d) Flow meter or air meter
e) Analyser for NO_x, CO etc.
f) Recording instrument
g) Analyser for O_3
h) Flow meter or air meter
i) Recording instrument
k) Dust collecting apparatus with pump and flow meter

Figure 3-5. Diagram of the Press/Florian fume chamber.[7]

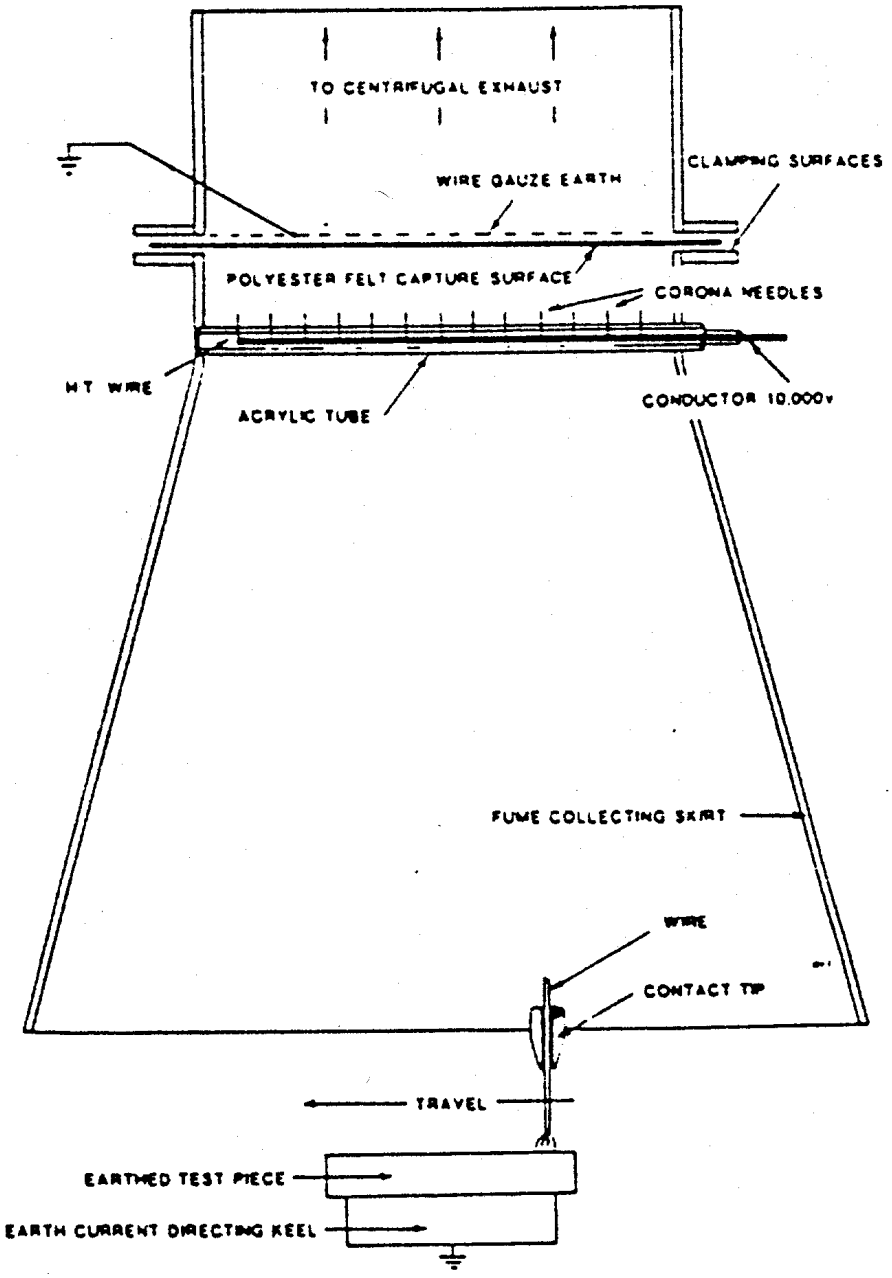

Figure 3-6. High intensity fume collector.[11]

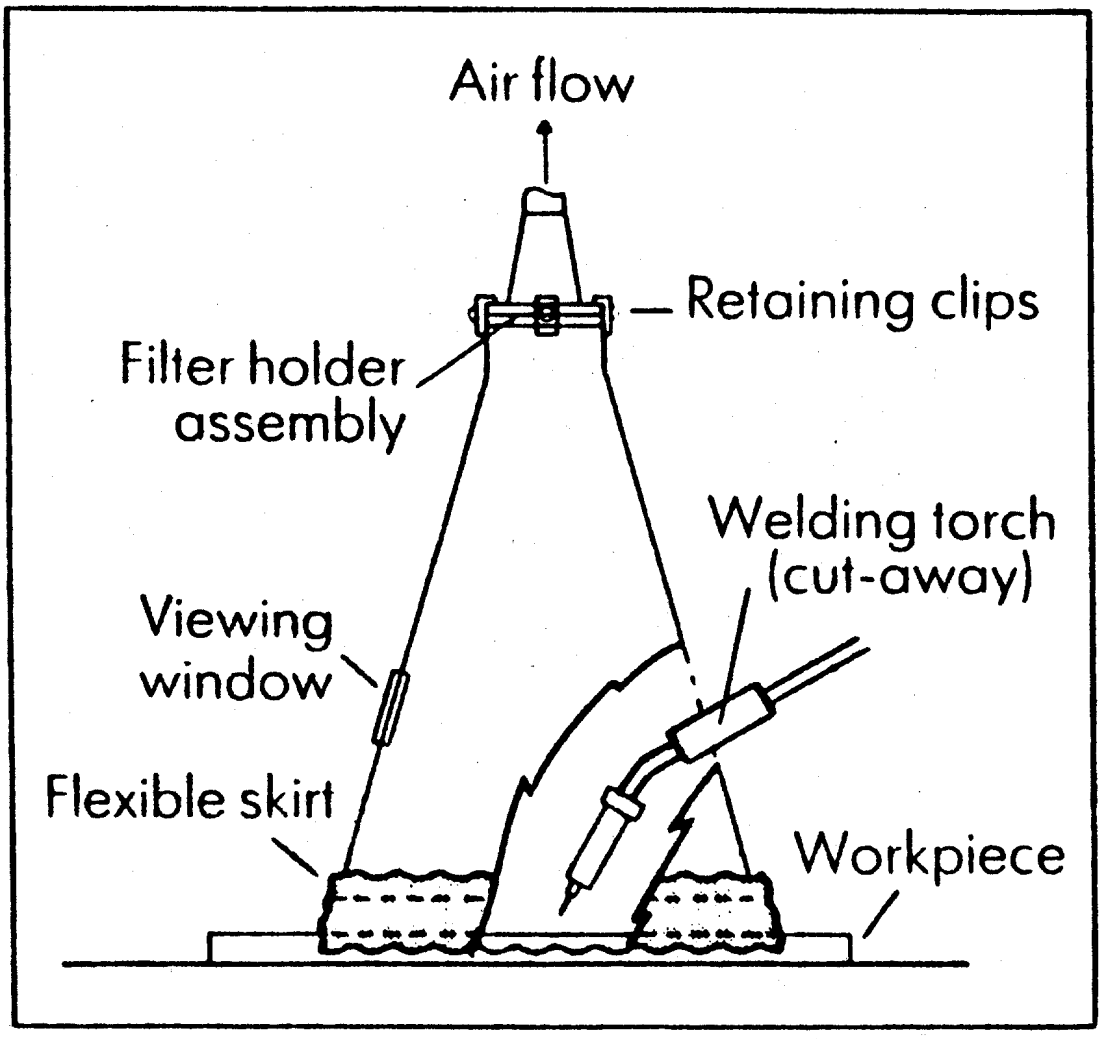

Figure 3-7. BOC fume chamber.[12]

The fume is collected on glass fiber filter paper supported by a stainless steel mesh with a rubber seal. A Nederman welding smoke extractor attached to the top of the chamber (with a 45-mm diameter hose) removes the fume from the chamber. Automatic welding is performed by moving the workpiece with a Kat Tractor system. A flexible skirt attached to the base of the box prevents fume loss.

3.4.9 Automatic Welder and Fume Collection System[13,14,15]

In research performed for the Australian Welding Research Association, an automatic welder and fume collection system was used (Figure 3-8). A 30 cm x 30 cm hood was located over the automatic welder operating on a horizontal work table. The fume generated was collected by high-volume air sampler. The sampler was fitted with 20 cm x 25 cm glass fiber filter paper.

3.4.10 Lund University Fume Hood[16]

A fume hood developed at Lund University in The Netherlands has been used to characterize welding fume emissions. A skilled welder maintained constant welding conditions for SMAW, and a fixed torch and workpiece mounted on a rail-operated wagon was used to evaluate the GMAW method.

The fume generated was drawn through an aluminum hood shown in Figure 3-9. A Battelle-type single orifice cascade impactor drawing 1 L/min was used to determine particle size distribution. A glass fiber filter sampled the fume to determine total mass emissions. A membrane filter was used to obtain a sample suitable for the determination of elemental composition.

3.4.11 Modified Stack Sampling Technique[17]

In the modified stack sampling technique, a duct (Figure 3-10) is placed over a stationary welding torch to collect most of the fume generated. Welds are performed on a rotating workpiece. An inclined manometer measures duct velocity. A probe inserted into the duct is connected to a filter and sampling pump. The velocity of the probe is set to match the velocity of the duct (i.e., isokinetic sampling). Welding began and steady-state conditions were established before sampling started. Glass- fiber filters are used to determine fume generation rates and triacetate filters are used to collect fume for chemical analysis.

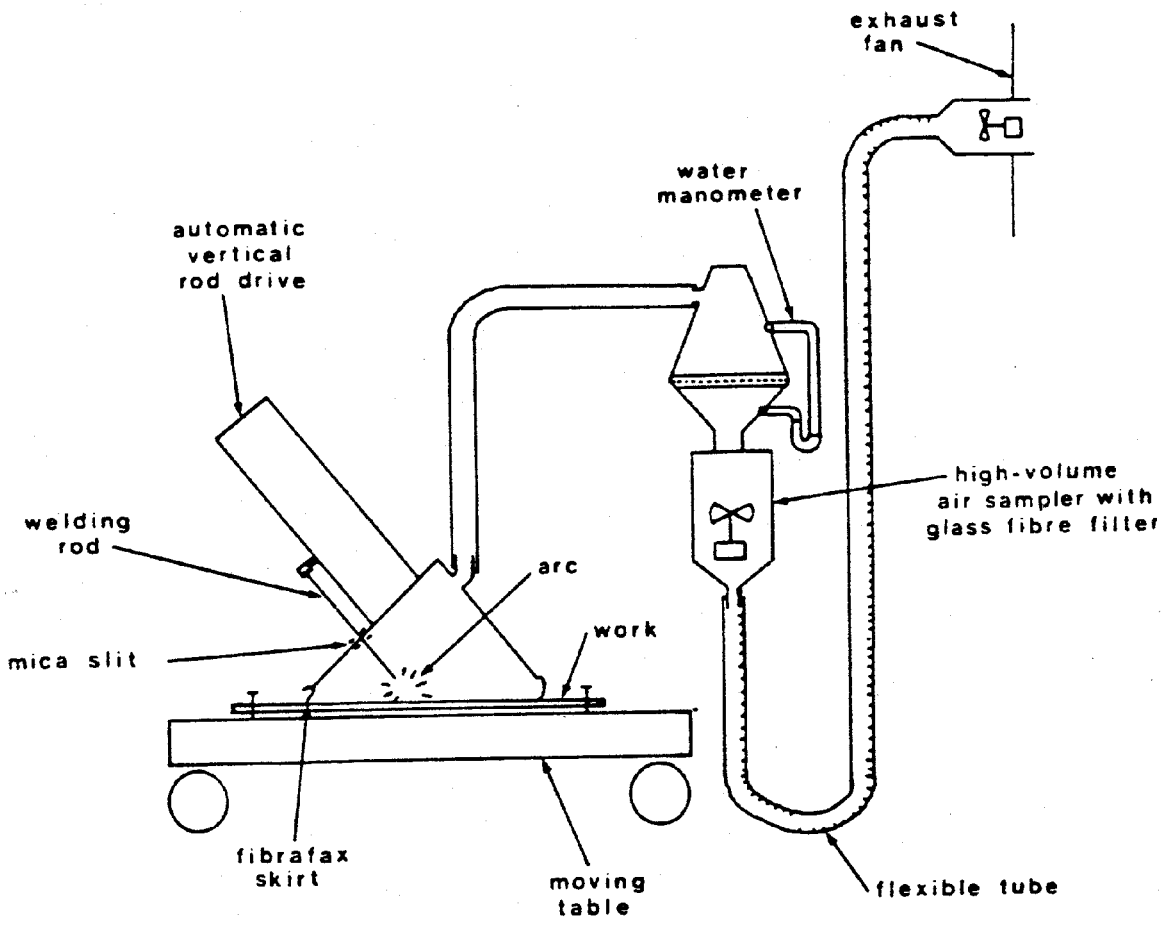

Figure 3-8. Schematic of the Australian welding and fume collection equipment.[14]

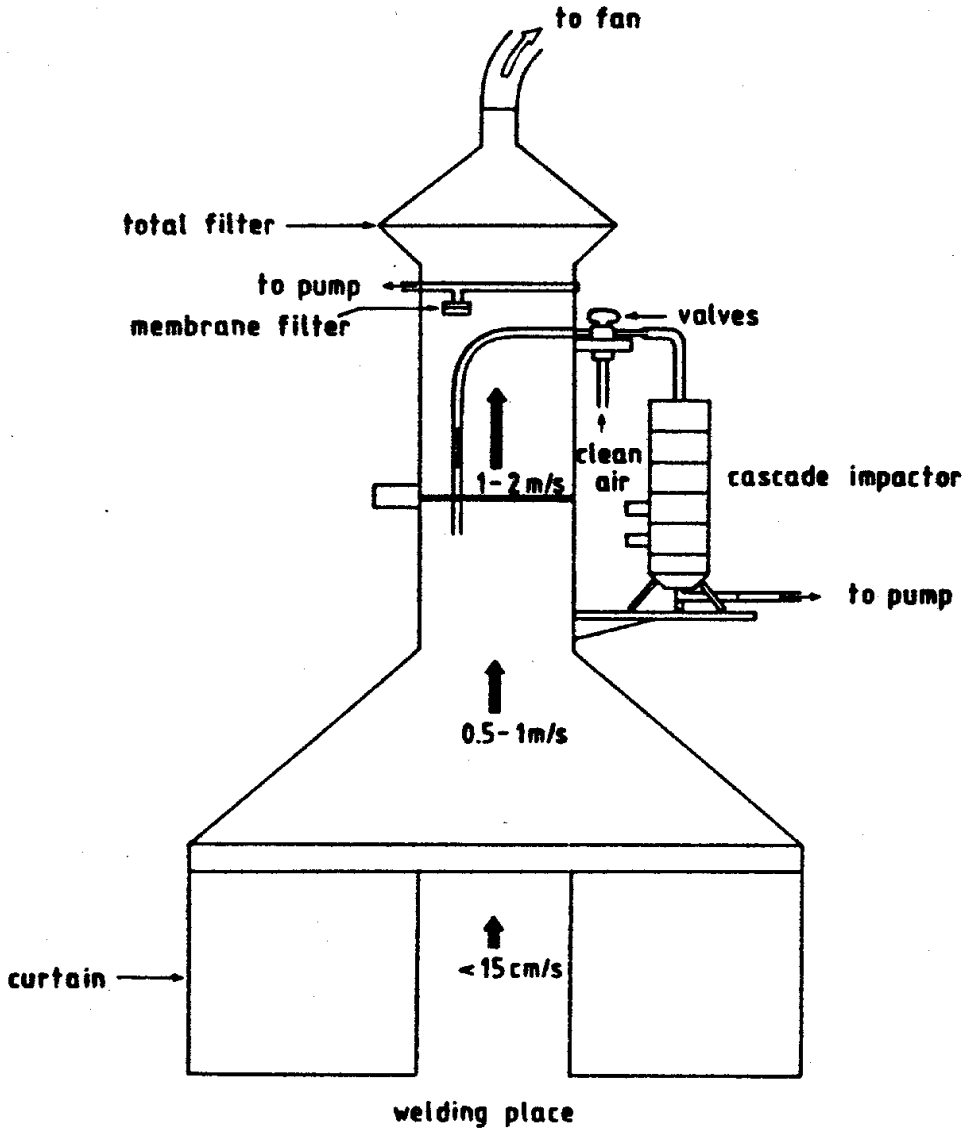

Figure 3-9. Lund University fume hood.[16]

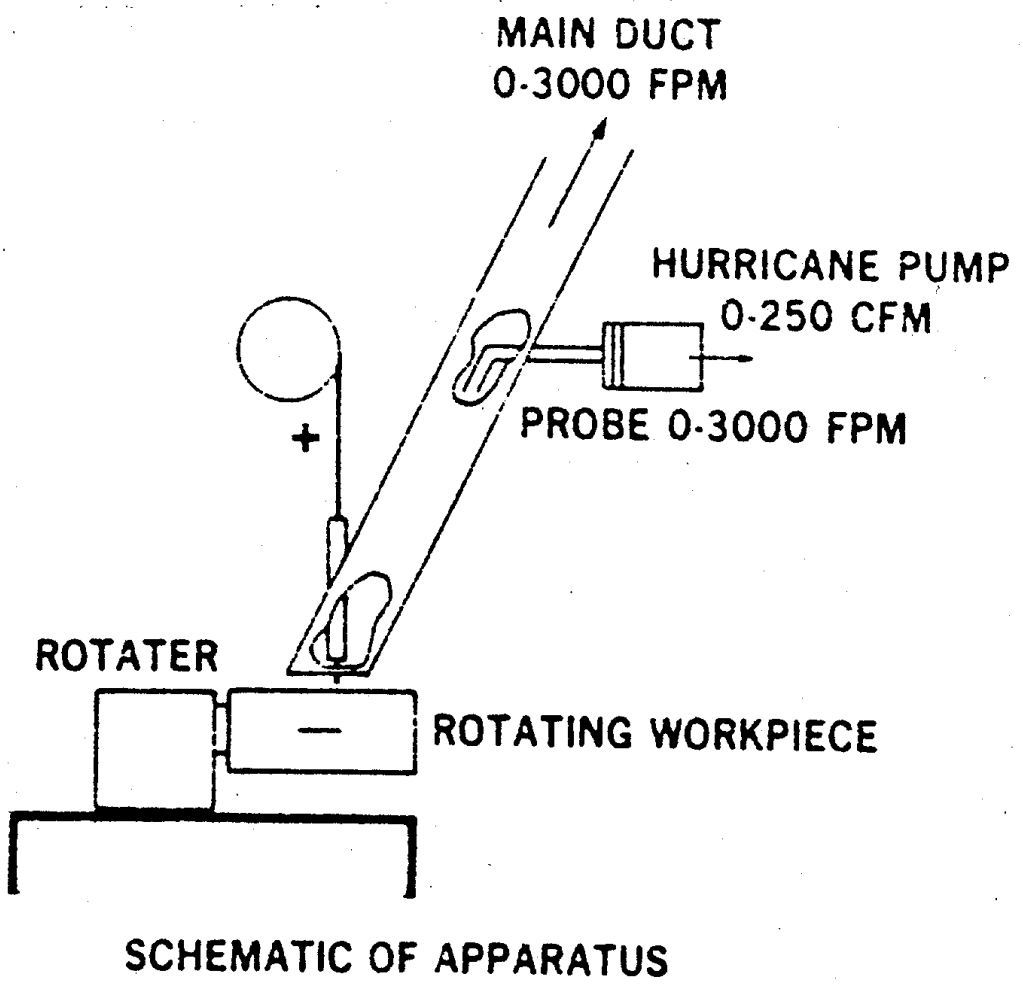

Figure 3-10. Diagram of modified stack sampling technique.[17]

3.4.12 BOHS Method[3,4]

The BOHS method was proposed by the British Occupational Hygiene Society (BOHS). The welder works in a enclosed room with a volume of approximately 20 m^3 in still air and no ventilation. The skilled welder lays down a single fillet weld in a mild steel workpiece using 300 mm of the electrode. Two minutes lapse to equilibrate the fume by a fan within the room, then the air is sampled using a high volume air sampler for 3 min.

3.4.13 Closed Environment[18]

Closed environment sampling has been performed to characterize welding fume. A polyvinyl chloride sheet is used to enclose the welding area up to the hood creating an area of 7 m^3 (Figure 3-11). After the welding process is completed, the environment is stirred up for 15 s with two small fans to obtain a homogeneous distribution of fumes and gases generated from welding. Sampling follows for 3 min from the breathing zone.

3.5 ANALYTICAL METHODS[19,20]

As stated above, particulate samples are normally collected on filter media for later chemical analysis. Of particular interest are heavy metals considered to be hazardous air pollutants (HAPs) under the Clean Air Act. These metals include: antimony (Sb); arsenic (As); beryllium (Be); cadmium (Cd); chromium (Cr); cobalt (Co); lead (Pb); manganese (Mn); mercury (Hg); nickel (Ni); and selenium (Se).

From the reviewed source tests, the most commonly used analytical methods are flame atomic absorption spectrometry and X-ray fluorescence. A brief description of these and several other common analytical methods are included in the following sections.

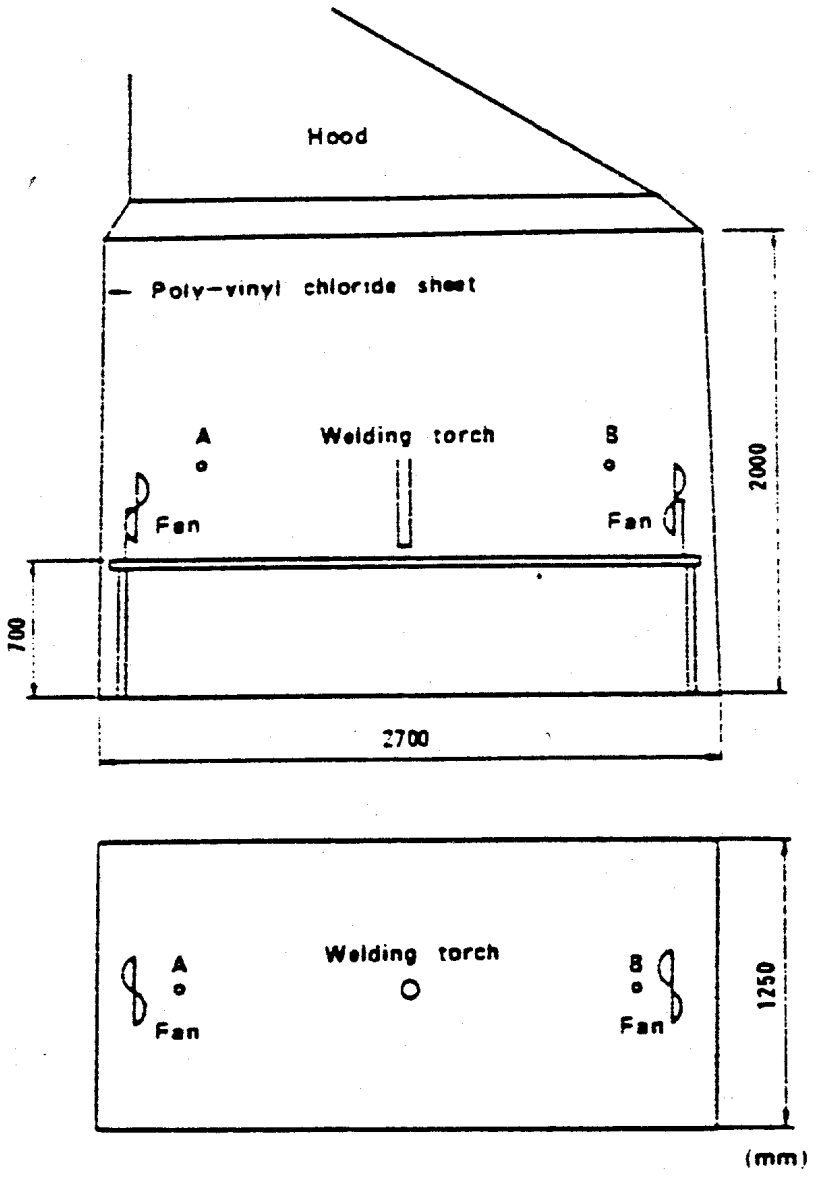

Figure 3-11. Closed environment for sampling of fumes and gases generated by welding.[18]

3.5.1 Inductively Coupled Plasma—Atomic Emission Spectrometry (ICP-AES)[21]

This analytical technique allows sequential or simultaneous quantitative analysis following acid digestion or dissolution of a number of elements in the parts-per-million to parts-per-billion range. An argon plasma is used to atomize or excite atoms to a higher state by collision with other atoms. These excited atoms *emit* their characteristic wavelength radiation as they return to a stable state. The emission of radiation at their characteristic wavelength is nearly proportional to the concentration of the element in the sample as compared to a known standard. This *quantitative* technique eliminates many elemental interferences as compared to using FAA and other methods.

3.5.2 Flame Atomic Absorption Spectrometry (FAA)[3,5,13,15,17,22,23,24]

In FAA, an energy source, such as a hollow cathode lamp, is used to atomize the sample following aspiration into the flame. The light energy *absorbed* at a characteristic wavelength is measured in units of absorbance and compared to the absorbance of a known standard. This *quantitative* technique is sensitive to sub-parts-per-million level for most elements following sample digestion.

3.5.3 X-Ray Fluorescence (XRF)[3,9,11,13,15,17,23]

This analytical technique involves the exposure of a specimen to an X-ray beam. The result is the *emission* of characteristic fluorescent line radiation for each element that is converted to electrical pulses presented as X-ray counts for quantitation. Due to X-ray spectra being quite simplistic, relatively few spectral interferences occur during analysis by XRF. Prior to analysis, the fume is typically fluxed and fused into a bead for analysis. Numerous interferences are common to XRF.

3.5.4 X-Ray Diffraction (XRD)[3,5,6,13,25]

XRD is a physical technique used to analyze crystalline compounds. Specimens are ground to a homogeneous powder or a single crystal may be radiated with the X-ray beam. This produces a unique diffraction pattern for each compound, which may be recorded photographically or electronically and compared to known catalogued patterns. The intensity and spacing of the diffraction angle (based on the wavelength) are the most important criteria in determining the compound(s) present. Problems in

qualitative identification of the diffraction patterns arise when several compounds are present in a single specimen.

3.5.5 Ion Specific Electrode[3,13,15]

Ion specific electrodes are used to measure ion activity within the sample dissolved in a liquid relative to the ion exchange process. Activity is a concentration indicator, which in dilute solutions approaches the ion concentration. The resulting ion activity (mV) reading from an ion specific electrode is compared to that of a calibration curve of known activity for evaluation purposes. Interferences can be quite apparent due to differences at phase boundaries and due to ion complexes with other free ions, which will decrease signal strength.

3.5.6 Flame Emission Spectroscopy[3]

This type of analysis is similar to ICP-AES in theory, but it uses thermal energy produced by the flame to excite the atoms to higher energy states. Upon returning to ground state, energy is *emitted* at the characteristic wavelength. Standards of known concentration are used as a reference to determine elemental concentration in samples. Due to the lower energy level of the flame as compared to the plasma, this technique is useful only for strongly emitting species.

REFERENCES FOR SECTION 3

1. *Technical Procedures for Developing AP-42 Emission Factors and Preparing AP-42 Sections*. EPA-454/B-73-050, U.S. Environmental Protection Agency, Office of Air Quality Planning and Standards, Research Triangle Park, North Carolina, October 1993.

2. American National Standards Institute, *Laboratory Method for Measuring Fume Generation Rates and Total Fume Emission of Welding and Allied Processes*, American Welding Society, Miami, Florida, January 25, 1985.

3. N. Jenkins et al., *Welding Fume, Sources*Characteristics*Control*, Volumes 1-3, The Welding Institute, Abington Hall, Cambridge, England, 1981.

4. P. J. Oakley, "Ways to Measure Rates of Fume Emission," *Welding Design and Fabrication*, 52:11, 74-76, November 1979.

5. R. M. Evans et al., *Fumes and Gases in the Welding Environment*, American Welding Society, Miami, Florida, 1979.

6. Battelle-Columbus Laboratories, *The Welding Environment, Parts IIA, IIB, and III*, American Welding Society, Miami, Florida, 1973.

7. H. Press and W. Florian, "Formation of Toxic Substances in Gas Shielded Arc Welding," *Welding in the World*, 23:1-23, 1985.

8. J. Moreton and R. V. Sharokes, "Fume Problems During Manual Metal-Arc Weld Surfacing," *Surfacing J. Inter.*, 1:4, 138-141, April 1986.

9. J. Moreton et al., "Fume Emission When Welding Stainless Steel," *Metal Construction*, 17:12, 794-798, December 1985.

10. J. Moreton, "Fume Emission Rates for Open-Arc Welding Processes," *Metal Construction*, 17:5, 308-310, May 1985.

11. I. D. Henderson et al., "Fume Generation and Chemical Analysis of Fume for a Selected Range of Flux-Cored Structural Steel Wires," AWRA Document P9-44-85, *Australian Welding Research*, 15:4-11, December 1986.

12. D. E. Hilton and P. N. Plumridge, "Particulate Fume Generation During GMAW and GTAW," *Welding and Metal Fabrication*, 59:10, 555 & 557-558, December 1991.

13. R. K. Tandon et al., "Chemical Investigation of Some Electric Arc Welding Fumes and Their Potential Health Effects," *Australian Welding Research*, 13:55-60, December 1984.

14. R. K. Tandon et al., "Fume Generation and Melting Rates of Shielded Metal Arc Welding Electrodes," *Welding Journal*, 63:8, 263s-266s, August 1984.

15. R. K. Tandon et al., "Variations in the Chemical Composition and Generation Rates of Fume from Stainless Steel Electrodes Under Different AC Arc Welding Conditions," AWRA Contract 90, *Australian Welding Research*, 11:27-30, December 1982.

16. K. G. Malmqvist et al., "Process-Dependent Characteristics of Welding Fume Particles," Presented at the International Conference on *Health Hazards and Biological Effects of Welding Fumes and Gases*, Commission of the European Communities. World Health Organization and Danish Welding Institute, Copenhagen, Denmark, February 1985.

17. R. F. Heile and D. C. Hill, "Particulate Fume Generation in Arc Welding Processes," *Welding Journal*, 54:7, 201s-210s, July 1975.

18. Y. Sugiyama et al., "Fumes and Gases Generated in Inert Gas Metal Arc Welding of Aluminum and Its Alloys," in Proceedings of the *Colloquium on Aluminum and Its Alloys in Welded Construction*, Porto, Portugal, September 8, 1981.

19. H. Willard, L. Merritt, J. Dean, and F. Settle Jr., *Instrumental Methods of Analysis, 6th Edition*, Wadsworth Publishing Co., Belmont, California.

20. D. Skoog, D. West, *Principles of Instrumental Analysis*, Holt, Rinehart and Winston, Inc., 1971.

21. *Development of Environmental Release Estimates For Welding Operations*, EPA Contract No. 68-C9-0036, IT Corporation, Cincinnati, Ohio, 1991.

22. J. F. McIlwain and L. A. Neumeier, *Fumes from Shielded Metal Arc (MMA Welding) Electrodes*, RI-9105, U. S. Department of the Interior, Bureau of Mines, Rolla Research Center, Rolla, Missouri, 1987.

23. J. Moreton et al., "Fume Emission Rate Measurements and Fume Analysis on Four Stainless Steel Welding Consumables," in *Health Hazards and Biological Effects of Welding Fumes and Gases*, 61-64, 1986.

24. C. N. Gray et al., "The Effect of Oxygen on the Rate of Fume Formation in Metal Inert Gas Welding Arcs," in *Proceedings of the International Conference on Weld Pool Chemistry and Metallurgy*, London, England, April 1980.

25. E. J. Fasiska et al., *Characterization of Arc Welding Fume*, American Welding Society, Miami, Florida, February 1983.

SECTION 4

EMISSION FACTOR DEVELOPMENT

After a review and analysis of the data obtained during the background search, the following test data and methodology were used to develop the draft AP-42 section for welding operations. Excerpts from the various tests reports are contained in Appendices A through M.

4.1 REVIEW OF SPECIFIC DATA SETS

Some 52 reference documents were collected and reviewed during the literature search. These documents are listed in Table 4-1 and are marked with an asterisk to indicate that the report contains potentially useful emissions data.

Utilizing the criteria outlined in Section 3.1, the original group of documents were reduced to a final set of 12 primary reports. Table 4-2 summarizes the reason(s) for the rejection of those documents not used. The data contained in each of the primary references are discussed below. The test data are presented in the units in which they were originally published.

4.1.1 Reference 11 (1987)

In these tests, fumes were generated and collected in an enclosed chamber, similar to the Battelle fume collection chamber (see 3.4.3). Shielded metal arc electrodes E308-16, E310-16 stainless steel, ECoCr-A, ENiCl Ni, Mn-Cr buildup alloy, E7018 carbon steel, E11018-M low alloy steel, and FCAW electrode E11018-M were tested for fume generation rate and chemical constituents. Between 11 and 35 test runs were made for each electrode. Welding was performed on a base metal of mild steel.

TABLE 4-1. REFERENCE DOCUMENTS OBTAINED
DURING LITERATURE SEARCH

1. S. A. David and T. DebRoy, "Current Issues and Problems in Welding Science," *Science*, 257:497-502, July 24, 1992.
2. B. Irving, "Inverter Power Sources Check Fume Emissions in GMAW, *Welding Journal*, 53-57, February 1992.
3. D. E. Hilton and P. N. Plumridge, "Particulate Fume Generation During GMAW and GTAW," *Welding and Metal Fabrication*, 59:10, 555 & 557-558, December 1991.
4. L. Bauer, "How to Select Exhaust Equipment," *Welding Design and Fabrication*, 64:7, 27-31, July 1991.
5. J. Medack and B. Heinze, "The Emission and Composition of Welding Fumes Generated During the MAG Welding of Metal Coated Sheet," *Welding International*, 4:11, 908-910, November 1990.
6. H. C. Campbell, "Some Effects of Welding on Health," *Welding Journal*, 69:4, 85-86, April 1990.
7. G. C. Barnes, "Control of Fumes in the Welding Environment," *Svetsaren*, 1:16-18, 1990.
8. I. D. Henderson et al., "Fume Rates of Gas-Shielded and Open-Arc Wires for Hardfacing and Surfacing," AWRA Research Contract 105, *Australian Welding Research*, 16:44-46, December 1988.
9. National Institute for Occupational Safety and Health, *Criteria for a Recommended Standard Welding, Brazing, and Thermal Cutting*, Publication No. 88-110, U. S. Department of Health and Human Services, Cincinnati, Ohio, April 1988.
10. F. Nielbock, "MAG Welding of Galvanized Steel Sheets," *Strips Sheets Tubes*, 4:2, 39-42, February 1987.
11.* J. F. McIlwain and L. A. Neumeier, *Fumes from Shielded Metal Arc (MMA Welding) Electrodes*, RI-9105, U.S. Department of the Interior, Bureau of Mines, Rolla Research Center, Rolla, Missouri, 1987.
12.* I. D. Henderson et al., "Fume Generation and Chemical Analysis of Fume for a Selected Range of Flux-Cored Structural Steel Wires," AWRA Document P9-44-85, *Australian Welding Research*, 15:4-11, December 1986.
13. J. Moreton and R. V. Sharokes, "Fume Problems During Manual Metal-Arc Weld Surfacing," *Surfacing J. Inter.*, 1:4, 138-141, April 1986.
14. S. G. Epstein et al., "Studies of Chemical and Physical Emissions from Aluminum Alloys," in Proceedings of the *Aluminum Joining Seminar*, Metairle, Louisiana, February 1986.
15.* K. G. Malmqvist et al., "Process-Dependent Characteristics of Welding Fume Particles," in *Health Hazards and Biological Effects of Welding Fumes and Gases*, R. M. Stern et al. eds., Excerpta Medica, Amsterdam, 1986, 31-46.
16. R. Eichhorn and T. H. Oldenburg, "Welding Fumes Emitted During Welding of High-Alloyed Materials--Evaluation of Amount, Chemical Composition and Morphology, Including the Influence of Welding Parameters," in *Health Hazards and Biological Effects of Welding Fumes and Gases*, R. M. Stern et al. eds., Excerpta Medica, Amsterdam, 1986, 51-54.
17. G. P. Gambaretto and G. Rausa, "Pollution Caused by Hand Arc Electric Welding," in *Health Hazards and Biological Effects of Welding Fumes and Gases*, R. M. Stern et al. eds., Excerpta Medica, Amsterdam, 1986, 55-59.
18. J. Moreton et al., "Fume Emission Rate Measurements and Fume Analysis on Four Stainless Steel Welding Consumables," in *Health Hazards and Biological Effects of Welding Fumes and Gases*, R. M. Stern et al. eds., Excerpta Medica, Amsterdam, 1986, 61-64.

19. J. F. K. Froats et al. "Work Exposure to Welding Fumes and Gases During Hydraulic Plant Turbine Repair," in *Health Hazards and Biological Effects of Welding Fumes and Gases*, R. M. Stern et al. eds., Excerpta Medica, Amsterdam, 1986, 137-140.

20. G. Casciani et al., "Welding Fumes Concentration in Heavy Carpentry Working Environment and Trial to Correlate Same with Gas and Powdered Fluorides," in *Health Hazards and Biological Effects of Welding Fumes and Gases*, R. M. Stern et al. eds., Excerpta Medica, Amsterdam, 1986, 153-157.

21.* J. Moreton et al., "Fume Emission When Welding Stainless Steel," *Metal Construction*, 17:12, 794-798, December 1985.

22. D. Northcote, "The GMA Welding Process. Ferritic Steels. An Evaluation: Solid Electrode Wires vs. Flux Cored Electrode Wires," *Australian Welding Journal*, 30:1, 9-11, Autumn 1985.

23. A. P. Glovatyuk and O. G. Levchenko, "Parameters of Mass Generation of Welding Aerosols and Their Use in Practice," *Welding Production*, 32:10, 42-44, October 1985.

24. J. Moreton, "Fume Emission Rates for Open-Arc Welding Processes," *Metal Construction*, 17:5, 308-310, May 1985.

25. A. P. Glovatyuk et al., "Rate of Formation of Aerosols During Manual Welding with Modulated Current," *Automatic Welding*, 38:2, 37-38, February 1985.

26. American National Standards Institute, *Laboratory Method for Measuring Fume Generation Rates and Total Fume Emission of Welding and Allied Processes*, American Welding Society, Miami, Florida, January 25, 1985.

27. H. Press and W. Florian, "Formation of Toxic Substances in Gas Shielded Arc Welding," *Welding in the World*, 23:1-23, 1985.

28.* R. K. Tandon et al., "Chemical Investigation of Some Electric Arc Welding Fumes and Their Potential Health Effects," *Australian Welding Research*, 13:55-60, December 1984.

29.* R. K. Tandon et al., "Fume Generation and Melting Rates of Shielded Metal Arc Welding Electrodes," *Welding Journal*, 63:8, 263s-266s, August 1984.

30. P. R. M. Dare and P. J. Hewitt, "Welding Fume: The Problems of Comparing Electrodes," *Welding and Metal Fabrication*, 52:2, 56-57, March 1984.

31. K. Houghton and P. Kuebler, "Consider a Low Fume Process for Higher Productivity," Paper 21 in *Proceedings, Joint Australasian Welding and Testing Conference*, Australian Welding Institute and Australian Institute for Nondestructive Testing, Perth, 1984.

32. M. E. Reinders, *Handbook of Emission Factors, Part 2, Industrial Sources*, Government Publishing Office, The Hague, Netherlands, 1984.

33. American Welding Society, *Filler Metal Comparison Charts*, American Welding Society, Miami, Florida, 1986.

34.* E. J. Fasiska et al., *Characterization of Arc Welding Fume*, American Welding Society, Miami, Florida, February 1983.

35. G. H. G. McMillan, "The Health of Welders in Naval Dockyards: Final Summary Report," *J. Roy. Nav. Med. Serv.*, 69:125-131, 1983.

36.* R. K. Tandon et al., "Variations in the Chemical Composition and Generation Rates of Fume from Stainless Steel Electrodes Under Different AC Arc Welding Conditions," AWRA Contract 90, *Australian Welding Research*, 11:27-30, December 1982.

37. H. Press and W. Florian, "An Investigation of the Production of Foreign Substances During Shielded-Arc Welding--TIG Welding of Alloy Steel and Aluminum Alloys," *Schweisen und Schneidan (Translation)*, 34:9, 437-440, September 1982.

38. C. N. Gray and P. J. Hewitt, "Control of Particulate Emissions from Electric-Arc Welding by Process Modification," *Ann. Occupy. Hyg.*, 25:4, 431-438, 1982.

39. I. S. Alekseeva et al., "Evaluation of the Health Aspects of the TIG Welding of Copper in Nitrogen," *Welding Production*, 28:10, 35-36, October 1981.

40. B. W. Goodwin and R. J. Wiseman, "Semi-Automatic Welding in Heavy Construction," in *Proceedings of the 2nd Joint AWI/NZIW Welding Convention*, Christchurch, New Zealand, October 12-16, 1981.

41. Y. Sugiyama et al., "Fumes and Gases Generated in Inert Gas Metal Arc Welding of Aluminium and Its Alloys," in Proceedings of the *Colloquium on Aluminium and Its Alloys in Welded Construction*, Porto, Portugal, September 8, 1981.

42. N. Jenkins et al., *Welding Fume, Sources*Characteristics*Control*, Volumes 1-3, The Welding Institute, Abington Hall, Cambridge, England, 1981.

43. C. N. Gray et al., "The Effect of Oxygen on the Rate of Fume Formation in Metal Inert Gas Welding Arcs," in *Proceedings of the International Conference on Weld Pool Chemistry and Metallurgy*, London, England, April 1980.

44. I. W. Head and S. J. Silk, "Integral Fume Extraction in MIG/CO_2 Welding," *Metal Construction*, 11:12, 633-638, December 1979.

45. P. J. Oakley, "Ways to Measure Rates of Fume Emission," *Welding Design and Fabrication*, 52:11, 74-76, November 1979.

46.* R. M. Evans et al., *Fumes and Gases in the Welding Environment*, American Welding Society, Miami, Florida, 1979.

47. *Criteria for a Recommended Standard . . . Occupational Exposure to Inorganic Nickel*, National Institute for Occupational Safety and Health, DHEW (NIOSH) Publication No. 77-164, U. S. Department of Health, Education, and Welfare, Cincinnati, Ohio, May 1977.

48.* R. F. Heile and D. C. Hill, "Particulate Fume Generation in Arc Welding Processes," *Welding Journal*, 54:7, 201s-210s, July 1975.

49. National Institute for Occupational Safety and Health, *Criteria for a Recommended Standard . . . Occupational Exposure to Chromium (VI)*, HEW (NIOSH) Publication No. 76-129, U. S. Department of Health, Education, and Welfare, Cincinnati, Ohio, 1975.

50.* Battelle-Columbus Laboratories, *The Welding Environment*, Parts IIA, IIB, and III, American Welding Society, Miami, Florida, 1973.

51.* *Development of Environmental Release Estimates For Welding Operations*, EPA Contract No. 68-C9-0036, IT Corporation, Cincinnati, Ohio, 1991.

52. *Welding Handbook, Welding Processes, Volume 2, Eighth Edition*, American Welding Society, Miami, Florida, 1991.

* Indicates potential sources of useful emissions data.

TABLE 4-2. DOCUMENTS NOT INCLUDED IN EMISSION FACTOR DEVELOPMENT

Reference No.	Cause for rejection
1	No emission test data.
2	No emission test data.
3	Cannot derive emission factor—emission rate data only.
4	No emission test data.

Reference No.	Cause for rejection
5	Insufficient information to determine emission factor.
6	Not original source of test data.
7	Not original source of test data.
8	Insufficient analytical description.
9	No emission test data.
10	Insufficient process description.
13	Not original source of test data.
14	No emission test data.
16	Insufficient process description.
17	Insufficient process description.
18	Same source test as Reference 21
19	Insufficient information to determine emission factor.
20	Insufficient information to determine emission factor.
22	Not original source of test data.
23	Insufficient process description.
24	Not original source of test data.
25	Insufficient process description.
26	No emission test data.
27	Insufficient process description.
30	No emission test data.
31	Not original source of test data.
32	Not original source of test data.
33	No emission test data.
35	No emission test data.
37	Insufficient information to determine emission factor.
38	No emission test data.
39	Insufficient process and analytical description.
40	Not original source of test data.
41	Insufficient process and analytical description.
42	Not original source of test data.
43	Insufficient information to determine emission factor.
44	No emission test data.
45	No emission test data.
47	No emission test data.
49	No emission test data.
52	No emission test data.

Two layers of 0.5 in (1.27 cm) thick fiberglass aircraft insulation were situated at the top of the chamber to collect fume for weight determination. Fume for chemical analysis was collected on Whatman No. 4 cellulose filters, backed by one layer of the glass material.

All procedures for collecting the fume followed ANSI Standard F1.2-79. Seven elemental compounds were analyzed using AAS, while titanium was analyzed colorimetrically. A summary of the test results appear below.

TABLE 4-3. SUMMARY DATA FROM REFERENCE 11

Welding process	Electrode type	Total fume emission factor (g/kg electrode)	Wt % HAP in fume[a]		
			Cr	Mn	Ni
SMAW	E308-16	10.9	–	–	–
	E310-16	15.1	–	–	–
	ECoCr-A	27.9	–	–	–
	ENiCl	18.8	–	–	–
	14Mn-4Cr	81.6	1.7	28.4	2.1
	E7018	17.7	–	6.4	–
	E11018-M	17.5	–	7.9	–
FCAW	E11018-M	57	1.7	24.5	–

[a] HAP = hazardous air pollutant as defined by the 1990 Clean Air Act Amendments.
Wt. % = weight percent of element measured in the total fume collected.

Upon review of Reference 11, it was found that a generally sound test methodology was used; however, a questionable type of filter media was used to collect the samples. Therefore, data were assigned a rating of C. Applicable portions of Reference 11 are included in Appendix A.

4.1.2 Reference 12 (1986)

Reference 12 reports the collected fume results from a range of nine classified wires using the flux cored arc welding (FAW) process. An Australian Welding Research chamber (Section 3.4.2), similar to the Swedish Fume Box, provided the

apparatus. An electrostatically assisted, felt filter system made from polyester fibers collected the fume. The base metal welded was not specified.

Test runs ranged from 10 s to 60 s. The voltage was kept constant and the current varied from 120 amps to 550 amps. The travel speed was recorded and varied from 110 mm/min to 675 mm/min. Fume analysis was performed by XRF.

The results presented in tables and on individual graphs show that gasless, wire-type electrodes have higher fume generation rates than the gas-shielded wires tested. A summary of the test results is shown in Table 4-4 below.

TABLE 4-4. SUMMARY DATA FROM REFERENCE 12

Welding process	Electrode type	Total fume emission factor (g/kg electrode)	Wt % HAP in fume[a]		
			Cr	Mn	Ni
FCAW	E70 T-1	7.3-12.0	0.01-0.04	7.2-13.5	0.03-0.08
FCAW	E71 T-1	7.3-13.4	0.01-0.03	7.8-13.5	0.03-0.06
FCAW	E70 T-G	4.7-9.8	0.01-0.03	13.3-15.6	0.03-0.65
FCAW	E70 T-2	9.8-11.9	0.01	10.5	0.02
FCAW	E70 T-4	14.6-26.0	0.01	0.7-1.9	0.02-0.06
FCAW	E70 T-5	8.8-22.3	0.01-0.03	7.7-12.0	0.01-0.04
FCAW	E70 T-7	23.0-41.0	0.01-0.15	0.74-0.76	0.03-0.04
FCAW	E110 T5-K3	20.8	0.01	9.7	0.54
FCAW	E71 T-11	17.0-21.0	0.01	1.2	0.03

[a] HAP = hazardous air pollutant as defined by the 1990 Clean Air Act Amendments.
Wt. % = weight percent of element measured in the total fume collected.

The test methods and analytical methods for the report proved to be sound and well defined. Because the report lacked the information necessary to verify results, the test data were given a B rating. A copy of the documents is provided in Appendix B.

4.1.3 Reference 15 (1986)

Reference 15 reports the results of tests conducted on 12 different electrodes and different welding processes, SMAW and GMAW. The Lund University fume hood (Section 3.4.10), which is similar to the Swedish Fume Box, was used as the test system. The fume was collected on a glass fiber filter and the air velocity near the welding point was < 0.15 m/s. The fume was collected for chemical analysis with a membrane filter arrangement and particle sizing was performed with a cascade impactor.

Particle Induced X-ray Emission (PIXE) was used in the tests for analytical quantitation of various metallic elements of interest. A special procedure was developed to determine the mass of soluble and less soluble Cr(III) and Cr(VI), which included PIXE, electron spectroscopy, a spectrophotometric method, and transmission electron microscopy.

A skilled welder performed the welding on a base metal of stainless steel while three to five samples were taken for each set of welding conditions. For shielding gas in the GMAW process, CO_2 was used for one electrode, an Ar/CO_2 mix for one electrode, and Ar for the other three GMAW electrodes. The fume generation in mass of fume per time, mass of fume per mass of electrode used, and the percentage composition for 16 elements are reported in tabular format. The mass median aerodynamic diameters were calculated and compared to past studies. A summary of the test results is presented in Table 4-5 below.

TABLE 4-5. SUMMARY DATA FROM REFERENCE 15

Welding process	Electrode type	Total fume emission factor (g/kg electrode)	Wt % HAP in fume				
			Cr	Cr VI	Mn	Ni	Pb
SMAW	E7028	15.7-21.7	0.07	–	2.8-5.9	–	0.07-0.10
SMAW	E7018	26	0.04	–	3.7	–	–
SMAW	E308 L-15	11.3	3.4	1.7	2.4	0.22	–
SMAW	E316 - 15	15.6	3.1	2.3	2.7	0.24	0.03
SMAW	OK 69.21[b]	12.4	3.0	1.6	14.0	0.44	0.04
GMAW	E70 S-6	5.4	0.07	–	7.3	–	–
GMAW	ER316 I-Si	3.8-5.7	10.0-12.0	0.2	4.8-5.3	4.8	–
GMAW	ER 1260	20.5	0.02	–	–	–	–
GMAW	ER 5154	24.1	0.04	–	0.14	–	–

[a] HAP = hazardous air pollutants as defined by the 1990 Clean Air Act Amendments. Wt. % = weight percent of element measured in the total fume collected.
[b] Swedish electrode designation (no AWS designation available).

Upon review of Reference 15, it was found that sound methodology was used during the testing and elemental analyses conducted. Since the source test report is an original

summary, insufficient information was available to verify the reported data; therefore, the data were given a rating of B. A copy of the test report is provided in Appendix C.

4.1.4 Reference 21 (1985)

Reference 21 focused on the welding of stainless steel. Several welding processes were measured using the Welding Institute fume box (Section 3.4.5) to collect the fume: manual metal arc welding (now SMAW), metal active gas welding (now GMAW) electrode with Ar-2%O_2 shielding gas, flux cored (FCAW) wire self-shielded electrode, and metal cored wire (now GMAW) gas shielded electrode.

Horizontal-vertical fillet welds were performed on 250 x 50 x 10 mm, 316 stainless steel test-pieces in the Welding Institute fume box. The fume was collected on 240-mm diameter, preweighed glass fiber filters. The voltage was held constant, and the current varied from 145 to 290 amps. The gas flow was maintained at 16 L/min.

Fume analyses included: pyro-hydrolysis for fluorine; alkaline extraction and *s*-diphenyl carbazide colorimetric finish for total hexavalent chromium; emission spectrophotometry for sodium and lithium; and XRF for the 16 other elements. Fume generation rates were presented in mass of fume per mass of electrode deposited and mass of fume per time. The results of the tests were presented in both tabular and graphical form. A summary of test results appears in Table 4-6.

Upon review of Reference 21, it was found that the test method used was similar to the AWS/ANSI standard and that a sound analytical methodology was employed. However, the test report contains only summary data; therefore, the data were given a rating of C. A copy of the documents is provided in Appendix D.

TABLE 4-6. SUMMARY DATA FROM REFERENCE 21

Welding process	Electrode type	Total fume emission factor[a] (g/kg electrode)	Wt % HAP in fume[b]			
			Cr	Cr VI	Mn	Ni
SMAW (MMA)	E316L-16	7.3-8.8	5	4.1	5	0.4
GMAW (MAG)	ER316L Si	3.9-4.1	13.4	0.2	12.6	4.9
FCAW (FCW)	E316LT-3	4.6-5.8	5.1	2.7	4.8	4.7
GMAW (MCW)	E316LT1,2,3	3.0-4.0	11.7	0.2	9.3	4.7

[a] Data from the presented graph.

[b] HAP = hazardous air pollutant as defined by the 1990 Clean Air Act Amendments. Wt. % = weight percent of element measured in the total fume collected.

4.1.5 Reference 28 (1984)

Reference 28 used the Australian automatic welder (Section 3.4.9) and five different electrode types to generate and collect fumes for metal analysis. All electrodes were used to weld 8-mm mild steel at a travel speed of 150 mm/min. The fumes were collected on glass fiber substrates and analyzed using XRF, XRD, atomic absorption, spectrophotometry, ion selective electrodes, and ion chromatography. The percentage of 19 elemental compounds found in the fume are presented in tabular form. The Hazardous Air Pollutants tested included Cr, Cr VI, Mn, and Ni. A summary of the analytical data is presented in Table 4-7 below. No emission factors were determined in the study.

TABLE 4-7. SUMMARY DATA FROM REFERENCE 28

Welding process	Electrode type[a]	Wt % HAP in fume[b] Cr	Cr VI	Mn	Ni
SMAW	(E01)	2.50	2.70	4.6	0.04
SMAW	E9018-G	0.03	0.03	5.0	0.20
SMAW	E9015-B3	0.50	0.60	3.9	0.02
SMAW	(E11)	0.05	0.03	26.1	1.40
SMAW	(E12)	4.70	1.70	6.5	0.04

[a] Australian Welding Research classification of electrodes.
[b] Determined using X-ray fluorescence spectroscopy. HAP = hazardous air pollutant as defined by the 1990 Clean Air Act Amendments.
Wt. % = weight percent of element measured in the total fume collected.

The tests described in Reference 28 varied slightly from the AWS/ANSI standard method. Although the tests used sound analytical methods, insufficient information was presented on the test protocol and the only data presented were in the form of summary tables. Therefore the data were assigned a rating of D. A copy of Reference 18 is provided in Appendix E.

4.1.6 Reference 29 (1984)

In Reference 29, the Australian automatic welding and fume collection system were used to measure the fume from five different electrode types using SMAW. Tests were performed with both an AC and DC power supply using the recommended optimal power setting. The electronic controller maintained a constant preset voltage, operated the horizontal drive table at 150 mm/min, operated the power supply, and displayed the voltage and current. An airflow of approximately 16 L/s was used. Glass fiber filters collected the fume sample for gravimetric analysis.

Graphs of fume formation rates in mass of fume per mass of electrode were provided for the electrodes at various power levels for DC and AC current. Results showed that AC and DC welding generated approximately the same fume rates when operated at the same power level. A summary of data collected in the study is presented in Table 4-8 below.

TABLE 4-8. SUMMARY DATA FROM REFERENCE 29

Welding process	Electrode type	Total fume emission factor (g/kg electrode)[a]
SMAW	(E01) 1855A4[b]	26-55
SMAW	E9018 G	15-25
SMAW	E9015 B3	10-22
SMAW	(E11) 1215A4	35-70
SMAW	(E12) 2355A1	40-75

[a] Range from presented graph.

[b] Australian Welding Research classification of electrodes.

Review of Reference 29 showed that the method varied substantially from the ANSI/AWS welding chamber technique. In addition, the only data presented were two summary graphs; therefore, the data were assigned a rating of D. A copy of the test report is provided in Appendix F.

4.1.7 Reference 34 (1983)

Reference 34 used the ANSI/AWS F1.1-79 standard method (see Section 3.4.1) with a conical chamber to sample six different types of electrodes for fume composition. Nuclepore filter samples were collected for analysis, which provided data from individual fume particles. Sample analysis was performed by energy dispersive X-ray analysis, XRD, automated electron beam analysis, gas chromatography-mass spectrometry, and scanning transmission electron microscopy.

The analytical data presented fume composition and particle sizing results. The average particle size for welding fumes ranged from 0.14 to 0.33 µm in physical diameter. No emission factors were presented in the reference. A summary of the analytical data is presented in Table 4-9 below.

TABLE 4-9. SUMMARY DATA FROM REFERENCE 34

		% HAP in fume[a]	
Welding process	Electrode type	Cr	Mn
SMAW	E6010	–	4.0
SMAW	E7018	–	4.6
GMAW	E70S - 3	–	7.8
FCAW	E70T - 1	–	11.1
SMAW	E308 - 16	5.6	6.2
GMAW	E5356	–	5.4

[a] HAP = hazardous air pollutant as defined by the 1990 Clean Air Act Amendments.
Wt. % = weight percent of element measured in the total fume collected.

After review of Reference 34, it was found that the test report lacked a detailed description of the test method. Although the test followed AWS standard method F1.1-79, no information was provided on the testing conditions. Due to the lack of background and test information, the data were given a D rating. A copy of the test report is provided in Appendix G.

4.1.8 Reference 36 (1982)

Reference 36 used an Australian automatic welding and fume collection system to determine the emissions for SMAW using a AWS A5.4 E316L-16 electrode. The welding was performed on 304 stainless steel base metal. During testing, the current varied from 80 amps to 120 amps, and voltage varied between 20 V and 40 V.

The fume, which generated from two to four electrodes, was collected on the paper filter, dried, weighed, and analyzed using atomic absorption spectroscopy. Results provided the mass of fume collected per mass of electrode used and the percent composition of 10 elemental compounds. The report stated that replicate values on fume generation were within ±5% of each other. A summary of test results are presented in Table 4-10 below.

TABLE 4-10. SUMMARY DATA FROM REFERENCE 36

Welding process	Electrode type	Total fume emission factor (g/kg electrode)[a]	Wt % HAP in fume[b]		
			Cr	Mn	Ni
SMAW	E316L-16	6-22	3.0-6.0	3.0-4.0	0.6-1.0

[a] Range from presented graph

[b] HAP = hazardous air pollutant as defined by the 1990 Clean Air Act Amendments.
Wt. % = weight percent of element measured in the total fume collected.

Upon review of Reference 36, it was found that the test method varied substantially from the accepted ANSI/AWS technique. Since the only data presented were two summary graphs, the data were assigned a rating of D. A copy of Reference 36 is provided in Appendix H.

4.1.9 Reference 46 (1979)

Reference 46 is a detailed laboratory investigation of the fume generation characteristics of representative electrodes for the following processes: SMAW, FCAW, GMAW, and GTAW. Testing was performed in a clean room with controlled humidity. The square Battelle fume chamber (see Section 3.4.3) was used for testing 38 different electrode types. Voltage was kept constant, and current was operated at recommended levels for each electrode, which ranged from 110 amps to 485 amps.

Samples were collected on prefilters and glass fiber absolute filters for determination of fume weight and on cellulose membrane filters for elemental analysis. All samples were collected in triplicate and showed little variation in the sample weight collected. Atomic absorption analysis was the primary analytical technique used in detecting elemental fume constituents. A summary of test results is presented in Table 4-11 below.

TABLE 4-11. SUMMARY DATA FROM REFERENCE 46

Welding process	Electrode type	Total fume emission factor (g/kg electrode)	Wt % HAP in fume[a]		
			Cr	Mn	Ni
SMAW	E6010	35.85	–	3.0-3.9	–
SMAW	E6013	14.16-25.75	–	4.1-5.1	–
SMAW	E7018	20.35-21.85	–	3.6-4.5	–
SMAW	E7024	8.92-11.11	0.01	5.3-7.8	–
SMAW	E8018 C3	15.92-17.89	0.1	7.2	0.3
SMAW	E9018 B3	11.19-14.94	1.6	5.9	0.1
SMAW	E316-15	8.02-11.08	1.6	7.7	1.1
SMAW	E316-16	6.56-11.92	6.5	8.8	1.5
SMAW	E410-16	11.75-13.97	5.0-10.0	5.2	0.1
SMAW	ENi-CI	12.90	–	0.3	6.9
SMAW	ENi-Cu-2	10.08	–	2.1	4.2
SMAW	ERNiCrMo-3 (Inconel 625)	9.24	5.9	4.6	–
SMAW	ENiCrMo-4 (Haynes C-276)	14.20	2.5	0.3	1.1
SMAW	Haynes 25	8.94	6.9	4.6	1.8
FCAW	E70T - 1	6.65-17.51	–	6.2-13.5	–
FCAW	E70T - 4	12.76-13.86	–	1.0-4.6	–
FCAW	E70T - 5	17.87-23.63	–	10.9-11.3	–
FCAW	81-C3	8.69	–	–	–
FCAW	91 - B3	8.42	–	–	–
FCAW	E308LT - 3	9.11	–	–	–
FCAW	E316LT - 3	6.97-12.32	12.5	7.3	1.06
			–	–	–
GMAW	E70S - 3	3.09-8.34	–	3.4-6.8	–
GMAW	E70S - 5	2.61-5.01	–	5.8	–
GMAW	ER316	0.58	–	–	–
GMAW	ERNiCu - 7	2.02	0.01	1.1	22.1

TABLE 4-11 (Continued)

Welding process	Electrode type	Total fume emission factor (g/kg-electrode)	Wt % HAP in fume[a] Cr	Mn	Ni
GMAW	ERNiCrMo-3 (Inconel 625)	0.87	15.4		27.2
GMAW	Haynes 25	1.38	14.9	15.4	7.1
GMAW	ENiCrMo-4 (Haynes C-276)	6.98	8.2	1	32.5

[a] HAP = hazardous air pollutant as defined by the 1990 Clean Air Act Amendments. Wt. % = weight percent of element measured in the total fume collected.

Sound methodology was used in Reference 46, and it contains excellent documentation of test procedures, results, and raw data collected. The data were assigned a rating of A. Applicable portions of the test report are provided in Appendix I.

4.1.10 Reference 48 (1975)

Reference 48 gives the results of tests conducted using a modified stack sampling technique on various welding methods. Ferrous material electrodes were used for SMAW, including cellulosic type, rutile type, rutile-iron powder type, and low hydrogen type. The FCAW samples used a rutile-base electrode with CO_2 shielding gas, a silica-base electrode with CO_2 shielding gas, and a fluorspar-base electrode with no shielding gas. The GMAW process used rutile-base flux, fluorspar-base flux, silica-base flux with CO_2 shielding gas. Several tests also were run with various Argon shielding gases. Voltage was kept constant and current ranged between 110 amps to 230 amps for all samples collected.

A probe in the fume stream collected samples on glass fiber filters to determine total mass emission rate and on triacetate filters to determine elemental composition of the fume. Sampling time varied between 10 s and 120 s. The tests determined the fume formation rate in mass per time and the mass of the fume generated per mass of metal deposited. The composition of the fume also was determined, but the only HAP measured was manganese. A summary of test results is presented in Table 4-12 below.

TABLE 4-12. SUMMARY DATA FROM REFERENCE 48

Welding process	Electrode type	Total fume emission factor (g/kg metal)	Wt % Mn in fume[a]
SMAW	E6010	19-24	–
SMAW	E6012	7-9	–

SMAW	E7018	8-18	–
SMAW	E7024	7-13	–
SMAW	E308-16	10-16	–
			–
FCAW	E70T - 1	11-12	5.0
FCAW	E70T - 5	18-22	4.0
FCAW	E70T - 4	18-20	2.0

[a] Mn = manganese.

Upon review of Reference 48, it was found that the tests were conducted with a generally sound methodology; however, the modified stack method differs considerably from the standard ANSI/AWS technique. The data were assigned a C rating. A copy of the test report is provided in Appendix J.

4.1.11 Reference 50 (1973)

In Reference 50, the fumes and gases produced during the welding of carbon steel by SMAW, GMAW, FCAW, and SAW were determined. Six different types of electrodes were evaluated in a square Battelle fume chamber during testing. Absolute filters with precleaners were used to collect the fume samples.

Total fume quantities were measured, the concentration of elemental compounds were determined, pollutant gases were analyzed, and particle size was characterized in the program. A mass spectrograph identified elemental composition, XRD identified major compounds in the sample, and optical emission spectroscopy helped verify and identify elemental composition. A cascade impactor inertially separated and classified the fume particles by aerodynamic diameter.

Table 4-13 summarizes the data presented in the report. The elemental compositions were reported as a concentration, and thus they were not in units useful for emission factor development.

TABLE 4-13. SUMMARY DATA FROM REFERENCE 50

Welding process	Electrode type	Total fume emission factor (g/kg electrode)
SMAW	E11018 - M	11.1
GMAW	E70S - 3	2.120-4.750
FCAW	E70T - 1	6.700-7.760
FCAW	E70T - 4	15.5-19.9
SAW	EM12K 1	0.034-0.041
SAW	F72-EM12K 2	0.0016-0.014

Sound test methodology was used in Reference 50 and adequate documentation was provided in the report to assess the quality of the data. The raw data were not included, however, and the test method varies slightly from the ANSI/AWS standard test method. With these considerations, the data were assigned a rating of B. Applicable portions of the test report are provided in Appendix K.

4.1.12 Reference 51 (1992)

Reference 51 is the report of a recent study performed for EPA. The document reported on tests of the 10 most commercially used electrodes for quantity and composition of fumes. Testing procedures followed the ANSI/AWS F1.2-85 standard method. Voltage was kept constant for each test, and current was operated at recommended conditions in the range of 130 amps to 180 amps. Fume was collected on glass-fiber filters located at the top of the welding chamber and weighed to determine total mass emissions. Composition of the sample for nine metals was determined using analysis techniques specified in EPA Method 6010 for evaluating solid waste. A summary of results for the electrodes tested is shown in Table 4-14 below.

TABLE 4-14. SUMMARY DATA FROM REFERENCE 51

Welding process	Electrode type	Total fume emission factor (g/kg electrode)	Wt % HAP in fume[a]			
			Cr	Co	Mn	Ni
SMAW	E6010 a	22.7	0.018	0.0023	3.9	0.026
SMAW	E6010 b	20.5	0.011	0.0035	4.4	0.008
SMAW	E6011	38.4	0.012	0.0025	2.6	0.014
SMAW	E6013	13.6	0.030	0.0030	4.1	0.018
SMAW	E308-16	6.4	6.200	0.0078	3.8	0.820
SMAW	E7018	15.7	0.024	0.0016	3.9	0.012
GMAW	E308L Si	8.6	6.000	0.0071	6.4	3.400
GMAW	E70S - 3	7.9	0.020	0.0017	6.7	0.007
GMAW	E70S - 6	5.4	0.015	0.0029	10.4	0.014
FCAW	E70T-1	8.7	0.013	0.0022	9.0	0.006
FCAW	E71T-1	12.0	0.014	0.0029	8.1	0.004

[a] HAP = hazardous air pollutant as defined by the 1990 Clean Air Act Amendments.
Wt. % = weight percent of element measured in the total fume collected.

Upon review of the information contained in Reference 51, it was found that the tests were conducted using sound methodology with good documentation; therefore, the data were assigned a quality rating of A. Applicable portions of the test report are provided in Appendix L.

4.2 DEVELOPMENT OF CANDIDATE EMISSION FACTORS

Emission factors were developed for the following welding operations: shielded metal arc welding (SMAW), gas metal arc welding (GMAW), flux cored arc welding (FCAW), and submerged arc welding (SAW). Other welding processes either did not have sufficient test data or did not generate sufficient emissions of concern. The following sections describe the development of emission factors for both total particulate matter and hazardous metals

4.2.1 Particulate Emissions

The data obtained from each of the primary references described earlier were combined to calculate candidate AP-42 emission factors for total particulate (fume) emissions. Since welding fume is essentially submicron in size (see Section 2.3), all particulate emissions are considered to be in the PM-10 (i.e., particles $\leq$ 10 µm in aerodynamic diameter) size range.

Candidate emission factors were developed for SMAW, GMAW, FCAW, and SAW processes using average data from each primary reference. Table 4-15 summarizes the average data used and the candidate emission factors obtained during this analysis. Also shown in Table 4-15 are the number of tests contained in each data set, as well as the average current and voltage used during testing.

To derive each candidate emission factor, arithmetic averages of the test data in each reference were calculated according to both the type of welding process(es) tested and the type of electrode(s) used. Next, the individual averages were grouped by process and electrode type in Table 4-15. Weighted averages, based on the number of tests conducted in each study, were then calculated to obtain the candidate emission factor for each process/electrode combination. A rating was assigned to each candidate factor based on the quality of the data used. Example hand calculations for obtaining the candidate emission factors are provided in Appendix M.

As shown in Table 4-15, the candidate emission factors are generally rated either C or D, depending on the quality of the individual data sets used in their derivation. All available data, regardless of quality, were used to develop each of the candidate emission factors. This approach was deemed to be most appropriate in order to obtain a more accurate representation of the fume generated by each process/electrode combination.

TABLE 4-15. SUMMARY OF PM-10 EMISSION DATA AND CANDIDATE EMISSION FACTORS[a]

Welding process	Electrode type	Reference No.	No. of tests conducted	Average current (A)	Average volt (V)	Average emission factor (g/kg electrode)[b]	Data quality rating	Candidate emission factor (g/kg electrode)[c]	Emission factor rating
SMAW	14Mn-4Cr	11	23	198	24	81.6	C	81.6	C
	E11018-M	11	30	161	24	17.5	C	16.4	C
	E11018-M	50	6	175	26	11.1	B		
	E308-16	11	35	174	23	10.9	C	10.8	C
	E308-16	48	2	185	26	13.0	C		
	E308-16	51	2	130	24	6.4	A		
	E308L-15	15	1	115	33	11.3	B		
	E310-16	11	26	164	24	15.1	C	15.1	C
	E316-15	15	1	140	24	15.6	B	10.0	C
	E316-15	46	9	151	26	9.8	A		
	E316L-16	21	2	145	29	8.1	C		
	E316L-16	36	22	102	26	10.5	D		
	E316-16	46	9	149	23	9.0	A		
	E410-16	46	9	153	23	13.2	A	13.2	D
	E6010	46	3	150	23	35.9	A	25.6	B
	E6010	48	2	140	30	22.0	C		
	E6010a	51	3	130	29	22.7	A		
	E6010b	51	3	130	29	20.5	A		
	E6011	51	6	145	34	38.4	A	38.4	C
	E6012	48	2	149	21	8.0	C	8.0	D
	E6013	46	9	154	23	21.0	A	19.7	B
	E6013	51	2	180	30	13.6	A		
	E7018	11	35	161	24	17.7	C	18.4	C
	E7018	15	1	140	23	26.0	B		
	E7018	46	12	175	23	20.9	A		
	E7018	48	2	190	24	13.0	C		
	E7018	51	2	155	25	15.7	A		
	E7024	46	3	207	40	10.2	A	9.2	C
	E7024	48	12	229	33	9.0	C		
	E7028	15	3	220	34	18.0	B	18.0	C
	E8018C3	46	7	164	23	17.1	A	17.1	C

TABLE 4-15 (CONTINUED)

Welding process	Electrode type	Reference No.	No. of tests conducted	Average current (A)	Average volt (V)	Average emission factor (g/kg electrode)[b]	Data quality rating	Candidate emission factor (g/kg electrode)[c]	Emission factor rating
SMAW	E9015B3	29	4	112	29	17.0	D	17.0	D
	E9018G	29	9	117	29	21.0	D	16.9	C
	E9018B3	46	10	168	23	13.3	A		
	ECoCr-A	11	27	138	25	27.9	C	27.9	C
	ENi-CI	11	27	139	23	18.8	C	18.2	C
	ENi-CI	46	3	135	21	12.9	A		
	ENiCrMo-4	46	6	139	34	11.7	A	11.7	C
	ENi-Cu-2	46	3	143	23	10.1	A	10.1	C
GMAW[d]	E308LSi	51	2	250	23	5.4	A	5.4	C
	E70S-3	46	37	252	31	5.2	A	5.2	A
	E70S-3	50	6	275	30	3.4	B		
	E70S-3	51	5	245	27	8.6	A		
	E70S-5	46	9	275	29	4.0	A		
	E70S-6	15	1	180	30	5.4	B		
	E70S-6	51	2	275	29	7.9	A		
	ER1260	15	1	180	20.5	20.5	B	20.5	D
	ER5154	15	1	160	24.1	24.1	B	24.1	D
	ER316I-Si	15	2	180	26	4.8	B	3.2	C
	ER316L-Si	21	8	220	22	4.0	C		
	ER316	46	3	170	32	0.6	A		
	ERNiCrMo	46	6	179	32	3.9	A	3.9	C
	ERNiCu-7	46	3	257	32	2.0	A	2.0	C
FCAW[d]	E110T5-K3	12	1	370	32	20.8	B	20.8	D
	E11018-M	11	11	303	30	57.0	C	57.0	D
	E308LT-3	46	3	400	32	9.1	A	9.1	C
	E316LT-3	21	2	290	24	5.2	C	8.5	B
	E316LT-3	46	6	382	29	9.6	A		

TABLE 4-15 (CONTINUED)

Welding process	Electrode type	Reference No.	No. of tests conducted	Average current (A)	Average volt (V)	Average emission factor (g/kg electrode)[b]	Data quality rating	Candidate emission factor (g/kg electrode)[c]	Emission factor rating
FCAW[d]	E70T-1	12	5	410	29	11.0	B	15.1	B
	E70T-1	46	15	451	31	11.7	A		
	E70T-1	48	4	375	30	12.0	C		
	E70T-1	50	6	450	31	7.2	B		
	E70T-1	51	2	425	31	8.7	A		
	E70T-2	12	2	340	28	11.0	B		
	E70T-4	12	6	420	29	20.0	B		
	E70T-4	46	10	391	31	16.4	A		
	E70T-4	48	4	375	32	20.0	C		
	E70T-4	50	6	450	31	17.7	B		
	E70T-5	12	8	370	29	15.5	B		
	E70T-5	46	6	441	31	20.8	A		
	E70T-5	48	4	375	30	20.0	C		
	E70T-7	12	3	340	25	31.3	B		
	E70T-G	12	5	370	32	8.2	B		
	E71T-1	12	7	280	28	9.4	B	12.2	B
	E71T-1	51	2	275	25	12.0	A		
	E71T-11	12	3	460	19	19.0	B		
SAW	EM12K1	50	5	450	32	0.04	B	0.05	C
	F72-EM12K2	50	5	550	31	0.01	B		

[a] All fume generated is < 10 µm in aerodynamic diameter (i.e., PM-10).

[b] Average emission factor obtained in test series expressed as mass of pollutant emitted per mass of electrode consumed.

[c] Mass of pollutant (PM-10) emitted per mass of electrode consumed determined as weighted average of all data sets.

[d] For GMAW and FCAW, the type of shielding gas employed will substantially influence the actual emissions generated.

4.2.2 Hazardous Metal Emissions

Candidate emission factors were also developed for hazardous metals listed in the 1990 Clean Air Act Amendments using the data available in each primary reference. Again, all HAP emissions are considered to be in the PM-10 size range as discussed above.

The same averaging approach used to develop the candidate emission factors for PM-10 emissions was used to derive similar factors for hazardous metals. A summary of the data used and the candidate emission factors obtained is provided in Table 4-16.

As was the case for total particulate, the candidate emission factors for hazardous metals are generally of poor quality. Again, all available data were used in an attempt to improve the representativeness of the candidate emission factors shown in Table 4-16.

TABLE 4-16. SUMMARY OF HAZARDOUS AIR POLLUTANT (HAP) EMISSION DATA AND CANDIDATE EMISSION FACTORS[a]

Welding process	Electrode type	Ref. No.	No of tests	Avg. current (A)	Avg. voltage (V)	Avg. emission factor (10^{-1} g/kg electrode or 10^{-1} lb/10^{3} lb electrode)[b] Cr	Cr(VI)	Co	Mn	Ni	Pb	Data rating	Candidate emission factor (10^{-1} g/kg electrode or 10^{-1} lb/10^{3} lb electrode)[c] Cr	Cr(VI)	Co	Mn	Ni	Pb	Emission factor rating
SMAW	14Mn-4Cr	11	23	198	24	13.97	--	--	232	17.14	--	C	13.9	--	--	232	17.1	--	C
	E11018-M	11	30	161	24	--	--	--	13.8	--	--	C	--	--	--	13.8	--	--	C
	E308-16	51	2	130	24	3.97	--	0.01	2.43	0.52	--	D	3.93	3.59	0.01	2.52	0.43	--	D
	E308L-15	15	1	115	33	3.84	3.59	--	2.71	0.25	--	B							
	E310-15	15	1	140	24	25.3	18.8	--	22.0	1.96	0.24	B	25.3	18.77	--	22.0	1.96	0.24	C
	E316-15	46	9	151	26	5.69	--	--	7.55	0.51	--	A	5.22	3.32	--	5.44	0.55	--	D
	E316L-16	21	2	145	29	4.05	3.32	--	4.05	0.32	--	D							
	E316L-16	36	22	102	26	4.94	--	--	3.68	0.84	--	D							
	E316-16	46	9	149	23	5.84	--	--	7.91	1.35	--	A							
	E410-16	46	9	153	23	--	--	--	6.85	0.14	--	A	--	--	--	6.85	0.14	--	C
	E6010	46	3	150	23	--	--	--	11.8	--	--	A	0.03	0.01	--	9.91	0.04	--	B
	E6010a	51	3	130	29	0.04	--	<0.01	8.85	0.06	--	A							
	E6010b	51	3	130	29	0.02	--	0.01	9.02	0.02	--	A							
	E6011	51	6	145	34	0.05	--	0.01	9.98	0.05	--	A	0.05	--	0.01	9.98	0.05	--	C
	E6013	46	9	154	23	0.24	--	--	10.3	--	--	A	0.04	--	<0.01	9.45	0.02	--	B
	E6013	51	2	180	30	0.04	--	<0.01	5.58	0.02	--	A							
	E7018	11	29	161	29	--	--	--	11.3	--	--	C	0.06	--	<0.01	10.3	0.02	--	C
	E7018	15	1	140	23	0.10	--	--	9.62	--	--	B							
	E7018	46	12	175	23	--	--	--	8.58	--	--	A							
	E7018	51	2	155	25	0.04	--	<0.01	6.12	0.02	--	A							
	E7024	46	15	225	34	0.01	--	--	6.29	--	--	A	0.01	--	--	6.29	--	--	C
	E7028	15	3	220	34	0.13	--	--	8.46	--	1.62	B	0.13	--	--	8.46	--	1.62	C
	E8018C3	46	7	164	23	0.17	--	--	12.3	0.51	--	A	0.17	--	--	12.3	0.51	--	C
	E9018B3	46	10	168	23	2.12	--	--	7.83	0.13	--	A	2.12	--	--	7.83	0.13	--	C
	ENi-CI	46	3	135	21	--	--	--	0.39	8.90	--	A	--	--	--	0.39	8.90	--	C
	ENiCrMo-3	46	3	145	25	5.45	--	--		4.25	--	A	4.20	--	--	0.43	2.47	--	C
	ENiCrMo-4	46	6	133	23	3.55	--	--	0.43	1.56	--	A							
	ENi-Cu-2	46	3	143	26	--	--	--	2.12	4.23	--	A	--	--	--	2.12	4.23	--	C
FCAW	E110T5-K3	12	1	370	32	0.02	--	--	20.2	1.12	--	B	0.02	--	--	20.2	1.12	--	D
	E11018-M	11	11	303	30	9.69	--	--	7.04	1.02	--	C	9.69	--	--	7.04	1.02	--	C
FCAW	E316LT-3	21	2	290	24	2.65	--	--	2.50	0.68	--	C	9.70	1.40	--	5.90	0.93	--	B
	E316LT-3	46	6	382	29	12.05	1.40	--	7.04	1.02	--	A							
	E70T-1	12	5	410	29	0.03	--	--	12.0	0.06	--	C	0.04	--	--	8.91	0.05	--	B
	E70T-1	46	15	451	31	--	--	--	10.8	--	--	A							
	E70T-1	48	4	375	30	--	--	--	6.00	--	--	C							

TABLE 4-16 (Continued)

Welding process	Electrode type	Ref. No.	No of tests	Avg. current (A)	Avg. voltage (V)	Avg. emission factor (10^{-1} g/kg electrode or 10^{-1} lb/10^{3} lb electrode)[b]						Data rating	Candidate emission factor (10^{-1} g/kg electrode or 10^{-1} lb/10^{3} lb electrode)[c]						Emission factor rating
						Cr	Cr(VI)	Co	Mn	Ni	Pb		Cr	Cr(VI)	Co	Mn	Ni	Pb	
	E70T-1	51	2	425	31	0.01	--	<0.01	7.83	<0.01	--	A							
	E70T-2	12	2	340	28	0.01	--	--	11.6	0.02	--	B							
	E70T-4	12	6	420	29	0.02	--	--	2.80	0.06	--	B							
	E70T-4	46	10	391	31	--	--	--	4.93	--	--	A							
	E70T-4	48	4	375	32	--	--	--	4.00	--	--	C							
	E70T-5	12	8	370	29	0.03	--	--	14.11	0.03	--	B							
	E70T-5	46	6	441	31	--	--	--	23.0	--	--	A							
	E70T-5	48	4	375	30	--	--	--	8.00	--	--	C							
	E70T-7	12	3	340	25	0.19	--	--	2.35	0.13	--	B							
	E70T-G	12	5	370	32	0.02	--	--	2.28	0.06	--	B							
	E71T-1	12	7	280	28	0.02	--	--	10.3	0.05	--	B	0.02	--	<0.01	6.62	0.04	--	B
	E71T-1	51	2	275	25	0.02	--	<0.01	9.72	<0.01	--	A							
	E71T-11	12	3	460	19	0.02	--	--	2.28	0.06	--	B							
GMAW	E308LSi	51	2	250	23	3.24	--	<0.01	3.46	1.84	--	A	3.24	--	<0.01	3.46	1.84	--	C
	E70S-3	46	37	252	31	--	--	--	2.75	--	--	A	0.01	--	<0.01	3.18	0.01	--	A
	E70S-3	51	5	245	27	0.02	--	<0.01	5.76	0.01	--	A							
	E70S-5	46	9	275	29	--	--	--	2.30	--	--	A							
	E70S-6	15	1	180	30	0.04	--	--	3.94	--	--	B							
	E70S-6	51	2	275	29	0.01	--	<0.01	8.22	0.01	--	A							
	ER1260	15	1	180	22	0.04	--	--	--	--	--	B	0.04	--	--	--	--	--	D
	ER5154	15	1	160	24.1	0.10	--	--	0.34	--	--	B	0.10	--	--	0.34	--	--	D
	ER316l-Si	15	2	180	26	5.28	0.10	--	2.45	2.26	--	B	5.28	0.10	--	2.45	2.26	--	D

TABLE 4-16 (Continued)

Welding process	Electrode type	Ref. No.	No of tests	Avg. current (A)	Avg. voltage (V)	Avg. emission factor (10^{-1} g/kg electrode or 10^{-1} lb/10^{3} 1b electrode)[b]						Data rating	Candidate emission factor (10^{-1} g/kg electrode or 10^{-1} lb/10^{3} lb electrode)[c]						Emission factor rating
						Cr	Cr(VI)	Co	Mn	Ni	Pb		Cr	Cr(VI)	Co	Mn	Ni	Pb	
GMAW	ERNiCrMo-3	46	3	192	34	1.34	--	--	--	2.37	--	A	3.53	--	--	0.70	12.5	--	B
	ERNiCrMo-4	46	3	165	30	5.72	--	--	0.70	22.7	--	A							
	ERNiCu-7	46	3	257	32	<0.01	--	--	0.22	4.51	--	A	<0.01	--	--	0.22	4.51	--	C

[a] All HAP emissions are in the PM-10 size range.

[b] Average emissions factors obtained in test series expressed as mass of pollutant emitted per mass of electrode consumed. Cr = chromium; Cr(VI) = chromium +6 valence state; Co = cobalt; Mn = manganese; Ni = nickel; and Pb = lead.

[c] Mass of pollutant emitted per mass of electrode consumed determined as weighted average of all data sets. Cr = chromium; Cr(VI) = chromium +6 valence state; Co = cobalt; Mn = manganese; Ni = nickel; and Pb = lead.

SECTION 5

PROPOSED AP-42 SECTION

The following pages contain the proposed new AP-42 section for welding operations as it would actually appear in the document.

APPENDIX A

REFERENCE 11

(McIlwain and Neumeier, 1987)

Report of Investigations 9105

Fumes From Shielded Metal Arc Welding Electrodes

By J. F. McIlwain and L. A. Neumeier

UNITED STATES DEPARTMENT OF THE INTERIOR
Donald Paul Hodel, Secretary

BUREAU OF MINES
David S. Brown, Acting Director

TABLE 1. - Weld deposit compositions (filler metal specifications) for welding electrodes (13), weight percent

AWS code and electrode type	Cc	Cr	Fe	Mn	Ni	Other[1]
A5.4:						
E308-16.....	NS..	18-21	Bal	0.5-2.5	9 -11	2.0
E310-16.....	NS..	25-28	Bal	1 -2.5	20 -22.5	2.0
A5.13:						
ECoCr-A.....	Bal.	25-32	Bal	2	3	10.9
A5.15:						
ENiCI.....	NS..	NS	5	1	85[2]	9.5
14 Mn-4 Cr[3].....	NS..	4- 5	8	.5-4.0	14 -16	.5
A5.1:						
E7018.....	NS..	.20	Bal	1.60	.30	1.1
A5.5:						
E11018-M.....	NS..	.40	Bal	1.3-1.8	1.25- 2.50	1.3

Bal Balance. NS Not specified.

[1]Maximum.

[2]Minimum.

[3]Not classified by AWS; data supplied by manufaccurers of electrodes used in this study.

hardfacing and rebuilding, welding is done in multiple layers of the weld filler metal. The weld alloy, rather than the original steel of the welded part, then becomes the substrate. To assess tne effect of this new substrate on fume generation, a double-layer bead pad of the weld alloy was deposited onto a mild steel plate. After sandblast cleaning, this pad served as the new substrate for fume generation tests of that same alloy, performed in the same manner as with the mild steel plate substrates. One brand from each of the five high-alloy SMAW groups was tested this way.

RESULTS

MILD STEEL SUBSTRATE

The data collected from the tests are the weight of the fume collected, the weight of the electrode consumed, the arc time, and the chemical analysis of the fume. Welding conditions such as voltage, current, plate speed, and electrode feed rate were recorded or derived for each test. For the alloy groups, two additional quantities, a maximum allowable fume exposure and an exposure rating, have been derived from the data.

Two quantities based on the weight of fume generated are the fume generation rate, FGR, and the fume weight per weight of electrode consumed, f_e. The FGR measures the fume generating tendencies of an electrode and is used to derive the exposure rating. Where the arc is operating intermittently, as during a work shift, f_e may be more useful in estimating the amount of fume generated. In either case, the data apply to the operating conditions stated and, for the FGR at least, to the size of the electrode given.

Fume generation data for the electrode groups are listed in table 2. Each electrode brand has been given a code letter or letters. Replicates were measured on one of the brands, code D, to get an estimate of the repeatability of the experiments and analyses. Code D was chosen at random from among the electrodes in this group. Comparisons of the derived FGR and f_e values between the replicates and the original data set, using the Student t statistic (14) at the 90-pct confidence level, show no significant differences. The coefficients of variation (CV) of the data sets of code D, for both FGR and f_e

TABLE 2. - Fume generation data for electrodes

Code	Runs	Average		FGR, mg/min	SD, mg/min	f_e, pct	SD, pct
		Voltage, V	Current, A				
TYPE E308-16--dc, ELECTRODE POSITIVE; 3.97-mm CORE DIAM; 280-mm/min TRAVEL SPEED; 1-min ARC TIME							
A	5	23	171	394	51	0.88	0.10
B	4	24	175	478	13	1.21	.18
C	5	24	173	514	27	1.31	.04
D	5	22	173	422	58	1.06	.14
	5	23	176	396	30	.95	.07
	6	23	174	415	27	1.04	.07
E	5	23	173	472	31	1.22	.07
Mean	NAp	23	174	440	55	1.09	.16
TYPE E310-16--dc, ELECTRODE POSITIVE; 4.76-mm CORE DIAM; 280-mm/min TRAVEL SPEED; 1-min ARC TIME							
F	3	24	163	446	26	1.11	0.06
G	6	23	166	540	37	1.47	.11
H[1]	6	24	164	659	31	2.17	.13
I	6	23	165	455	33	1.20	.13
J	5	25	160	527	32	1.39	.10
Mean	NAp	24	164	534	84	1.51	.40
TYPE ECoCr-A--dc, ELECTRODE POSITIVE; 3.97-mm CORE DIAM; 280-mm/min TRAVEL SPEED; 45-s ARC TIME							
K	5	26	140	766	59	2.58	0.20
L	5	26	137	571	77	1.77	.32
M	6	25	134	713	23	2.31	.07
N	6	24	139	1,086	74	4.29	.32
O[2]	5	28	176	1,041	46	2.86	.11
Mean[3]	NAp	25	138	795	204	2.79	1.01
TYPE ENiCI--dc, ELECTRODE POSITIVE; 3.97-mm CORE DIAM; 280-mm/min TRAVEL SPEED; 1-min ARC TIME							
P	6	24	135	612	12	2.08	0.06
Q	6	22	140	538	13	1.90	.08
R	4	24	143	598	12	1.78	.06
S	6	24	138	560	18	2.14	.11
T	5	23	139	461	16	1.38	.06
Mean	NAp	23	139	554	54	1.88	.28
14 Mn-4 Cr SURFACING ALLOY--dc, ELECTRODE POSITIVE; 4.76-mm CORE DIAM; 280-mm/min TRAVEL SPEED; 20-s ARC TIME							
U	4	24	200	3,010	140	8.08	0.37
V	3	24	199	3,280	82	9.16	.10
W	5	24	198	3,170	270	7.81	.43
X	5	24	197	3,280	200	8.82	.50
Y	6	24	196	2,380	250	7.13	.55
Mean	NAp	24	198	2,980	420	8.16	.79

See explanatory notes at end of table.

TABLE 2. - Fume generation data for electrodes--Continued

Code	Runs	Average		FGR,	SD,	f_e, pct	SD, pct
		Voltage, V	Current, A	mg/min	mg/min		
TYPE E7018--dc, ELECTRODE POSITIVE; 3.97-mm CORE DIAM; 280-mm/min TRAVEL SPEED; 1-min ARC TIME							
CC	6	24	161	459	30	1.55	0.10
DD	5	24	159	515	20	1.81	.08
EE	6	24	165	653	40	2.17	.15
FF	6	24	158	475	21	1.62	.07
GG	6	24	164	511	21	1.70	.08
Mean	NAp	24	161	523	75	1.77	.24
TYPE E11018-M--dc, ELECTRODE POSITIVE; 3.97-mm CORE DIAM; 280-mm/min TRAVEL SPEED; 1-min ARC TIME							
HH	6	24	163	445	16	1.46	0.06
II	6	24	160	561	12	1.96	.05
JJ	6	24	160	518	15	1.72	.06
KK	6	24	163	560	20	1.90	.06
LL	6	24	158	513	34	1.70	.10
Mean	NAp	24	161	520	47	1.75	.19
Mn-Cr SURFACING ALLOY FLUX-CORED WIRE--dc, ELECTRODE POSITIVE; 2.78-mm DIAM, 38-mm WIRE STICKOUT; 430-mm/min TRAVEL SPEED; 2,200-mm/min WIRE FEED; 1-min ARC TIME; NO SHIELD GAS							
Z[4]	6	30	288	5,070	200	6.2	0.24
BB[4]	5	29	317	4,320	190	5.2	.23
Mean	NAp	30	303	4,700	530	5.7	.73
AA[5]	6	30	287	5,410	620	6.1	.70

f_e Fume weight per weight of electrode consumed.
FGR Fume generation rate.
NAp Not applicable.
SD Standard deviation.

[1]Composite core.
[2]4.76-mm core diameter.
[3]Excludes code O data.
[4]Nominally 15 pct Mn, 4 pct Cr.
[5]Nominally 1.5 pct Mn, 16 pct Cr.

determinations, vary from 6.5 to 13.7 pct. These are similar to values computed for the other brands in this group.

For the most part, the results presented in the tables are straightforward. Code H electrodes, in the type E310-16 series, give higher fume generation data than do others in the group. This may be due to their unique construction. Unlike the solid filler core of the other electrodes, code H electrodes consist of a hollow tube filled with granular metal. This construction results in a larger surface area per unit weight of filler metal, thus generating more fume. Because the code O electrodes are of a larger diameter than are the other type ECoCr-A electrodes, they were tested at commensurately higher voltage and current settings, and their data were not included in calculating the means for the group. However, its FGR value, if reduced by the ratio of the group electrode cross section to its own cross section, is not significantly different from the group mean. Note also that its fume fraction, f_e, which effectively corrects for the difference in size, is quite close to that of the group mean.

TABLE 3. - Chemical composition of fumes generated from electrodes, weight percent--Continued

Code	Al	Ba	Ca	Co	[1]Cr	[2]Cr^{5+}	F	Fe	K	Mn	Na	Ni	Si	Sr	Ti
14 Mn-4 Cr SURFACING ALLOY															
U					1.9		NA	35.4		24.4	2.0	3.1	0.6		
V					1.6		NA	33.1		36.0	1.0	.3	1.8		
W					1.3		NA	36.8		26.6	1.7	2.9	2.3		
X					1.7		0	37.9		25.5	.8	2.7	.6		
Y					2.1		1.1	30.2		29.4	1.1	1.3	2.2		
Mean					1.7		.6	34.7		28.4	1.3	2.1	1.5		
SD					.30		.78	3.1		4.6	.50	1.2	.83		
TYPE E7018															
CC	0.7		10.8				1.2	29.1	14.6	8.6	3.1		5.1	NA	
DD	.6		11.0				.9	37.0	12.3	9.5	2.9		6.0	NA	
EE	1.1		11.3				0	25.3	5.0	3.9	2.7		1.3	NA	
FF	.4		10.8				9.3	24.3	11.1	5.5	1.9		4.9	NA	
GG	.2		11.4				5.8	31.9	6.7	4.5	3.9		6.3	1.0	
Mean	.6		11.1				3.4	29.5	9.9	6.4	2.9		4.7	1.0	
SD	.36		.28				4.0	5.2	4.0	2.5	.72		2.0	NAp	
TYPE E11018-M															
HH			13.0				4.7	24.5	6.8	14.5	4.4		2.0	1.2	
II			6.3				2.0	33.1	6.6	6.5	3.4		6.1	0	
JJ			10.6				8.1	33.0	.7	6.0	4.9		.4	0	
KK			10.1				5.6	36.6	3.5	6.1	5.0		2.7	0	
LL			12.9				.9	26.1	7.3	6.6	4.1		1.5	1.1	
Mean			10.6				4.3	30.7	4.4	7.9	4.4		2.5	.5	
SD			2.7				2.9	5.1	2.9	3.7	.65		2.2	.63	
Mn-Cr SURFACING ALLOY FLUX-CORED WIRE															
Z					1.7		1.7	43.4		22.3		2.0			
BB					1.7		2.4	43.9		26.6		.4			
Mean					1.7		2.0	43.7		24.5		1.2			
AA					10.5		.1	54.8		3.1		.3			

NA Not analyzed.
NAp Not applicable.
SD Standard deviation.

[1]Determined by acid leach-titration.
[2]Determined by INCO method.
[3]Single analysis run on separate sample.

NOTE.--No entry in a column indicates that element was not a fume constituent.

elements, the exposure value was calculated as

$$C_{i,max} = [\Sigma(f_{i,fume}/TLV_i)]^{-1}. \quad (3)$$

The resulting relative exposure indices for the electrode brands are given as C_m values in table 5.

A second index, the exposure rating, R, is derived from C_m and the FGR, as

$$R(m^3/min) = \frac{FGR}{C_m}. \quad (4)$$

If taken literally, it represents the amount of fresh air per minute needed to dilute the fume being generated to a safe level. It is essentially equivalent to the nominal hygienic air requirements (NHL) developed in Sweden to rate the fume hazards of electrodes numerically (14-15). The NHL, however, combines all of the components, using equation 3, thereby leading to higher values of the ratings. Also, lower TLV's, such as for Cr or Ni, are used. The NHL is given in cubic meters per hour. Because of these differences, the exposure rating R is used in this report. Values for the electrode brands appear in table 5. According to this ranking, the ECoCr-A

TABLE 4. - Threshold limit values (TLV's) for fume constituents (4), milligrams per cubic meter

	TLV		TLV		TLV
Al....	10	Cr^{6+}..	0.05	Na....	(2)
Ba....	.5	F.....	2.5	Ni....	1
Ca....	[1]1.4	Fe....	5	Si....	[3]2.8
Co....	.1	K.....	(2)	Sr....	(2)
Cr....	.5	Mn....	1	Ti....	(4)

[1]Based on 2-mg/m³ TLV for CaO.
[2]None established in reference.
[3]Based on 6-mg/m³ TLV for amorphous SiO_2.
[4]TLV for TiO_2 deleted from reference.

TABLE 5. - Exposure index (C_m) and exposure rating (R) values for welding electrodes

Group and code	C_m, mg/m³	R, m³/min	Group and code	C_m, mg/m³	R, m³/min	Group and code	C_m, mg/m³	R, m³/min
E308-16:			ECoCr-A--Con:			Mn-Cr buildup wires--Con:		
A.....	1.1	370	Mean[1]....	0.40	1,980	BB[2].....	3.8	1,150
B.....	1.2	400	2 SD.....	±.10	±1,420	Mean.....	4.1	1,140
C.....	.89	580	ENiCI:			2 SD.....	±1.0	±30
D.....	.92	440	P.....	1.8	340	AA[3].....	4.8	1,140
E.....	.94	500	Q.....	1.6	340	E7018:		
Mean.....	1.0	460	R.....	1.7	350	CC.....	11.6	40
2 SD.....	±.27	±170	S.....	1.5	370	DD.....	10.5	49
E310-16:			T.....	1.2	390	EE.....	19.8	33
F.....	1.1	410	Mean.....	1.6	360	FF.....	18.2	26
G.....	1.0	520	2 SD.....	±.26	±43	GG.....	15.7	32
H.....	1.1	590	Mn-Cr buildup:			Mean.....	15.2	36
I.....	.92	500	U.....	4.1	730	2 SD.....	±8.1	±18
J.....	.84	630	V.....	2.8	1,180	E11018-M:		
Mean.....	1.0	530	W.....	3.8	840	HH.....	6.9	64
2 SD.....	±.23	±170	X.....	3.9	840	II.....	15.1	37
ECoCr-A:			Y.....	3.4	700	JJ.....	13.6	38
K.....	.36	2,150	Mean.....	3.6	860	KK.....	13.7	41
L.....	.43	1,320	2 SD.....	±1.0	±380	LL.....	11.1	46
M.....	.46	1,540	Mn-Cr build-up wires:			Mean.....	12.1	45
N.....	.37	2,910				2 SD.....	±6.5	±22
O.....	.44	2,380	Z[2].....	4.5	1,130			

2 SD 2 standard deviations.
[1]Excludes code 0 data. [2]Nominally 15 pct Mn, 4 pct Cr.
[3]Nominally 1.5 pct Mn, 16 pct Cr.

electrodes, as a group, are 55 times more hazardous to use than the carbon steel E7018 electrodes. Included in the data are two standard deviation (2 SD) values calculated from the data listed. Although not strictly justifiable from the small number of samples used, this statistic should encompass most of the electrode brands not tested.

The data in figures 2 through 5 were tested to determine fits to curves of the form $f_f = a_o + a_1 f_e$ and $f_f = a_o + a_1 f_e^{1/2} + a_2 f_e$, where f_f and f_e are the elemental fractions in the fume and electrode, respectively. Although the second curve gave slightly better fits for each of the elements, negative values for the coefficient a_1 for Cr and Fe argued in favor of linear fits for these data. Figure 2 plots data for five of the electrode groups in which Cr was a contributor to the fume. The least-squares fit shown is

$$f_{Cr,\ fume} = -0.31 + 0.66\ f_{Cr,\ elec}, \quad (5)$$

with deviations of about 24 pct. All fume fractions in equations 5 through 10 are in weight percent. More precise fits result from separately grouping the ECoCr-A or the stainless steel electrodes with Mn-Cr electrodes, giving for the ECoCr-A group

$$f_{Cr,\ fume} = -0.11 + 0.75\ f_{Cr,\ elec}, \quad (6)$$

and for the stainless steel E308-16 and E310-16 electrodes combined

$$f_{Cr,\ fume} = -0.054 + 0.57\ f_{Cr,\ elec}. \quad (7)$$

Shown also in the figure are mean values of the weld-metal specifications for Cr in these alloy groups. These values, representing the Cr level in the weld deposit, are the only Cr fractions generally available.

Levels of hexavalent Cr in the fumes did not follow a pattern with respect to total Cr content in the electrode. The valence of the Cr is sensitive to the flux composition, which is quite complex for these electrodes.

A linear fit to the Fe data (fig. 3) is given by

$$f_{Fe,\ fume} = 0.916 + 0.45\ f_{Fe,\ elec}. \quad (8)$$

Again, scatter is significant at about 30 pct. The weld-metal specification values are shown also. The Mn and Ni data are described by the relations

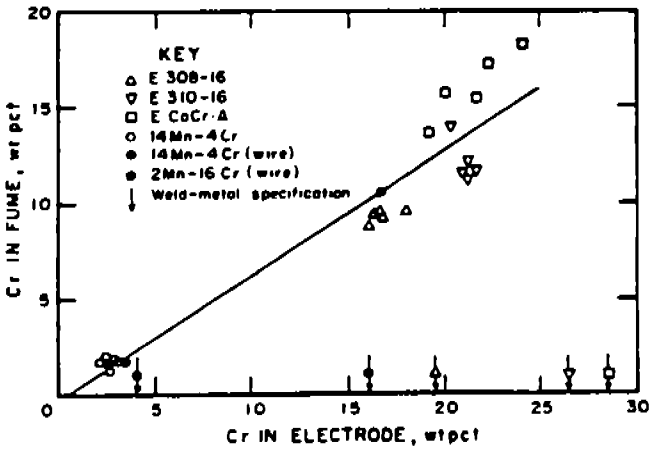

FIGURE 2.—Chromium fraction in fume as function of Cr content of electrode, including flux coating. Welding onto mild-steel plate.

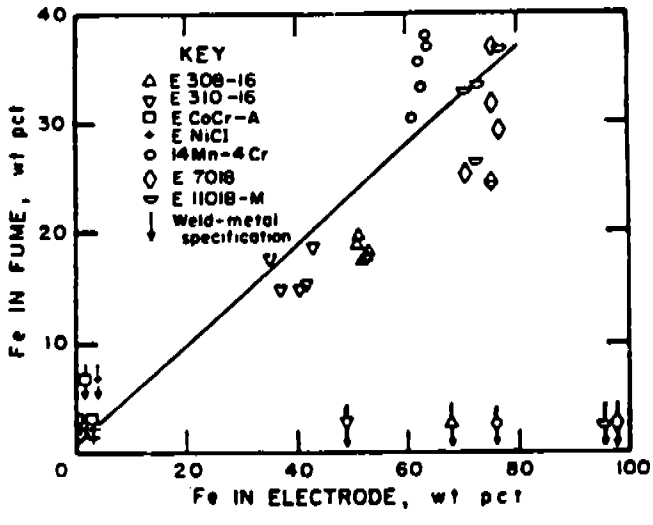

FIGURE 3.—Iron fraction in fume as function of Fe content of electrode, including flux coating. Welding onto mild-steel plate.

$$f_{Mn,fume} = -0.99 + 4.60\, f^{1/2}_{Mn,elec} + 0.57\, f_{Mn,elec}, \quad (9)$$

and

$$f_{Ni,fume} = -0.78 + 1.59\, f^{1/2}_{Ni,elec} - 0.04\, f_{Ni,elec}, \quad (10)$$

respectively. Figures 4 and 5 give the data and the weld-metal specification values. Mn comes the closest to matching these values in terms of the total electrode content. Its propensity to fume is substantially greater than that of the other metals shown, while Ni displays the least. The curves, combined in figure 6, show that these metals fume in ascending order as Ni, Fe, Cr, and Mn, roughly in proportion to their vapor pressures.

Because Co was not present in the other electrodes, the data for it were not plotted. The mean ratio of fume to electrode fractions for the five ECoCr-A electrodes is 0.54±0.06. If its fuming rate were linear with electrode content, Co would fall between Fe and Cr in fuming propensity. It does not follow in order of its vapor pressure, which is lower than that of Ni.

Partly because of the low fuming potential of Ni, the exposure index for the ENiCI electrodes was determined primarily by the Ba content of the fume, with secondary contributions from Sr and Ca. Although the fuming potentials for these elements, as determined by ratios of fume to electrode fractions, were

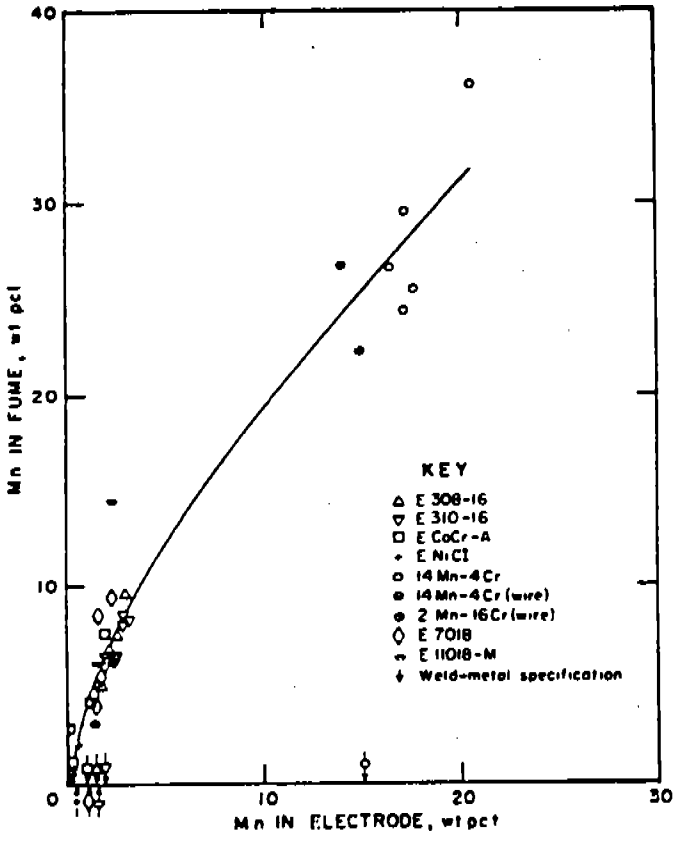

FIGURE 4.—Manganese fraction in fume as function of Mn content of electrode, including flux coating. Welding onto mild-steel plate.

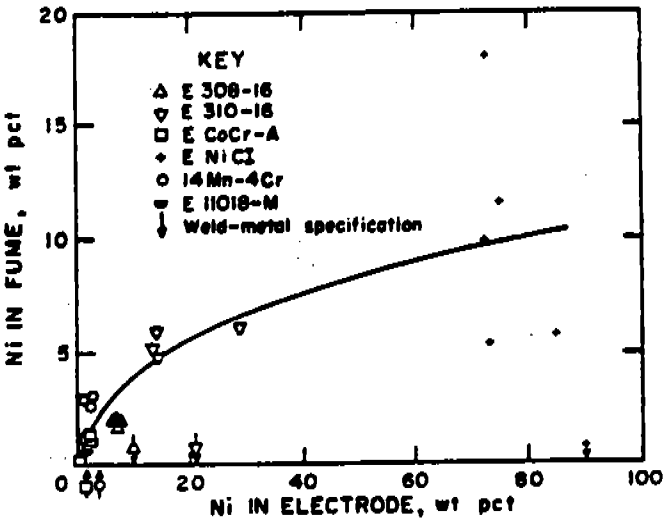

FIGURE 5.—Nickel fraction in fume as function of Ni content of electrode, including flux coating. Welding onto mild-steel plate.

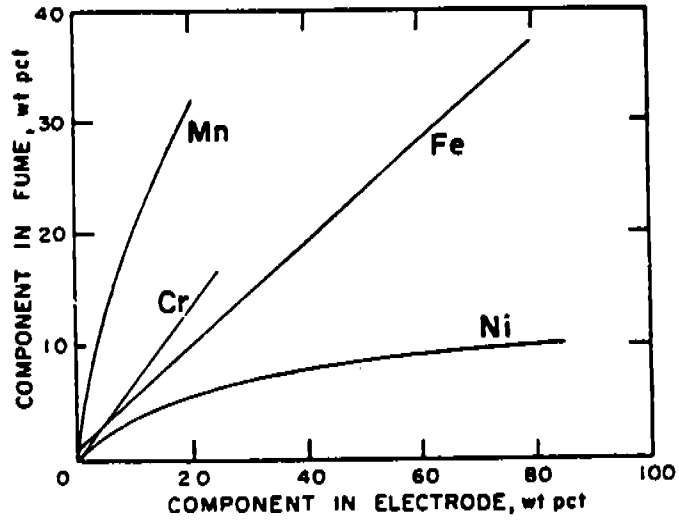

FIGURE 6.—Comparison of elemental components of fume to their respective contents in electrode.

substantially higher than for the filler metal components, the scatter was too great to be of use in predicting fume contents of untested electrodes.

ALLOY SUBSTRATE

The components of interest in the fumes of electrodes deposited onto double-layer alloy deposits (the substrate) are those found in the deposited filler metal. Fume compositions for the five electrodes tested this way appear in table 6. Except for hexavalent Cr, elements not exceeding 1 pct in the fume from mild steel welding were not analyzed for in the alloy welding fumes. Below each element fraction in the table is the ratio of it to the corresponding mild steel weld component from the fume of the same electrode code. The uncertainties are calculated from the code D replicate data (table 3) using the t statistic. Values for hexavalent Cr and Co were estimated at ±9.5 and ±6.3 wt pct, respectively. In only a few cases do the results indicate a significant increase in the component fraction arising from the alloy substrate. The 9-pct rise in Co and a 16-pct rise in Cr in the code L electrode fume are troublesome in terms of welder exposure because of their already high level in the fume. The other elements showing large fractional increases are at low enough levels as to cause minimal concern.

TABLE 6. - Chemical composition of fumes generated from electrodes weld-deposited onto double-layer alloy substrates, weight percent

	E		I		L		S		Y	
	Fume	Ratio[1]	Fume	Ratio[1]	Fume	Ratio[1]	Fume	Ratio[1]	Fume	Ratio[1]
Co.....	NA	NA	NA	NA	25.4	1.09±0.07	NA	NA	NA	NA
[2]Cr.....	8.7	1.0 ±0.1	12.5	1.08±0.1	18.2	1.16± .11	NA	NA	2.1	1.0 ±0.1
Cr^{6+}....	4.2	.88± .08	4.8	.87± .08	2.0	.87± .08	NA	NA	.36	1.4 ± .1
Fe.....	17.6	.94± .05	16.2	1.06± .06	2.2	.67± .04	2.7	0.93±0.05	30.8	1.02± .06
Mn.....	7.2	.96± .05	7.8	.94± .05	.12	.04± .00	NA	NA	29.2	.99± .05
Ni.....	2.8	1.4 ± .1	5.6	1.1 ± .1	1.1	.92± .07	10.4	.90± .07	2.5	1.9 ± .1
Si.....	4.2	.95± .06	3.8	.84± .06	NA	NA	1.7	.63± .04	3.5	1.6 ± .1

NA Not analyzed.
[1]Alloy-generated component to mild-steel-generated component.
[2]Determined by acid leach-titration.

DISCUSSION

The exposure indices determined for the electrodes can be useful in a number of ways. The mining personnel responsible for specification of welding consumables could use these data to guide their selection of electrodes. Often, more highly alloyed austenitic stainless steel fillers are used to repair quenched-and-tempered steel structural components because they are considered more "forgiving" to less than optimum welding practices (16). The order of magnitude difference in exposure indices between the stainless steels and the E7018 or E11018-M steels should bias the selection towards the leaner electrodes. (It might be noted that a t statistic test shows no significant differences between the indices of E308-16 and E310-16 or between E7018 and E11018-M. A larger sampling might confirm the slight differences seen in the table.)

Knowledge of relative exposure hazards of the various types of electrodes would also alert the welder to take extra precautions during welding when using electrodes with higher exposure indices. Those with knowledge of any total fume

APPENDIX B

REFERENCE 12

(Henderson, 1986)

FUME GENERATION AND CHEMICAL ANALYSIS OF FUME FOR A SELECTED RANGE OF FLUX-CORED STRUCTURAL STEEL WIRES — AWRA DOCUMENT P9-44-85 (REVISED 15/9/86)

By I.D. Henderson*, U.E. Senff and A.J. Wilson*****

ABSTRACT

This report sets down the collected fume results from a range of nine classified wires supplied by five welding companies. The intention was to look at commonly used flux-cored wires in the structural welding field and investigate the fume characteristics by operating the wires at the manufacturers' recommended conditions.

In part, the results have been compared with similar work completed by AWS and they show reasonable correlation. The report also describes the methods employed in collecting the fume by an electrostatically assisted filter and the technique of elemental chemical analysis using x-ray fluorescence spectrometry.

INTRODUCTION

This investigation which is an extension of the AWS data on flux-cored welding wires was intended to give an overview of the consumables used in this segment of the industry to see:

(a) what level and type of particulate fume was generated, and

(b) how this would show up in the classified divisions of the consumables.

The following classified electrodes were employed in the exercise.

AWS	SAA	TYPE
E70T	ETD-Cp-W502H	Gas shielded
E71T *	ETP-Cp-W502H & Mp	Gas shielded
E70T	ETP-Cp-W502H & Mp	Gas shielded
E70T	* —	Gas shielded
E70T--	ETD-Np-W500	No gas shield
E70T-5	ETD & P-Cp & Mp-W503	Gas shielded
E70T-7	ETD-Nn-W500	No gas shield
E110T5-K3	Not classified	Gas shielded
E71T-11	ETP-Nn-W500	No gas shield

* Not nominated by the supplier.

These classifications are defined in the AWS Codes A5.20[1] and A5.29[2] and the Australian Standard AS2203[3].

The programme was divided into sections. The CSIRO Division of Manufacturing Technology in Adelaide carried the operation of running the wire at the recommended welding parameters and measuring the fume rate (g/hr) and the fume produced per kg of consumable (g/kge).

Samples of fume, electro-deposited on hard filter paper and then collected by scraping, were then sent to BHP Steel International Port Kembla for chemical analysis.

In order to facilitate the testing operation the following information was requested from the electrode supplier for each consumable: current; arc voltage; wire feed rate; travel speed; contact tip to work distance; gas shielding; chemical elements in the wire; and electrode angle to work.

1 FUME MEASUREMENT EQUIPMENT

CSIRO Division of Manufacturing Technology developed an electrostatically assisted felt filter system to cope with the high fume generated by the flux-cored range of wires. The AWS experiments on flux-cored wires of the E70T-1 type showed that deposits were of the order of 12 g per square metre of filter and this was collected in 30 seconds.

Since some wires would produce fume at a rate of 10 times this figure, the limit of 12 g/m² would be reached in 3 seconds, which is too short for testing these wires.

The AWS report also mentioned clogging and overloading being a problem possibly occurring at the high generation rate of 200 g/hr, and if a reasonable filter load before clogging is taken to be 15 g/m² the maximum arc time would be of the order of 13.5 seconds.

When a tubular open arc hardfacing electrode was tested locally in a device similar to a Swedish Fume Box and using a membrane of 200 mm diameter (area 0.03 m²), the system was hopelessly clogged very shortly after the test began. From the visual evidence of fume production as compared to a flux-cored, gas shielded electrode, it was apparent that a system less susceptible to clogging would have to be designed.

The immediate search for a filter medium of greater flow, perhaps compensated by a larger effective area and thicker cross-section (ie. longer trapping path), was centred on the materials used in bag-houses such as exist at lead

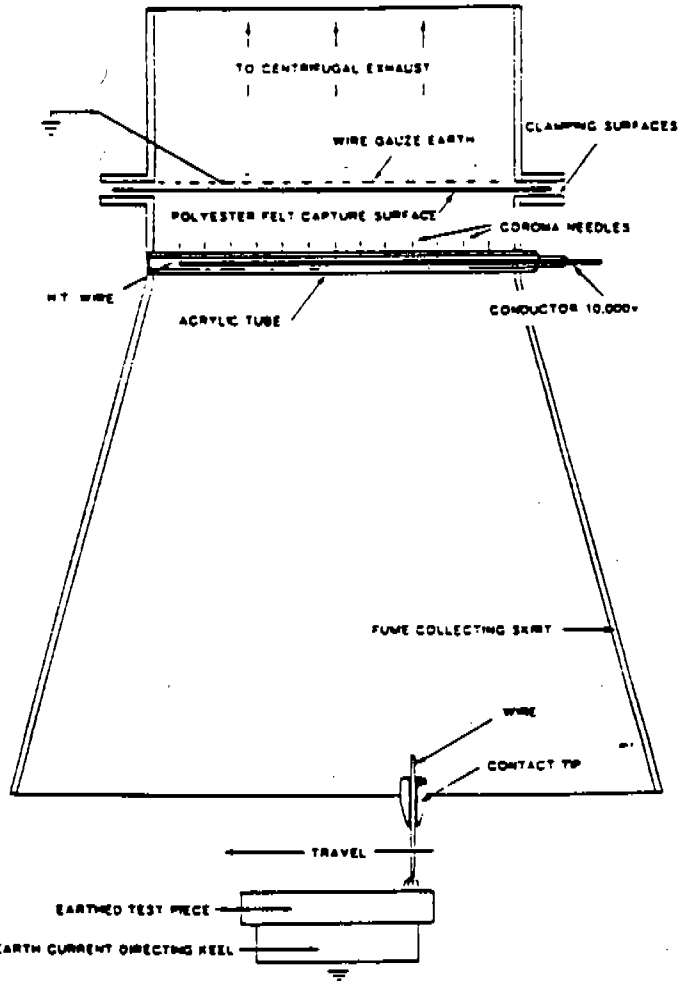

FIG 1. HIGH INTENSITY FUME COLLECTOR.

* CSIRO Adelaide Laboratory
** BHP Steel International
*** AWRA

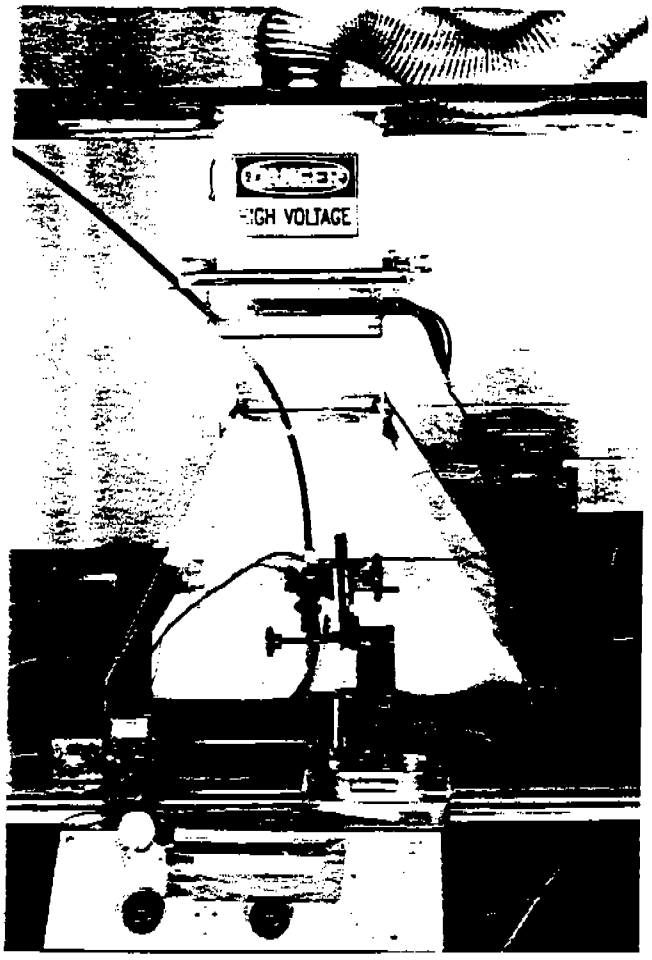

FIG 2. FUME BOX ASSEMBLY (WITH FRONT PERSPEX PANEL REMOVED).

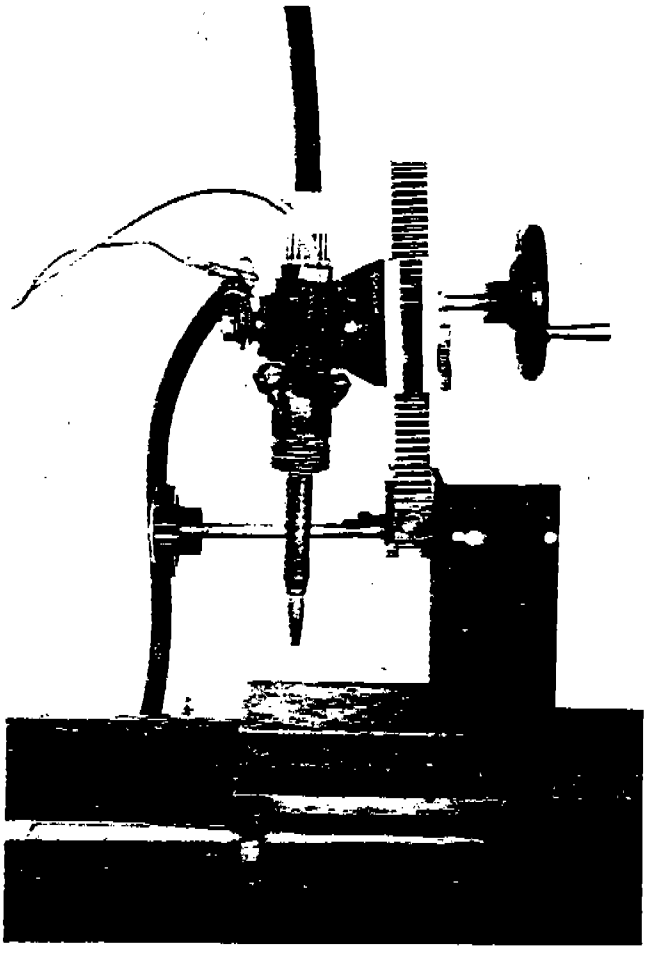

FIG 3. CLOSE-UP OF TORCH SHOWING THE MECHANISM FOR GUN ADJUSTMENT.

smelting works (ie. CSIRO considered filters used at the Port Pirie Smelters). All possible sources of filters, felt cloths and the like were contacted for samples and information. In order to reduce the tendency of fine particles to pass through the intersticies between filter fibres or the like, it was decided that a corona beam should supply gaseous current in the direction of flow of the particles in the air stream, to constrain the particles to a path perpendicular to the equipotential planes and hence to a site on a solid surface, ie. the filter fibre. The thoughts behind the electrostatic aid to filtration follow naturally from the behaviour relationships between charged substances, ie. thick film insulators discharge mechanisms of absorbed gas layers and other electrostatic phenomena.

The final choice was a felt made from polyester fibres, and an array of needle points at 12,000 volts producing point to plane electrical corona discharges to this felt (see Figure 1).

Fume monitoring requires that the rate of collection versus time be constant, ie. at the first indication of a diminished rate of capture, which is defined as the onset of clogging, the fume collection must be ceased.

Typical CSIRO collection times for fume rates of 200 g/hr (which is quite a high rate) was 30 seconds and for very high rates of 600 g/hr the times were reduced to 10 seconds.

Onset of clogging was found to occur at a filter loading of 15 g/m^2 of filter area or higher.

Figures 2 and 3 show the Fume Box arrangement and the gun adjustment mechanism for adjusting electrical stickout.

2 METHOD OF CHEMICALLY ANALYSING THE FUME

Known weights of the welding fume samples ranging from 0.1 to 0.5 grams, depending on sample availability were mixed with 6.0 grams of a lithium borate flux (12 parts lithium tetraborate to 22 parts lithium metaborate) in Pt-Rh-Au alloy crucibles. This mixture was fused in a muffle furnace for 15 minutes at 1000°C swirling the metal at five minute intervals to ensure complete sample dissolution and homogeneity. The metal was then cast into Pt-Rh-Au alloy moulds also heated to 1000°C. On cooling, this produced glass beads 40 mm in diameter suitable for analysis on x-ray fluorescence (XRF) spectrometers.

The concentration of all elements in Table 2 except fluorine were determined on a PW1400 wavelength dispersive XRF spectrometer. The spectrometer was equipped with a chromium tube powered at 50 kV and 50 mA. Measurements were made on the Lα line of barium and Kα lines of the remaining elements. All measured lines were corrected for background and line overlaps if present. Matrix effects were accounted for using matrix coefficients obtained from a fundamental parameters programme written by one of us (UES) which is based on the method of de Jongh[4].

The concentration of fluorine was not determined in the PW1400 due to the low excitation efficiency of the chromium tube for this element.

Fluorine concentrations were therefore determined on a PW1600 wavelength dispersive XRF spectrometer using a rhodium tube at 40 kV and 50 mA. The concentra-

TABLE 1 RESULTS OF FUME TESTING BY CSIRO ADELAIDE FUME GENERATION DATA

Flux Cored Welding Wires (Gasless and Gas Shielded)

M_1 = 25% CO_2 in argon
M_2 = 16% CO_2, 2.5% O_2 in argon

	SAA Classification	AWS Classification	Wire dia mm	Current	Voltage	Travel Speed mm/min	Fume Generation Rate g/hr	Fume Generation per kg of electrode g/kge
1	ETD Cp-W502H	E70 T-1-CO_2	1.6	275	28	360	50	12.0
2	ETD Cp-W502H	E70 T-1-CO_2	1.6	350	28.5	510	58	7.3
3	ETD Mp-W502	E70 T-1-M_1	1.6	400	30	610	100	15.4
4	*	E70 T-1-CO_2	2.4	450	28	465	75	9.4
5	*	E70 T-1-CO_2	2.4	550	33	575	90	9.0
6	ETP Mp-W502	E71 T-1-M_1	1.2	240	26	310	45	9.0
7	ETP Cp-W502H	E71 T-1-CO_2	1.2	240	28	345	45	9.0
8	ETP Cp-W502	E71 T-1-CO_2	1.2	250	31	410	40	7.3
9	ETP Mp-W502H	E71 T-1-M_1	1.6	275	26	310	40	7.5
10	ETP Cp-W502H	E71 T-1-CO_2	1.6	275	27	310	50	9.7
11	ETD Mp-W504H	E71 T-1-M_1	1.6	300	28	360	58	13.4
12	ETP Cp-W502	E71 T-1-CO_2	1.6	350	32	510	68	10.1
13	ETD Mp-W502H	E70 T-G-M_2	1.6	340	30	470	48	7.5
14	ETD Cp-W502H	E70 T-G-CO_2	1.6	340	32	465	52	8.3
15	ETD Mp-W502H	E70 T-G-M_2	1.6	350	32.5	490	30-60	4.7-9.4
16	ETD Cp-W502H	E70 T-G-CO_2	1.6	380	33	560	63	8.4
17	ETD Cp-W502H	E70 T-G-CO_2	2.4	450	32	550	70	9.8
18	*	E70 T-2-CO_2	1.6	300	27	350	60	11.9
19	*	E70 T-2-CO_2	1.6	375	30	480	72	9.8
20	ETD Np-W500	E70 T-4	2.4	325	28.5	360	95	17
21	ETD Np-W500	E70 T-4	2.4	350	30	400	112	14.6
22	ETD Np-W500	E70 T-4	3.0	400	28	360	115	21.8
23	ETD Np-W500	E70 T-4	3.0	420	28	340	180	19
24	ETD Np-W500	E70 T-4	3.0	470	28-29	385	240	23
25	ETD Np-W500	E70 T-4	3.0	550	31-32	530	350	26
26	ETD Mp-W503H	E70 T-5-M_1	1.6	300	26	340	48	8.8
27	ETD Cp-W503H	E70 T-5-CO_2	1.6	300	28	370	65	11.3
28	ETP Cp-W503H	E70 T-5-CO_2	1.6	360	32	510	105	14.7
29	ETD Mp-W503H	E70 T-5-M_1	1.6	400	30	500	85	12.2
30	*	E70 T-5-CO_2	2.4	300	26	290	95	18.8
31	ETD Cp-W503H	E70 T-5-CO_2	2.4	400	28	470	100	17.3
32	ETP Cp-W503H	E70 T-5-CO_2	2.4	400	32	480	110	18.4
33	*	E70 T-5-CO_2	2.4	500	32	609	196	22.3
34	ETD Nn-W500	E70 T-7	2.4	200	21	160	70	23
35	ETD Nn-W500	E70 T-7	2.4	340	25	310	180	29
36	ETD Nn-W500	E70 T-7	2.4	490	30	550	430	41
37	**	E110 T5-K3 CO_2	2.4	370	32	360	120	20.8
38	ETP Nn-W500	E71 T-11	1.7	120	19	110	25	19
39	ETP Nn-W500	E71 T-11	1.7	140	19	120	40	21
40	ETP Nn-W500	E71 T-11	1.7	200	19	160	50	17

* *Supplier has not provided Australian Classification.*
** *There is no Australian Classification.*

B-5

ORDER OF EXPRESSION FOR AUSTRALIAN SAA CLASSIFICATION SYSTEM (AS 2203)

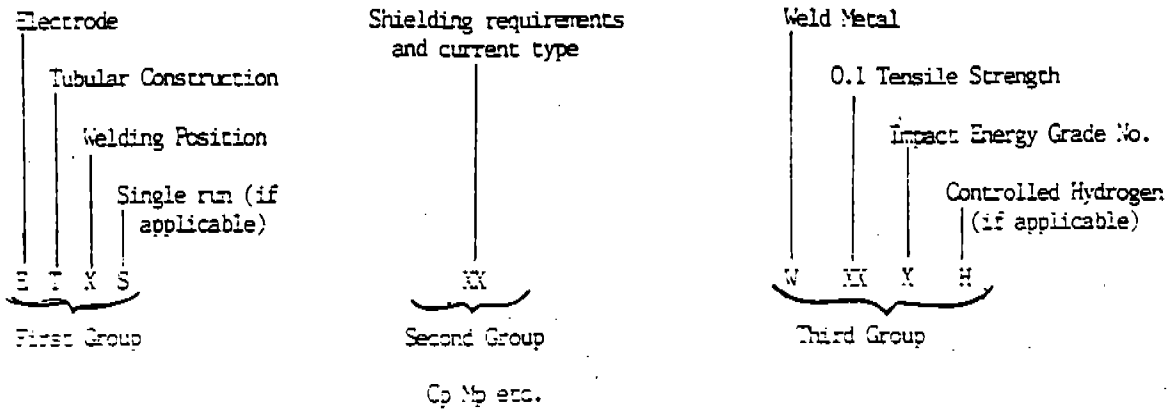

tions of the remaining elements of Table 2 with the exception of V, Ni, Cu and Ba were also determined on this instrument for use in correcting for matrix effects on the fluorine Kα radiation and to provide a check on the PW1400 results.

Concentrations of V, Ni, Cu and Ba were not determined on the PW1600 because existing calibrations on this instrument did not include these elements.

Since a glass bead technique was used to prepare the samples, particle size and mineralogical effects on the intensities of the analyte lines are eliminated and matrix effects are greatly reduced. The effect of omitting the fluorine matrix correction to the determined concentrations of the remaining elements measured on the PW1400 was thus expected to be small due to the small matrix coefficient of fluorine on the remaining elements. The effect of excluding V, Ni Cu and B matrix corrections in the PW1600 results were also expected to be small due to the low concentrations of these elements in the fume samples. These expectations were confirmed by the close agreement between results obtained on both instruments.

3 RESULTS

The wires have been classified according to AWS and SAA. The essential parameters listed for each are shown in the Tables.

Table 1 shows the fume generation data (intrinsic or total particulate matter generated over a specific arcing time). The generation rate is measured in gms/hour. There is also a figure showing generation in gms/kg of electrode wire to show the effect of welding productivity, which is a feature of these wires.

Table 2 shows the elemental analysis of fume deposits as a percentage by weight.

Table 3 shows the weld parameters nominated by manufacturers for their particular flux-cored wires.

Table 4 shows the comparison between CSIRO and AWS fume results for 3 wire types E70-T1, E70-T4 and E70-T5. (AWS had a limited range of F/C wires.)

Figure 4 shows fume generation graphs in g/hr related to the welding current for various types of wire. The graphs are shown for each wire classification and freehand curves have been drawn between the points.

Figure 5 shows the weight of fume per kg of electrode consumed, related to welding current for various types of wire.

4 DISCUSSION

The method of fume collection established by CSIRO Adelaide is an important one for coping with the high fume generation processes associated with flux-cored wires. The ability to operate the welding for long periods before the onset of clogging means that the results can be more accurate due to longer averaging times.

Comparing the results with some similar work completed by AWS in 1979 shows by and large agreements in the major fume measuring parameters for three types of wire. Table 4 is a comparison that has been made on results for the type wires E70-T1, E70-T4 and E70-T5. The comparison is limited because the other wire types were not tested by AWS. There were also limitations in the wire sizes available for comparison as the more recent trend is to use thinner wires particularly for out of position welding. Given the changes in welding conditions between the two sets of test figures there is reasonable correlation between the results.

The work completed in this study extends previous data[5] on fume generation and analysis to electrodes covered by the AWS classifications E71T1, E70T6, E70T2, E70T7, E110T5-K3 and E71T11.

By using XRF to analyse the fume, the presence of elements of atomic number greater than eight could be detected and quantitatively determined. However, the method precluded a study on the lithium content of the fume, a component known to be a minor constituent in some electrodes.

Small quantities of strontium were found in the E71T11 electrode fume. This is not considered significant in terms of health risk.

The various wire classifications conformed in a general way chemically, despite the variety of wires being tested from five different companies, ie. the gasless wires contain levels of aluminium, magnesium, calcium and fluoride, the basic wires are high in fluoride and calcium whilst the rutile electrodes are higher in titanium, etc.

The significance of these results is that they can be used for estimating the requirements of ventilation. The limitation of respirable air for dust loading at 5 mg/cubic metre will be rapidly exceeded by many of these wires in a confined location. The individual element limitation for iron oxide and fluorides is also likely to be exceeded in confined areas.

Overall, the results show that gasless wires type E70T4, E70T7 and E71T11 have higher fume generation than gas-shielded wires although the figures are modified when the deposition rate is considered.

Small amounts of barium were measured in the gasless wires E70T7 and E71T11 but only negligible amounts in the E70T4 type.

The gasless wires have the ability to withstand wind

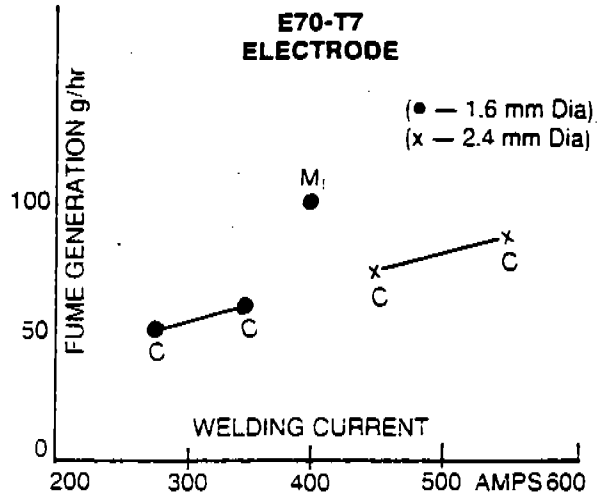

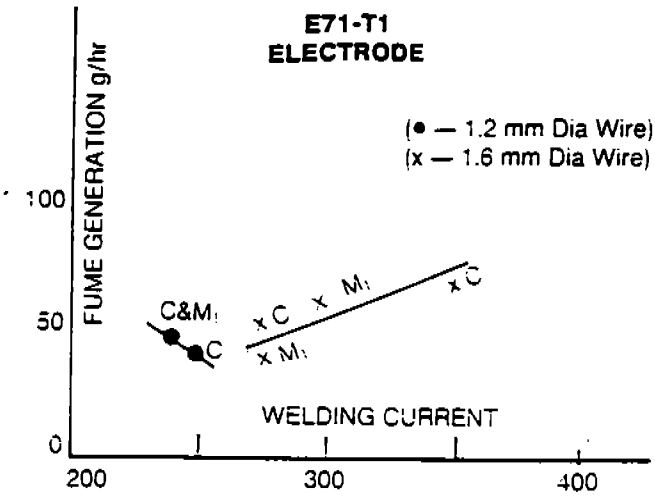

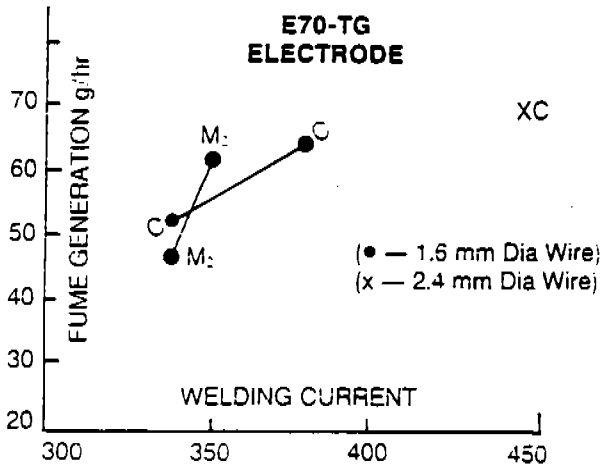

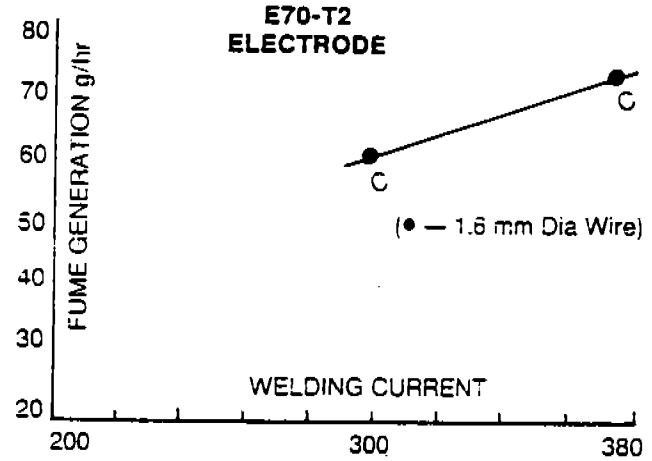

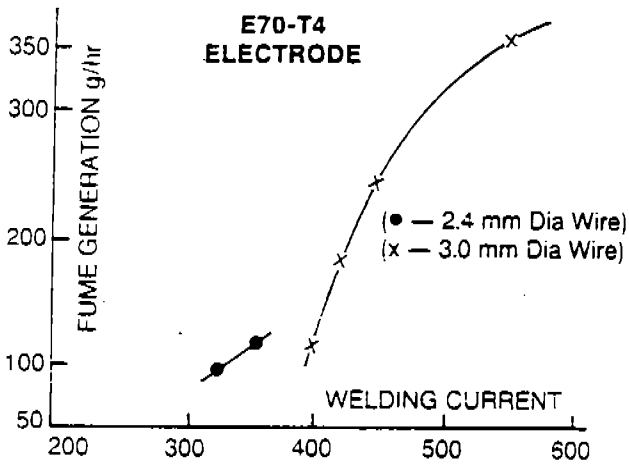

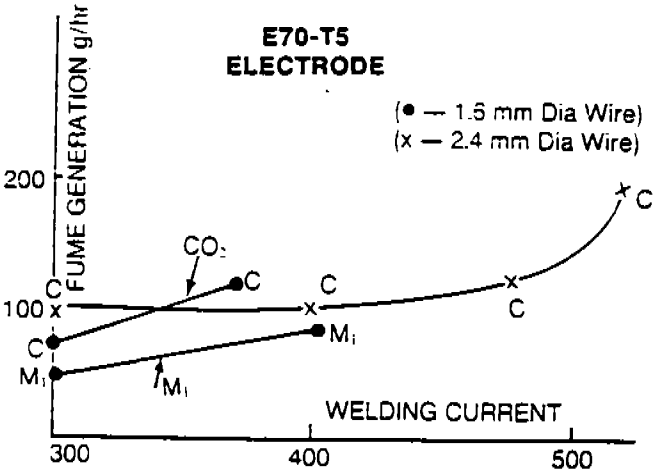

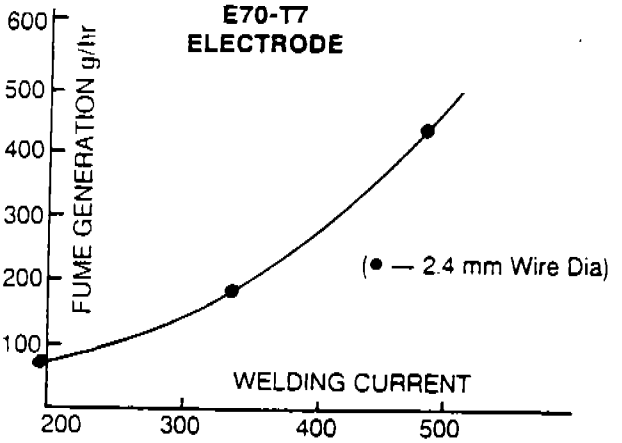

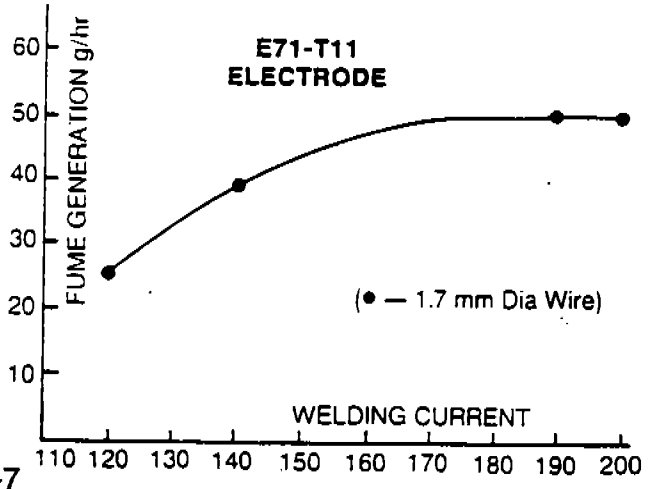

FIG. 4. FUME GENERATION RATE.

TABLE 2 WELDING FUME ANALYSIS

	Classification	Sample No.	Elemental Composition in % Ti	Si	Fe	Al	Mn	Ca	Mg	S	K	Na	Cr	F	Zn	Ni	Cu	Ba	V	Sr
1	E70T-1CO2	4	2.5	5.5	45.5	.03	10.8	.11	<.01	.05	.06	3.0	.02	<.1	.10	.03	.18	.01	.03	ND
2	E70T-1CO2	18	2.8	5.5	37.8	.48	9.5	.29	.48	.09	2.1	5.3	.02	9.4	15	.03	.15	<.01	04	ND
3	E70T-1M1	3	.11	5.4	52.5	.27	7.2	.36	.30	.05	.03	.96	<.01	<.1	02	04	.17	<.01	.009	ND
4	E70T-1CO2	40	2.2	7.5	43.1	.03	13.5	.07	.05	.04	.29	.10	.04	<.1	04	.08	.32	<.01	.03	ND
5	E70T-1CO2	41	2.2	7.5	43.1	.03	13.5	.07	.05	.04	.29	.10	.04	<.1	.04	.08	.32	<.01	.03	ND
6	E71T-1-M1	1	3.7	6.5	39.7	.11	13.5	.25	.09	.04	.12	3.9	.03	<.1	.08	.04	.17	<.01	.05	ND
7	E71T-1-CO2	2																		
8	E71T-1-CO2	11	5.5	3.4	39.9	.79	10.0	.14	.72	.10	1.1	4.5	.01	1.5	15	.03	.12	<.01	.09	ND
9	E71T-1-M1	9	3.5	7.7	34.1	.03	14.3	.29	.12	.10	.08	3.8	.02	<.1	.06	.05	.19	<.01	.06	ND
10	E71T-1-CO2	8	3.5	7.7	34.1	.03	14.3	.29	.12	.10	.08	3.8	.02	<.1	.08	.05	.19	<.01	.06	ND
11	E71T-1-M1	6	2.7	2.9	48.3	.11	7.8	.14	.45	.05	.12	4.5	.03	1.4	.06	.04	.11	<.01	.04	ND
12	E71T-1-CO2	12	5.0	3.6	43.0	.64	10.5	.14	.60	.07	.83	3.6	.02	1.0	.12	.06	.20	<.01	.08	ND
13	E70T-G-M2	25	3.1	4.6	43.1	.32	14.3	.07	.05	.05	1.7	.31	.01	<.1	40	29	.29	<.01	.04	ND
14	E70T-G-CO2	22	6.9	4.1	39.0	.74	14.0	.50	.12	.04	1.3	.16	.03	<.1	44	55	.21	<.01	.10	ND
15	E70T-G-M2	10	.13	6.6	46.5	.11	13.3	.14	.42	.07	.02	.05	.01	<.1	.14	.03	.13	<.01	.009	ND
16	E70T-G-CO2	26	6.9	4.1	39.0	.74	14.0	.50	.12	.04	1.3	.16	.03	<.1	44	55	.21	<.01	.10	ND
17	E70T-G-CO2	23	4.9	4.6	40.5	.58	15.6	.26	.07	.05	1.3	.13	.03	<.1	.1	41	.25	.02	.08	ND
18	E70T-2-CO2	42	1.7	4.3	47.4	.05	10.5	.07	.05	.08	.15	4.1	.01	<.1	.02	.02	.08	<.01	.02	ND
19	E70T-2-CO2	43	1.7	4.3	47.4	.05	10.5	.07	.05	.08	.15	4.1	.01	<.1	.02	.02	.08	<.01	.02	ND
20	E70T-4	16	.01	.28	21.3	8.2	.7	19.8	8.0	.05	.15	1.1	<.01	18.5	.03	.05	.05	<.01	<.005	ND
21	E70T-4	7	.02	.61	20.1	8.2	1.4	13.9	12.1	.09	3.1	.10	<.01	15.6	.04	.02	.08	<.01	<.005	ND
22	E70T-4	15	.01	.28	28.1	8.2	1.0	14.5	7.5	.08	.12	.9	<.01	13.5	<.01	.06	.06	.01	<.005	ND
23	E70T-4	32	.01	.19	25.0	7.1	1.8	14.7	10.1	.05	1.9	.07	.01	15.4	.09	.03	.05	.04	<.005	ND
24	E70T-4	31	.01	.19	23.9	6.4	1.6	13.9	9.7	.07	2.0	.08	<.01	15.4	*	.02	.05	.04	<.005	ND
25	E70T-4	30	.01	.19	24.3	6.4	1.9	15.1	10.0	.06	2.1	.13	<.01	16.6	1	.02	.06	.04	<.005	ND
26	E70T-5-M1	24	.15	2.2	32.7	1.4	7.7	12.9	1.2	.04	4.4	.13	<.01	19.1	.14	.04	.45	<.01	.005	ND
27	E70T-5-CO2	20	.12	2.8	39.2	1.6	7.8	13.9	1.1	.03	4.9	.14	.01	21.1	.16	.03	.39	<.01	.005	ND
28	E70T-5-CO2	14	.04	3.8	41.1	.11	7.7	10.0	3.1	.04	.06	.19	.02	6.6	.04	.02	.14	<.01	.01	ND
29	E70T-5-M1	5	.19	2.9	36.7	.27	8.4	12.4	<.01	.05	.21	2.0	<.01	15.6	.06	.03	.20	.03	.008	ND
30	E70T-5-CO2	44	.29	3.3	34.3	.53	12.0	10.7	.14	<.01	2.7	.17	.02	15.5	.04	.01	.09	.01	.01	ND
31	E70T-5-CO2	21	.24	3.4	25.9	1.4	9.8	15.6	1.7	.10	5.2	.11	.02	22.5	.07	.02	.14	<.01	.005	ND
32	E70T-5-CO2	13	.06	3.5	38.8	.11	8.0	12.0	3.0	.05	.06	.15	.03	9.3	.07	.03	.18	<.01	.02	ND
33	E70T-5-CO2	46	.29	3.3	34.3	.53	12.0	10.7	.14	<.01	2.7	.17	.02	15.5	.04	.01	.09	.01	.01	ND
34	E70T-7	38	.01	.15	21.6	7.5	.74	10.1	17.4	24	1.7	.10	.15	9.8	.02	.04	.04	.6	<.005	ND
35	E70T-7	37	.01	.12	20.8	7.7	.74	11.0	16.8	.4	1.7	.05	.01	11.7	.02	.04	.05	.7	<.005	ND
36	E70T-7	36	.01	.08	26.2	7.9	.76	6.2	13.9	.16	1.4	.10	.01	10.4	.02	.03	.04	.6	<.005	1.2
37	E110T5-K3CO2	19	1.0	4.9	37.5	.32	9.7	3.7	<.01	.05	.03	4.6	.01	13.0	.04	.54	.18	<.01	.02	ND
38	E71T-11	35	.01	<.01	38.1	5.9	1.2	<.05	8.0	.03	<.01	.33	.01	4.4	.02	.03	.06	.4	<.005	12.0
39	E71T-11	34	<.01	<.01	31.1	6.6	1.2	<.05	11.3	.07	<.01	.45	.01	6.1	.03	.03	.04	.5	<.005	14.2
40	E71T-11	33	<.01	<.01	28.7	7.1	1.2	<.05	11.1	.05	<.01	.42	<.01	5.9	.03	.03	.04	.5	<.005	15.9
	TLV TWA (mg m³ (Air))		—	—	5	5	1	2	10	5	—	—	Cr 2,3,6 5	.05	2	5	1	2	.5	.05	x
	TLV STEL (mg m³ (Air))		—	20	10	—	3	—	—	10	—	—	—	—	4	10	3	—	—	—	—

TLV levels for Time Weighted Average (TWA) and Short-Term Exposure Limits (STEL) are taken from the National Health and Medical Research Council (Threshold Limit Values 1983-84).

ND = Not Detected
TWA = Time Weighted Average
STEL = Short-Term Exposure Limit
TLV = Threshold Limit Value
Cr,2, 3, 6 = Are different forms of Chromium with specific TLV levels.
X = Considered to be very similar to Ca.

effects to a resonable degree and hence these wires are commonly used in field applications, thus minimising the problems of ventilation.

REFERENCES

1 ANSI/AWS A5.20-80 — Specification for carbon steel electrodes for flux-cored arc welding.

2 AWS A5.29-80 — Specification for low alloy steel electrodes for flux cored arc welding.

3 AS2203-1981 — Carbon steel electrodes, cored (for arc welding).

4 X-ray Spectrom by W.K. de Jongh. 2(1973) 151.

5 Fumes and Gases in the Welding Environment. American Welding Society (1979).

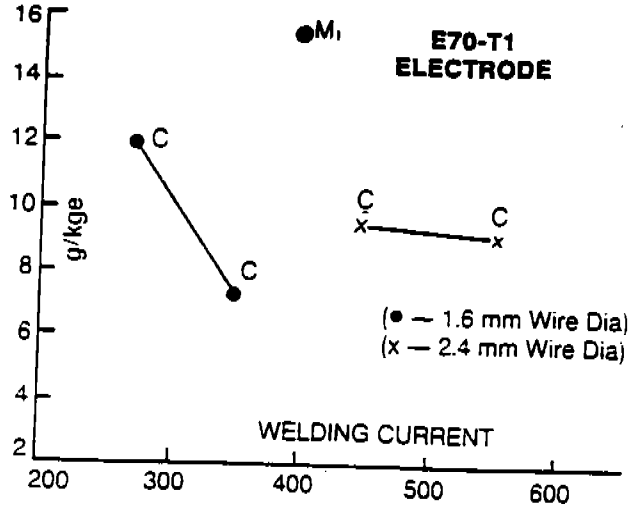

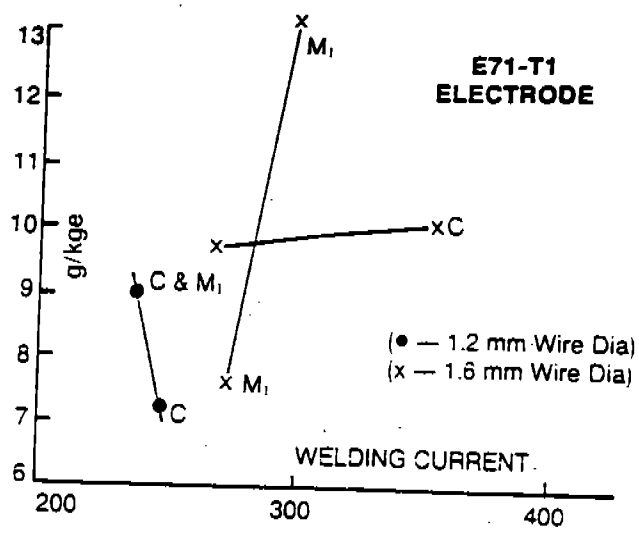

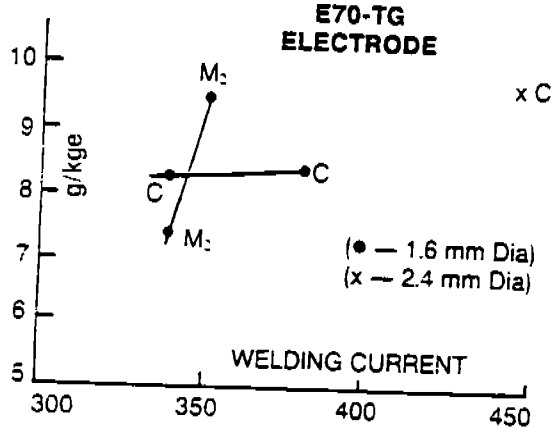

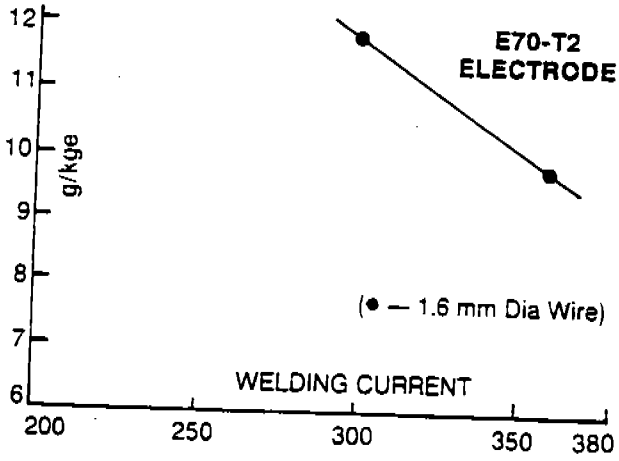

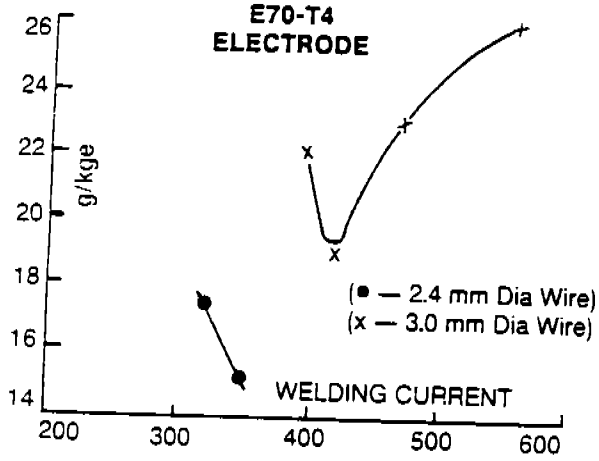

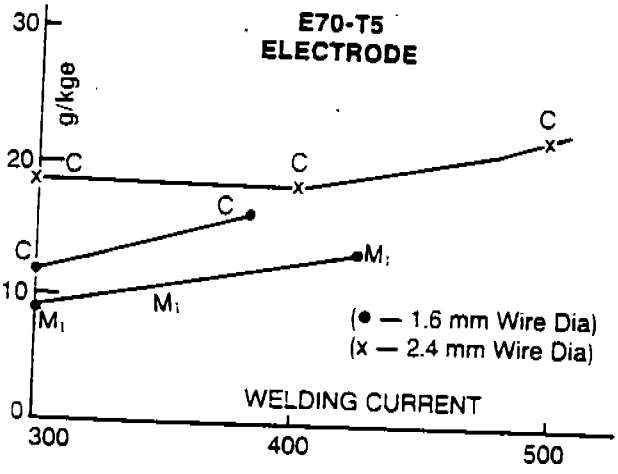

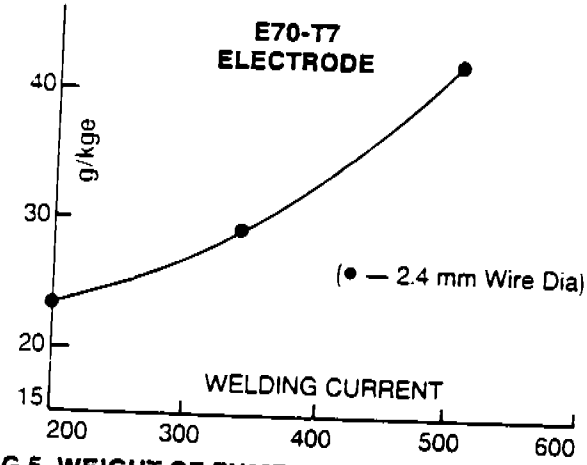

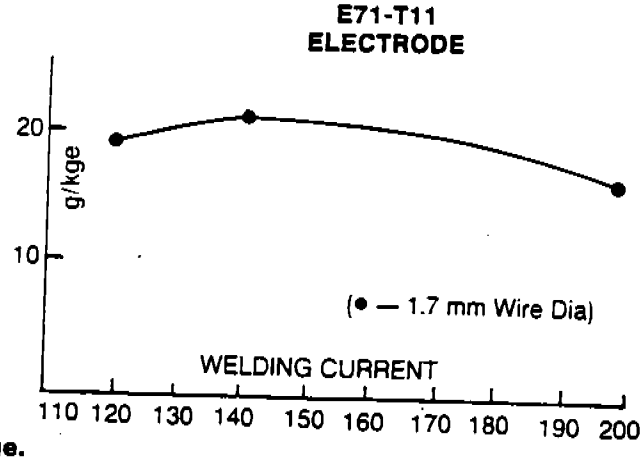

FIG 5. WEIGHT OF FUME PER kg OF ELECTRODE g/kge.

TABLE 3 WELDING PARAMETER DETAILS

	Classification	Gas Flow litres/ min	Torch Angle degrees	Stick-out mm	Wire Feed metres/ min
1	E70T-1CO2	15	80	20	5.0
2	E70T-1CO2	20	90	25	10.8
3	E70T-1M1	15	80	20	7.4
4	E70T-1CO2	20	75	25	4.4
5	E70T-1CO2	20	75	25	5.4
6	E71T-1-M1	15	80	20	12.6
7	E71T-1-CO2	—	—	—	—
8	E71T-1-CO2	20	90	25	12.8
9	E71T-1-M1	15	80	20	5.7
10	E71T-1-CO2	15	80	20	5.6
11	E71T-1-M1	15	80	20	5.2
12	E71T-1-CO2	20	90	25	10.4
13	E70T-G-M2	10	75	25	8.4
14	E70T-G-CO2	20	75	25	8.2
15	E70T-G-M2	20	90	25	7.9
16	E70T-G-CO2	20	75	25	9.8
17	E70T-G-CO2	20	75	25	4.2
18	E70T-2-CO2	15	75	20	6.4
19	E70T-2-CO2	15	75	20	9.1
20	E70T-4	—	90	40	3.8
21	E70T-4	—	80	60	4.8
22	E70T-4	—	90	40	2.2
23	E70T-4	—	60	70	3.8
24	E70T-4	—	60	70	4.45
25	E70T-4	—	60	70	5.7
26	E70T-5-M1	10	75	25	7.6
27	E70T-5-CO2	10	75	25	8.0
28	E70T-5-CO2	20	90	25	9.0
29	E70T-5-M1	15	80	20	8.5
30	E70T-5-CO2	20	75	25	2.7
31	E70T-5-CO2	10	75	25	3.4
32	E70T-5-CO2	20	90	25	3.5
33	E70T-5-CO2	20	75	25	5.1
34	E70T-7	—	60	40	1.9
35	E70T-7	—	60	40	3.8
36	E70T-7	—	60	40	6.85
37	E110T5-K3CO2	20	90	25	3.3
38	E71T-11	—	75	20	1.5
39	E71T-11	—	75	20	1.9
40	E71T-11	—	75	20	2.8

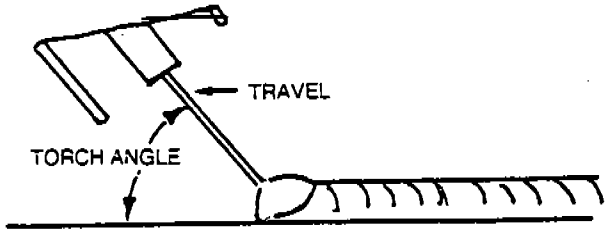

TABLE 4 COMPARISON OF FUME GENERATION RESULTS (AWS[a] AND CSIRO)

Reference and Classification	Wire Size (mm)	Current — amps / Melt Rate (kg/hr)		Voltage (volts dc)		Fume Gen' g/hr		Fume Weight to Weight El' g/kge		Stick Out (mm)	
		AWS	CSIRO	AWS	CSIRO	AWS	CSIRO	AWS	CSIRO	AWS	CSIRO
E70-T1 (AWS 44[c], Tables B12 and B43)[b] (CSIRO Nos. 4 & 5)	2.4	445/(8.17)	450 (7.9)	29	28	61	75	7.5	9.4	25.4	25
		515/(8.9)	550/(9.9)	28	33	79.2	90	7.9	9.0	25.4	25
E70-T4 (AWS 48[c], Table B12)[b] (CSIRO Nos. 20 & 21)	2.4	385/(9.2)	350/(7.6)	32	30	178	112	19.2	14.6	70	60
		390/(9.2)	325(5.5)	31	28.5	177.6	95	19.1	17	70	40
E70-T5 (AWS 44[c], Table B13)[b] (CSIRO Nos. 31 & 32)	2.4	425/(8.7)	400/(5.7)	30	28	136.2	100	15.5	17.3	38	25
		445/(8.8)	400(5.9)	31	32	135.6	110	15.4	18.4	38	25

a = American Welding Society Data taken from, "Fumes and Gases in the Welding Environment". 1979.
b = Appendix B of AWS publication (see a).
c = Electrode Code No. in AWS Publication (see a).

APPENDIX C

REFERENCE 15

(Malmquist et al., 1986)

PROCESS-DEPENDENT CHARACTERISTICS OF WELDING FUME PARTICLES

KLAS G MALMQVIST[1], GERD JOHANSSON[2,3], MATS BOHGARD[1,2] AND K ROLAND AKSELSSON[2]

1. Department of Nuclear Physics, Lund University Institute of Science and Technology, Box 118, S 221 00 Lund, SWEDEN
2. Department of Working Environment, Lund University Institute of Science and Technology, Box 118, S 221 00 Lund, SWEDEN
3. Department of Enviromental Health, University of Lund, Sölvegatan 21, S 223 62 Lund, SWEDEN

INTRODUCTION

In electric-arc welding operations more or less hazardous particles are generated. Thus there is a need for actions against health effects such as changes of welding techniques and welding parameters, changes of joining technique, local exhausts, respiratory protective equipment, job rotation and robotization. To give priority to actions involving economic as well as health factors, there is a need for reliable dose-response relations and for good exposure data. For both of these needs extensive data on process-dependent characteristics of welding fume particles are of utmost importance.

This paper describes a comprehensive investigation of the total mass emission, particle size distribution and elemental composition for 13 different welding methods at different currents and voltages. The oxidation state of chromium was also investigated where applicable. See ref. 1 for an extensive report of this work performed at the Lund Institute of Technology. The results are discussed in the light of some recent results from the literature.

EXPERIMENTAL ARRANGEMENTS

Sampling equipment

Figure 1 shows the design of the sampling arrangement. The welding takes place beneath the aluminium hood. The velocity of the air is low (<0.15 m/s) around the welding point to ensure that the welding process and the aerosol formation are not significantly affected. To obtain the size distribution the welding aerosol was sampled by a Battelle-type single orifice cascade impactor[2] drawing 1 litre/min. For an accurate investigation of the elemental composition of the welding aerosols, a membrane filter arrangement was used. The flow-rate was 1-3 l/min. To determine the total mass of the welding aerosol a glass fibre filter was used.

Analytical methods

In this investigation more than 3000 samples have been analysed for many elements. The multi-elemental analysis method PIXE[3], Particle Induced X-ray Emission, was used for quantification of all elements heavier than phosphorous. A nuclear reaction, $^{19}F(p,\alpha\gamma)^{16}O$, was used for fluorine analysis[4]. An analytical

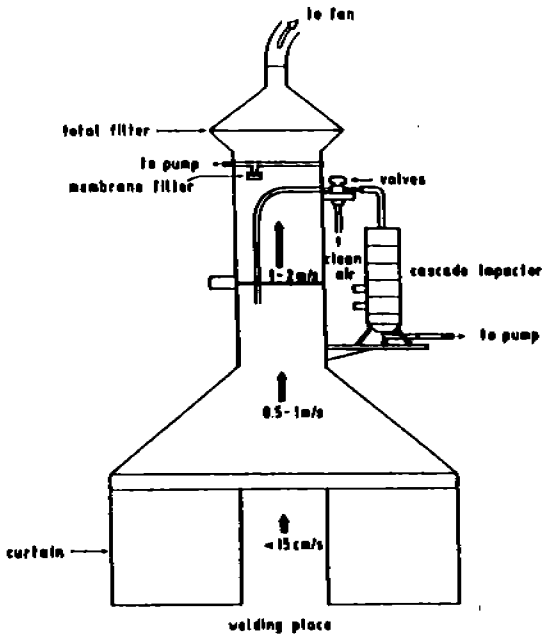

Fig. 1. Sampling equipment for the characterization of welding aerosols. The arrows indicate the air velocity in different parts of the system.

procedure was developed to quantify the masses of soluble and less soluble Cr(III) and Cr(VI) (ref. 5). This procedure includes the PIXE method, electron spectroscopy for chemical analysis (ESCA), a spectrophotometric method and transmission electron microscopy (TEM).

EXPERIMENTS

Sampling procedures

Table 1 shows the electrodes used in this investigation. For each of the electrodes the welding current was varied within the intervals recommended for each of the electrodes by the manufacturer, while the welding voltage was varied in an interval significantly larger than the recommended in order to enhance any systematic effect on the fume production.

For the direct current SMAW (Shielded Metal Arc Welding) methods reversed polarity (positive electrode) was used. The welding was performed manually by

Electrode	Type	Coating/Gas	AWS[a]-class.	Diam.(mm)
1 OK 38.65	SMAW	iron powder, low hydr. zirconium added	E 7028	3.25
2 OK 38.85	SMAW	iron powder, low hydr. rutile	E 7028	5
3 OK 38.95	SMAW	iron powder, low hydr. zirconium added	E 7028	4
4 OK 48.00	SMAW	iron powder, low hydr.	E 7018	2,3.25,4
5 OK 61.41	SMAW[b]	rutile	E 308 L-15	3.25
6 OK 63.35	SMAW[b]	low hydrogen	E 316-15	2.5,3.25,4.5
7 OK 69.21	SMAW[b]	low hydrogen-rutile	-	3.25,4,5
8 OK 12.51	GMAW	CO_2	E 70 S-6	1.2
9 OK 16.32	GMAW[b]	Ar	ER 316 L Si	1.2
10 OK 16.32	GMAW[b]	Ar/CO_2	ER 316 L Si	1.2
11 OK 18.01	GMAW[c]	Ar	Er 1260	1.2
12 OK 18.13	GMAW[c]	Ar	ER 5154	1.2

a) AWS-class. = American Welding Society classification
b) welding on stainless steel; c) welding on aluminium

Table 1. A list of the welding methods included in this study. The numbers are used for identification in the various figures.

a skilled welder exerting himself to maintain constant welding conditions.

For the GMAW (Gas Metal Arc Welding) methods the welding gun was mounted in a fixed position perpendicular to the work piece, which was fixed onto a wagon running on rails. The speed of the wagon could be varied to simulate the normal welding speed.

For each set of welding parameters three to five measurements were carried out. The results are given as averages.

RESULTS AND DISCUSSION

Total Fume Emission

For the comparison of fume production from different welding techniques, two entities can be defined, viz. the total fume emission rate, E (g/min), and the relative fume formation index, R, which is the total mass of emitted fume normalized to the mass of the deposited consumable (excluding slag) in mg/g. In Table 2, our experimental values of E and R are summarized.

The total fume emission rate is dependent on electrode dimensions and electric power. Due to variations in these parameters, E varies in the interval 0.2 to 2 g/min for the methods in the present study (except for GTAW). As can also be seen

Electrode	Diam.(mm)	I(A)[1]	U(V)[1]	E(g/min)	R(mg/g)
OK 38.65	3.25	160	35	0.58	16.7[3]
OK 38.85	5	300	34	1.30	15.7
OK 38.95	4	210	32	0.93	21.7
OK 38.95[2]	4	205[2]	30[2]	0.75	19.2
OK 48.00	3.25	140	23	0.45	26.0
OK 61.41	3.25	115	33	0.38[3]	11.3[3]
OK 63.35	4	140	24	0.39	15.6[3]
OK 69.21	4	140	22	0.29	12.4
OK 12.51 CO_2	1.2	180	30	0.23[4]	5.4[4]
OK 16.32 Ar	1.2	180	26	0.20	3.8
OK 16.32 Ar/CO_2	1.2	180	26	0.29[3]	5.7
OK 18.01 Ar	1.2	180	22	0.49	20.5
OK 18.13 Ar	1.2	160	24	0.91	24.1

1) Direct current; reversed polarity (electrode as anode).
2) Alternating current.
3) Standard error of the mean: 5-10%.
4) Standard error of the mean: 10-15%.

Table 2. The welding situations referred to in the text as "normal" welding, implying that the welding currents were chosen to be in the middle of the intervals recommended. E and R denote the total fume emission rate and the relative fume formation index respectively. The standard errors on the mean were less than 5% if not explicitly given.

from Table 2, large variations in the relative fume formation index are found between the different methods (3-35 mg/g). It may also be inferred that, with the one exception of GMAW on aluminium, the SMAW methods generally give higher values than the GMAW methods for both E and R.

The results in Table 2 can be compared with those obtained in the systematic study presented in ref. 6. The differences are normally smaller than 10%. The discrepancies might be explained by somewhat different sampling and welding conditions as well as by variations in different brands of welding consumables of the same classification and between different conditions and ages of the covered electrodes.

Shielded Metal Arc Welding. Despite their different dimensions, coatings and core compositions, the seven SMAW methods in this study seem to have approximately the same current dependence (see fig. 2). These results are in good agreement with those of refs. 6 and 7.

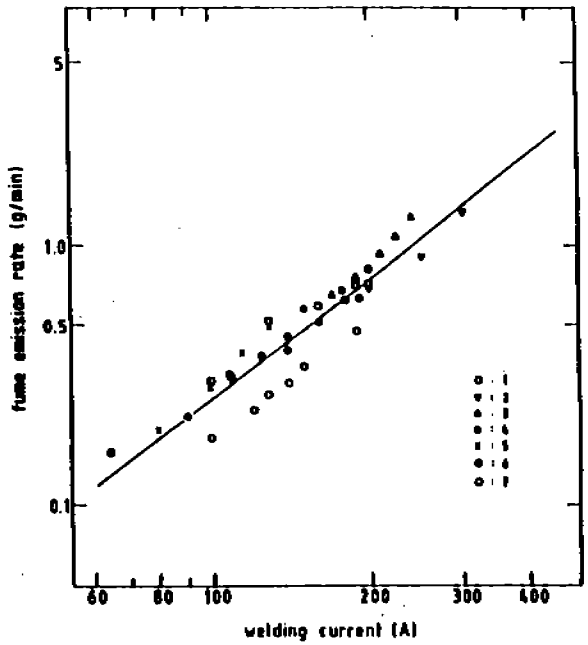

Figure 2. Total fume emission rates for all the SMAW methods in this study plotted versus welding current ($r^2 = 0.88$). The number at each symbol refers to the corresponding welding method in Table 1.

For the relative fume formation index, the influence of welding current is normally low.

In figs. 3 and 4 the total fume emission rate, E, and the relative fume formation index, R, for three SMAW methods are plotted versus welding voltage. Increases in both E and R are observed with increasing voltage. A high voltage, i.e. a long electric arc, implies an increased residence time for the transferred melted material before reaching the weld pool, thus increasing the fume formation. The covering forms a protective crater for the arc hindering oxygen penetration into the arc region. When the arc length is increased this protection may be less efficient and oxygen may interfere in the arc region. This normally promotes fume formation (ref. 8). The long arc also suffers from more severe wire explosions and bubble bursting of boiling material. The instantaneous evaporation in wire explosions and the spatter from bubble bursting have been shown by Gray et al[9]

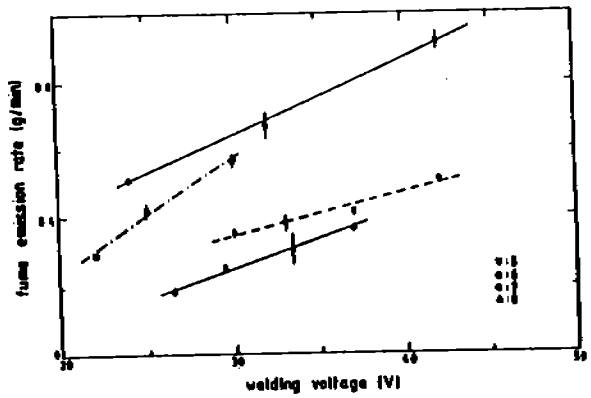

Figure 3. Total fume emission rates for three SMAW methods (stainless steel welding) and for the GMAW method with CO_2 as protective gas (mild steel welding) plotted versus welding voltage. The number at each symbol refers to the corresponding welding method in Table 1. The welding currents were 115, 160 and 140 A for methods 5,6 and 7 respectively, and 200 A for method 9. The error bars show one standard error on the mean.

to be significant sources of fumes. In GMAW the spatter produced up to 30% of the fume and is probably also important in SMAW.

The increase in the emission rate with voltage as seen in fig. 3 is very similar to that observed in other studies (10,11). From fig. 4, it is evident that the influence of the welding voltage on the fume formation index is dependent on the type of coating on the electrode in question. Part of the explanation for this finding may be the coating dependent relation between voltage and arc length. A significant impact from coating composition on fume formation has been demonstrated by Kobayashi et al[12].

Gas Metal Arc Welding. In semi-automatic gas metal arc welding the influence of the protective gas on the electric arc and on the metal transport process makes the fume emission a complex function of the welding parameters.

With pure CO_2 the transfer of the melted metal from the electrode tip to the work piece is characterized by large globules (diameter: 2 to 3 mm). If, however, the protective gas is argon or mixtures of argon and CO_2, different modes of transfer will occur. For low voltage and very low current the transfer will be short-circuiting and for somewhat higher current the transfer will be globular with decreasing size and increasing number of globules for increasing current. In these modes the tendency towards wire explosions and bubble bursting

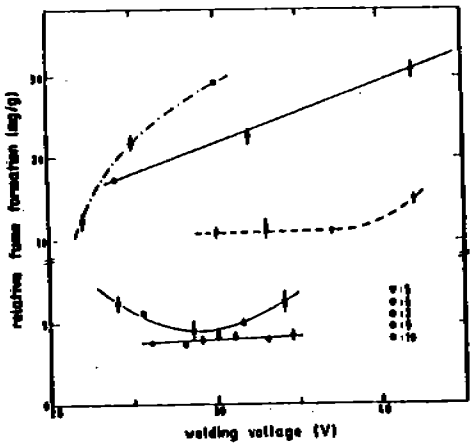

Figure 4. Relative fume formation index plotted versus welding voltage for the same SMAW methods as in figure 3 and for the GMAW method with pure argon (●) and an argon/CO_2 mixture (■) as protective gas respectively. The number at each symbol refers to the corresponding method in Table 1. The welding current in method 9 and 10 was 180 A. The error bars show one standard error on the mean. Note the shift of scale on the ordinate axis.

is rather high with spatter yielding significant fume emission as was shown by Gray et al[9]. For high voltage and high current, metal transfer becomes a spray of smaller droplets (diameters between 0.5 and 1 mm). The drop size remains essentially constant when the current is increased. The detachment of the small droplets from the electrode is due partly to the magnetic "pinch effect" and transport along the arc is due mainly to the plasma jet[13]. The value of the current at which this transition occurs is proportional to the diameter of the electrode and dependent on the material and electrode extension[14].

In fig. 4 the relative fume formation index, R, is plotted versus welding voltage with pure argon and with a mixture of 80% argon and 20% CO_2 as protective gases. While for pure argon, R is almost independent of the welding voltage, there is a well-defined minimum at a specific voltage for the Ar/CO_2 mixture. The magnitude of R is higher for all voltages when CO_2 is mixed in the gas. The oxides of several elements have higher vapour pressure than the pure elements, thus promoting fume formation in an oxidizing atmosphere (oxygen enhanced evapora-

	Elements															
No[1]	F	Cl	K	Ca	Ti	Cr	Mn	Fe	Ni	Cu	Zn	As	Rb	Zr	Mo	Pb
1	7.1		8.8	2.6		.07	5.9	32		.08	.17[3]	.06[3]		.54		.10[3]
2	11	.26[3]	15	.62	.54		4.7	24			.29[4]					
3	11	.33[3]	15	2.0			3.4	23			.04[3]			.23[3]		.07[3]
3[2]	14	.54[3]	19	1.8			2.8	11			.04[3]			.36[3]		.07
4	16		16	9.5	.45	.04	3.7	19		.01	.13	.03[3]				
5	21		18	1.3	2.1	3.4	2.4	3.7	.22	.01	.25		.02			
6	24	.34	22	10	.62	3.1	2.7	3.3	.24		.11		.01		.03	.03
7	16	.20	22	3.5	2.3	3.0	14	3.4	.44[3]		.14				.09[3]	.04[3]
8						.07[4]	7.3	45		.26[3]	.04[4]					
9						10	5.3	28	4.5	.06	.17				.95	
10						12	4.8	31	4.8	.09	.18				.92	
11						.02[4]		.12[4]		.03						
12						.04	.14	.06			.02					

1) See Table 1; 2) Alternating current; 3) Standard error of the mean: 10-20%
4) Standard error of the mean: >20%

Table 3. Relative elemental compositions (expressed as per cent of the total mass of aerosol) of the welding fumes from the welding situations described in Table 2 as determined in this study. The standard errors of the mean are less than 10% if not explicitly shown.

tion). This effect has been discussed in detail in refs. 8 and 15.

The welding current for the GMAW methods in Fig. 4 (I = 180 ± 5 A) is above the transition level for spray transfer for this particular electrode[16]. The minimum of R for the Ar/CO_2 mixture coincides with the lowest voltage at which a stable spray arc can exist. Once a stable spray arc is established, R will increase with voltage in the case of Ar/CO_2 gas but remain constant for pure argon. The increased voltage corresponds to a longer electric arc with a consequently longer residence time for the droplets in the oxidizing atmosphere while being transferred to the work piece, and hence, according to what is stated above, an increased probability for fume formation. The inert argon atmosphere, which surrounds the arc, protects the droplets from oxygen during transfer.

In pure CO_2 welding the fume emission rate increases strongly with voltage, as can be seen from fig. 3. This dependence is in good agreement with the results of refs. 17 and 18, where the same or very similar welding parameters have been used. Part of this increase with voltage is due to increased oxygen penetration into the arc but since the oxidizing CO_2 is used as a protective gas the instability and high degree of spatter is probably a more important source of increased fume production. If, instead, the welding current is increased at constant voltage, the wire feeding speed increases with decreasing length of the welding arc[17]. Due to the decreasing time for the globules in the CO_2 atmosphere, R decreases with increasing current[8]. As an example, for method 8 (see table 1) at 30 V the relative fume formation index decreased from 10 mg/g to 5 mg/g and further to 3.5 mg/g when the welding current was increased from 150 A to 200 A and further to 300 A.

Elemental Composition

In Table 3, the elemental compositions of welding aerosols including fluorine and elements heavier than sulphur are given for the different welding processes for the same parameter values as those given in Table 2.

Basically, the elemental composition of a welding aerosol reflects the composition of the consumable electrode used but often with an altered relative abundance. In the electric-arc column the highest temperature is found at the axis near the melting tip of the electrode[19]. Consequently, fumes will come mainly from the welding electrode and from the surface of the droplets being transferred in the arc. This statement is supported by the findings in ref. 20.

Table 4 gives fractionation factors of the different metals in the welding aerosol relative to the welding consumable for four different welding methods. Noticeable are the high factors for manganese (2-7) while the factors of the other elements are well below unity. This is in good agreement with the results from Kobayashi et al[20]. Since manganese has a much higher vapour pressure than, e.g. chromium and iron, it will also have a high tendency towards fume formation.

	Shielded metal arc welding		Gas metal arc welding	
	Low alloy electrodes (n=4)	Stainless steel electrodes (n=3)	CO_2 - gas Low alloy steel (n=1)	Argon - gas Stainless steel (n=2)
Cr		0.17-0.21		0.68-0.70
Mn	2.2-6.1	2.3-3.8	6.9	4.2-5.2
Fe	0.22-0.33	0.055-0.066	0.49	0.47-0.50
Ni		0.025-0.040		0.36-0.41
Mo		0.027-0.052 (n=2)		0.24-0.32

Table 4. The elemental concentrations in the fume divided by the elemental concentrations in the welding consumables. The intervals are defined by the minimum and maximum values. n = the number of methods included.

Shielded Metal Arc Welding. The voltage dependence of the relative abundances of elements in the fume is varying between different electrodes. Nevertheless, potassium and fluorine constitute one group and the core metals another group with inter-group covariations. In our results the elements of typical flux origin, e.g. fluorine and potassium, show a decrease with increasing arc voltages at low voltages. These results may seem to be contradictory to the findings by Gray et al[10]. However, the discrepancy might be explained by differences in welding parameters and electrodes used in the two investigations.

In a systematic study, Kobayashi et al[12] have shown how the concentrations of the elements in the covering are reflected in the fumes. Generally, a positive linear relation holds for all elements except fluorine and iron. The coefficients of regression depend on the vapour pressures of the respective elements. The concentrations of alkaline metals, such as potassium, are much higher in fumes from electrodes with a lime-type covering than in fumes from non-lime electrodes. The presence of calcium, especially CaF_2, in the covering seems to be the main source of this special characteristic.

The contribution to the fume from the elements in the metal core will depend on the arc voltage and on the flux composition in the covering. Generally, when the voltage is increased elements with low vapour pressures, e.g. iron, are enhanced relative to those with high vapour pressures, e.g. manganes (see fig. 5). For the electrodes OK 48.00 and OK 63.35, which have relatively equal flux compositions, this effect is pronounced. The main reason for this dependence is a relative increase in the unfractioned fume production due to increased severity of wire explosions followed by instantaneous non-fractionated vaporisation of the elements[10].

As seen in Table 3 a change from DC to AC may cause a drastic change in the relative composition. The temperature at the electrode tip depends on the

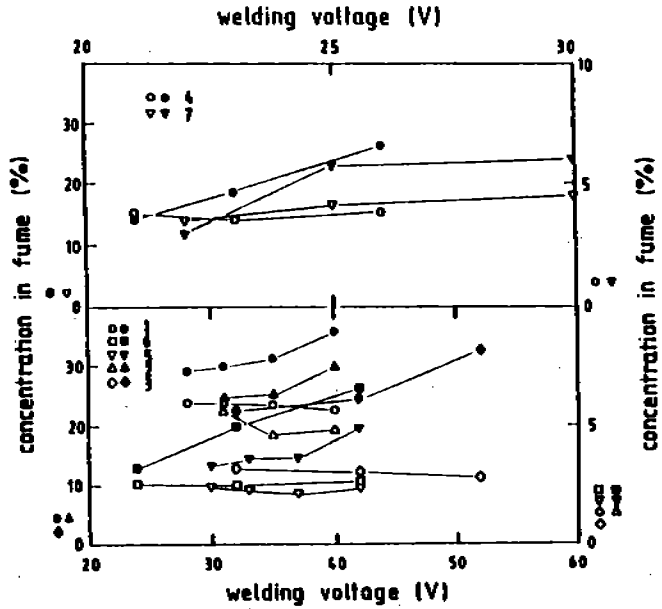

Figure 5. Iron (filled symbols), and manganese (unfilled) concentrations in the welding fume versus welding voltage for seven SMAW methods. The numbers refer to the methods given in table 1. The ordinate axis corresponding to each symbol is indicated by the symbols close to origin of each axis respectively.

polarity and consequently the use of an alternating current is expected to change the conditions for fume production and hence the chemical composition.

Gas Metal Arc Welding. In the semi-automatic GMAW methods the composition of the welding fumes is determined by the composition of the metal wire and by the character of the protective gas.

For mild steel a CO_2 atmosphere is normally used giving globular transfer. When the welding parameters are varied, no significant variation in the elemental composition has been observed in the present study. This observation is in good agreement with the results from other studies[8,21].

In fig. 6, the concentrations of five elements in the fumes versus voltage for an argon GMAW method are shown. When comparing with an argon/CO_2 mixture (80/20) all elements except manganese have higher abundances with the mixture than with

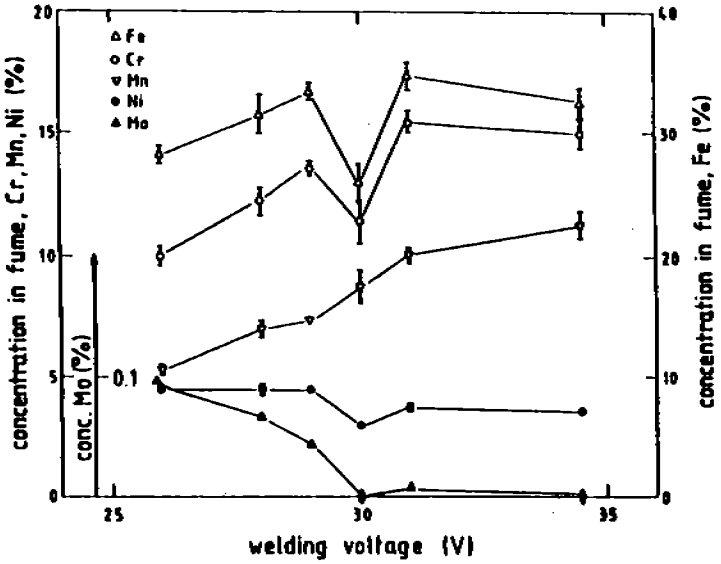

Figure 6. Relative elemental abundances from stainless steel welding with GMAW (OK 16.32, 100% argon, I = 180 A) plotted versus welding voltage. The errors indicated are one standard error on the mean.

the pure argon. For both protective gases, the general trend for chromium and manganese is an increase with voltage, while the iron concentration is essentially constant and nickel and molybdenum concentrations decrease with increasing voltage. However, in pure argon, a dip in the relative abundance is observed (at 30 V) for all elements except manganese. This minimum voltage is the lowest for which stable spray transfer can be sustained. A tentative explanation for this may be that the very stable arc, essentially free from spatter and turbulence, significantly reduces oxygen-enhanced vaporisation in the inert argon gas. When the voltage is further increased the increasing arc length makes the arc less stable again. Since CO_2 is oxidizing the same effects are not observed for argon/CO_2 as shielding gas.

In fig. 6 it can be seen that the concentration of molybdenum decreases rapidly with voltage, disappearing when the material transfer changes. Apparently the major mechanism for molybdenum to produce a fume is non-fractionated instantaneous vaporisation in connection with wire explosions which are more frequent for

globular transfer. The voltage dependence of molybdenum is in good agreement with the results obtained in a study by Gray et al[9].

Oxidation State of Chromium

See Table 5. In aerosols from the three SMAW methods for stainless steel welding, more than 50% of the chromium was found to be soluble and hexavalent. Between 60 and 100% of the chromium in the particle surface layers was hexavalent as determined by ESCA analysis, but decreases after washing the aerosol with a buffer solution (pH 7.4). Apparently most of the hexavalent chromium on the particles surfaces leaches out during washing. TEM studies have shown that after washing, the core particles consist of smaller homogeneous particles with diameters of about 0.01 µm. The ESCA results are representative of about 80% of the volume of the particles of this size. The formation of hexavalent chromium depends on which elements have been added to the coating and it has been shown by Kimura et al[22] that it is possible to reduce the amounts of hexavalent chromium by changing the additives to the coatings and still perform technically acceptable welding.

For argon gas metal arc welding only about 2% of the total chromium is soluble and hexavalent and for both the unwashed and washed aerosol samples the concentrations of hexavalent chromium on the particle surface are below the detection limit of the ESCA method (< 15%).

Within the uncertainties of the differences in welding conditions and parameters, the results concerning the content and oxidation state of chromium in welding aerosols found here are consistent with those of other studies[23-25].

Method number[1]	Diam. (mm)	I(A)	U(V)	Cr-tot (%)	A	B	C
5	3.25	100	35	3.4	.50	.60	.27
6	3.25	100	22	4.4	.73	1.00	<.15
7	3.25	105	21	2.9	.52	1.00	<.15
9	1.2	180	26	12	.019	<.15	<.15

1) see table 1
A) Cr(VI)-soluble/Cr total
B) Cr(VI)/Cr-total on the particle surfaces
C) Cr(VI)/Cr-total on the particle surfaces after washing

Table 5. Results from the determination of oxidation state and solubility of chromium in welding aerosols from stainless steel welding.

Particle Size Distribution

The mass median aerodynamic diameters (MMAD) were calculated for each element. For SMAW and GMAW methods the MMAD is between 0.35 and 0.6 μm. The variation with element is small. A typical value of the geometrical standard deviation of the distribution is 1.5. Thus the particles in all welding aerosols studied are respirable and have a rather high probability of being deposited in the lower parts of the respiratory tract. The results of refs. 6, 8, 18, 26-28 are essentially in agreement with those of the present study.

The particles emitted in SMAW methods contain significant concentrations of highly soluble and hygroscopic compounds derived from elements such as fluorine, potassium and sodium in the electrode coating. The high relative humidity of the human respiratory tract, RH > 99% in the subglottic region[29], enables the particles to rapidly absorb water, which may significantly alter the pattern of regional lung deposition.

Particle size determinations have been carried out for all methods and sets of parameters. Only negligible variations (< 10%) in the particle diameter occured. The variation in the MMAD between elements for a certain method is also negligible.

SUMMARY

Several welding methods were characterized using a specially designed collection apparatus which has been found to be reliable and to yield accurate and representative sampling of welding aerosols. The results are compared with some recent results from the literature.

The highest fume emission in this study is found for SMAW methods and for GMAW methods on aluminium followed by GMAW methods on steel. The fume emission rate (E) is determined primarily by the welding current. Similar current dependence is found for all SMAW methods if used at normal voltage. The voltage also effects E but to a smaller extent. The relative fume formation index (R) varies drastically among the methods and is dependent on the welding parameters. For gas metal arc welding of mild steel with pure CO_2 as the protective gas, R essentially decreases with increasing current.

The composition of the shielding gas in GMAW is important for the fume production. The fume formation index is higher in the case of argon/CO_2 mixture than in the case of pure argon. The influence of the welding parameters on the fume formation is altered by mixing CO_2 into the argon. This study supports the findings of earlier works, viz. that the oxidizing potential of the gas surrounding the electric arc is of considerable importance in determining the fume production, with increased fume production when the oxidation potential of the protective gas is increased.

The fume contains the same elements as the consumable but with the relative abundances changed due to fractionation effects. This is explained by the different properties of the elements, e.g. with regard to vapour pressures of the pure elements and their compounds. For SMAW only minor variations occur when the current is changed. Welding voltage and current mode (AC/DC) have drastic effects on the elemental composition of the fumes. This is probably due to changes in electric-arc length and arc characteristics. The elemental composition of a GMAW aerosol is also dependent on the protective gas. Thus, a relative decrease in several elements is noted when the transition from globular to spray transfer takes place in the argon atmosphere.

While the chromium in the SMAW aerosols is almost entirely hexavalent (and soluble), only trivalent chromium is found in the GMAW aerosols.

The particles in the welding aerosols are below 1 μm in diameter and consequently respirable. Mass median aerodynamic diameters vary from 0.35 μm to 0.6 μm and seem to be essentially independent of the welding parameters. Hygroscopicity may be an important factor in evaluating lung deposition of aerosols from SMAW methods.

ACKNOWLEDGEMENTS

We are indebted to Dr Folke Brundin for many stimulating discussions throughout this work and for putting welding equipment and other resources at our disposal at the Department of Production and Material Engineering. The skilled and patient welding of hundreds of welding joints by Mr Alex Simonsson is gratefully acknowledged as is much good advice throughout the course of this study. We have also highly appreciated the equipment built by Mr Knut Sjöberg. This study has been supported financially by the Swedish Work Environment Fund.

REFERENCES

1. G.I. Johansson, K.G. Malmqvist, M. Bohgard and K.R. Akselsson, "Characteristics of Welding Fumes", In "Proton Induced X-ray Emission - mass calibration, computer analysis and applications to work environment aerosols", (thesis, 1981); Department of Nuclear Physics, Lund University Institute of Science and Technology, Box 118, S 221 00 Lund, Sweden
2. R.I. Mitchell and J.M. Pilcher, Ind. and Eng. Chem., 15 (1959) 1039
3. S.A.E. Johansson and T.B. Johansson, Nucl. Instr. and Meth., 137 (1976) 473
4. K.G. Malmqvist, G.I. Johansson and K.R. Akselsson, J. of Radioanal. Chem., 74 (1982) 125
5. M. Bohgard, B.L. Jangida and K.R. Akselsson, Ann. Occup. Hyg., 22 (1979) 241
6. Fumes and Gases in the Welding Environment, American Welding Society, Miami (1979)
7. M. Kobayashi, S. Maki and J. Ohe, Inst. of Welding, Doc VIII-670-76 (1976)
8. R.F. Heile and D.C. Hill, Welding Journal, 54 (1975) 201s

9. C.N. Gray, P.J. Hewitt and P.R.M. Dare, Welding and Metal Fabrication, (okt 1982) 393
10. C.N. Gray, P.J. Hewitt and P.R.M. Dare, Welding and Metal Fabrication (jan/feb 1983) 52
11. F. Eichhorn and F. Trösken, Technical Report DVS Berichte 1977 (in German)
12. M. Kobayashi, S. Maki, Y. Hashimoto and T. Suga, Welding Journal, 62 (1983) 190s
13. J.C. Needham, C.J. Cooksey and D.R. Milner, Brit. Weld. J., 7 (1960) 297
14. A. Lesnewich, Welding Journal, (sept 1958) 418s
15. I.R. Patskevich and O.A. Rykov, Avt. Svarka, 8 (1971) 15, in Russian
16. L.F. Defize and P.C. van den Willigen, Brit. Weld. J., 7 (1960) 297
17. B. Haas and H.V. Pomaska, Proc. of Coll. on Welding and Health, (1980) No 10
18. F. Eichhorn and F. Trösken, Industrie Anzeigen, 101 (1979) 31, in German
19. L.A. King and J.A. Howes, Proc. Physics of the Welding Arc, (1962) 180
20. M. Kobayashi, S. Maki, Y. Hashimoto and T. Suga, Weld. in the World., 16, No 11/12 (1978) 238
21. M.J. Erman, E.E. Raiskiy and A.G. Potapevskiy, Autom. Weld., 21, No 4, (1968) 65
22. S. Kimura, M. Kobayashi, T. Godai and S. Minato, Proc. of Coll. on Welding and Health, (1980) No 16
23. G.M. Lautner, J.C. Carver and R.B. Konzen, Am. Ind. Hyg. Ass. J., 39 (1978) 651
24. S. Kimura, M. Kobayashi, T. Godai and S. Minato, Weld. Journal, 58 (1979) 195 s
25. E. Thomsen and R.M. Stern, Scand. J. Work Environ. Health, 5 (1979) 386
26. The Welding Environment, American Welding Society, Miami (1973)
27. R.M. Stern, "The production and characterization of a reference standard welding fume", Part 2, SVC/SF 78-08, The Danish Welding Institute, Copenhagen (1978)
28. I.M. Naumenko and L.V. Ferdman, Svar.Proizvod., 8 (1974) 50, in Russian
29. J. Postendörfer, J. Aerosol Science, 2 (1971) 73, in German

EXPOSURE MONITORING AND CHEMICAL ANALYSIS OF WELDING FUME

E. THOMSEN, Chemconsult, Oldvejen 7, Rågerup, DK 4050 Skibby
R.M. STERN, Danish Welding Institute, Park Alle 345, DK 2600 Glostrup.
B. PEDERSEN, Danish Institute of Occupational Health, Baunegårdsvej 73, DK 2900 Hellerup.

INTRODUCTION

Standardised and quality assured sampling and analysis procedures for welding fumes are essential in efforts to demonstrate causality between occupational exposures and possible health effects. Three important but frequently overlooked sources of significant errors are: Loss of reactive species during collection and storage. Losses due to incomplete digestion of refractory matricies. Changes in species (solubility, oxidation state) during analysis.

In the case of metal inert gas (MIG) and electrode (MMA) welding of stainless steel (SS), it has been shown that over 90% of the Cr content of MMA/SS fume of 5-8% is in the form of stable water soluble Cr(VI), MIG/SS fume may contain 11-13% Cr, of which only 50-75% is detected by standard aqua regia digestion procedures. Complete digestion with perchloric acid can lead to significant loss due to formation of volatile CrO_2Cl_2 (1). The water soluble Cr(VI) content, thought to be 0,1-0,5% decays towards zero in the solid MIG/SS fume after collection on membrane filters independent of filter type (2). When collected in an impinger filled with water short arc MIG/SS fume appears to contain of the order of 3% stable water soluble Cr(VI) (3). This ample evidence that monitoring and analysis dependent effects can lead to severe underreporting of exposures to toxic species such as Cr(VI) suggest the need for establishing standardized and appropiate protocols for use with welding fumes, as reported below.

MATERIALS AND METHODS.

MIG/SS Welding Fumes are produced in downhand welding on stainless plate with the aid of a robot (ESAB 3RS17 1.2mm wire, 20 l/min Ar or Ar+2%O_2, 30 cm bead, 10 cm/min). The fumes are collected via a 20 cm diameter 1.5 m column on Watman 41 paper filters, and/or in an impinger (0.2-0.5 mm orifice, 1-1.2 l/min, 50 ml liquid volume (destilled water) having parallel filter cassette for absolute determination of fume densities: fume concentrations are typical 200 mg/m3 with filter placed in top of column. Aliquots are removed convenient at intervals for analysis.

Chemical Analysis is performed either on total fume scraped from the membrane filters or collected in the impinger, or on water soluble species (30 min. at 20°C under agitation) and precipitate seperately, using atomic absorption (AAS). In some cases the filter is carried along with the sample to determine filte-matrix effects if any. Cr(VI) is determined using the standard diphenylcarbazide technique (DPC).

Fume Digestion is performed using a series of methods to enable a determination of procedures dependence if any as

APPENDIX D

REFERENCE 21

(Moreton, 1985)

Fume emission when welding stainless steel

Health aspects of chromium compounds in welding fume are a subject of much current concern, and hence there is particular interest in measurements of fume emission in stainless steel welding. **J Moreton, E A Smårs** and **K R Spiller** measured fume emission rates from a variety of stainless consumables, and demonstrated effects of changing welding process and conditions.

A previous article described measurement of fume emission rates using a fume box technique, and subsequent chemical analysis of fumes from a range of open arc welding processes.[1] The feasibility of testing consumables from different processes by the fume box method allows between-process comparisons to be made for fume emission potential, especially in cases where the quantity and/or toxicity of the fume may be critical. With the current worldwide concern regarding health aspects of chromium compounds in welding fume,[2] measurements of fume emission during welding of stainless steel are of special interest.

In the study reported here, fume emission rate measurements were made by the fume box technique[3] on typical 18:10:3 Cr:Ni:Mo stainless consumables, as follows:

A—manual metal arc (MMA) electrode;

B—metal active gas (MAG) consumable with Ar-2%O_2 shielding gas;

C—flux cored wire (FCW) self-shielded consumable;

D—metal cored wire (MCW) gas shielded consumable.

Specifications are given in Table 1. All these consumables can be used for the same welding application. The MAG consumable B was also tested (B1-B5) under five different welding conditions, to provide an indication of the possible range of fume emission rates for a single consumable within a process. Because of the possibilities of using dip, globular, spray and pulse modes of metal transfer, the range of corresponding fume emission rates with a given MAG consumable is probably greater than with those consumables used for the other processes.

Although there is a considerable practical demand for a fume emission rate test method, no standard for such a method currently exists in the UK. The method used is derived from the Swedish Standard[4] for measurement of fume emission rates and related parameters for MMA consumables only. Therefore, the work described employs what are currently Welding Institute in-house test methods. The results, however, have a general comparative significance.

Janet Moreton, MA, is a Principal Research Chemist in the Materials Department of The Welding Institute; Erik Smårs, DEng, is Manager of R & D in Welding Technology, AGA, Lidingoe, Sweden; and Bob Spiller is a Senior Welding Engineer in the Production Systems Department of The Welding Institute.

EMISSION RATE MEASUREMENTS

Welding fume emission rate (FER) measurements were made on consumables A, B, C and D using the fume box described in ref. 1. Horizontal-vertical fillet welds were made on 250×50×10mm, 316 stainless steel testpieces in the fume box, and the particulate fume emitted was extracted on to a 240mm diameter preweighed filter. The weight of fume collected per unit arcing time (or per unit weight of deposited metal) gives the FER of the consumable.

Welding details are given in Table 1. Results of the fume analyses are given in Table 2. The analysis of the stainless steel base plate materials used in the test, and of the consumables (coatings, cores, sheaths and wires) was made by Xray fluorescence spectroscopy, and is reported in Table 3. Because of the diversity of welding conditions required by the different consumables, it was not possible to use the same welding equipment for all tests. The fume emission rate of the MAG wire, B, was investigated under a range of parameters, with Ar-2%O_2 gas shield: dip transfer, B1a and B1b, globular, B and B2, spray, B3 and B4, and pulse, B5.

For the MAG welding tests (B1-B5 inclusive), it was considered important to define closely the mode of transfer of each test, not only in terms of monitored welding parameters (Table 1), but also to ensure that the welds produced in the fume box were of a comparable standard to those common in industry. Prior to welding, the required parameters for the various modes of metal transfer were established. The fillet weld specimens were then completed by a welder of average ability who had experience in using the gas shielded arc welding process. Tests B1a and B1b, using a dip transfer condition are replicate sets using two different welding power sources and illustrate that possible varying inductances and widely differing open circuit voltages at constant arc voltage appear not to influence the FER results. It was not practicable in either power source to adjust the inductance, this being a preset factor within the power units for a given wire diameter. In all MAG tests, each fillet weld was made using the conventional leftward technique, *i.e.* traversing the welding gun from right to left, the gun preceding the deposited weld bead. Throughout the trials the nozzle of the welding gun to work distance was maintained to within 10-15mm. Observations of the welding operation and of the fillet welds produced using each of the selected modes of metal transfer and associated welding parameters clearly indicated that acceptable welds were being produced. On completion of the welding programme, the fillet welded specimens were seeded into their representative groups and visually examined, with measurements being taken to determine the leg lengths of each weld. The results of this examination, albeit a subjective one, are summarised in Table 4.

For each set of experiments, A-D, B1-B5, gravimetric tests were made with humidity-stable glass fibre filters. The filters were weighed before and after welding, as were the corresponding test plates. These weights, and the relevant arcing times were used to calculate the fume emission rates illustrated in Fig. 1 in terms of mg/g of deposited metal and mg/sec of arcing time.

For the MMA consumable (A), nominal arcing time was 60sec, for the MAG wire (B) it was usually 30sec, and for the FCW and MCW consumables, C and D respectively, it was reduced to 20sec.

During sampling, for each experiment, a bulk sample of at least 1g fume was collected where possible, on a 240mm diameter filter paper. This fume was removed by careful brushing with a camel hair brush, and stored in a dry box for analysis, by the following techniques:

a Fluorine (samples A and B only) by pyrohydrolysis, using a volumetric finish with thorium nitrate:

Table 1 Consumables and welding parameters

Code	Process	Standard grade	Dia, mm	Welding parameters: Current, A	Voltage, V	O/C, V	WFS, m/min	Stickout, mm	Gas shield	Gas flow, l/min
A	Manual metal arc (MMA)	BS 2926 (1970) 19 12 3LR AWS A5. 4 81 E316L-16	4.0	145±10	28-29	70DC+				
B	Gas shielded solid wire (MAG)	BS 2901 Pt 2. 316S 93 AWS A5. 9 77 ER316L Si	1.2	190±10	19-20	35DC+	6.0	15	Ar/2%O_2	16
C	Flux cored wire (FCW) self-shielded	AWS A5. 22 80 E316LT-3	2.0	250±10	24	37DC+	5.5	20-25		
D	Metal cored wire (MCW) gas shielded	AWS A5. 22 80 E316LT, 1, 2, 3	1.6	290±10	24-25	32DC+	7.2	15-20	Ar/2%O_2	16
B1a	MAG dip transfer	As B	1.2	150-160	17.9 (mean)	68DC+	4.2	10	Ar/2%O_2	16
B1b	MAG dip transfer	As B	1.2	150-160	17.0 (mean)	26DC+	4.8	10	Ar/2%O_2	16
B2	MAG globular transfer	As B	1.2	210-220	21.6 (mean)	70DC+	6.7	15	Ar/2%O_2	16
B3	MAG spray transfer	As B	1.2	275-280	25.2 (mean)	36DC+	11.6	15	Ar/2%O_2	16
B4	MAG spray transfer	As B	1.2	280-290	27.6 (mean)	41DC+	9.3	15	Ar/2%O_2	16
B5	MAG pulse transfer	As B	1.2	165-170 (mean)	22.0 (mean)	74DC+	4.6	10	Ar/2%O_2	16

Table 2 Chemical analyses of fumes, wt %

Code	Si	Ti	Zr	Al	Fe	Mn	Ca	Mg	Na	K	Li	F	Ba	Ni	Mo	Nb	V	Cu	Cr	Total CrVI
A	10.0	2.1	<0.2	1.4	5.1	5.0	0.4	<0.2	7.3	19.9	<0.2	14.9	<0.1	0.4	<0.2	<0.1	<0.1	<0.1	5.0	4.1
B	1.7	0.1	<0.2	0.2	33.3	12.6	<0.2	<0.2	0.2	<0.1	<0.2	–	<0.1	4.9	0.6	<0.1	<0.1	0.6	13.4	0.2
C	4.0	2.7	<0.2	2.4	13.4	4.8	1.9	0.9	17.0	3.0	<0.2	15.5	<0.1	1.3	0.4	<0.1	<0.1	<0.1	5.1	2.7
D	3.6	0.2	<0.2	0.8	31.9	9.3	<0.2	<0.2	0.4	<0.1	<0.2	–	<0.1	4.7	0.8	<0.1	<0.1	<0.1	11.7	0.2
B1a					27.6	11.0	<0.1	<0.1		<0.1			<0.1	3.8	0.8	<0.1	<0.1	0.2	9.5	0.3
B2					29.9	9.9	<0.1	<0.1		<0.1			<0.1	4.5	0.8	<0.1	<0.1	0.2	10.0	0.3
B3					34.5	7.5	<0.1	<0.1		<0.1			<0.1	5.7	1.1	<0.1	<0.1	0.2	8.9	0.4
B4*					36.0	14.7	<0.1	<0.1		<0.1			<0.1	4.4	<0.1	<0.1	<0.1	0.5	11.6	0.2
B5*					22.4	17.6	<0.1	<0.1		<0.1			<0.1	2.6	<0.1	<0.1	<0.1	0.4	8.2	0.2

* *Reduced analytical accuracy since only 0.3g fume available.*

Table 3 Consumables analysis, wt %

a) **Plates**

Plate	C	S	P	Si	Mn	Ni	Cr	Mo	V	Cu	Nb	Ti	Co
23587	0.046	0.014	0.047	0.70	2.01	10.5	17.0	2.38	0.06	0.38	<0.01	<0.1	0.25
23776	0.043	0.020	0.036	0.70	1.57	9.6	17.7	0.31	0.03	0.28	<0.01	0.30	0.16

b) **MMA coating**

Consumable coating	Si	Ti	Zr	Al	Fe	Mn	Ca	Mg	Na	K	Li	F	CO_2	Ba	Ni	Cr	Mo	Nb	V	Cu
A	9.1	17.9	0.2	2.0	9.8	4.8	4.3	0.4	1.4	2.3	<0.2	2.3	2.8	0.1	1.0	11.1	0.3	0.1	0.2	<0.1

c) **Consumables**

	C	S	P	Si	Mn	Ni	Cr	Mo	V	Cu	Nb	Ti	Co
MMA core, A	0.014	0.005	0.013	0.06	1.32	12.8	18.5	2.68	0.04	0.10	<0.01	0.01	0.05
MAG wire, B	0.027	0.005	0.024	0.71	1.89	12.1	18.4	2.53	0.06	0.22	<0.01	0.02	0.05
MCW wire, D	0.015	0.016	0.011	0.78	1.43	11.5	18.5	2.23	0.01	0.03	<0.01	0.01	0.01
MAG wire, B1-5	0.029	0.010	0.026	0.82	1.59	12.7	18.9	2.52	0.05	0.14	<0.01	0.02	0.09

Note: Consumable C has not been included, since it was impossible to separate core and sheath of a 2.0mm diameter FCW in a satisfactory manner for analysis.

b Total hexavalent chromium, by alkaline extraction and s-diphenyl carbazide colorimetric finish, based on the method described by Moreton *et al.*[5] Total chromium figures were obtained by a fusion technique described in the same paper;

c Sodium and lithium (samples A, B, C and D only) by fume emission spectrophotometry;

d Xray fluorescence analysis was performed for the remaining elements, on a bead fused from a mixture of fume, lanthanum oxide and lithium tetraborate.[6]

RESULTS AND DISCUSSION

Application of the fume box

This study confirms previous findings that the fume box is an appropriate tool for fume sampling, and measurement of fume emission rates of MMA, MAG, and flux and metal cored wire welding. Compared with the Swedish Fume Box,[7] designed solely for MMA tests, the revised box allows improved access of the MAG gun in gas shielded arc welding and a more conventional gun angle, while the larger chamber volume means that there is less disturbance of the gas shield. The only difficulties were encountered with the pulse arc condition, MAG wire, test B5, when the fume emission rate was so low that there were problems in collecting sufficient fume sample for analysis.

me emission rates

..eproducibility of fume emission rate results, as illustrated in Fig. 1, has been shown[6, 8] to depend critically on variations in current, and particularly voltage during tests, and is similar for all four processes tested. No values for standard deviations (sd) were calculated, since only three or four replicate tests were made for each consumable, but previous work suggests a value for 2sd of about ±10%. Figure 1 shows, for each set of tests, the *range*, which in all cases is about 10% of the value of the *average* for a set of observations.

FER results for MMA, MAG and MCW consumables lie within the respective ranges predicted by previous results held on the Fume Emission Database (FED),[1, 9] although the number of results held on the database is still small, and does not allow a balanced statistical assessment. Similarly, results for the MAG tests B, B1a or B1b, B2 and B4 lie within the range expected from the corresponding results on the Database. The low arc voltage spray condition, B3, produces an FER greater than average, whereas the pulse condition, B5 gives an FER considerably less than the expected range for MAG. However, no tests had been performed previously on the pulse arc MAG condition.

Chemical analysis

The results of chemical analysis of the fume (Table 2) are in line with previous analogous results.[5] Of particular occupational hygiene interest are the chromium contents of the fumes. Since the Occupational Exposure Limit (OEL)[10] for the trivalent form, CrIII is 0.5 mg/m³, whilst the OEL for the hexavalent species, CrVI, is 0.05 mg/m³, there is clearly a strong incentive to reduce amounts of chromium in fume in general, and proportions of CrVI in fume in particular.

Fumes A and C give 5% total chromium, for the MMA and FCW tests respectively. The CrVI contents for A and C of 4.1 and 2.7% respectively, represent a large proportion (*i.e.* 80 and 60%) of the total Cr. Such proportions of CrIII/CrVI in the fume have been noted previously with MMA and FCW consumables.[1, 5, 11]

Wire B is a solid MAG wire, and wire D an MCW type described by the manufacturer as containing no flux. It is in accord with previous experience that the total chromium in fume from MAG wire is about 12% and that very little of this chromium is in the hexavalent state (Table 2).[5, 12] For the tests B and B1-B5, MAG wire, the CrVI amounts in the fume obtained by alkaline leach and the s-diphenyl carbazide method were low for all samples, and only just above the limit of detection (0.1-0.2%). Total Cr was obtained on small weight fume samples B1-B5 by a fuming technique, and there was no marked compositional variation through the set.

Previous fume analyses from the same wire were 9-13% by six co-operating analysts.[5]

Nickel contents of the fumes are as expected from previous experience.[5] It is known that Ni is present in an insoluble form as the oxide in welding fumes and therefore the OEL[10] of 1 mg/m³ is relevant. One anomaly in the results (Table 2) is the small amount of sodium, at the detection limit, in fume B, from the MAG process. This is thought to be caused by airborne contamination, but is not important from an occupational hygiene viewpoint. Also, in fume B, the copper amount of 0.6% is higher than normal, but similar levels have been found previously in fume from this consumable.[5]

The reduced analytical accuracy resulting from small fume sample weights

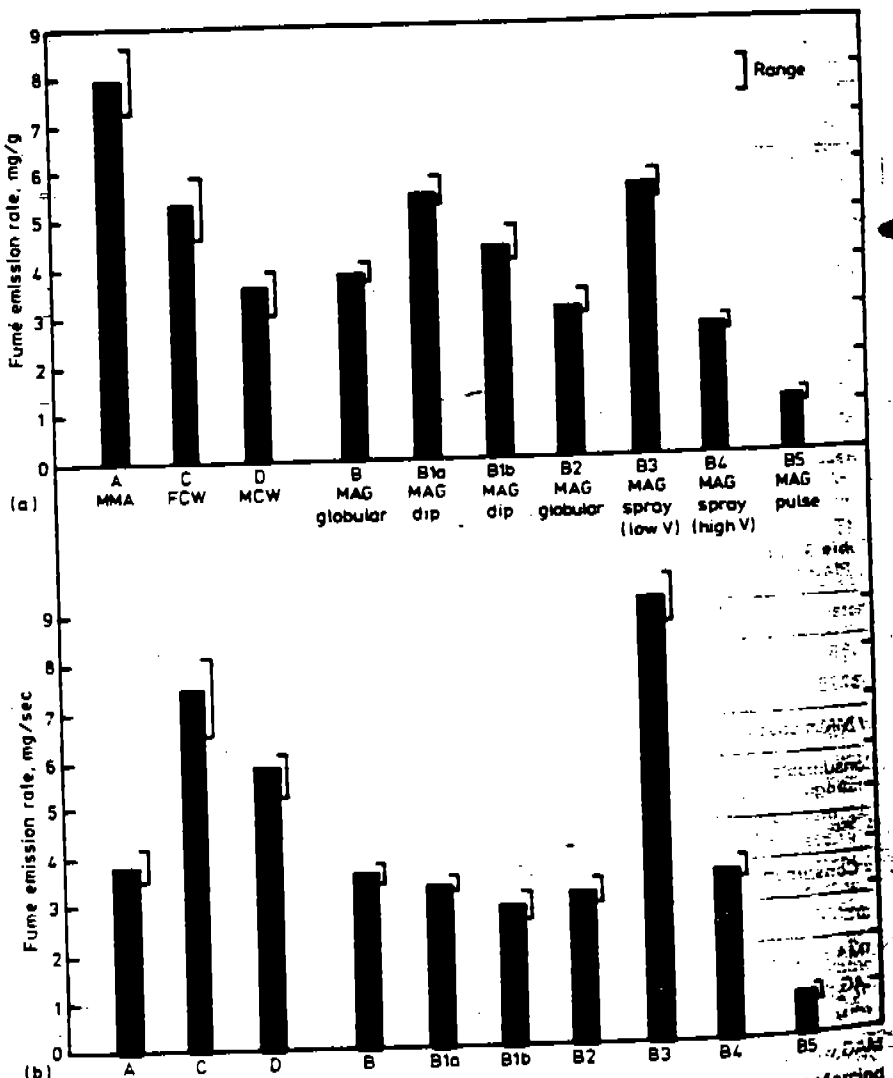

1 Fume emission rates: *a*/ Expressed in mg/g of deposited metal; *b*/ Expressed as mg/sec of arcing time.

Table 4 Summary of results following visual assessment of welded specimens

Test specimen numbers	Mode of metal transfer	General comments
B1a (3 specimens)	Dip	Bead profile convex with a slightly pronounced rippled surface. The weld toes fusing into each plate with a 5mm leg length fillet weld present. Fine spatter adhering to the plates.
B1b (3 specimens)	Dip	Bead profile convex, the convexity being more pronounced than those produced in group B1a. The bead was however of a smoother rippled surface. The weld toes, although fused into each plate, were distinctly rolled along the base plate with a 5mm leg length. There was also marked reduction in the fine spatter formation.
		Welds B1a and B1b may be considered as typical of industrial practice for this joint type and plate thickness.
B2 (3 specimens)	Globular	Bead profile only slightly convex with a herringbone rippled surface. The weld toes fusing smoothly into the parent plates but assuming a 'scalloped' effect with a 6mm leg length. Some fine spatter.
B3 (3 specimens)	Spray (low volts)	Bead profile slightly convex with a smooth fine herringbone rippled surface. The weld toes fusing into the parent plates with a slight 'scalloping' along the base plate toe, with a 7mm leg length. No spatter.
B4 (3 specimens)	Spray (high volts)	Bead profile flat to slightly concave with a smooth very fine herringbone rippled surface. The weld toes fusing smoothly into the parent plates with a 6mm leg length. No spatter.
B5 (3 specimens)	Pulse	Bead profile flat to slightly convex with a semi herringbone rippled surface. The weld toes, although fused into the parent plates were slightly irregular along the length of the specimen with a 7mm leg length. No spatter.

available in tests B4 and B5 means that no firm conclusions should be based on the compositional variations of Fe, Ni, Mn, *etc.* of tests B1-B5. However, fume analyses for test B, with the same wire, were in good agreement with fume analyses carried out in 1983,[5] where 31-33%Fe, 12-15%Mn and 3-5%Ni were found by six analysts. These results are thus in general agreement with the series B1-B5.

Table 3 provides data on consumable analyses. Two separate reels of wire B were used for the tests, and had marginally different composition. Such differences were not thought to be significant. Results are not given for wire C, as it was not found possible to separate the core and sheath of this flux cored consumable for analysis.

IMPLICATIONS FOR STAINLESS STEEL WELDING

This work with MMA, FCW, MCW and MAG processes (all of which are applicable to routine stainless steel fabrication) illustrates the range of fume emissions which can be obtained, and suggests that use of the MAG process is feasible to reduce the CrVI/CrIII ratio to one which is preferable from an occupational hygiene viewpoint. This is the case providing that total fume amounts are also adequately controlled by local extraction. It should be borne in mind that whilst it is fairly well documented that MAG welding invariably produces only low amounts of hexavalent chromium in the fume,[5, 11, 12] there are differences in FERs and fume composition with different MAG consumables. Shielding gas mixtures may also have an effect. However, equally notable are the variations in FER which can be obtained by use of different welding conditions applied to the same consumable, within a band of commercially acceptable resultant weld qualities. Thus, it has been shown possible when employing a low voltage spray arc mode of transfer in test B3 to obtain a very high fume emission rate. This result points to the importance of considering fume formation during preliminary trials to establish welding procedures for fabrication purposes.

Far more important is the discovery that conventional pulse arc welding is capable of producing very low fume amounts indeed (commensurate with conventional TIG and the hot wire TIG process[1]) at the same time as having a deposition rate of the order of the dip mode. Although it is known that the pulse arc condition is guilty of producing enhanced amounts of ozone (not readily measurable in the fume box), this test points the way to a possible considerable overall reduction in pollutant levels, particularly in situations where the reduction of particulate fume is critical (*e.g.* welding in a hyperbaric environment).[13] Figure 2 shows the results in terms of a measure of the toxicity of fume from different processes. The value of the FER has been divided by an additive threshold limit value[14] for fume given by:

$$TLV_{fume} = \frac{1}{\frac{A}{a} + \frac{B}{b} + \frac{C}{c} \ldots} \text{ mg/m}^3$$

where A, B, C are the % weights of elements of hygienic significance in the fume, and a, b and c are the corresponding occupational exposure limits.

This calculation is one step in the classification of fumes into classes, which forms part of the Swedish Standard.[4] This standard, and in particular, its adoption of fume classes is not accepted in the UK, nor is the method of adding together components of a mixture of pollutants presently accepted by the Health and Safety Executive, although the additive formula above is used by the American Conference of Governmental Industrial Hygienists (ACGIH)[14] for airborne pollutant mixtures in general.

Nevertheless, as an aid to considering the relative hazards of fumes from different processes and consumables used for welding stainless (and high alloy) steels, the diagram can be thought provoking. Using UK OEL values[10] in the calculation, the combination of low FER, and the absence of significant amounts of CrVI in the fume potentially makes the fume from pulse arc welding (test B5) an order of magnitude less hazardous than the equivalent MMA conditions during the deposition of equal amounts of weld metal. For conventional dip and spray MAG conditions, the three factors of: *a)* very low CrVI; *b)* average FER; and *c)* high total Cr (12-15% compared with 4-8% for MMA), have to be borne in mind when considering control of fume emission at source.

These considerations thus suggest that it is perhaps unacceptable to adopt the same value of OEL for particulate welding fume[10] from two different processes, although nominally these processes may deposit weld metal of similar composition. The authors suggest that considerably more research is required into fume emission rates of competing open arc processes (*e.g.* different shielding gas mixtures, and a range of stainless and highly alloyed MAG wires) before any firm conclusions can be drawn.

CONCLUSIONS

1 The fume box has proved a useful tool for measurement of fume emission rates of consumables from the MMA, MAG, FCW and MCW processes.

2 Fume emission rates found in this investigation lie within the ranges, process by process, expected from previous experience.

3 The MAG process, with a single stainless steel wire, type 316S93, and Ar-2%O_2 shielding gas, used under a wide range of welding conditions, has shown itself capable of lower fume emission rates than the self-shielded (MMA and FCW) processes.

4 For the MAG process, small alterations in arc voltage within the spray range can have marked (factor of three) effects on total fume emission. The higher fume

emission rates were obtained with the low arc voltage.

5 The pulse arc transfer mode during MAG welding has extremely low fume emission rates.

6 Of particular interest is the presence of hexavalent chromium, CrVI in fume, because of the recent debate concerning possible carcinogenic hazards relating to CrVI. These investigations indicate that gas shielded welding gives emission rates of CrVI that are lower than those given by self-shielded methods by a factor of 1/15 to 1/25. For pulse transfer MAG welding, the same factor is of the order of 1/100. If a 'low' voltage spray transfer mode is used, the factor reverts to 1/4 to 1/5.

7 No measurements of ozone formation were made. In considering the potential air pollution problems when welding stainless steels, attention should also be paid to the ozone, particularly when using the pulse arc MAG process.

Acknowledgements

This project was initiated by AGA Sweden, and sponsored by AGA AB and Sandvik AB, Sweden. The authors are grateful to those companies for permission to publish this work. The experimental studies were carried out at The Welding Institute, and the authors acknowledge with thanks the assistance and advice of colleagues within the arc welding and chemical laboratories.

References

1 Moreton J: 'Fume emission rates for open arc welding processes'. *Metal Construction* 1985 17 (5) 308-310.

2 Jenkins N: 'Conference considers health hazards and effects of welding fume'. *Metal Construction* 1985 17 (5) 319-320.

3 Moreton J: 'An improved fume box for measurement of fume emission rates'. *Welding Institute Research Bulletin* 1984 25 (7) 230-233.

4 'Welding electrodes—covered electrodes—fume classes.' Swedish Standards SS 06 2801, SS 06 2806 (in Swedish). Draft English translation IIW Doc IIE-285A and 3.

5 Moreton J, Bettelley J, Mathers H, Nicholls A, Perry R W, Ratcliffe D B and Svensson L: 'Investigation of techniques for the analysis of hexavalent chromium, total chromium and total nickel in welding fume: a co-operative study'. *Annals Occup Hygiene* 1983 27 (2) 137-156.

6 Jenkins N, Moreton J, Oakley P J and Stevens S M: 'Welding fume: sources, characteristics, control'. Publ. The Welding Institute, Vol. I, II 1981, Vol. III 1983, Abington, Cambs.

7 Magnusson E J: 'The problems of fumes in welding'. *Svetsaren* 1974 3 1-8.

8 Gray C N, Hewitt P J and Dare P R M: 'New approach would help control fumes at source. Part two: MIG fumes'. *WMF* 1982 (Oct) 393-397.

9 Moreton J and Stevens D C: 'FED—a data base to assist with welding fume problems'. *Welding Institute Research Bulletin* 1984 25 (9) 301-304.

10 'Occupational Exposure Limits, 1985.' Guidance Note EH40 from the Health and Safety Executive, April 1985, HMSO, London.

11 Van Bemst A, Beaufils D, Hewitt P J and Stern R M: 'Interlaboratory calibration of a standardised analytical method of hexavalent and total chromium in welding fume'. *Welding in the World* 1983 (1/2) 10-15.

12 Zatka V J: 'Specification of hexavalent chromium in welding fumes: interference by air oxidation of chromium'. *Amer Ind Hygiene Assoc J* 1985 46 (6) 327-331.

13 Molyneux M K, Worrall D A, Gibson D E, Smith D D and Peterson R E: Norske Hydro/Norske Shell. 'A study of welding fumes and gases under experimental hyperbaric conditions.' DEEP EX 81, Deep Weld, Oct 1982.

14 'TLV's Threshold limit values for chemical substances and physical agents in the work environment and biological exposure indices with intended changes for 1984-85.' American Conference of Governmental Industrial Hygienists, ACGIH, 6500 Glenway Ave, Bldg D5, Cincinnati, OH 45211, USA.

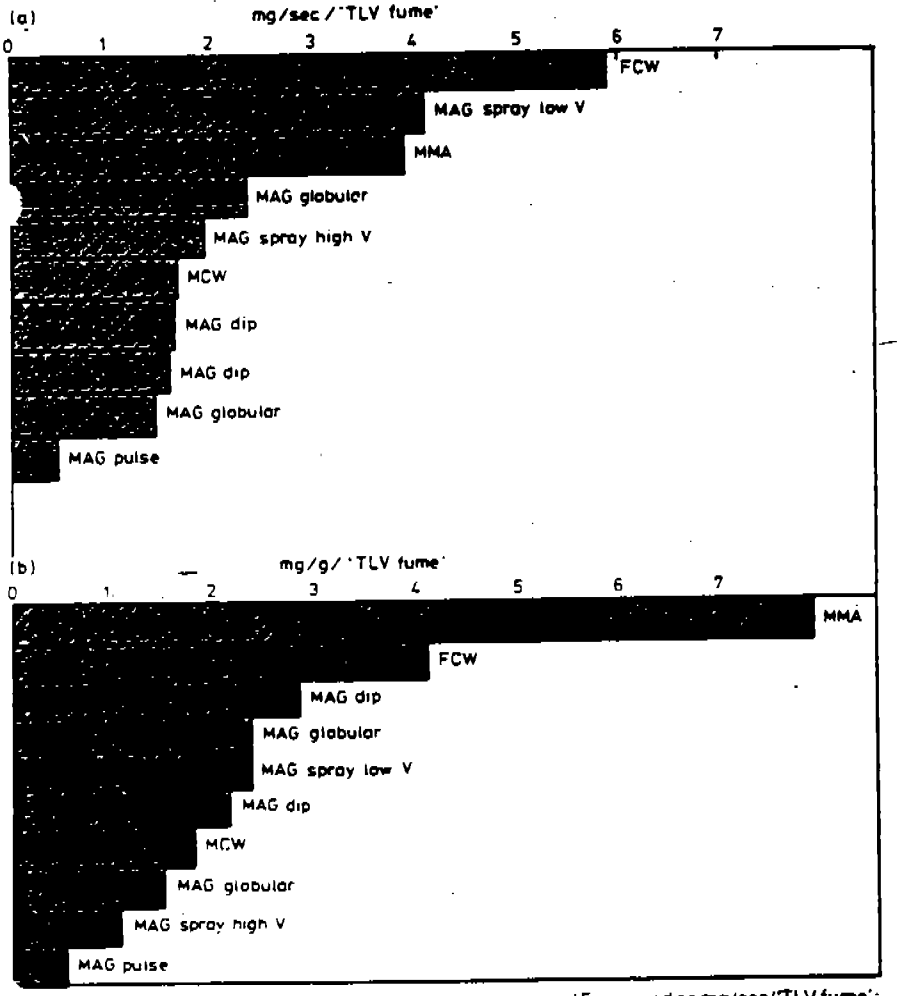

2 Relative toxicity of fume from different welding processes: *a)* Expressed as mg/sec/'TLV fume'; *b)* Expressed as mg/g 'TLV fume'.

METCON FILE

Authors Moreton J, Smârs E A and Spiller K R

Title **Fume emission when welding stainless steel**

Reference Metal Construction 1985 17 (12) 794-798

Fume emission rates were determined for MMA (AWS A5.4 81, E316L-16), MAG ($Ar+2\%O_2$, metal cored wire AWS A5.22 80, E316 LT, 1, 2, 3 or solid wire AWS A5.9 77, ER316L Si, dip, spray (various voltage levels), globular or pulsed metal transfer), or self-shielded flux cored wire welding (AWS A5.22 80, E316LT-3). Horizontal-vertical fillet welds were made in a fume box on Type 316 stainless steel (17%Cr, 10%Ni, 2.38 or 0.31%Mo) and particulate fume was collected for weighing and chemical analysis (especially for total chromium and hexavalent chromium). Pulsed MAG welding gave very low levels of fume.

APPENDIX E

REFERENCE 28

(Tandon et al., 1984)

CHEMICAL INVESTIGATION OF SOME ELECTRIC ARC WELDING FUMES AND THEIR POTENTIAL HEALTH EFFECTS – AWRA CONTRACT 90, AWRA DOCUMENT P9-14-85

By R.K. Tandon[1], P.T. Crisp[1], J. Ellis[1], R.S. Baker[2], B.E. Chenhall[3].

ABSTRACT

An understanding of the chemical composition of welding fumes is of value in predicting and controlling the occupational health risk to welders. This paper describes the determination of 19 elements in the flux and fume from three types of hardfacing and two types of high-strength, low-alloy steel flux-covered electrodes. A number of experimental techniques were used in the analyses. These included x-ray fluorescence, x-ray diffraction, atomic absorption spectrophotometry, ion-selective electrode and ion-chromatography. Fe_3O_4, K_2CrO_4, CaF_2 and NaF were the only crystalline compounds detected in the fumes by qualitative x-ray diffraction. The results from the various quantitative analyses were reproducible to within ±5%. Excellent agreement was found between x-ray fluorescence and atomic absorption methods. Mass balances (> 90% of total) were obtained for the flux, fume and water-soluble fume fractions. The iron contents of the fumes are related to their fume generation rates (FGRs). There is also an inverse relationship between fluoride concentrations in the fumes and FGRs. The water-soluble chromium (VI)/total chromium in the fume is highly correlated with the percentage of Na + K in the flux (r = 0.92). The various analytical results are discussed side by side with existing toxicological information.

Key terms: Chemical composition, chromium, fluoride, mass balance, toxicity, welding environment.

Welders constitute about 0.5 – 2% of the total work force in most technologically advanced countries[34]. In the work environment, welders experience varying amounts of chronic exposure to aerosols which contain ozone, nitrogen oxides, metal oxides, fluorides and other compounds[5,41]. The occupational health effects of the various components of welding aerosols are well documented in the literature[5,6,8,11,33]. A study by the American Welding Society[5] lists cadmium, chromium, lead, titanium, magnesium, manganese, mercury, molybdenum, nickel, vanadium, zinc and fluorides in the fume particles as potentially hazardous. However, only nickel and chromium (VI) are suspected human carcinogens and these metals occur in significant concentrations only in fumes from the welding of stainless steel and nickel-coated mild steel[35].

The toxic action of welding fumes, metal fumes and related metal salts on target organs is known to have a chemical basis[20,21,43]. The toxicity or inertness of welding fume particulates may therefore be assessed by factors such as solubility, chemical composition (both surface and bulk), chromium oxidation state and crystallinity of constituents[2,38,40]. In this paper, we examine some of these factors and present a detailed chemical analysis of the flux, fume and water-soluble fume fractions from three types of hardfacing and two types of high-strength low-alloy (HSLA) steel manual metal arc welding (MMAW) electrodes. MMAW is one of the two most commonly practiced welding technologies[33], and hardfacing and HSLA-steel electrodes are a major class of electrodes used in the welding industry[37]. The work is part of a multi-disciplinary project which involves physical, chemical and biological investigations of fume from these electrodes[9,37,39].

MATERIALS AND METHODS

Electrodes

The electrodes used in the study are listed in table 1. The electrodes were stored in an oven at 100°C. Electrodes exposed to moisture were dried at 200°C for two hours prior to welding.

Chemicals

All chemicals (reagents, standards, etc) were of analytical grade or better. Triple glass-distilled water was used. The hydrochloric, nitric and perchloric acids used were BDH, Aristar (ultrapure). Atomic absorption spectrophotometry (AAS) standards (1,000 mg/L stock solutions) were prepared from pure metals (99.9 – 99.999%) or from pure salts (≥ 99.9%) using standard methods[42]. The working AAS standards were prepared freshly each day. The AAS standard for total chromium determination was made by dissolving 99.999% chromium metal in hydrochloric acid (1,000 mg/L Cr^{3+} stock solution). Both AAS and colorimetric standards for Cr(VI) determinations were made from a stock solution of 1,000 mg/L potassium dichromate. Sym-diphenylcarbazide (s – DPC) reagent was prepared by dissolving 0.50g of the solid in a mixture of 100mL acetone and 100mL of distilled water. The solution was stored in an opaque bottle at 4°C (stable for up to a month).

Fume sampling

Fume from the electrodes was generated using an automatic arc welder and collected on glass fiber media[36]. All the electrodes were welded bead-on-plate to 8mm mild steel at speeds around 15cm min^{-1}. Operating conditions for the different electrodes are described in table 1. The fume particles collected were carefully brushed from the

TABLE 1 DESCRIPTION OF ELECTRODES AND OPERATING CONDITIONS FOR GENERATION OF WELDING FUME

Code	Type	Diameter (mm)	Mode[a]	Welding Current (A) and voltage (V)
E01	Hardfacing, medium-chromium	3.25	AC	125A,24V
E04	HSLA-steel[b]	3.25	AC	125A,25V
E05	HSLA-steel	3.25	DCEP	125A,23V
E11	Hardfacing, high-manganese	4.0	AC	200A,26V
E12	Hardfacing, high-chromium	6.0	AC	128A,22V

[a] The manufacturer specified DC electrode positive (DCEP) welding for E05; all the other electrodes were suitable for welding on either AC or DC.
[b] HSLA = high-strength, low-alloy.

1 Department of Chemistry, University of Wollongong.
2 Commonwealth Institute of Health, University of Sydney.
3 Department of Geology, University of Wollongong.

glass fiber substrates and dried at 100°C prior to analysis. Fume was generally analyzed immediately after collection. Some fume samples (dried) were stored in sealed glass vials in a vacuum desiccator at 4°C for up to two weeks before analysis was commenced.

ANALYSIS

Weld deposit

Each manufacturer provided data based on the analysis of a typical batch of electrodes. Weld metal deposit compositions are similar to the compositions of the electrode core metal except where there is a contribution from the metal present in the flux.

Flux

Analysis of the flux (outer coating) of the electrodes was carried out by:

(i) x-ray fluorescence ($Li_2B_4O_7/LiBO_2$ fushion; Philips PW 1600; ZAF corrections program) and

(ii) combustion (Leco EC 12) for total carbon.

Fume

X-ray fluorescence (XRF) analysis was carried out as for flux. X-ray diffraction (XRD) was carried out using Philips PW 1316/90 specimen/camera housing with PW 1050/70 goniometer (CuK_α radiation; graphite crystal monochromator; 2θ calibrated with silicon crystal).

The following analyses were also performed:

(i) AAS: Duplicate 0.1g samples of fume from electrodes E01, E04, E05 and E11 were dissolved in 6M hydrochloric acid at 60°C[10]. Fume samples from electrode E12 were dissolved by adding nitric, perchloric and hydrofluoric acids and evaporating to dense white fumes[15]. These techniques resulted in > 90% dissolution of the fume samples. Samples for total chromium analysis were also prepared by the alternative method of $KHSO_4$ fusion followed by dissolution of the product in 3M sulfuric acid[26]. All solutions (standards and unknowns) for the AAS analyses were made in 0.1M hydrochloric acid. AA measurements were made on an Instrumentation Laboratory Model 551 instrument using flame atomization with automatic background correction in the double beam mode. The air-acetylene flame was used for all elements except aluminium, calcium and chromium, for which nitrous oxide-acetylene was used. Standard measuring conditions (wavelength, hollow cathode lamp setting, slit width, etc) were used[14]. The wavelength corresponding to the highest sensitivity was chosen. Appropriate ionization suppressants and releasing agents were added to both standards and unknowns for the analysis of sodium, magnesium, aluminium, potassium and calcium[36,42].

(ii) Cr(VI): Samples for total Cr(VI) determinations (0.1g; in duplicate) were prepared by extracting the fumes with sodium carbonate/sodium hydroxide at ~ 90°C and pH = 12.5[24]. A diluted NIOSH solution[46] was used for the AAS analysis. Total Cr(VI) was also determined by colorimetry[1] using sym-diphenylcarbazide (Hitachi Model 101 spectrophotometer; 1cm cuvettes; green filter; λ = 546nm). Because large concentrations of iron (III) interfere with the determination[24,29], it was removed by extraction with 8-hydroxyquinoline at pH 4.

(iii) Ion-selective electrode (ISE): For total fluoride analyses, duplicate 0.1g samples of fume from electrodes E01, E04, E05 and E11 were dissolved in 6M hydrochloric acid and those from E12 by digestion in nitric/hydrochloric acid. An Orion Model 901 Ionanalyser and a Model 94-09 fluoride-selective electrode were used. Standards were

TABLE 2 ANALYTICAL DATA FOR ELECTRODE E01 (MEDIUM-CHROMIUM HARDFACING)

Element	Abundance (% w/w) Weld deposit	Flux	Fume	Water-soluble fume
C	0.4[a]	5.7[b]	N.D.	●
F	●	8.4[c]	8.9[c], 7.6[d]	3.2[d], 2.8[e]
Na	●	0.7[c]	2.4[c], 2.8[f]	1.2[f]
Mg	●	0.5[c]	0.4[c], 0.3[f]	0.2[f]
Al	●	0.6[c]	0.4[c], 0.4[f]	0.03[f]
Si	●	5.2[c]	2.5[c]	●
P	●	0.03[c]	0.03[c]	●
S	●	0.04[c]	0.08[c]	●
Cl	●	0.2[c]	0.4[c]	0.4[e]
K	●	1.5[c]	7.8[c], 8.6[f]	6.8[f]
Ca	●	18.7[c]	9.4[c], 9.9[f]	1.5[f]
Ti	●	1.9[c]	0.2[c]	●
V	0.5[a]	n.d.[c]	n.d.[c]	●
Cr	7.0[a]	15.9[c]	2.5[c], 2.5[f]	●
Cr(VI)	●	●	1.7[f], 1.9[g]	1.5[f], 1.5[g]
Mn	0.3[a]	2.8[c]	4.6[c], 3.6[f]	0.003[f]
Fe	91.3[n]	8.8[c]	32.1[c], 32.3[f]	0.05[f]
Ni	●	0.1[c]	0.04[c], 0.03[f]	n.d.[f]
Cu	●	N.D.	0.03[c], 0.03[f]	n.d.[f]
Zn	●	<0.01[c]	0.04[c]	N.D.
Zr	●	<0.1[c]	<0.1[c]	●
Mo	0.5[a]	0.6[c]	0.1[c]	●
Total	100.0	71.8	71.8	14.7

a Data provided by the manufacturer.
b by combustion.
c by x-ray fluorescence.
d by ion-selective electrode.
e by ion-chromatography.
f by atomic absorption spectrophotometry.
g by sym-diphenylcarbazide colorimetric method.
n by difference.
● = category not applicable.
N.D. = not determined.
n.d. = not detected.

TABLE 3 ANALYTICAL DATA FOR ELECTRODE E04 (HSLA-STEEL)

Element	Abundance (% w/w) Weld deposit	Flux	Fume	Water-soluble fume
C	0.07[a]	2.7[b]	N.D.	●
F	●	8.1[c]	14.4[c], 13.1[d]	8.5[d], 9.9[e]
Na	●	0.4[c]	2.8[c], 3.5[f]	1.5[f]
Mg	●	0.2[c]	0.1[c], 0.1[f]	0.06[f]
Al	●	0.5[c]	0.5[c], 0.6[f]	0.04[f]
Si	0.04[a]	4.7[c]	2.8[c]	●
P	●	0.01[c]	0.02[c]	●
S	●	0.03[c]	0.1[c]	●
Cl	●	0.1[c]	0.2[c]	0.2[e]
K	●	1.2[c]	13.7[c], 13.7[f]	12.3[f]
Ca	●	15.0[c]	7.3[c], 9.1[f]	1.2[f]
Ti	●	2.5[c]	0.4[c]	●
Cr	●	0.07[c]	0.03[c], 0.03[f]	●
Cr(VI)	●	●	0.03[f], 0.03[g]	0.02[f], 0.02[g]
Mn	1.0[a]	2.6[c]	5.0[c], 4.4[f]	0.006[f]
Fe	97.0[n]	29.7[c]	19.8[c], 17.8[f]	0.07[f]
Ni	1.6[a]	2.8[c]	0.2[c], 0.1[f]	n.d.[f]
Cu	●	N.D.	0.03[c], 0.06[f]	n.d.[f]
Zn	●	<0.01[c]	0.03[c]	N.D.
Zr	●	<0.1[c]	<0.1[c]	●
Mo	0.3[a]	0.6[c]	0.1[c]	●
Total	100.0	71.2	66.9	24.6

a-n, ●, N.D., n.d., See footnotes to table 2.

prepared containing the same concentrations of aluminium and iron (III) as the unknowns. All fluoride concentrations were measured at pH ≈ 6 using the trishydroxymethyl-aminomethane method[25,36].

Water-soluble fume

Fume samples (in duplicate) were dissolved by stirring in water at 60°C for two hours (0.1g fume; 100mL water). For calcium determinations, 0.1g of the fume sample was dissolved in 1L water. Solubility determinations were made by recovering the insoluble portion of the fume by filtration through a 0.45 μm nylon membrane filter, drying in a desiccator and weighing to constant weight.

Water-soluble fractions were analyzed for:

(i) metals by AAS as for fume;
(ii) Cr(VI) using sym-diphenylcarbazide (colorimetry), and by AAS;
(iii) fluoride using an ion-selective electrode as for fume; and
(iv) chloride and fluoride by suppressor column ion-chromatography (Korth and Ellis[17] – 3.0 mM Na_2CO_3 + 2.4 mM $NaHCO_3$ eluent; peak height measurements).

A least-squares linear regression program (Apple II; Pascal) was used to determine the correlation between water-soluble chromium (VI)/total chromium in the fume and Na + K in the flux. All five types of electrodes were considered.

Results

Spectrographic analysis of the mild steel base metal (workpiece) gave: Fe – 98.02%; Mn – 1.46%; Si – 0.22%; C – 0.10%; Al – 0.05%; V – 0.05%; Cr – 0.02%; P – 0.02%; Nb – 0.02%; Ni – 0.015%; Cu – 0.01%; S – 0.005%; Mo – 0.003% and Sn – 0.002%. The major non-metallic constituents of the flux in the different electrodes were: E01 and E04 – $CaCO_3$, CaF_2, silicates, TiO_2; E05 – $CaCO_3$, CaF_2, K_2SiO_3, TiO_2; E11 – $CaCO_3$, CaF_2, silicates, TiO_2, cellulose; and E12 – $CaCO_3$, CaF_2 silica, silicates and cellulose. The crystalline compounds identified in the fume from the different electrodes were: E01 and E04 – Fe_3O_4, K_2CrO_4, CaF_2, NaF; E05 – Fe_3O_4, K_2CrO_4, CaF_2; E11 – $(Fe, Mn)_3O_4$; and E12 – Fe_3O_4, CaF_2. The following d-spacing values (Å) were measured from the x-ray diffractograms which could be matched with known compounds in the JCPDS (Joint Committee on Powder Diffraction Standards) card system: 2.53, 2.97, 1.48 (Fe_3O_4); 3.08, 2.99, 2.96 (K_2CrO_4); 1.93, 3.15, 1.65 (CaF_2); and 2.32, 1.65, 2.68 (NaF). Fume from electrode E11 (high-manganese hardfacing) gave XRD peaks at d (Å) = 2.56, 3.01, 1.52, which we ascribed to a Fe_3O_4 – Mn_3O_4 solid solution[19]. The solubilities of the fumes in water (w/w) were found to be: E01 – 22.5%; E04 – 28.0%; E05 – 37.5%; E11 – 3.0%; and E12 – 26.3%.

All the analytical data relating to the five types of electrodes are presented in tables 2 – 6. Duplicate chemical analyses varied by an average of 2% (maximum of 10%). For total chromium, samples prepared by $KHSO_4$ fusion gave similar results to those prepared by acid-digestion.

Table 7 shows the concentrations of chromium (III), water-insoluble chromium (VI) and water-soluble chromium (VI) in the fumes from the five types of electrodes. The concentrations of chromium in the weld deposit and in the flux, and of sodium and potassium in the flux, are also included in the table for comparison.

DISCUSSION

The crystalline compounds detected in the welding fumes by x-ray powder diffraction are similar to those identified in other studies[4,16,32,38]. The results show magnetite (Fe_3O_4) and calcium fluoride (CaF_2) to be prominent in the crystal phases of four of the five fumes tested. No transition-metal fluorides were detected in any

TABLE 4 ANALYTICAL DATA FOR ELECTRODE E05 (HSLA-STEEL)

Element	Abundance (% w/w) Weld deposit	Flux	Fume	Water-soluble fume
C	0.045[a]	3.1[b]	N.D.	●
F	●	8.0[c]	18.7[c], 18.5[c]	8.2[d], 10.8[e]
Na	●	0.4[c]	1.9[c], 2.4[f]	0.5[f]
Mg	●	0.1[c]	0.1[c], 0.1[f]	0.06[f]
Al	●	1.9[c]	2.2[c], 2.1[f]	0.05[f]
Si	0.38[a]	8.2[c]	4.5[c]	●
P	0.022[a]	0.03[c]	0.03[c]	●
S	0.019[a]	0.06[c]	0.08[c]	●
Cl	●	n.d.[c]	0.1[c]	0.1[e]
K	●	2.4[c]	16.3[c], 17.3[f]	15.1[f]
Ca	●	19.1[c]	9.5[c], 12.5[f]	2.1[f]
Ti	●	5.2[c]	0.9[c]	●
Cr	2.12[a]	4.2[c]	0.5[c], 0.7[f]	●
Cr(VI)	●	●	0.6[f], 0.7[g]	0.7[f], 0.6[g]
Mn	0.72[a]	2.2[c]	3.9[c], 3.6[f]	0.006[f]
Fe	95.74[h]	11.6[c]	11.6[c], 11.5[f]	0.04[f]
Ni	●	0.02[c]	0.02[c], 0.01[f]	n.d.[f]
Cu	●	N.D.	0.03[c], 0.04[f]	n.d.[f]
Zn	●	<0.01[c]	0.05[c]	N.D.
Zr	●	<0.1[c]	<0.1[c]	●
Mo	0.95[a]	1.9[c]	0.1[c]	●
Total	100.0	68.4	72.5	28.1

[a-n], ●, N.D., n.d., See footnotes to table 2.

TABLE 5 ANALYTICAL DATA FOR ELECTRODE E11 (HIGH MANGANESE HARDFACING)

Element	Abundance (% w/w) Weld deposit	Flux	Fume	Water-soluble fume
C	0.065[a]	3.7[b]	N.D.	●
F	●	0.2[c]	1.5[c], 2.2[d]	1.5[d], 0.8[e]
Na	●	1.0[c]	4.1[c], 3.5[f]	0.9[f]
Mg	●	1.5[c]	0.4[c], 0.2[f]	0.1[f]
Al	●	0.05[c]	0.1[c], 0.1[f]	n.d.[f]
Si	0.14[a]	3.0[c]	1.1[c]	●
P	⩽0.05[a]	0.03[c]	0.03[c]	●
S	0.01[a]	0.08[c]	0.08[c]	●
Cl	●	n.d.[c]	0.1[c]	0.1[e]
K	●	0.08[c]	0.3[c], 0.1[f]	0.1[f]
Ca	●	3.1[c]	0.4[c], 0.5[f]	0.15[f]
Ti	●	5.7[c]	0.4[c]	●
Cr	●	0.2[c]	0.05[c], 0.05[f]	●
Cr(VI)	●	●	0.03[f], 0.03[g]	0.03[f], 0.02[g]
Mn	14.5[a]	36.3[c]	26.1[c], 31.0[f]	0.05[f]
Fe	80.75[h]	7.2[c]	28.1[c], 27.3[f]	0.09[f]
Ni	3.2[a]	8.2[c]	1.4[c], 2.0[f]	n.d.[f]
Cu	●	N.D.	0.03[c], 0.07[f]	n.d.[f]
Zn	●	<0.01[c]	0.02[c]	N.D.
Zr	●	<0.1[c]	<0.1[c]	●
Mo	0.75[a]	2.3[c]	0.4[c]	●
Total	100.0	72.6	57.0	2.7

[a-n], ●, N.D., n.d., See footnotes to table 2.

TABLE 6 ANALYTICAL DATA FOR ELECTRODE E12 (HIGH-CHROMIUM HARDFACING)

Element	Abundance (% w/w) Weld deposit	Flux	Fume	Water-soluble fume
C	4.5[a]	17.1[b]	N.D.	●
F	●	14.7[c]	6.8[c], 5.2[d]	2.7[d], 1.9[e]
Na	●	<0.01[c]	1.9[c], 1.4[f]	0.4[f]
Mg	●	0.3[c]	0.6[c], 0.3[f]	0.2[f]
Al	●	0.2[c]	4.7[c], 4.1[f]	0.01[f]
Si	●	12.2[c]	13.3[c]	●
P	●	0.02[c]	0.01[c]	●
S	●	0.01[c]	0.07[c]	●
Cl	●	0.2[c]	3.6[c]	4.5[e]
K	●	0.02[c]	1.9[c], 2.4[f]	2.2[f]
Ca	●	19.5[c]	14.5[c], 16.0[f]	3.9[f]
Ti	●	0.02[c]	0.03[c]	●
Cr	32.5[a]	0.1[c]	4.7[c], 5.5[f]	●
Cr(VI)	●	●	1.7[f], 1.2[g]	0.4[f], 0.5[g]
Mn	3.3[a]	0.3[c]	6.5[c], 6.5[f]	0.02[f]
Fe	59.7[n]	1.0[c]	11.1[c], 13.2[f]	0.03[f]
Ni	●	0.1[c]	0.04[c], 0.03[f]	n.d.[f]
Cu	●	N.D.	0.03[c], 0.05[f]	n.d.[f]
Zn	●	<0.01[c]	0.05[c]	N.D.
Zr	●	<0.1[c]	<0.1[c]	●
Mo	●	<0.01[c]	<0.01[c]	●
Total	100.0	65.8	70.9	14.0

[a-n], ●, N.D., n.d., See footnotes to table 2.

TABLE 7 COMPARISON OF CHROMIUM (III) AND CHROMIUM (VI) CONCENTRATIONS IN THE WELDING FUME WITH CHROMIUM AND ALKALI-METAL CONCENTRATIONS IN THE FLUX AND CORE METAL

Source	Species	% element (w/w) E01	E04	E05	E11	E12
Fume	total Cr	2.6	0.03	0.7	0.05	5.1
	Cr(III)	0.3	0.0	0.0	0.02	3.6
	wis[a]Cr(VI)	0.3	0.01	0.0	0.0	1.0
	ws[b]Cr(VI)	1.5	0.02	0.7	0.03	0.5
Weld deposit	Cr	7.0	≈0[c]	2.12	≈0[c]	32.5
Flux	Cr	15.9	0.07	4.2	0.2	0.1
	Na	0.7	0.4	0.4	1.0	<0.01
	K	1.5	1.2	2.4	0.08	0.02

[a] wis = water-insoluble.
[b] ws = water-soluble.
[c] Not determined by manufacturer, implying negligible concentration.

of the fumes. Crystalline silica (SiO_2) and/or metal silicates were also not observed in the x-ray diffractograms of any of the fumes, implying that silicon was present as amorphous silica or silicates. Although crystalline silica could potentially act as a tumour enhancing agent due to chronic irritative and tissue wounding effects, there is no evidence relating to any biological activity of amorphous silica[3]. The presence of crystalline potassium chromate (K_2CrO_4) in fume from electrode E04 (soluble Cr(VI) – 0.02%) and its absence in fume from electrode E12 (soluble Cr(VI) – 0.5%; K – 2%) is somewhat puzzling. It is possible other Cr(VI) compounds were present in the fume from E12 and in addition XRD techniques will not detect crystalline substances in particles < 0.05 – 0.1 μm in diameter[44].

The AAS and XRF techniques together provide analytical data for all elements except oxygen. Where elements were determined by both methods, the agreement was excellent (tables 2-6). Volatilization losses during fusion at 1050°C with $Li_2B_4O_7/LiBO_2$ probably contribute to some of the lower Na, K and Ca concentrations measured by XRF. Ion-chromatography and ion-selective electrode methods for measuring water-soluble fluorides varied on an average by ± 12% (maximum variation ± 30%). Ion-chromatography[28] has not been used before in welding fume analysis and is probably the more accurate technique. Ionic interferences with ion-selective electrodes are common[25,45] and may not have been completely eliminated by our matrix matching methods.

Mass balances (up to 85-95% of total) may be obtained for the flux, fume and water-soluble fume by including the mass of oxygen which would be associated with elements such as Si(SiO_2, SiO_4^{4-}), Ti(TiO_2, TiO_4^{4-}), Cr(Cr_2O_3, CrO_4^{2-}), Al(Al_2O_3, AlO_4^{5-}), Mn(MnO, MnO_2, Mn_2O_3, Mn_3O_4, MnO_4^{2-}) and Fe(Fe_2O_3, Fe_3O_4, FeO_4^{2-})[4]. Contributions from elements which were not determined are in general minor. The maximum deviation from mass balance is in the case of the water-soluble fume fraction from electrode E01 (table 2). The total after including the mass of oxygen is ≈ 17.5% w/w which is 5% less than the total based on the solubility determination (22.5% w/w). The 5% deficiency may be due to the presence of water-soluble sodium and potassium silicates (2.5% Si in fume).

The enrichment of fume in flux elements (expressed as the ratio of their concentrations in fume and flux) generally follows the order: K > Na > F > Si > Ca > Ti. This is related to the volatility of the associated compounds[38] and to the prevailing chemical-thermodynamics[36]. The enormous enrichment of fume in Na, K and Cl for electrode E12 may be due to the formation of highly volatile compounds such as NaCl, NaF, KCl and KF. If F were present as CaF_2 and Si as SiO_2 in the original flux, this would further explain the Na and F flux results (table 6).

Iron is the most abundant element in the fumes. Stokinger[35] has reviewed the literature on iron oxides and concluded that they have no adverse health effects. The comparatively low iron content of the fume from electrode E05 (table 4) may be attributed to the low fume generation rate (FGR) of the electrode[23,37,39]. Similarly, the higher than expected iron content of the fume from electrode E11 (table 5) may be derived from the high FGR of the electrode[23,37,39].

Metals such as iron, chromium, manganese, molybdenum and nickel are added to the electrode flux to increase deposition efficiency[3]. Gray et al.[13] have pointed out that metal added as a powder in the flux makes a larger contribution to the fume than a similar weight of metal present in the electrode core. Gray et al. emphasize that toxic metals should, wherever possible, be incorporated in the core metal and not added as metal powders in the flux. There is some evidence from the present results that contributions of manganese (see tables 3 and 6) and nickel (see tables 3 and 5) to the fume are greater from the flux than from the core metal (estimated on the basis that the electrodes contain 65-80% core metal and 20-35% flux by weight).

The fluorine compounds present in welding fumes

have been found to be physiologically active[27,31]. Basic electrodes[30] give rise to mainly NaF, KF and CaF_2 in the fume[26] [all the electrodes used in the present study are basic electrodes, except E11 (high-manganese hardfacing), which is a neutral electrode[30]]. The transition-metal fluoro-complexes found in the water-soluble fume fractions from basic electrodes may lower the biological activity of fluoride[27]. Our results show that the actual amount of fluoride formed in the fume is the same for the four types of basic electrodes, ie, 2.2 – 2.4 g/kg electrode melted (see refs 37, 39 for FGR data). This means that there is an inverse relationship between fluoride concentration and FGR. The result is not unexpected and is related to the high volatility of NaF, KF and CaF_2[7,38]. There is no significant correlation between the percentage of fluoride in the fume and the percentages of fluoride, sodium, potassium or calcium in the flux (tables 2-6). It appears therefore that fluoride formation in the fume is controlled mainly by volatilization processes and not by specific high temperature stoichiometric reactions. The differences in concentrations of NaF, KF and CaF_2 in the flux from the different electrodes are probably manifested in the slag compositions and/or in the concentrations of chromates, silicates, etc in the fumes.

The chromium speciation results (table 7) deserve special attention. Chromium (III) compounds are biologically inert[20] and have in fact been used in nutritional medicine[22]. Chromium (VI) compounds can penetrate cell membranes more easily and oxidize biological material, thereby adversely affecting cellular function and causing toxic effects[20]. The carcinogenic activities of chromium (VI) compounds are related to their solubilities in body fluids[3,18]. Relatively insoluble Cr(VI) compounds (eg, $ZnCrO_4$, $PbCrO_4$) have been clearly shown to be carcinogenic in laboratory animals[8]. However, the carcinogenicity of highly soluble Cr(VI) compounds (eg, Na_2CrO_4, K_2CrO_4, CrO_3) is not yet well established[8]. Our results indicate that Cr(III), water-insoluble Cr(VI) and water-soluble Cr(VI) in the fume originate both from the electrode core and flux. Core metal must favour the formation of Cr(III) compounds (eg, Cr_2O_3, $FeCr_2O_4$)[40]. The most important finding from the results in table 7 is that there is a high correlation ($r = 0.92$) between water-soluble Cr(VI), total Cr in the fume and the Na + K in the flux. Kimura et al.[16] tested several types of flux-coated electrodes and have reported a similar finding with the one type of electrode containing different amounts of Na and K in the flux. The electrodes used in our study are of five different types but it seems that the sodium and potassium in the flux are present chiefly as silicates with similar high temperature (> 3,000°C) reactivity. Reduction of the Na and K content of electrode fluxes might be a useful means of reducing the proportion of Cr(VI) in welding fumes.

CONCLUSION

The results obtained in the current investigation may be used to calculate ventilation requirements in welding workshop environments by applying the relevant threshold limit value (TLV) indices[12,23]. Fume generation rate (FGR) data for the electrodes are reported elsewhere[37,39]. The present results relate to fumes produced and collected under controlled conditions at the recommended optimum welding current and voltage. It should be recognized that fume composition may vary with arc voltage[13,36] and to a lesser extent with AC and DC welding[23]. However, the data presented may provide guidance to industrial hygienists and occupational health physicians in appraising specific situations related to fume exposure, fume toxicity and the health status of welders.

Biological tests on the 5 types of fume and their water-soluble extracts, have been completed and are being published in the "Journal of Applied Toxicology".

ACKNOWLEDGEMENTS

We thank Mr I.S. Barrow, Australian Iron and Steel, Port Kembla, for performing the XRF measurements, Mr W. Korth for carrying out the ion-chromatographic determination of fluoride and chloride and Mr D. Cheesman for writing the linear regression program. The technical assistance of Mr T.W. Lewis and Miss E.A.I. Wilke is also acknowledged. The authors are indebted to Mrs C. Peacock for her care in typing the manuscript. The work was supported by a grant from the Australian Welding Research Association.

REFERENCES

1 Abell M.T., Carlberg J.R. A simple reliable method for the determination of airborne hexavalent chromium. *Am Ind Hyg Assoc J* 35 (1974) 229-233.

2 American Welding Society. *The Welding Environment*. AWS, Miami 1973.

3 American Welding Society. *Welding Handbook*. Seventh edition, Volume 1. AWS, Miami 1976, pp 69-70.

4 American Welding Society. Characterization of arc welding fume. AWS, Miami 1982. 55p.

5 American Welding Society Safety and Health Committee. *Effects of Welding on Health*. AWS, Miami 1979. 121p.

6 American Welding Society Safety and Health Committee. Effects of welding on health. *Aust. Welding J* 24 (1980) 7-15.

7 Aylward G.H., Findlay T.J.V. Chemical data book. John Wiley, New York 1966.

8 Baker R.S. Nickel and chromium (VI): evaluation of carcinogenic materials and cancer in welders. *Aust. Welding J* 27 (1982) 53-57.

9 Baker R.S., Arlauskas A., Tandon R.K., Crisp P.T., Ellis J. Effect of welding fume particles on sister chromatid exchange in cultured Chinese-hamster cells. In preparation.

10 British standards institution. Methods for the sampling and analysis of fume from welding and allied processes. Part 1, particulate matter. *International Institute of Welding Doc. VIII – 729-77*.

11 Clapp D.E., Owen R.J. An investigation of potential health hazards of arc welding fume growth with time. *Welding J* 56 (1977) 380-s-385-s.

12 Gray C.N., Hewitt P.J., Dare P.R.M. New approach would help control weld fumes at source Part 1: biomedical ground. *Welding and Metal Fabrication* 50 (1982) 318-324.

13 Gray C.N., Hewitt P.J., Dare P.R.M. New approach would help control weld fumes at source Part 3: MMA fumes. *Welding and Metal Fabrication* 51 (1983) 52-55.

14 Instrumentation Laboratory Incorporated. Atomic absorption methods manual: Volume 1 Standard conditions for flame operation. Massachusetts 1979.

15 Japanese welding engineering standard 9003k – 1976. Methods for chemical analysis of weld fumes. *International Institute of Welding Doc.* VIII – 717-77.

16 Kimura S., Kobayashi M., Godai T., Minato S. Investigations on chromium in stainless steel welding fumes. *Welding J* 59 (1979) 195-s-204-s.

17 Korth W., Ellis J. Ion-chromatographic determination of chloride and fluoride in electrolyte from the halogen tin-plating process. *Talanta* 31 (1984) 467-468.

18 Koshi K., Iwasaki K. Solubility of low-solubility chromates and their clastogenic activity in cultured cells. *Ind health* 21 (1983) 57-65.

19 Kubaschewski O., Hopkins B.E. Oxidation of metals and alloys. Butterworths, London 1962. pp 1-15.

20 Langard S. Absorption, transport and excretion of chromium in man and animals. In: Langard S., ed. Biological and environmental aspects of chromium. *Elsevier* 1982. 149-169.

21 Luckey T.D., Venugopal B. Metal toxicity in mammals: Volume 1 Physiologic and chemical basis for metal toxicity. Plenum press, New York 1977. 238p.

22 Mertz W. Effects and metabolism of glucose tolerance factor. *Nutr Rev* 33 (1975) 129-135.
23 Miller T.M., Jones R.C. An assessment of the fume characteristics of Australian electrodes – for manual metal arc welding. *Aust Weld Res* 6 (1979) 1-9.
24 NIOSH Measurements Research Branch. Latest NIOSH method for hexavalent chromium. 1981. 319-1-319-7.
25 Orion Research Incorporated. Orion ionalyzer instruction manual. Form IM 94, 96-09/7721. Massachusetts 1977.
26 Pantucek M. Influence of filler materials on air contamination in manual metal arc welding. *Am Ind Hyg Assoc J* 32 (1971) 687-692.
27 Pantucek M.B. Hygiene evaluation of exposure to fluoride fume from basic arc-welding electrodes. *Ann Occup Hyg* 18 (1975) 207-212.
28 Pohl C.A., Johnson E.L. Ion chromatography – The state-of-the-art. *J Chromatogr Sci* 18 (1980) 442-452.
29 Sandell E.B. Colorimetric determination of traces of metals. 3rd ed., Interscience Publishers, New York 1959, pp 392-397.
30 Sandvik A.B., Sandviken, Sweden. *Sandvik Welding Handbook*. Pannebald, Goteborg 1977, pp 34-35.
31 Sjogren B. Urinary fluoride concentration as an estimator of welding fume exposure from basic electrodes. *Brit J Ind Med* 41 (1984) 192-196.
32 Stern R.M. Production and characterization of a reference standard welding fume: introduction. Danish Welding Institute Rep. 76.00.
33 Stern R.M. Process-dependent risk of delayed health effects for welders. *Environ Health Perspect* 41 (1981) 235-253.
34 Stern R.M. Assessment of risk of lung cancer for welders. *Arch Environ Health* 38 (1983) 148-154.
35 Stokinger H.E. A review of world literature finds iron oxides noncarcinogenic. *Am Ind Hyg Assoc J* 45 (1984) 127-133.
36 Tandon R.K., Crisp P.T., Ellis J., Baker R.S. Variations in the chemical composition and generation rates of fume from stainless steel electrodes under different AC arc welding conditions. *Aust Welding J* 28 (1983) 27-30.
37 Tandon R.K., Ellis J., Crisp P.T., Baker R.S. Fume generation and melting rates of shielded metal arc welding electrodes. *Welding J* 63 (1984) 263-s-266-s.
38 Tandon R.K., Payling R., Chennall B.E., Crisp P.T., Ellis J., Baker R.S. Application of x-ray photoelectron spectroscopy to the analysis of stainless-steel welding aerosols. *Appl Surf Sci.* in press.
39 Tandon R.K., Crisp P.T., Ellis J., Baker R.S. Generation rate, particle-size and chemical measurements of fumes from some hardfacing and HSLA-steel electrodes. *Welding and Metal Fabrication*. In press.
40 Thomsen E., Stern R.M. Collection, analysis and composition of welding fumes. *Danish Welding Institute Rep.* 81.09.
41 Ulfvarson U. Survey of air contaminants from welding. *Scand J Work Environ Health* 7 (1981): suppl 2, 28 p.
42 Varian Techtron. Analytical methods for flame spectroscopy. *Australia* 9/72.
43 Venugopal B., Luckey T.D. Metal toxicity in mammals: Volume 2 Chemical toxicity of metals and metalloids. Plenum press, New York 1978, 409 p.
44 Voitkevich V.G. Methods of investigating welding fumes review. *Avt Svarka* 3 (1982) 51-54.
45 Willard H.H., Merritt Jr. L.L., Dean J.A., Settle Jr. F.A. Instrumental methods of analysis. Wadsworth Publishing Company, Belmont, California 1981, pp 640-663.
46 Interlaboratory calibration of a standardized analytical method of hexavalent and total chromium in welding fumes. *Welding in the World* 21 (1983) 10-14.

APPENDIX F

REFERENCE 29

(Tandon et al., 1984)

purity. Although sodium is known to be present in the binder, it does not appear in any SPEC chemical category. Elements are detected by EDXA in the SPEC system. Sodium can be detected, but the sensitivity is low. When X-rays from very small particles are counted for short times (1 second), the likelihood for observing Na above background noise is not very good.

2. E7018

The wet chemical analysis showed 0.9 percent aluminum, 20.6 percent calcium, 19.5 percent fluorine, 24.6 percent iron, 12.5 percent potassium, 4.6 percent manganese, 3.3 percent sodium, and 2.8 percent silicon. Analysis of the elements present in the bulk sample by EDXA showed major amounts of potassium, calcium and iron, intermediate amounts of silicon and manganese, and trace amounts of aluminum, sulfur, and chlorine. XRD analysis of the bulk sample showed that the major crystalline phase is potassium-calcium fluoride, KF-CaF_2. Intermediate phases include magnetite, Fe_3O_4, calcium fluoride, CaF_2, and jacobsite, $MnFe_2O_4$. It should be mentioned again that the element fluorine, although prominent in the crystal phases, is very difficult to detect by EDXA.

The SPEC system was used to analyze approximately 1000 particles by chemistry and by size. The average diameter (by number) for all particles was 0.182 ± 0.117 μM. The categories identified by computer search are shown below.

E7018 Composition by Category

Category	Percent by Number	Average Diameter	Composition (Volume Weighted X-ray %)
16. K-Fe	14%	0.179 μM	Si(18) K(36) Fe(28)
18. Ca-Fe	15	0.158	Al(7) Si(17) Ca(25) Fe(37)
19. K-Ca-Fe	48	0.188	Al(4) Si(10) K(28) Ca(22) Fe(23)

Chromium, copper, and manganese are present in the particles in low concentrations in 8, 8, and 23 percent, respectively. These elements are found in mixtures of the particles classified in the three main categories. In a typical particle, for example, X-ray percentage may be either 35 Ca, 14 Cr, and 51 Fe, or 22 Si, 15 K, 14 Ca, 21 Mn, and 27 Fe. Lead is found in low concentrations in only 5 percent of the particles in mixtures similar to those described above. (Details of the other particle categories are given in Tables 5b, 6b, 7b, and 8b.)

The STEM analysis of this fume was made difficult by the irregularities of the particles. They were either too thick to obtain diffraction patterns or, where thin enough, appeared to be multi-crystalline giving diffraction patterns too irregular to be indexable. Occasionally, particles could be found that showed only an Fe peak (see Fig. 10). These patterns were again consistent with Fe_3O_4.

The particles in this fume are mixtures of potassium/calcium fluorides and iron/manganese oxides. Fe_3O_4 and $MnFe_2O_4$ are observed and probably non-stoichiometric oxides of iron and manganese are present as well. No pure manganese oxide is likely since particles with a very high Mn concentration are not found. No crystalline silicon compounds are observed, and the behavior of silicon is similar to that discussed for the E6010 fume.

3. E70S-3

The wet chemical analysis showed 0.4 percent copper, 57.0 percent iron, 7.8 percent manganese, and 3.3 percent silicon. Analysis of the elements present in the bulk fume by EDXA showed the elements iron and minor amounts of silicon and manganese. XRD analysis of the bulk sample showed that the major crystalline phase was magnetite, Fe_3O_4. XRD also indicated a trace of metallic iron.

The SPEC system was used to analyze approximately 1000 particles by chemistry and by size. The average diameter (by number) for all particles was 0.135 ± 0.114 μM. The main categories identified by the computer search are shown below.

E70S-3 Composition by Category

Category	Percent by Number	Average Diameter	Composition (Volume Weighted X-ray %)
2. Fe	9%	0.153 μM	Si(7) Fe(90)
3. Fe/Low Si	14	0.173	Si(10) Mn(6) Fe(76)
5. Fe-Mn	17	0.129	Si(12) S(4) Mn(13) Fe(62)
6. Fe-Cr	5	0.129	Si(16) Cr(10) Fe(53) Zn(5)
12. Fe-Al	6	0.103	Al(18) Fe(69)
16. K-Fe	6	0.111	Si(6) K(16) Mn(6) Fe(58)
18. Ca-Fe	10	0.118	Al(7) Si(13) Ca(15) Mn(5) Fe(48)
34. Fe-Rich	8	0.148	Al(4) Si(5) K(6) Fe(71)

Copper, chromium, and lead are found in low concentrations in 8, 10, and 7 percent of the particles, respectively. Once again, these trace elements are not found as a small number of particles of the pure oxide, but rather spread in small amounts through a large number of particles. For example, in the bulk fume 0.4 percent by weight is copper (see Table 8). Yet copper is found in 8.5 percent of the particles which make up 13.3 percent by weight of the fume sample analyzed by SPEC. Manganese comprises 7.8 percent by weight of the bulk fume, but 25 percent of the particles contain manganese at low concentrations in mixtures of iron, manganese, and silicon. An additional 3 percent contain intermediate amounts of manganese in particles of similar chemistry. It is unlikely that pure oxides of manganese are present. (Details of the other particle types are given in Tables 5c, 6c, 7c, and 8c.)

Fume Generation and Melting Rates of Shielded Metal Arc Welding Electrodes

Electronically controlled welding apparatus is used to determine the fume generation rates and melting rates of some hardfacing and HSLA steel SMAW electrodes

BY R. K. TANDON, J. ELLIS, P. T. CRISP, AND R. S. BAKER

ABSTRACT. An electronically-controlled welding apparatus with a fume collection system was used for shielded metal arc welding (AC and DC) of three hardfacing and two high-strength, low-alloy steel electrodes at optimum current settings for each electrode.

At each current setting, fume generation rates (FGR's, *i.e.*, g fume/kg electrode melted) varied by a factor of 1.5 to 2.0 while acceptable arc length was maintained. FGR's increased almost linearly with voltage and with power, and decreased almost linearly with current. AC welding gave FGR's which ranged from 50% greater (hardfacing high-manganese electrode) to 30% less (hardfacing medium-chromium electrode) than DC welding at the same current. No difference was found in FGR's between DCEN or DCEP welding* with a hardfacing high-manganese electrode.

Electrode melting rates (EMR's, kg electrode melted/h) increased almost linearly with current, and decreased almost linearly with voltage and power. For the same current with a hardfacing high-manganese electrode, EMR's varied as follows: AC < DCEP < DCEN.

The processes responsible for the observed variations are discussed, and the need for study of metal arc physics is emphasized.

*AC – alternating current; DCEP – direct current, electrode positive; DCEN – direct current, electrode negative.

R. K. TANDON, J. ELLIS and P. T. CRISP are with the Department of Chemistry, University of Wollongong, and R. S. BAKER is with the Cell Biology Laboratory, Commonwealth Institute of Health, University of Sydney, in New South Wales, Australia.

Introduction

A large proportion of the electrodes currently produced are of the hardfacing and high-strength-low-alloy (HSLA) steel types. Special shielded metal arc welding (SMAW) electrodes are extensively used for hardfacing in agriculture, mining and engineering where resistance to abrasion, impact and erosion are essential weld requirements (Refs. 1, 2). HSLA steel SMAW electrodes have numerous industrial applications, such as the welding of tubes and vessels in chemical plants and steam generating equipment (Ref. 2).

Both types of electrodes contain varying amounts of chromium which, when released as chromium (VI) in fume, is suspected of causing lung cancers (Ref. 3), but this has not been established in welding health studies (Ref. 4). It is important, therefore, to study the formation rate and chemical composition of the fume emitted from such electrodes.

In this paper, data are presented for three hardfacing-SMAW and two HSLA steel SMAW electrodes in order to show the effect of electrical variables on fume generation rates and electrode melting rates. Both welding and fume collection were carried out under precisely controlled and reproducible conditions. This study is the first phase of a project in which it is planned to carry out physical, chemical and biological investigations of fume particles from hardfacing SMAW and HSLA steel SMAW electrodes.

Experimental Procedure

The equipment and method used for generating and collecting welding fume have already been described by the authors (Ref. 5). A schematic diagram of the equipment is shown in Fig. 1.

An electronic controller maintains a constant preset welding voltage by adjusting the arc length via an electrode feeder mechanism. The electronic controller also operates the horizontal drive table and welding power supply while continuously displaying the welding current and voltage; both current and voltage can be continuously recorded. The electrode feeder mechanism comprises an insulated electrode holder mounted on a worm thread which is driven by a DC servo-motor. The horizontal table moves on rollers with a total movement of 500 mm (19.7 in.) at speeds adjustable from 100 to 700 mm/min (3.94 to 27.6 ipm).

For AC welding (Ref. 5), the low current range (open circuit = 78 V) was used for all electrodes except E11 (Table 1); for the E11 electrode, a high current range (open circuit = 55 V) was used. DC welding was performed with a Lincwelder DC 250 MK generator (open circuit = 60V).

For both AC and DC welding, the current on the power supply was set to the mid-point of the recommended operating range, and welding was performed at arc voltages between 20 and 35 V. The use of automatic welding apparatus simulated both practical welding conditions and unstable long-arc conditions. The latter were included in the study in order to probe the physical and chemical processes occurring in the welding arc.

All measurements were made at a welding speed of 150 mm/min (5.9 ipm), with the electrode feeder mechanism set at an angle of 45 deg to the table. All welding was done on 8 mm (0.31 in.) thick mild steel plates. Voltage measurements were made between the top of the electrode and the work table and between points 50 mm (1.97 in.) apart near the top of each electrode; current

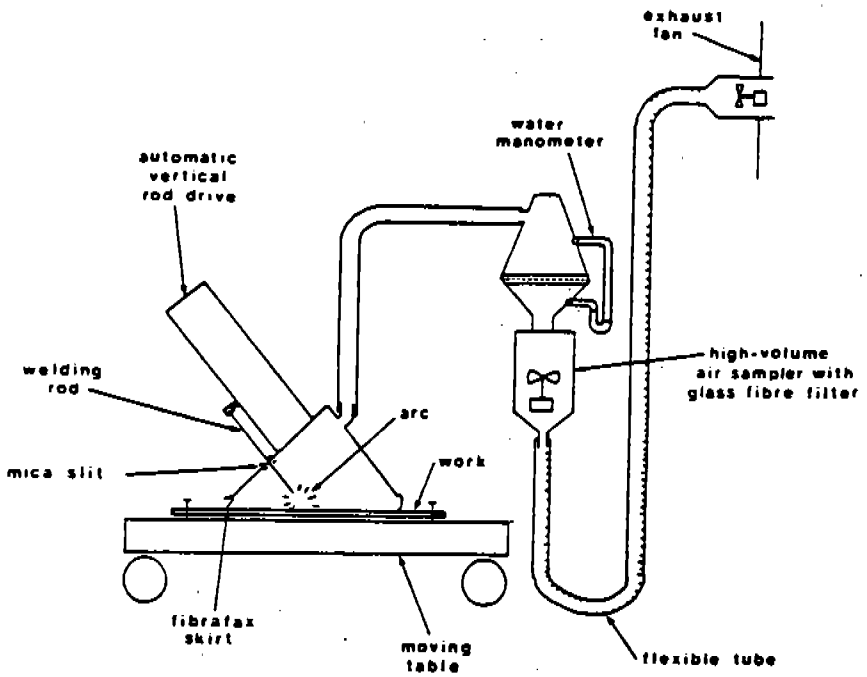

Fig. 1—Schematic of the welding and fume collection equipment. Reproduced from Australian Welding Journal *with permission (Ref. 5)*

was determined by measuring the voltage drop across a shunt of known resistance. Dynamic properties of the arc (Ref. 6) and phase angle were measured using a cathode-ray oscilloscope.

Fume collection was carried out following the procedures described by the American Welding Society (Ref. 7) and the Australian Welding Research Association (Ref. 8). An air flow rate of approximately 16 L/s (2034 cfh) was used; this is within the range of fume-plume conditions in practical welding.

Results

The electrodes used in the study and their recommended operating conditions are given in Table 1. The relationships between the electrical variables—current, voltage and power—are shown in Fig. 2, and the variations in fume generation rate and electrode melting rate with current are shown in Figs. 3 and 4.

It must be borne in mind that both fume generation rates and electrode melting rates relate to a situation where power (V · A) is increasing as voltage (V) is increasing and current (A) is decreasing (see Fig. 2). We are thus working along points on the voltage-current curve at constant current setting on the power supply. The experiments were not designed to make comparisons of fume generation rates at equivalent power levels (power (kW) = current (A) X voltage (V) ÷ 1000). However, in all instances where equivalent power levels were obtained, higher fume generation rates were found with higher arc voltages.

Values for average current, fume generation rate, and electrode melting rate were reproducible within ±5% using the same voltage setting on the electronic controller and electrodes of the same production batch. During welding, voltage and current fluctuated within ±1 V, ±1 A with electrode E11 and within ±2.5 V, ±5 A for the other electrodes.

Resistive heating of the unused portion of electrode was small, since the voltage drop along the electrode was 20–50 mV/cm (≃ 51–127 mV/in.), corresponding to ≈ 1 V along a full rod. Current and arc voltage were in phase (phase angle <3 deg), confirming the absence of significant capacitance or inductance in the arc. All electrodes formed a gun barrel tip during use, and the welded seams were generally flat and uniform. Electrodes E11 and E12 formed considerably less slag than the other electrodes.

No leakage of fume around the collecting hood was visible during welding, and loss of fume due to deposition in the steel tubing and hood was <5%. The glass-fiber filter collects particles below 0.3 μm with decreasing efficiency, but such particles constitute only a small percentage of the total mass collected on the filter (Ref. 9).

Discussion

The fume generation rates (FGR's) for each electrode varied by a factor of approximately two while acceptable arc length was maintained using the recommended nominal current settings on the power supplies. FGR's increased almost linearly with voltage and with power, and decreased almost linearly with current—Figs. 3 and 4.

It is likely that the power of the arc is the principal factor determining the FGR's (Refs. 5, 10), since an increase in the rate of heat input to the arc should lead to greater evaporation and sputtering of molten metal and molten flux. The arc voltage may also be important since it

Table 1—Description of the Hardfacing and High-Strength, Low-Alloy Steel Electrodes Used

Code[a]	Type	Diameter, mm	Recommended operation and current, A	Nominal weld deposit analysis, wt-%
E01	Hardfacing, medium-chromium	3.25	AC : 90-135 DCEP: 90-135	Cr:7, C:0.4, Mo:0.5, Mn:0.3, V:0.5
E04	High-strength, low-alloy steel	3.25	AC :105-150 DCEP:105-150	Ni:1.6, C:0.07, Mn:1.0, Si:0.04, Mo:0.3
E05	High-strength, low-alloy steel	3.25	DCEP: 75-130	Cr:2.12, C:0.045, Mo:0.95, P:0.022, Mn:0.72, S:0.019, Si:0.38
E11	Hardfacing, high-manganese	4.0	AC :125-230 DCEP:125-210 DCEN:125-210	Mn:14.5, Si:0.14, Ni:3.2, P: ≦ 0.05, Mo:0.75, S:0.01, C:0.65
E12	Hardfacing, high-chromium	6.0	AC :120 DCEP:120	Cr:30-35, Mn:3-3.5, C:4-5

(a) AWRA system of classification corresponding to code designations: E01—1855A4; E04—E9018C; E05—E901583; E11—1215A4; E12—2355A1.

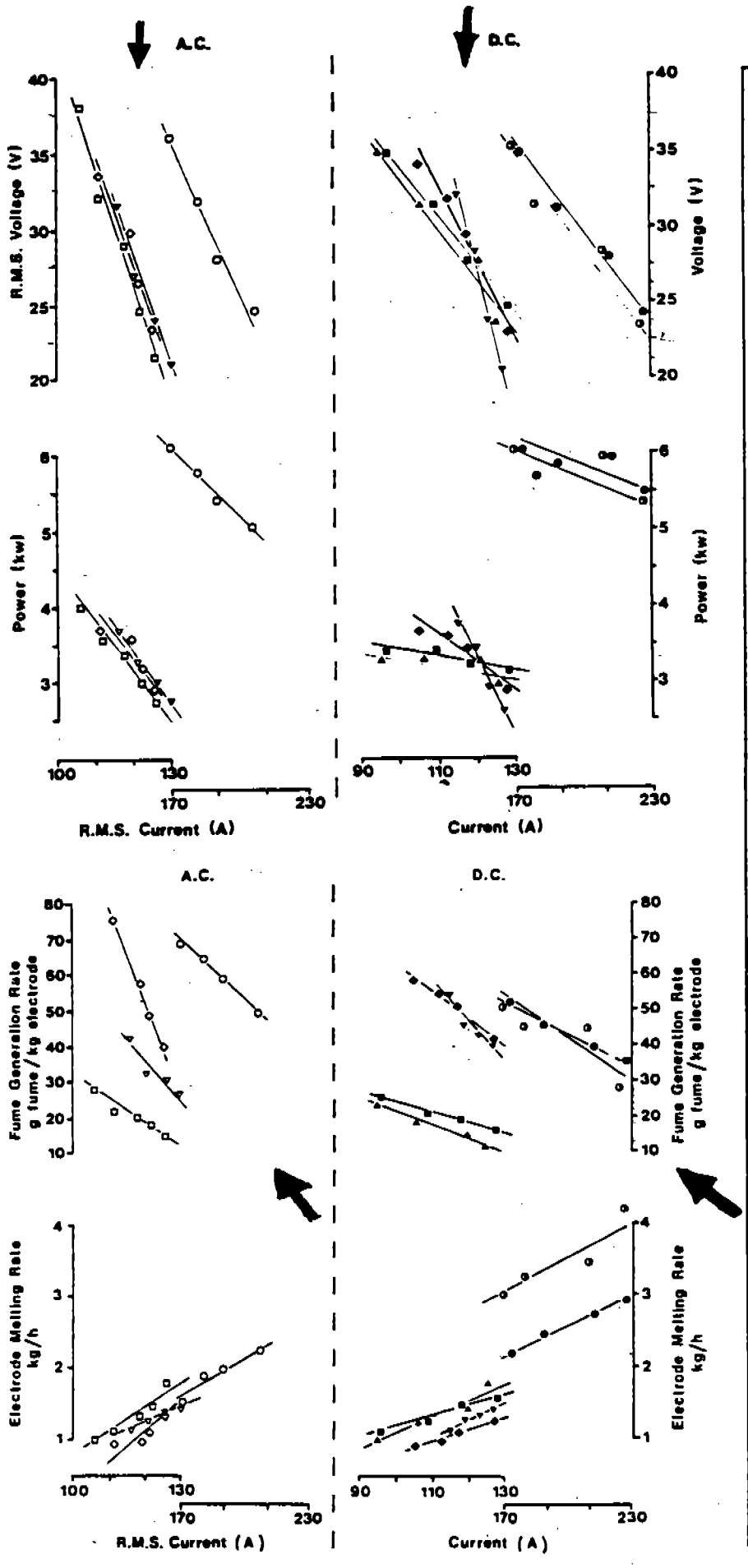

Fig. 2 – Effect of current on arc voltage and power using specific electrodes by code designation (see Table 1): E01 with AC – ▽, with DCEP – ▼; E04 with AC – □, with DCEP – ■; E05 with DCEP – ▲; E11 with AC – ○, with DCEP – ●, with DCEN – ⊕; E12 with AC – ◇, with DCEP – ◆

determines the arc length (Ref. 1) and, thus, the following:

1. The surface area of the plasma column through which material can escape.
2. The time the material spends in the plasma (Ref. 5).

No systematic difference was observed in FGR's with AC compared with DC welding. The results obtained here do not agree with the findings of Eichhorn *et al.* (Ref. 11) that AC welding generally produces less fume than DC welding.

The mechanism of metal transfer during SMAW welding is difficult to establish but under optimum conditions consists of a showery spray of metal and slap droplets (Ref. 1). Gray *et al.* (Ref. 12) proposed that, during spray transfer, the bulk of the fume formation occurs in the arc plasma by evaporation of droplets in the plasma jet rather than by processes at the cathode or anode. This proposal explains the similar FGR's obtained with DCEN and DCEP welding for electrode E11; it also explains the generally similar fume generation rates obtained with AC and DC welding at the same power – Fig. 4.

The electrode melting rates (EMR's) displayed opposite behavior to the FGR's in their variation with the electrical conditions. EMR's increased almost linearly with current and decreased almost linearly with voltage and power. EMR's obtained using AC and DCEP were generally similar, but the EMR for electrode E11 using DCEN was approximately 40% greater than that using DCEP.

The high melting rates obtainable with DCEN arcs are well known (Refs. 1, 13). The transfer of metal is globular and spattery, unless trace constituents such as metal oxides and calcium salts are included in the flux to make the cathode more thermionic; if this is done, spray transfer of metal predominates and the melting rate decreases (Ref. 1). It appears, therefore, that the differences in EMR's with different DC polarities arise from differences in the proportions of globular transfer (fast) and spray transfer (slow).

We suggest that globular transfer occurs when there are relatively few arc roots releasing heat ("plasma emission," Ref. 13) and that spray transfer occurs when the arc roots are relatively numerous ("field emission," Ref. 13). The

Fig. 3 – Effect of current on the fume generation rate and electrode melting rate (see Fig. 2 caption for symbols corresponding to electrode code designations)

increase in EMR's with increasing current may be due to the increasing frequency of charge-transfer processes per unit area of the electrode surface, resulting in a greater rate of heat dissipation.

It is notable that EMR's increase with decreasing power. This is probably due to the relatively small amount of radiative heating of the electrode by the plasma or workpiece surface (Ref. 1); resistive heating of these components of the arc, therefore, has little bearing on events at the electrode surface.

Interpretation of fume-generation and electrode-melting data for covered electrodes is hindered by the limited information available on the physics of metal arcs. Processes occurring at the anode and cathode surfaces are poorly understood and, to date, studies of the arc plasma have concentrated on the simplest cases, *i.e.*, inert-gas shielding, nonconsumable electrode and cooled workpiece (Refs. 12, 14).

The flux coatings of covered electrodes provide additional charge carriers to the plasma (readily ionizable elements such as sodium, potassium and calcium); these modify the emissivity of the cathode and anode surfaces (metal oxide and ionizable atomic films) and probably affect most other arc variables. Further interpretations of fume-generation and electrode-melting data must wait until the chemical physics of flux coatings and electrode processes are better understood.

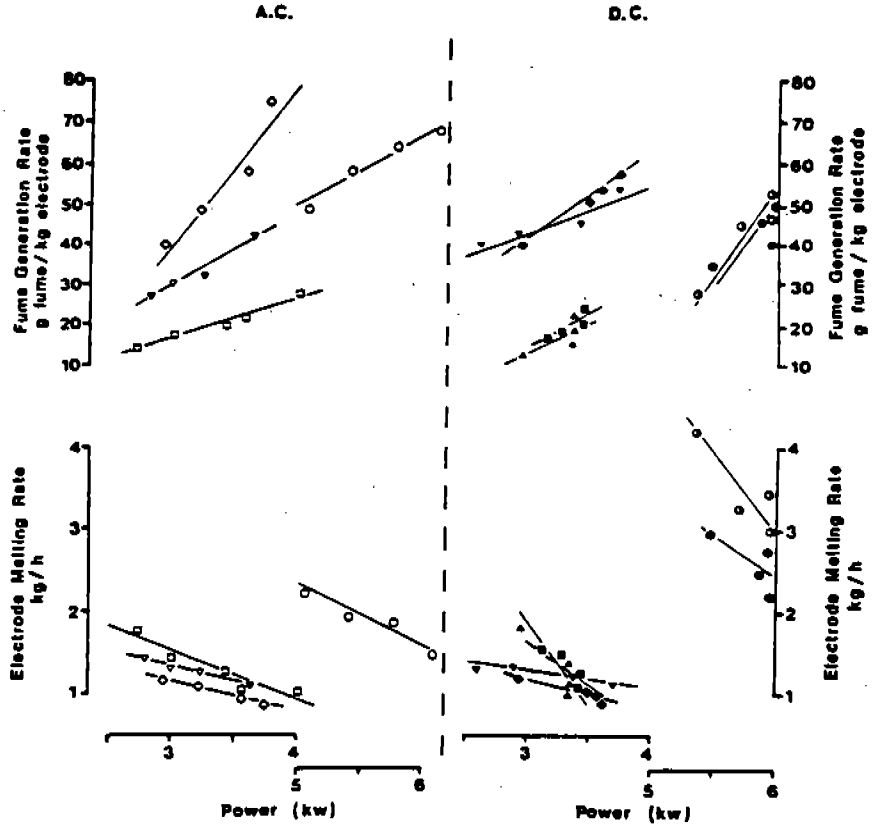

Fig. 4 — Effect of power in the fume generation rate and electrode melting rate (see Fig. 2 caption for symbols corresponding to electrode code designations)

Conclusion

Wide variations in fume generation rate occur with different electrodes and with the same electrode under different welding conditons. In particular, the highest fume generation rates were observed with a high-chromium hardfacing electrode; this result may be important due to the present concern about chromium (VI) toxicity.

Variations in fume generation rates are important for determining the precautions which should be taken during welding operations and must be known for chemical and biological studies of fume toxicity. In addition, fume generation rate data for welding processes under different conditions must be available so that hypotheses concerning electrode and plasma behavior may be tested.

Acknowledgments

This work was supported by a research grant from the Australian Welding Research Association (AWRA). The authors wish to thank Mr. A. Wilson and Mr. I. McGeachie of AWRA for their assistance. We gratefully acknowledge receipt of electrodes from the various manufacturers and thank Welding Industries Aust. Ltd. for providing an AC power supply, and Lincoln Electric Pty. Ltd. for the loan of a DC generator. The assistance of the University of Wollongong Science Faculty Workshop staff is much appreciated. One of us (R.K.T.) gratefully acknowledges the award of an AWRA research fellowship.

References

1. American Welding Society. 1976. *Welding handbook:* 7th ed., vol. 1. Miami, Florida.

2. Welding Industries of Australia (WIA) catalogue 2012/20/180.

3. Baker, R. S. 1982. Nickel and chromium (VI): evaluation of carcinogenic materials and cancer in welders. *Australian Welding Journal* 27(3):53-57.

4. Palmer, W. G. 1983. Effect of welding on health IV. Miami, Florida: American Welding Society.

5. Tandon, R. K., Crisp, P. T., Ellis, J., and Baker, R. S. 1983. Variations in the chemical composition and generation rates of fume from stainless steel electrodes under different AC arc welding conditions. *Australian Welding Journal* 28(1): 27-30. (IIW/IIS VIII-1098-83.)

6. Sandvik, A. B. 1977. *Sandvik welding handbook.* Sandviken, Goteborg, Sweden.

7. American Welding Society. *Laboratory method for measuring fume generation rates and total fume emission of welding and allied processes.* AWS F 1.2-79. Miami, Florida. (IIW/IIS VIII-932-81.)

8. Australian Welding Research Association. *AWRA standard laboratory method for measuring fume generation rates and total fume emission from wire welding processes.* AWRA Panel 9-8-82. Sydney.

9. General Metal Works Inc. *Glass fibre filter specifications.* Ohio.

10. Kimura, S., Kobayashi, M., and Maki, S. 1976. Some considerations about fumes generated in arc welding processes. IIW/IIS VIII-687-76.

11. Eichhorn, F., Trösken, F., and Oldenburg, T. 1982. The production of air-contaminating substances during manual arc welding: *Schweissen und Schneiden,* translation 2/1982. Paper presented at the special DVS conference on "Health and Safety during Welding" held in Essen, West Germany, 16 and 17 February 1982.

12. Gray, C. N., Hewitt, P. J., and Dare, P. R. M. 1982. New approach would help control fumes at source, part two: MIG fumes. *Welding and Metal Fabrication:* 50(8): 393-397.

13. Houldcroft, P. T. 1967. *Welding Processes:* 15-22 London: Cambridge University Press.

14. Glickstein, S. S. 1983. Basic studies of the arc welding process. *Trends in welding research in the United States,* S. A. David, ed., pp. 3-51. Metals Park, Ohio: American Society for Metals.

APPENDIX G

REFERENCE 34

(Fasiska et al., 1983)

Characterization of Arc Welding Fume

Research performed by the Mellon Institute Materials Characterization Center, Pittsburgh, Pennsylvania, under contract with the American Welding Society and supported by industry contributions.

Performed By:

Edward J. Fasiska
Howard W. Wagenblast
Margaret Nasta
Mellon Institute MCC
Pittsburgh, PA 15213

February, 1983

Prepared for:

Safety and Health Committee
AMERICAN WELDING SOCIETY
550 N.W. LeJeune Road
Miami, FL 33126

Characterization of Arc Welding Fume

I. Introduction

During the process of welding, metal vapors are produced in the electric arc. As these vapors cool and solidify, a fume is formed that may be a potential health hazard to the welder and to others working in the same area. Such fine aerosols are all irritating to the respiratory system. Yet some fumes may potentially be more dangerous than others because of the specific substances present.

The purpose of this study is to provide a data base of chemical, crystallographic, and physical data for representative welding fume types which will aid in the understanding of the interactions of these particles with the human respiratory system. Such interactions are affected by many variables. Therefore, a simple percent weight analysis for various elements does not provide adequate information since individual particle size and chemistry affect toxicity. For example, a few large particles may dominate a percent by weight analysis. However, if these particles were over 10 μM in diameter, they might not reach the lower respiratory system at all, while compounds present in thousands of fine particles would penetrate to the alveoli of the lungs and could be absorbed into the blood. Particle morphology is also significant since particles with sharp edges or fibers are more irritating to the lungs than smooth, sphere-shaped objects. Finally, specific compounds must be identified since such factors as crystallinity, solubility, and oxidation state affect toxicity. Such information may influence the determination of federal standards for occupational exposure.

These objectives were accomplished by using various macro and micro scale techniques. Initially, energy dispersive X-ray analysis (EDXA) and X-ray diffraction (XRD) were used to obtain background information on bulk fume properties. The focus of this work was the analysis of the welding fume on a particle by particle basis. Automated electron beam analysis (SPEC) was used to analyze large numbers of particles, and specially designed computer software sorted the particle data by size and chemistry. Finally, a scanning transmission electron microscope (STEM) was used for a manual examination of a smaller number particles for size, chemical composition, and crystallinity. An examination of all of the data available for a fume can then be used to decide whether toxicological testing may be advisable.

II. Sampling Techniques

Two general types of samples were required for the investigation: bulk fume samples which could be used for the analytical techniques requiring large amounts of sample material, and lightly dispersed samples for the techniques which provide analyses of individual particles.

A. Bulk Samples

The bulk samples were collected by AWS in a conical chamber as described in AWS F1.1-79, *Laboratory Method for Measuring Fume Generation Rates and Total Fume Emission of Welding and Allied Processes.* This provides a sample of several grams needed for certain analytical procedures such as X-ray diffraction.

B. Dispersed Samples

For the analytical techniques which provide data from individual particles of the fume, it is required that the particles be dispersed in such a manner that the individual particles are not contingent so that individual particle data is not altered by adjacent particles. In principle, this can be accomplished in two ways. One method would be to redeposit portions of bulk samples to provide a non-contingent dispersion. This approach, however, has some danger in that there is no absolute assurance that the redeposition process does not break up naturally occuring particle agglomerates, dissolve certain particle types, or lose either large or small particle sizes.

The other approach is to collect the particles in a dispersed state on a suitable substrate directly from the weld fume. The only concern about this approach is that the collection times are necessarily short (a few seconds) and may not accurately represent an 8-hour average.

Three direct sampling techniques were investigated in order to determine a method that would reliably sample representative portions of the various arc welding fumes.

1. Nuclepore Filter Samples

Fume samples were collected by suction (2 liter/min) onto polyester Nuclepore filters (pore size 0.2 μM) loaded into standard plastic cassettes. There was some tendency for particles to agglomerate around the pores, but this was not a serious problem if sampling times were kept relatively short and the filter loadings were light. It was most convenient to collect several samples 18 inches above the arc at times such as 1, 3, and 5 seconds in order to bracket the optimum filter loadings needed for the various analytical techniques such as SPEC and STEM.

This technique is a standard method for collection of ambient air particulates analyzed in this laboratory. It also appears to be the best method for collecting fume samples defined for characterization of the individual particles rather than by bulk analysis.

2. Electrostatic Collector

With this technique, the particles were collected on smooth surfaces such as a glass slide or plastic tape using an electrostatic collector and charge neutralizer system. Although this technique reduced the tendency of the particles to agglomerate, the method was discarded because some agglomeration was still observed and because the long sampling tube needed for this instrument may be causing some size and chemical discrimination in particle collection. Further, it was felt that the electrostatic charge neutralizer in the system might be breaking up naturally-occurring agglomerates and, therefore, altering the actual state of the weld fumes.

3. Sticky Films

Samples were collected simply by holding a glass slide coated with a very thin film of a sticky substance such as Vaseline directly in the fume. This method was also discarded because the smallest particles are not representatively collected due to the air stagnation zone that develops at the surface of the slide.

Therefore, Method 1, the collection of the fume on Nuclepore filters, was selected as the primary sampling technique. The samples that were collected were compatible with the scanning electron microscope and the scanning transmission electron microscope, the instruments needed to measure size and chemistry of the submicron particles that are characteristic of welding fume.

III. Analytical Techniques and Sample Preparation

A. X-ray Diffraction (XRD)

Portions of the as-received bulk fume samples were loaded into glass trays to provide a smooth, even surface of the material. The trays were then placed in an X-ray diffractometer and exposed to copper K-alpha radiation over the Bragg reflection angle of 6 degrees to 100 degrees using a focusing graphite crystal, diffracted-beam monochromator. The output data from an X-ray diffraction analyses typically consists of peaks of different intensities at various Bragg reflection angles. These peaks result from the unique structures of crystalline materials with definite relationships of the distances and angles between the constituent atoms. Thus, proper indexing of the reflections from an X-ray diffraction pattern will reveal the specific crystalline compounds and phases which are present. It is important to mention that X-ray diffraction will not indicate the presence of amorphous materials or materials with particle sizes less than approximately 0.03 μM.

In the present study, the peaks on the patterns were generally relatively sharp indicating that at least portions of the sample materials were fairly well crystallized. The results of the analyses for the six samples are described in the Discussion Section of the report.

B. Energy Dispersive X-ray Spectrometry (EDXA)

Portions of the bulk samples were mounted on high purity graphite wafers with Duco Cement, coated with 0.02 μM of carbon, and examined in the scanning electron microscope (SEM) using a 24 KV accelerating voltage and a tilt angle of approximately 45 degrees. The microscope is equipped with an energy-dispersive X-ray analyzer which detects and semi-quantitatively measures all elements with atomic numbers greater than ten. (The elements not detected by EDXA are: hydrogen, helium, lithium, beryllium, boron, carbon, nitrogen, oxygen, fluorine, and neon. It is sometimes possible to detect fluorine if the concentration is at least 5 percent.) EDXA works by virtue of the fact that the high energy electron beam excites all elements in the sample and causes them to emit characteristic X-rays whose energies are unique to the emitting element. The X-rays are detected and energy-sorted by a solid-state detector, providing a spectral presentation of all elements present in concentrations greater than approximately one-half percent.

Further, the analysis can be confined to specific sample features as small as approximately 1 micron or, as in the present case, scanned over areas as large as approximately 4 mm x 4 mm to provide averages typical of the bulk concentration.

C. Suspended Particulate Evaluation and Classification (SPEC) System

The SPEC system combines three basic analytical instruments to produce its particle-by-particle particulate analysis. An electron beam image analyzer is joined to a scanning electron microscope (SEM) and an energy-dispersive X-ray analyzer (EDXA). The motion of the electron beam is digitized, allowing the position of the beam to be completely controlled by a mini computer. Using contrast variations resulting from differences in chemistries between the particles and the substrate, a description of particle size, shape, and chemistry can be rapidly generated and stored in a computer for the subsequent retrieval.

The fume samples were prepared for analysis by cutting a segment of approximately one square centimeter from the middle of the Nuclepore filter. These were mounted on an aluminum SEM stub using an amorphous graphite solution, then coated with approximately 0.02 μM of carbon by exposure to a carbon arc in vacuum. At least 1000 particles were analyzed for each fume type. Particle density on the filters ranged from 10^5 to 10^7 particles per square centimeter. Because of the random distribution of the fume particles, the analytical results are equivalent to those that would be obtained if all of the particles on the filter were analyzed.

The basic operational steps of the SPEC system are as follows:

- Generation of a search grid system
- Detection of particles intersecting the search grid system
- Size and shape analysis of particles
- Chemical analysis of particles
- Data reduction and particle type classification.

1. Generation of a Search Grid System

A digital scan generator is used to convert the normal SEM beam scanning motion of a stepping motion with regular intervals. The spacing between grid points is chosen in such a manner as to intersect a representative fraction of the particles on the SEM viewing screen. For this study, a grid size was selected such that all particles greater than 0.07 μM diameter would be detected 100 percent of the time. The grid size was chosen after examination of high magnification SEM and STEM pictures. Particles as small as 0.01 μM were observed, but the vast majority were 0.1 μM or larger. Subsequent analysis of particle size distribution graphs for the six fumes tested in this study indicated that particules smaller than 0.07 μM constituted 0.1 to 1 percent by weight and 1 to 25 percent by number. After the grid is defined, the computer instructs the electron beam to pause at each grid point while a particle detection is performed.

2. Detection of Particles Intersecting the Search Grid System

The particles are detected on the grid points by monitoring a backscattered electron signal. A signal above an adjustable threshold value indicates that the beam is on a particle. If the signal is below the threshold, the computer selects the next coordinate of the grid.

3. Size and Shape Analysis of Particles

After a particle is located, a subroutine is used to drive the beam in a preset pattern to determine the particle size and shape. The preset pattern consists of eight diagonals, each of which is terminated when a grid point is monitored and found to be off the particle. The pattern is repeated twice — once to locate the particle and once to determine the lengths of the diagonals through its centroid. The minimum diagonal becomes the particle Width. The maximum diagonal becomes the particle Length. Its Average Diameter is the arithmetic average of the eight diagonals. Finally, the data is stored and the beam is positioned to chemically analyze the particle.

4. Chemical Analysis of Particles

The chemical analysis of a particle is performed by a computer command which positions the electron beam at the measured centroid of the particle for a preset time, usually one or two seconds. The electron beam excites X-rays characteristic of all the elements present in the particle. All elements present in the periodic table are detected simultaneously. Their signal levels are stored in the memory of the computer for subsequent retrieval. For this study, the following 18 elements were monitored: sodium, magnesium, aluminum, silicon, phosphorus, sulfur, chlorine, potassium, calcium, titanium, vanadium, chromium, manganese, iron, copper, zinc, bromine, and lead. Unfortunately, this original list of elements did not contain nickel, an element present in stainless steel. Therefore, the one stainless steel fume was reanalyzed using a 19-element file that monitored nickel.

5. Data Reduction and Particle Type Classification

Typically, a thousand particles per sample are analyzed. Additional information other than lineal dimensions is derived by calculating the volume and surface area. Each particle is assumed to be a prolate spheroid with the Length as the major axis and the Width as the minor axis.

The volume equation is:

$$V = \frac{4}{3}\pi ab^2$$

where: a = 1/2 Length
b = 1/2 Width

The surface area equation is:

$$S = 2\pi[b^2 + ab/e\ \mathrm{Sin}^{-1}e]$$

where: e, Eccentricity, $= [1 - (b^2/a^2)]^{1/2}$

Next, the particles are separated into different types based on present chemistries derived from the X-ray spectra.

Two new chemistry definition files have been developed for the present study — one for the ferrous base fumes containing thirty nine particle categories, the other for the aluminum base fume containing twenty one particle categories. These categories are expressed in elemental form, and not as compounds. EDXA identifies only elements with atomic number greater than ten. Therefore, low atomic number elements (e.g., oxygen, fluorine) are not mentioned in the chemical categories since they cannot be observed. It is to be understood, however, that the elements mentioned in a particular category are virtually always present as complex oxides and not as metals. In addition, fluorides may be present in certain fumes such as E7018 and E308-16, where fluorides were used as fluxes in the original welding consumable.

The ferrous base fume categories are:

(1) Carbon/Organic
(2) Iron
(3) Iron with Low Silicon
(4) Iron with High Silicon
(5) Iron-Manganese
(6) Iron-Chromium
(7) Iron-Chromium-Manganese
(8) Iron-Copper
(9) Iron-Vanadium
(10) Iron-Zinc
(11) Iron-Titanium
(12) Iron-Aluminum
(13) Iron-Sulfur
(14) Iron-Chlorine
(15) Potassium-Chromium
(16) Potassium-Iron
(17) Potassium-Chromium-Iron
(18) Calcium-Iron
(19) Potassium-Calcium-Iron
(20) Potassium-Manganese
(21) Potassium-Titanium
(22) Calcium-Chromium
(23) Calcium-Manganese
(24) Calcium-Titanium
(25) Potassium-Calcium
(26) Potassium-Rich
(27) Calcium-Rich
(28) Lead-Rich
(29) Chromium-Rich
(30) Manganese-Rich
(31) Copper-Rich
(32) Titanium-Rich
(33) Vanadium-Rich
(34) Iron-Rich
(35) Sodium-Rich
(36) Magnesium-Rich
(37) Aluminum-Rich
(38) Silicon-Rich
(39) Miscellaneous

The aluminum base fume categories are:

(1) Carbon/Organic
(2) Aluminum
(3) Aluminum-Copper
(4) Aluminum-Magnesium
(5) Aluminum-Iron
(6) Aluminum-Silicon
(7) Aluminum-Chromium
(8) Aluminum-Titanium
(9) Aluminum-Vanadium
(10) Aluminum-Sulfur

(11) Aluminum-Chlorine
(12) Aluminum-Potassium
(13) Aluminum-Calcium
(14) Aluminum-Manganese
(15) Copper-Rich
(16) Chromium-Rich
(17) Manganese-Rich
(18) Iron-Rich
(19) Magnesium-Rich
(20) Aluminum-Rich
(21) Miscellaneous

Category definitions can range from very specific to very general. For example, a particle identified as *Iron* shows an iron peak with a relative X-ray intensity of at least 85 percent. It is to be understood that the iron is present as an oxide. Other elements are present only in trace amounts. For the "Iron with Low Silicon" category, up to 50 percent may come from silicon with the rest from iron. Other elements are present only in trace amounts. For "Iron with High Silicon", silicon produces 50 percent or more of the X-rays. Again, these are complex mixtures of iron oxides and silicon oxides. For categories such as "Iron-Manganese" or "Iron-Titanium", the elements mentioned may be present in any proportion. These categories also allow for aluminum and silicon to be present. Specific definitions were developed when an analysis of the particle-by-particle printout showed that these species were present in relatively large numbers. Other particles are collected into more generally defined categories such as "Chromium-Rich" or "Copper-Rich". The element mentioned will produce at least 25 percent of the X-rays, but particules such as Copper-Phosphorus, Copper-Manganese, and Copper-Silicon will all be collected into the same Copper-Rich category.

The Carbon/Organic category collects particles composed of elements of atomic numbers less than ten, primary carbonaceous material, and the final Miscellaneous category collects those which do not fit into any previous category. After the particles are sorted by chemical category, the program completes its work by calculating size distributions for each particle type and for the whole sample.

The specific definitions of the categories will be found in Tables 1 and 2.

In addition, the data was re-analyzed to investigate the distribution of specific elements: copper, chromium, lead, and manganese. Only three simple categories were used: High, with the element producing over 50 percent of the X-rays; Medium, 25-50 percent; and Low, 1-24 percent. The Miscellaneous category then collected all of the particles that did not contain that element.

D. Transmission Electron Microscopy (TEM) and Scanning Transmission Electron Microscopy (STEM)

Samples for the TEM and STEM were prepared by overlaying a portion of the Nuclepore collection filter with approximately 0.02 μM of carbon by evaporation. The fume particles were retained in the carbon film while the filter substrate was dissolved in chloroform. The carbon film was transferred to a standard 300 mesh copper TEM grid. The grids were washed in chloroform before use. The grid and sample were washed again to insure complete removal of the filter media. The STEM was used to obtain electron diffraction and EDXA date.

The prepared grids of each fume were examined in a scanning transmission electron microscope operating at 120 kV. The microscope was equipped with an energy dispersive X-ray analyzer.

STEM analysis was undertaken because it can obtain morphological, chemical and crystallographic information from the same region. While it thus has a great potential for this type of problem, it is inherently more time-consuming than the SPEC analysis, and it was realized that it could not be compared statistically with the SPEC data. The approach chosen, therefore, was to perform analyses on 5-10 particles per fume to determine if the chemistries detected by SPEC could be directly related to the crystal structures determined by XRD. The identification of electron diffraction patterns is, in many cases, more ambiguous than X-ray patterns since only a single slice of reciprocal space is obtained in a single pattern. For this reason, the crystal structures were not determined directly from the electron diffraction data. Instead, the electron diffraction patterns were indexed against the structures observed by XRD.

Of the several modes of electron diffraction available in the STEM, convergent beam diffraction in the TEM mode was chosen. In this technique, the electron beam is focused down to a spot about 0.1 μM in diameter which is then placed on the particle to be analyzed. In this way, the electron diffraction pattern and the X-ray spectrum of the particle were recorded simultaneously. The X-ray spectrum records the elements present. The diffraction pattern determines the crystal structure and interatomic distances. Particular compounds are identified by indexing this data against values for known substances. While smaller spot sizes are attainable in this type of instrument, they were not used here for two reasons. First, they produce a high contamination rate on the specimen which leads to a rapid deterioration of the diffraction pattern and second, the angle of view in the diffraction pattern is somewhat restricted.

The particles analyzed in each fume were about 0.1 μM

in diameter or larger. The particles were chosen to encompass the range of morphologies observed. Since the diffraction data was important, many particles of each type were often examined before one with a diffraction pattern suitable for indexing was found. Then the X-ray spectrum was taken and the particle's image recorded. In some cases no satisfactory diffraction patterns could be obtained for any of the particles in a given morphological class. This occurred both for particles that were too small (so that diffraction patterns showed spots from too many individual particles) and too thick (so that the transmitted intensity was too weak or non-existent).

Because of the relatively complex structure of some of the phases, the indexing of the electron diffraction patterns was performed with the aid of a computer program.

E. Gas Chromatography-Mass Spectrometry (GC-MS)

During the analysis of size and chemistry by the SPEC system, a portion of the particles could not be classified by chemical composition because they yielded an X-ray count below the threshold limit. This could result from a very small particle that did not produce enough X-rays to trigger the detector or from a particle containing carbon compounds that would not be detected by EDXA.

Since carbon combustion products can be carcinogenic, a brief study was undertaken to eliminate the possibility of these substances existing in the fume. 0.5-gram samples of two of the bulk fumes (E7018 and E70S-3) were extracted with 20 ml of dichloromethane for 8 hours using a Soxhlet extractor. The solvent was concentrated to one milliliter, and a portion of this concentrate was analyzed by GC-MS. No organic compounds were observed. Thus, it is more likely that the unclassified particles are simply too small for a good EDXA analysis. [AWS comment: Organics would not be expected to be present because of composition when exposed to arc temperatures that can exceed 6000°K.]

IV. Results and Discussion

The fumes from six different types of welding rods and wires have been analyzed to determine the size and shape of the particles and the crystalline phases present. These included low carbon steel solid, coated, and flux cored rods and wires (E6010, E7018, E70S-3, E70T-1), a stainless steel coated rod (E308-16), and an aluminum wire (E5356). The properties of the bulk fumes were analyzed by EDXA and X-ray diffraction. Then, particles collected on Nuclepore filters were analyzed for their individual size and chemistry. Data for approximately 1000 particles were stored on floppy disc and size distributions by number, by surface area, and by mass were calculated. Finally, selected particles were examined by electron diffraction using STEM analysis.

In the following sections, the data from the SPEC system are compared with other properties, such as the EDXA spectra and crystalline compound/phase constituents. SEM photographs of the fumes are shown in Figs. 1a through 1f. EDXA spectra in Figs. 2a through 2f. Table 3 lists the size distributions for the total fume sample from the SPEC analysis by number, by surface area, and by mass. Table 4 shows the average particle diameters for the total fume sample. Values for percent composition by category are given in Tables 5a through 5e for the steel fumes. Tables 6a through 6e list size distributions by number, and Tables 7a through 7e list size distributions by mass for the steel fumes. Average values for diameter, volume, and surface area by category are given in Tables 8a through 8e for the steel fumes. Data for the aluminum fume given in Tables 9a through 9d. The composition of these fumes by standard wet chemical analysis techniques is given in Table 10.

A. Particle Size

The particle size distributions were similar for all six fumes and can be discussed together. (Graphs of the size distributions by number, by surface area, and by mass are given in Figs. 3-8.)

The particles were all very small. Less than 1 percent of the particles were larger than 1 μM (see Figs. 9-14). The largest particle observed was 2.8 μM. STEM pictures showed that particles as small as 0.01 μM exist. A study done by the Task Group on Lung Dynamics in 1966 indicated that particles approximately 5 to 10 μM or smaller are respirable. The exact point varies with the individual. Thus, all of the fume particles observed were in the respirable range.

The size distributions for the six fumes tested were all very similar. There seems to be little variation with the type of welding consumable or with individual particle chemistry.

For example: Number Average Diameter 0.14-0.33 μM
Area Average Diameter 0.21-0.41
Volume Average Diameter 0.34-0.64

There is little variation in average diameter among the chemical categories within a given fume.

For example: E6010 0.09-0.54 μM
E70S-3 0.06-0.30
E308-16 0.06-0.27

The reverse is also true. There is little variation among the different fumes for a given chemical category.

For example: Fe 0.14-0.17 μM
Fe-Mn 0.13-0.20
K-Fe 0.11-0.18

None of these size variations would greatly influence the amount of each type of material that reaches the lower respiratory system.

The particles from all six fume types seem to obey the log normal distribution. This can be seen from the straight lines produced when the values for cumulative percent composition (for particles less than 1 μM) are plotted against the log of the particle diameter on probability graph paper. (See Figs. 3 through 8 and Tables 3 and 4.) Values for the geometric mean diameters are located at the points where the lines intersect 50 percent. For these graphs, 1 μM was used as an arbitrary upper limit. Ninety nine percent of the particles are less than 1 μM in diameter. There are so few particles greater than 1 μM that average diameters derived from this data would not be statistically significant.

B. Particle Chemistry

The chemical composition of the fumes was evaluated by three methods: X-ray diffraction of the bulk fume, STEM analysis of a few individual particles, and SPEC analysis of a large number of particles. A wet chemical analysis was also provided by the AWS. These particles appeared as spheres or as chains or clusters of spheres. Some appeared to be just touching, attracted by static electricity or by magnetic forces. Others appeared to have fused at high temperatures. Even though no crystal planes were evident, particles examined by STEM produced electron diffraction patterns, indicating that crystalline material was present. Some of the particles might even be single crystals.

1. E6010

The wet chemical analysis showed 46.0 percent iron, 4.0 percent manganese, 6.3 percent sodium, 7.5 percent silicon, and 0.2 percent titanium. Analysis of the elements present in the bulk sample by EDXA showed a large amount of iron, intermediate amounts of silicon and manganese, and a trace amount of titanium. XRD of the bulk sample showed that the major crystalline phase was magnetite (Fe_3O_4).

The SPEC system was used to analyze approximately 1000 individual particles by chemistry and by size. The mean diameter (by number) for all particles was 0.192 $\pm$ 0.146 μM. The main categories identified by the computer search are shown in the following table.

E6010 Composition by Category

Category	Percent by Number	Average Diameter	Composition (Volume Weighted X-ray %)
3. Fe/Low Si	31%	0.188 μM	Si(36) Mn(4) Fe(56)
4. Fe/High Si	10	0.245	Al(21) Si(46) K(9) Fe(21)
5. Fe-Mn	16	0.202	Si(36) Mn(14) Fe(44)
18. Ca-Fe	8	0.169	Si(37) Ca(13) Fe(43)

Chromium is present at low concentrations in 7 percent of the particles. The chromium seems to replace iron in the various types of iron-silicon particles. Copper is present at low concentrations in 3 percent of the particles and it is also found in iron-silicon mixtures. Lead is present at low concentrations in only 2 percent of the particles containing aluminum, silicon, potassium, and iron. The behavior of manganese is similar to chromium and copper. Thirty percent of the particles contain some manganese in mixtures of iron and silicon. Only 0.5 percent of the particles contain intermediate amounts of manganese. These are also iron-silicon-manganese mixtures, and pure manganese oxides is unlikely to exist. (Details of the other particle categories are given in Tables 5a, 6a, 7a, and 8a.)

STEM analysis showed particles that were predominantly iron with varying amounts of manganese and silicon. All of the electron diffraction patterns were indexable as $(Fe,Mn)_3O_4$.

Only 3 percent of the particles were categorized as "Iron," probably as Fe_3O_4. Nearly half of the particles were iron-manganese oxides listed either as Fe/Low Si" or "Fe-Mn". A pure manganese oxide is unlikely to exist since no particles with a very high manganese concentration were observed. Even though most particles contained some silicon, no crystalline silica or transition metal silicates could be detected. Particles analyzed by STEM contained iron with varying smaller amounts of manganese and silicon. (See Fig. 9.) However, all of the electron diffraction patterns are similar, indicating a mixed iron-manganese oxide $(Fe,Mn)_3O_4$. Silicon must be present either as an amorphous oxide or in solid solution in the magnetite lattice. The water glass binder of the electrode contains sodium and perhaps potassium oxides and silicon dioxide. Other silicates and ferro-silicon are also present. These and all other materials in the electrode are partially vaporized by the arc and interact to form new compounds as the fume condenses. Iron compounds appear to crystallize, but the silicon compounds do not. Thus, a particle in the "Fe/High Si" category is probably a magnetite sphere either coated with condensed amorphous silicate or fused to another sphere which is primarily amorphous silicate. Particles in the "Ca-Fe" category are mixtures of magnetite and binder containing a calcium im-

purity. Although sodium is known to be present in the binder, it does not appear in any SPEC chemical category. Elements are detected by EDXA in the SPEC system. Sodium can be detected, but the sensitivity is low. When X-rays from very small particles are counted for short times (1 second), the likelihood for observing Na above background noise is not very good.

2. E7018

The wet chemical analysis showed 0.9 percent aluminum, 20.6 percent calcium, 19.5 percent fluorine, 24.6 percent iron, 12.5 percent potassium, 4.6 percent manganese, 3.3 percent sodium, and 2.8 percent silicon. Analysis of the elements present in the bulk sample by EDXA showed major amounts of potassium, calcium and iron, intermediate amounts of silicon and manganese, and trace amounts of aluminum, sulfur, and chlorine. XRD analysis of the bulk sample showed that the major crystalline phase is potassium-calcium fluoride, KF-CaF_2. Intermediate phases include magnetite, Fe_3O_4, calcium fluoride, CaF_2, and jacobsite, $MnFe_2O_4$. It should be mentioned again that the element fluorine, although prominent in the crystal phases, is very difficult to detect by EDXA.

The SPEC system was used to analyze approximately 1000 particles by chemistry and by size. The average diameter (by number) for all particles was 0.182 ± 0.117 μM. The categories identified by computer search are shown below.

E7018 Composition by Category

Category	Percent by Number	Average Diameter	(Volume Weighted X-ray %)
16. K-Fe	14%	0.179 μM	Si(18) K(36) Fe(28)
18. Ca-Fe	15	0.158	Al(7) Si(17) Ca(25) Fe(37)
19. K-Ca-Fe	48	0.188	Al(4) Si(10) K(28) Ca(22) Fe(23)

Chromium, copper, and manganese are present in the particles in low concentrations in 8, 8, and 23 percent, respectively. These elements are found in mixtures of the particles classified in the three main categories. In a typical particle, for example, X-ray percentage may be either 35 Ca, 14 Cr, and 51 Fe, or 22 Si, 15 K, 14 Ca, 21 Mn, and 27 Fe. Lead is found in low concentrations in only 5 percent of the particles in mixtures similar to those described above. (Details of the other particle categories are given in Tables 5b, 6b, 7b, and 8b.)

The STEM analysis of this fume was made difficult by the irregularities of the particles. They were either too thick to obtain diffraction patterns or, where thin enough, appeared to be multi-crystalline giving diffraction patterns too irregular to be indexable. Occasionally, particles could be found that showed only an Fe peak (see Fig. 10). These patterns were again consistent with Fe_3O_4.

The particles in this fume are mixtures of potassium/calcium fluorides and iron/manganese oxides. Fe_3O_4 and $MnFe_2O_4$ are observed and probably non-stoichiometric oxides of iron and manganese are present as well. No pure manganese oxide is likely since particles with a very high Mn concentration are not found. No crystalline silicon compounds are observed, and the behavior of silicon is similar to that discussed for the E6010 fume.

3. E70S-3

The wet chemical analysis showed 0.4 percent copper, 57.0 percent iron, 7.8 percent manganese, and 3.3 percent silicon. Analysis of the elements present in the bulk fume by EDXA showed the elements iron and minor amounts of silicon and manganese. XRD analysis of the bulk sample showed that the major crystalline phase was magnetite, Fe_3O_4. XRD also indicated a trace of metallic iron.

The SPEC system was used to analyze approximately 1000 particles by chemistry and by size. The average diameter (by number) for all particles was 0.135 ± 0.114 μM. The main categories identified by the computer search are shown below.

E70S-3 Composition by Category

Category	Percent by Number	Average Diameter	Composition (Volume Weighted X-ray %)
2. Fe	9%	0.153 μM	Si(7) Fe(90)
3. Fe/Low Si	14	0.173	Si(10) Mn(6) Fe(76)
5. Fe-Mn	17	0.129	Si(12) S(4) Mn(13) Fe(62)
6. Fe-Cr	5	0.129	Si(16) Cr(10) Fe(53) Zn(5)
12. Fe-Al	6	0.103	Al(18) Fe(69)
16. K-Fe	6	0.111	Si(6) K(16) Mn(6) Fe(58)
18. Ca-Fe	10	0.118	Al(7) Si(13) Ca(15) Mn(5) Fe(48)
34. Fe-Rich	8	0.148	Al(4) Si(5) K(6) Fe(71)

Copper, chromium, and lead are found in low concentrations in 8, 10, and 7 percent of the particles, respectively. Once again, these trace elements are not found as a small number of particles of the pure oxide, but rather spread in small amounts through a large number of particles. For example, in the bulk fume 0.4 percent by weight is copper (see Table 8). Yet copper is found in 8.5 percent of the particles which make up 13.3 percent by weight of the fume sample analyzed by SPEC. Manganese comprises 7.8 percent by weight of the bulk fume, but 25 percent of the particles contain manganese at low concentrations in mixtures of iron, manganese, and silicon. An additional 3 percent contain intermediate amounts of manganese in particles of similar chemistry. It is unlikely that pure oxides of manganese are present. (Details of the other particle types are given in Tables 5c, 6c, 7c, and 8c.)

STEM analysis showed particles containing iron with 6-12 percent manganese and 3-7 percent silicon. The crystal structure of all of the particles was the same (space group FD3M) and could be indexed as $(Fe, Mn)_3O_4$. (See Fig. 11.)

This fume is quite similar to the E6010. Most of the iron exists as Fe_3O_4. Other transition metals easily substitute for iron in the magnetite lattice. Manganese is most commonly observed in these substitutions since its concentrations are the highest. Manganese constitutes 8 percent by weight of this fume, but no individual particles with a very high Mn concentration were found, indicating that a pure Mn oxide is unlikely. Other transition metals, present at even lower concentrations, are also not likely to be found as the pure oxide. For example, copper was found in low concentrations in 8 percent of the particles even though it made up only 0.4 percent by weight of the fume. Copper then exists as a very dilute $(Fe,Cu)\ Fe_2O_4$ solid solution. The XRD data also showed a weak peak that resulted from the presence of traces of metallic iron. This is the only fume in which the metallic form of an element was observed.

In the original electrode, silicon was present in the steel, not as an amorphous water glass binder. Nevertheless, no crystalline silica or silicates were observed. Silicon appears to become trapped in the rapidly condensing magnetite fume, possibly substituting for iron at random sites. It is also possible that amorphous silicates are present which cannot be detected by the methods used in this study.

4. E70T-1

The wet chemical and analysis showed 38.1 percent iron, 0.3 percent potassium, 11.1 percent manganese, 8.9 percent sodium, 5.1 percent silicon, and 0.8 percent titanium. Analysis of the elements present in the bulk fume by EDXA showed iron and manganese, an intermediate amount of silicon, and trace amounts of sodium and titanium. XRD analysis of the bulk fume showed that the major crystalline phase was jacobsite, $MnFe_2O_4$, with an intermediate amount of magnetite, Fe_3O_4.

The SPEC system was used to analyze approximately 1000 particles by chemistry and by size. The average diameter (by number) was $0.163 \pm 0.126\,\mu M$. The main categories identified by the computer search are shown below.

E70T-1 Composition by Category

Category	Percent by Number	Average Diameter	Composition (Volume Weighted X-ray %)
2. Fe	14%	0.140 μM	Fe(99)
3. Fe/Low Si	25	0.160	Si(25) Fe(72)
5. Fe-Mn	37	0.178	Si(8) Ti(11) Mn(19) Fe(59)

Manganese is present in just over half of the particles. Thirty two percent contain low amounts of manganese and are similar to the "Fe-Mn" particles described above. 18 percent contain intermediate amounts of silicon, iron, and manganese. One percent of the particles contain over 50 percent manganese. Half of these particles are mixtures of iron and manganese, or iron, manganese, and silicon. The others seem to be a mixture of manganese and silicon. These may be a manganese silicate or a manganese oxide covered with an amorphous silica layer. However, the small number of these particles makes their exact identification impossible by techniques such as XRD or STEM.

Copper, chromium, and lead are present in low concentrations in 1, 2, and 0.5 percent of the particles, respectively. Particles with higher concentrations of these elements are present in less than 0.5 percent of the particles. They are, in general, included in mixtures of iron, manganese, and silicon. (Details of other particle types are given in Tables 5d, 6d, 7d, and 8d.)

STEM analysis showed particles containing iron with 6-12 percent manganese. Only two particles contained silicon (3-4 percent). The crystal structure of all of the particles was the same (space group FD3M) and could be indexed as $(Fe,Mn)_3O_4$. (See Fig. 12.)

In fumes in which the manganese to iron ratio is low, no particles with a high manganese concentration are observed. On the other hand, if the manganese to iron ratio is high enough, manganese oxides may form. In the E70T-1 fume the Mn/Fe ratio is 1/3.5 by wet chemical analysis. One percent of the particles contained manganese in large amounts (>50 X-ray percent). Since the other oxides present (Fe_3O_4, $MnFe_2O_4$) have the X_3O_4 stoichiometry, Mn_3O_4 may be present, but in concentrations too small to be observed by XRD. No crystalline silicates were observed. Silicon is present either as an amorphous silicate or in solid solution in the metal oxides.

5. E308-16

The wet chemical analysis showed 5.6 percent chromium, 16.8 percent fluorine, 10.8 percent iron, 18.9 percent potassium, 6.2 percent manganese, 10.4 percent sodium, 0.75 percent nickel, and 4.9 percent silicon. Analysis of the elements present in the bulk fume by EDXA showed silicon, potassium, chromium, manganese, and iron with trace of fluorine, sodium, and titanium. XRD analysis of the bulk fume showed mixed oxides of manganese and iron $(Fe,Mn)_3O_4$ and $MnFe_2O_4$, jacobsite. Transition metals were also observed as potassium salts, potassium chromate, K_2CrO_4, and potassium ferrate, K_2FeO_4. Villiaumite, NaF, was present in intermediate amounts.

The SPEC system was used to analyze approximately

1000 particles by chemistry and by size. The average diameter (by number) was 0.160 ± 0.090 μM. The main categories identified by computer search are shown below.

E308-16 Composition by Category

Category	Percent by Number	Average Diameter	Composition (Volume Weighted X-ray %)
5. Fe-Mn	5%	0.166μM	Si(32) Ti(5) Mn(26) Fe(26)
15. K-Cr	5	0.155	Al(6) Si(19) K(31) Cr(17) Mn(9)
16. K-Fe	18	0.169	Si(22) K(27) Mn(10) Fe(22)
17. K-Cr-Fe	5	0.176	Si(14) K(28) Ti(10) Cr(24) Fe(21)
18. Ca-Fe	7	0.144	Si(24) Ca(18) Mn(12) Fe(23)
19. K-Ca-Fe	7	0.159	Si(25) K(20) Ca(15) Mn(6) Fe(17)
20. K-Mn	8	0.161	Al(6) Si(25) K(29) Mn(22)
26. K-Rich	7	0.174	Si(26) Cl(5) K(50) Ca(5)
38. Si-Rich	6	0.161	Si(56) S(8) K(8)

Copper is present in low concentrations (12 X-ray percent) in 7 percent of the particles and in medium concentrations (28 X-ray percent) in 1 percent of the particles. These are primarily K-Cu or K-Fe-Mn-Cu particles. Lead is present in low concentrations in 6 percent of the particles. These are composed of K, Fe, Mn, and Pb. Only 1 percent contained mixtures of chromium and lead (together with iron and manganese) that might be present as lead chromate. Chromium is present in low concentrations in 16 percent of the particles and in medium concentrations in 5 percent of the particles. These appear to be K_2CrO_4 or mixtures of K_2CrO_4 and K_2FeO_4. In addition, slightly less than 1 percent of the particles contained nearly pure chromium oxide. Manganese was present in 40 percent of the particles. Thirty percent contain low amounts of manganese usually in particles which would be categorized as "K-Fe" or "K-Cr." Nine percent contained intermediate amounts of manganese, usually as "K-Mn" and "Fe-Mn" particles. One percent of the particles contained high concentrations of manganese. Some of these particles are mixtures of metal oxides (Mn with Fe, V, Cu). However, in this fume, particles of pure manganese oxide are observed in very small numbers (0.4 percent). Once again the very small numbers of these particles make their location and identification very difficult. (Details of the other particle categories are given in Tables 3e, 4e, 5e, and 6e.)

Since nickel was not among the elements in the original analysis, the stainless steel fume was reanalyzed to look for nickel-bearing particles. Nickel was observed in low concentrations in 2 percent of the particles. Like copper at low concentrations, nickel seems to be substituting for the more abundant transition metals in Fe_3O_4 or $K_2(CrFe)O_4$.

The STEM data for this fume differed from those discussed previously because of the elemental complexity of the particles analyzed. For example, Fig. 13 shows a particle high in Cr, Ca, and S with smaller amounts of Fe, Mn, K, and Na. In no case was nickel detected. No identifiable diffraction patterns could be obtained for any of these particles.

The E308-16 fume was the most complex examined. Fluroine was observed (XRD) only as NaF, although it is not impossible that other alkali fluorides are present. The "K-Rich" category is probably KF. Iron and manganese are again observed as $(Fe,Mn)_3O_4$. The Mn/Fe ratio is only one-half by wet chemical analysis. One percent of the particles contained high manganese concentrations and Mn_3O_4 may be present. The nickel in the stainless steel fume, like copper in the E70S-3 fume, is present only in low concentrations, probably as $(Fe,Ni)Fe_2O_4$. Chromium exists as a $K_2(Fe,Cr)O_4$ solid solution. Manganese is probably also present in this solution. Some $KMnO_4$ may also exist since a few percent of the particles are categorized as "K-Mn", although other explanations are possible. The Cr/Fe ratio is also one-half. One percent of the particles contained Cr in high concentrations (>50 X-ray percent). These may well be a chromium oxide, although the concentration was too small to be observed by XRD. Another one percent of the particles contained mixtures of Pb and Cr and may be $PbCrO_4$. Once again no crystalline silicates are observed.

6. E5356

The wet chemical analysis showed 45.0 percent aluminum, 0.5 percent copper, 0.2 percent iron, and 5.4 percent magnesium. EDXA analysis of the elements present in the bulk sample showed a large amount of aluminum with trace amounts of iron and copper. The XRD data from the bulk sample showed that the major crystalline phase was α-alumina (Al_2O_3). Smaller amounts of magnetite (Fe_3O_4) and $(Cu,Fe)Al_2O_4$ were present.

The SPEC system was used to analyze approximately 1000 individual particles by chemistry and by size. The average diameter (by number) for all particles is 0.328 ± 0.201 μM. The main categories identified by the computer search are shown below.

E5356 Composition by Category

Category	Percent by Number	Average Diameter	Composition (Volume Weighted X-ray %)
2. Al	86	0.327 μM	Al(99)
3. Al-Cu	7	0.318	Al(65) Cu(35)

Chromium, manganese, and lead are not present in this fume. Copper is present in 8 percent of the particles although it is present only 0.5 percent by weight (Table 10). However, the distribution of copper contrasts con-

siderably with that observed in the steel fumes. In the steel fumes, copper is present at low concentrations, presumably substituting for iron in the crystal lattice. In the E5356 fume, only 1 percent of the particles had a low Cu concentration (20 X-ray percent). Five percent had a medium copper concentration (32 X-ray percent) and 2 percent had a high Cu concentration (64 X-ray percent). At least half of these particles contained nearly pure copper, probably as the oxide.

STEM analysis of this fume showed all of the particles to be Al_2O_3 without any detectable Mg. A typical spectrum is shown in Fig. 14 which has been expanded along the horizontal axis so that the shape of the aluminum K-alpha peak can be clearly seen. The K-alpha marker for magnesium is also shown in this Figure to indicate where magnesium would appear if present.

Only one aluminum fume was examined. Most of the fume (80 percent by weight) was α-alumina. Copper was present as an aluminate $(Cu,Fe)Al_2O_4$. Two percent of the particles contained Cu in high concentrations and may contain a copper oxide although this could not be detected by XRD. The magnesium present in this fume is not well characterized. No Mg compounds were observed by XRD or STEM. Few particles containing magnesium were identified by the SPEC system. In EDXA, the signal from magnesium at 1.25 KeV lies next to that from aluminum at 1.49 KeV. The strong peak from aluminum may be masking the magnesium signal. A second explanation is also possible. The sensitivity of EDXA for sodium and magnesium is low. (See the discussion of sodium in Section 1.) The small particle size and short counting times make the observation of these elements difficult. However, using new software developed since these fumes were analyzed, it may be possible to improve the ability to detect these two elements. Most of the Mg containing particles found in the SPEC analysis were Mg/Al combinations and may be a mixed oxide such as $MgAl_2O_4$.

V. SUMMARY

The welding fumes were composed of very fine particles with a log normal size distribution and average diameters in the easily respirable range of 0.1 to 1.0 μM. Average particle size does not vary greatly among the fumes examined.

The particles appeared as individual spheres or as clusters of spheres that have been fused at high temperatures. The planes and angles that characterize crystalline material that has cooled slowly were absent in these particles. Nevertheless, much crystalline material was present. Every particle examined by STEM produced an electron diffraction pattern. Some patterns indicated that the particle was a single crystal. Others showed the complex overlapping patterns characteristic of the presence of several crystals within a single particle.

For the ferrous fumes, particle chemistry was dependent on the iron content of the fume. When large amounts of iron are present, the main crystalline phase is magnetite and other transition metals exist as $(Fe,X)_3O_4$. Only when the iron concentration is relatively low, is there a possibility that pure oxides of other transition metals are present. Other oxidation states for iron may then be present also, such as the $K(Fe,CR)O_4$ found in the stainless steel fume.

If fluorides were present in the original consumable, then sodium, potassium, and calcium fluorides were found in the fume. No transition metal fluorides were detected.

Crystalline silica and transition metal silicates were also not observed in the fume. The silicon either formed an amorphous silica or was in solid solution with the iron oxide.

Only one non-ferrous electrode was treated, an aluminum wire. The major fraction of this fume was alumina, Al_2O_3. Other elements present in small concentrations in the starting material reacted to form aluminates, XAl_2O_4.

This study has shown that automated electron beam image and chemistry analysis (SPEC) used with bulk X-ray diffraction and micro electron diffraction (STEM) techniques is an effective method for screening welding fumes for potential health hazards. The composition of the fumes from several different ferrous electrodes was similar. Therefore, a single list of chemical categories for the SPEC system can be tailored to identify particle types in a wide variety of fumes. A detailed analysis of all of the data can then be used to describe the behavior of all of the elements in the fume, even those present at low concentrations.

APPENDIX H

REFERENCE 36

(Tandon et al., 1982)

VARIATIONS IN THE CHEMICAL COMPOSITION AND GENERATION RATES OF FUME FROM STAINLESS STEEL ELECTRODES UNDER DIFFERENT AC ARC WELDING CONDITIONS – AWRA CONTRACT 90

By R.K. Tandon*, P.T. Crisp*, J. Ellis* and R.S. Baker**

ABSTRACT

The generation rate and chemical composition of fume from manual metal arc welding type AWS A5.4 E316L-16 electrodes (3.15 mm) were studied under a wide range of current (80-120A) and voltage (20-40V) conditions using an AC electrode deposition machine. Welding conditions, generation rates and chemical analyses were reproducible to within 5%. For each setting on the power supply, there was an optimum arc length which minimised fume generation. The rates of fume generation were up to 4 times greater than the minimum under high voltage conditions and up to 1.5 times greater under low voltage conditions. Marked variations were found in the elemental composition of fume produced under different welding conditions using power supply settings of 100 and 120A. The metal content of the fume increased under low voltage conditions, except in the case of chromium at 100A where a linear increase with arc voltage was observed. At 100A, sodium and potassium had similar abundances in the fume, while at 120A potassium was nine times as abundant as sodium.

The results are discussed in terms of arc temperature, gas shielding effects and the volatility and thermodynamic stability of fume components. For each power supply setting, the rates of release of individual metals in fume (g metal/kg electrode) have minimum values at the same arc conditions as the minimum in total fume generation rate; rates of metal release under unfavourable conditions may be up to three times the minimum value. Data on rates of fume generation and element release permit the occupational health aspects of welding to be evaluated and may lead to improvements in the formulation and operation of welding rods to minimise the emission of potentially toxic constituents.

1 INTRODUCTION

Welders commonly experience increased fume production when the arc length is increased beyond its normal value or when the current setting on the power supply is raised. Variations in the rate of fume generation have been reported for a variety of electrodes under different current and voltage conditions [1-3]. Kimura *et al.* [3] found that the rate of fume generation increases with the apparent power (V.A) of the arc. The elemental composition of welding fume has also been shown to vary with the arc conditions [2]. Studies to date have concentrated on examining a broad range of electrodes and provide only a small amount of data for each electrode under different arc conditions. We report here the first phase of an exhaustive study of the welding fume from a single type of stainless steel MMA electrode under a wide range of precisely controlled arc conditions. The data may be used to test proposed theories of fume formation and is essential for evaluating the toxicology of stainless steel welding fume.

2 EXPERIMENTAL

2.1 Equipment for fume generation and collection

The automatic welder and fume collection system (Figures 1 and 2) comprised the following:

(i) An AC Weldarc 230 power supply with rated input current 13.5A at 415V, set on low current range (open circuit voltage 78V).

(ii) An automatic deposition machine (Steel Mains Pty Ltd) with a horizontal work table driven by a variable speed motor set at 150 mm min^{-1} and an electrode feeder mechanism set at 45° to the table.

(iii) An electronic controller (Steel Mains Pty Ltd) for the electrode feeder mechanism which maintains a constant preset voltage between the electrode and the work by raising or lowering the electrode.

(iv) A galvanised steel hood (base dimensions 30 cm x 30 cm) with a Fibrafax skirt connected by galvanised

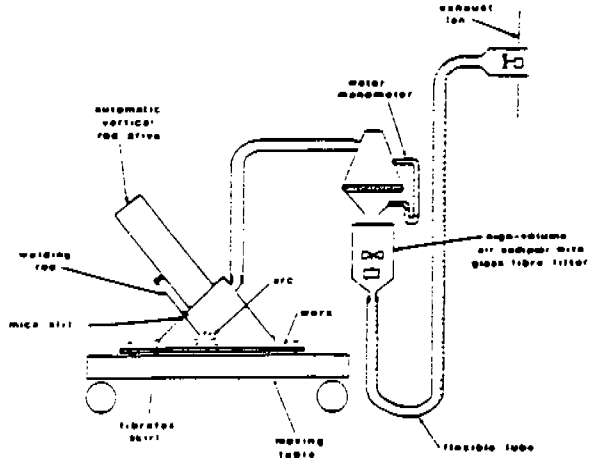

FIG 1 SCHEMATIC DIAGRAM OF AUTOMATIC WELDER AND FUME COLLECTION SYSTEM

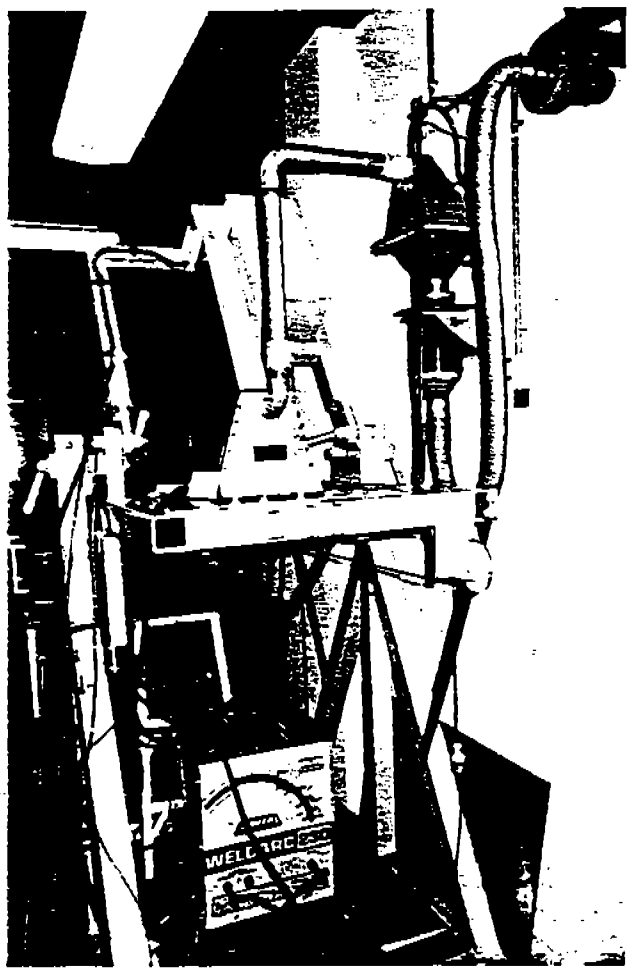

FIG 2 THE WELDING AND FUME COLLECTION SYSTEM

* University of Wollongong.
** Commonwealth Institute of Health, University of Sydney.
AWRA Document P9-49-82.

steel tubing (15 cm I.D. wrinkles at bends filled with plastic) to a galvanised steel cowl (base dimensions 25 cm x 20 cm).

(v) A high-volume air sampler (General Metal Works Model 2000) with motor speed regulated by a variable transformer and fitted with a 20 cm x 25 cm glass-fibre filter paper (flow rate ≈ 14 ℓs^{-1}).

Welding was initiated by placing a 1 cm ball of steel wool between the electrode and the work. The voltage setting on the electrode feed controller kept the arc length within close limits with a hunting action of ± 2 mm superimposed on the downward feed. The flow rate of the high-volume air sampler was the minimum required to prevent escape of fume from beneath the hood skirt.

2.2 Chemical analysis of fume and flux

Fume was generated using 3.15 mm E316L-16 electrodes on stainless steel 304 plates 6.25 mm thick. Fume from 2-4 electrodes was collected on the filter paper, dried at 100°C and weighed prior to the chemical analysis. The fume deposit was carefully brushed from the filter paper. The deposit was examined for glass fibres or brush hairs and contaminated samples were rejected. Duplicate 0.1g samples of fume were extracted with nitric/hydrochloric and nitric/perchloric acids following the method described by Miller and Jones [4]. Acid insoluble material was removed by filtration, ignited and weighed. The filtrate was analysed for the metals iron, chromium, manganese, nickel, copper, potassium, sodium, calcium, magnesium, using atomic absorption spectrophotometry and for fluoride using an ion selective electrode. Atomic absorption measurements were made on an Instrumentation Laboratory Model 551 instrument using flame atomisation with automatic background correction in the double beam mode. An air-acetylene flame was used for all elements except chromium and calcium, where nitrous oxide-acetylene was used. The matrices of standard and unknown solutions were matched and standard instrument and analytical conditions [5] were used. Appropriate ionisation suppressants and releasing agents were added to standards and unknowns for the following elements: potassium (1000 ppm caesium), sodium (2000 ppm potassium), calcium (2000 ppm potassium) and magnesium (10000 ppm lanthanum). Fluoride analyses were made using an Orion Model 901 ionanalyser and a Model 94-09 fluoride selective electrode. Standards were prepared containing the same concentration of iron (III) as the unknowns and all fluoride concentrations were measured using solutions at pH = 5-6 containing sodium acetate (0.9M), hydrochloric acid (5M), sodium tartrate (0.5M) and trishydroxymethylaminomethane (0.9M). A second-order polynomial least-squares fit was applied to the fume generation data using standard programmes on a Univac 1100 computer.

Qualitative analyses of the electrode flux coating were carried out by x-ray fluorescence (XRF) spectrometry. Samples of flux coating were pelletized by fusing with lithium metaborate and analysed using a United Scientific instrument fitted with an energy dispersive Si (Li) detector and a Tracor Northern TN2000 multichannel analyser.

3 RESULTS

The compositions of the stainless steel 304 base metal and the weld deposit from E316L-16 electrodes are given in Table 1. Qualitative XRF analysis of the electrode flux indicated the following components: titanium, zirconium, (major); potassium, calcium, chromium, manganese, nickel, silicon, niobium (minor); iron, rubidium, strontium, aluminium (trace). Phosphorus, molybdenum, sulphur and chlorine were not detected; magnesium and sodium were not determined.

The reproducibility of fume generation rates using the automatic deposition machine (relative standard deviation of six determinations) was 2% at 21.5V, 91A and 1% at 37.5V, 101A. Replicate values for the rates of fume generation during sample collection were determined periodically and lay within 5% of each other. The hunting action of the electrode feeder mechanism (designed to mimic the manipulation by an experienced welder) caused a variation of ± 0.5V and ± 8A. Average voltage and current values at a particular power supply setting varied by ±3%.

Variations in the rate of fume generation under different welding conditions are shown in Figure 3. Points with similar fume generation rates were contoured using a least squares curve fit to yield "isofume" lines (goodness of fit 88%). The effect of V.A. upon the rate of fume generation is given in Figure 4. The effects of arc voltage on the fume composition and rates of element release in fume are given in Figures 5 and 6 for 100A and 120A power settings. Duplicate chemical analyses differed by an average of 2% (maximum 5%). Approximately 20% of the fume was acid insoluble.

TABLE 1 COMPOSITION OF THE BASE METAL (S.S.304) AND THE WELD DEPOSIT (E316L-16 ELECTRODES)

Element	Percentage by weight[1]	
	Base metal (S.S.304)	Weld deposit[2] (E316L-16)
Fe	70.64	64.98
Cr	18.35	19.02
Mn	1.29	1.76
Ni	8.85	11.34
Cu	0.05	0.04
Mo	0.17	2.27
Nb	≤ 0.005	0.02
Ta	–	0.01
Ti	–	0.02
Si	0.54	0.49
C	0.05	0.023
P	0.03	0.017
S	0.02	0.004

1. Percentage values for iron were obtained by difference.
2. Certificate of analysis provided by the manufacturer for a batch of electrodes.

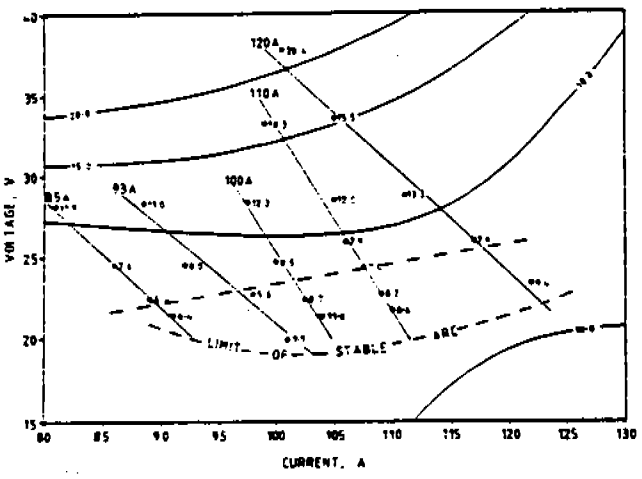

FIG 3 ISOFUME CURVES FOR 3.15 mm E316L-16 ELECTRODES. MACHINE – ELECTRODE CHARACTERISTIC CURVES AT 85, 93, 100, 110 AND 120A SETTINGS ARE SHOWN AS LINES OF BEST FIT TO THE EXPERIMENTAL DATA POINTS (•). FUME GENERATION RATES (g FUME/kg ELECTRODE MELTED) ARE INDICATED AT EACH POINT ON THE MACHINE-ELECTRODE CURVES. ISOFUME CURVES (10.0, 15.0, 20.0 g FUME/kg ELECTRODE) ARE DRAWN USING A BIVARIATE LEAST-SQUARES POLYNOMIAL FIT. THE DASHED LINE (- - - -) INDICATES THE MINIMUM FUME GENERATION RATE IN EACH OF THE MACHINE-ELECTRODE CURVES

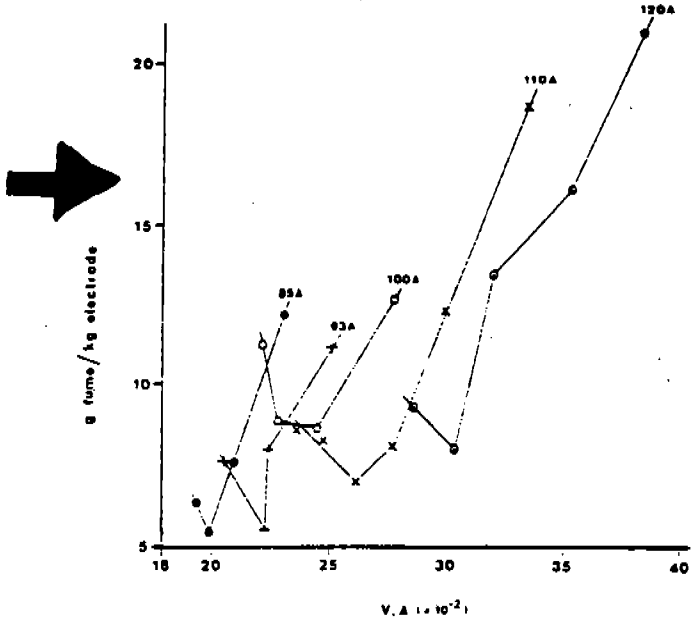

FIG 4 EFFECT OF APPARENT POWER (V.A.) ON THE RATE OF FUME GENERATION USING 3.15 mm E316L-16 ELECTRODES AT POWER SUPPLY SETTINGS OF 85, 93, 100, 110 AND 120 AMPS.

4 DISCUSSION

Within the limits of stable arc, fume generation rates varied by a factor of four (Figure 3). For each electrode-machine curve, there was an arc length (corresponding to particular current and voltage values) which resulted in a mimimum fume generation rate. The rate of fume generation varied so critically with arc length that even an experienced welder might choose to operate under conditions which would result in substantially more than the mimimum rate of fume generation. An inexperienced welder using the same machine setting might easily produce fume at twice the minimum rate. The highest and lowest voltages do not represent practical welding conditions, but were chosen in order to probe the physical and chemical processes occurring in the arc. The increase in fume production with increasing arc length (increasing voltage) is probably due to more vapour being expelled from the arc [3] as it becomes larger and hotter (greater rate of energy dissipation). The relationship between fume generation rate and apparent power in the arc (Figure 4) supports this view: for each setting of the power supply, the relationship is approximately linear in the region away from the short arc (low voltage) condition. Kimura *et al.* [3] have reported a similar linear relationship between fume generation rate and apparent power for a variety of electrodes. The increase in fume generation under short arc conditions does not appear to have been reported previously. It may result from the erratic operation of the arc causing spattering and loss of gas shielding.

The fumes generated at power supply settings of 100A and 120A have generally similar elemental compositions (Figure 5). The most notable exceptions are sodium and potassium: at 100A sodium and potassium have similar abundances, while at 120A potassium is nine times as abundant as sodium. Sodium and potassium salts with the same anion boil at similar temperatures [6] and are likely therefore to have similar volatilities in the arc. Ejection of liquid droplets from the arc is unlikely to favour one alkali metal over another. The different ratios of sodium to potassium may be explained by each metal being associated with a different anion (either in the original flux or in the arc) to produce compounds with different volatilities. Although the ratio of sodium to potassium varied, the sum of mean sodium and potassium concentrations in fume evolved at 100A and 120A settings respectively was constant.

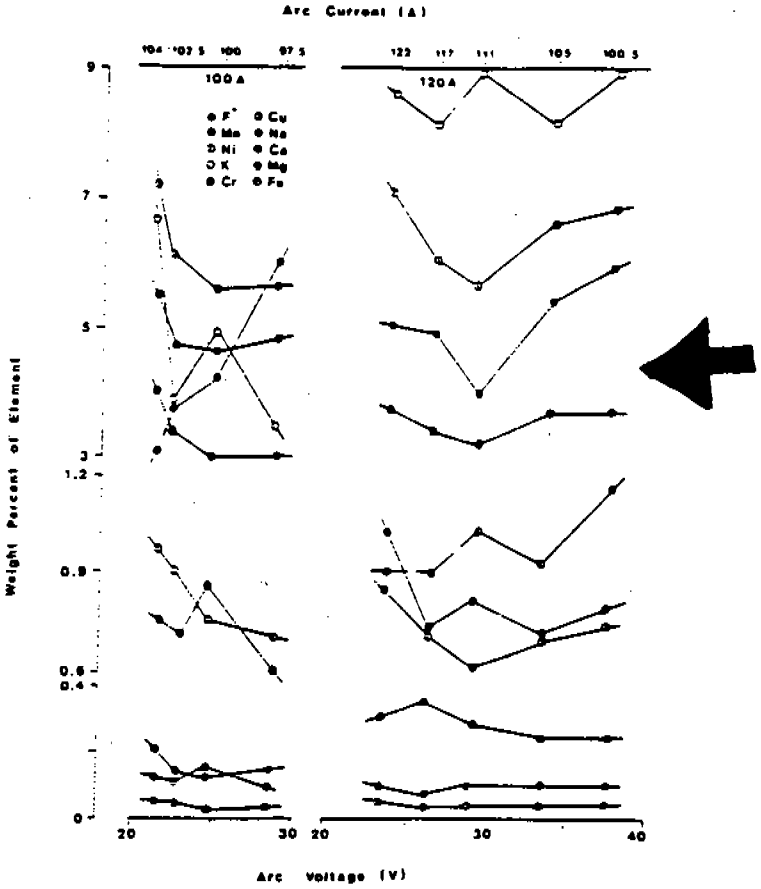

FIG 5 EFFECT OF ARC VOLTAGE ON THE COMPOSITION OF WELDING FUME FROM 3.15 mm E316L-16 ELECTRODES AT 100A AND 120A POWER SUPPLY SETTINGS

TABLE 2 PHYSICAL AND THERMODYNAMIC PROPERTIES OF RELEVANT METALS AND METAL OXIDES

Metal	Boiling point[1] (°C)	Composition of stable oxide at 2000°C	Melting point of oxide[2] (°C)	ΔG_f° of metal oxide per mole of metal[3] (kJ mol^{-1} at 2000°C
Iron	2750	FeO	1424	−120
Chromium	2480	Cr_2O_3	2400	−255
Manganese	2100	MnO	1875	−200
Nickel	2730	NiO	1960	− 30
Copper	2600	Cu_2O	1230	− 15

1. Handbook of Chemistry and Physics, 55th edition, 1974-75.
2. Kubaschewski, O. and Hopkins, B.E., Oxidation of Metals and Alloys, Butterworths, London, 1962.
3. Richardson, F.D. and Jeffes, J.H.E., J. Iron St. Inst., 1948, 160, 261.

There is a marked increase in the abundance of most elements in fume produced under low voltage conditions, especially with a power supply setting of 100A. These increased abundances must be associated with decreased abundances of constituents which have not yet been determined (e.g. titanium and zirconium). Under the cooler conditions of a short arc, metals such as titanium and zirconium, which form refractory compounds, may be relatively less volatile than at higher temperatures. Chromium is exceptional in having a lower abundance in fume

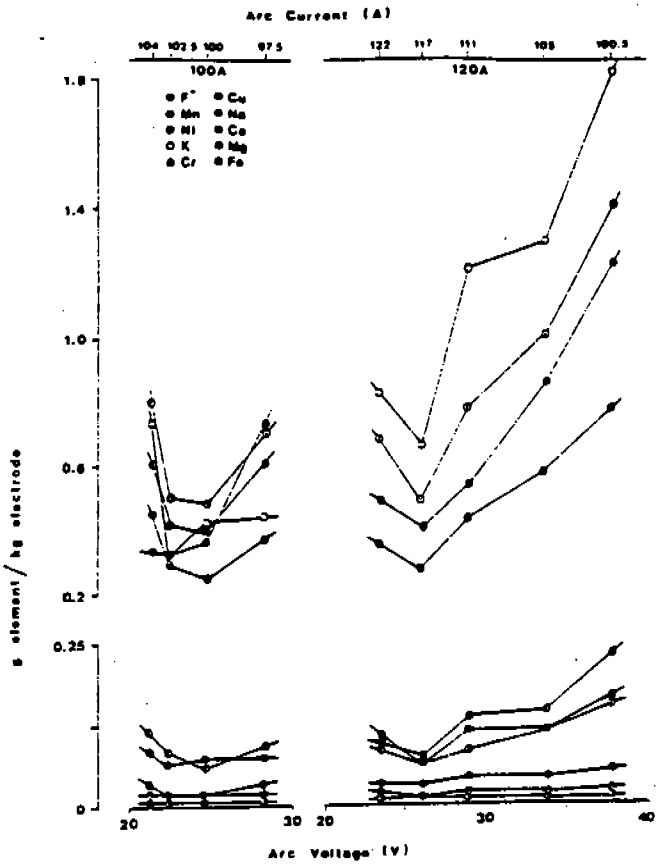

FIG 6 EFFECT OF ARC VOLTAGE ON THE RATES OF ELEMENT RELEASE IN FUME FROM 3.15 mm E316L-16 ELECTRODES AT 100A AND 120A POWER SUPPLY SETTINGS

produced under low voltage conditions than under normal welding conditions at 100A. This may be due to an increased concentration of oxygen in the erratic arc leading to the formation of poorly-volatile chromium (III) oxide. Chromium (III) oxide is more stable than iron, manganese, nickel and copper oxides at 2000°C (Table 2) and should be formed preferentially from the vapour of the electrode alloy. While reliable data for the boiling points of metal oxides could not be obtained, the order of the melting points (Table 2) indicates that chromium (III) oxide should be less volatile than the other metal oxides.

The approximately linear relationship between the chromium content of the fume and arc voltage at a power supply setting of 100A is notable: the abundance of chromium in the fume doubles as the arc voltage increases from 20 to 30V. Since chromium compounds are suspected of having adverse health effects [7], this result may be significant.

The composition of the welding fume is very different from the composition of the electrode metal. Comparative figures for the electrode core wire and fume generated with a 120A power supply setting are given in Table 3 (average fume compositions at 100A are similar). It appears from the work of Gray *et al.* (8) that the volatilisation of elements from the molten electrode core wire is an important mechanism for the formation of fume particles in the arc. The simplest model assumes that the metals behave ideally and that their partial pressures above the liquid alloy surface may be calculated from Raoult's Law [9]. Due to the dilution of electrode core wire elements in the fume by volatilised flux constituents, comparisions must be made relative to a particular element. Table 3 gives this comparison in terms of "enrichment factors" relative to iron. For the major elements, chromium, manganese and nickel, direct application of Raoult's Law provides values which are in fair agreement with the experimental values. However, the concentration of copper in the fume

TABLE 3 COMPARISON OF ELECTRODE AND FUME COMPOSITION USING THE 120A POWER SUPPLY SETTING

Metal	% in electrode core wire[1]	% in fume[2]	Relative enrichment factors[3] Experimental	Raoult's[4] Law	Gray *et al.*[5]
Fe	65.0	6.5	1	1	1
Cr	19.0	5.1	3	4	2
Mn	1.8	3.3	19	11	27
Ni	11.3	0.7	0.6	0.9	0.5
Cu	0.04	0.04	10	185	–

1. Values for the weld deposit metal have been used.
2. Average of values obtained at 23.4, 26.0, 28.8, 33.6 and 37.8V.
3. The relative enrichment factor (E) for each metal (relative to iron) is given by

$$E = \frac{C_{\text{metal in fume}} \times C_{\text{iron in electrode}}}{C_{\text{metal in electrode}} \times C_{\text{iron in fume}}}$$

where C values are concentrations expressed as percentage by weight.
4. Calculated from the composition of the equilibrium vapour obtained by direct application of Raoult's Law to liquid electrode alloy at 2600°C (total vapour pressure = 1 atm).
5. Based on Raoult's Law calculations by Gray *et al.* [8] for a similar electrode alloy (64.7% Fe, 18.7% Cr, 1.9% Mn, 12.9% Ni, 2.3% Mo) using estimated activity coefficients.

differed by an order of magnitude from the Raoult's Law prediction, and this may reflect non-ideal behaviour of this trace constituent in the liquid metal solution. A more rigorous model is one which takes into account the activity coefficients of the metals in the liquid alloy. Such a model has been used by Gray *et al.* [8] for metal inert gas welding using an electrode core wire of similar composition to that used here. Their results have been used to calculate enrichment factors which are presented in Table 3 for comparison. The concentration of nickel in the fume is better represented by this model.

The amount of each element released in fume per kilogram of electrode consumed (Figure 6) may vary by a factor of between two and four under different welding conditions. The variation with arc voltage is larger at the higher power supply setting (120A). The minimum rate of all elements released in the fume (g element/kg electrode consumed) occurs under arc conditions corresponding to the minimum rate of total fume generation (Figure 4). The results demonstrate the importance of welding under optimum arc conditions in order to minimise the release of metal aerosols to the work environment.

5 CONCLUSIONS

Within the limits of stable arc, the quantity and chemical composition of welding fume from a stainless steel electrode varies greatly and for reasons which are not clearly understood at present. Due to increasing concern about the occupational health aspects of stainless steel welding, it is important that the extent and causes of these variations be determined. Such knowledge should enable welding rods to be chemically formulated and operated in a manner which will minimise the release of potentially toxic constituents. The present study will be continued to provide further data on the chemical composition of fume and it is hoped that this may contribute to an understanding of the mechanisms of fume generation.

6 ACKNOWLEDGEMENTS

This study was made possible by a grant from the Australian Welding Research Association (AWRA). The authors wish to thank Dr A.J. McLeod from this organisation for his advice and assistance throughout the study. We are grateful to Mr R. Gebhardt of Sandvik Australia Pty Ltd for his assistance, and to Welding Industries Aust Ltd for providing an AC power supply. We thank Dr B.E. Chenhall for performing the XRF analyses. One of us (R.K.T.) gratefully acknowledges the award of an AWRA research fellowship.

7 REFERENCES

1 Kimura, Y., Ichahara, I. and Kobayashi, M., *IIW/IIS Doc.* VIII-574-74.

2 Technical Committee Welding Filler Metal Division The Japan Welding Engineering Society, *IIW/IIS Doc.* II-956-81.

3 Kimura, S., Kobayashi, M. and Maki, S., *IIW/IIS Doc.* VIII-687-76.

4 Miller, T.M. and Jones, R.C., *Aust. Weld. Res.*, 1979, 6, 1.

5 Instrumentation Laboratory atomic absorption methods manual, Massachusetts, USA, 1979.

6 Handbook of Chemistry and Physics 55th edition, Chemical Rubber Co., Cleveland, Ohio, 1974-75.

7 Leonard, A. and Lauwerys, R.R., *Mutation Res.*, 1980, 76, 227.

8 Gray, C.N., Hewitt, P.J. and Hicks, R., Weld Pool Chemistry and Metallurgy International Conference, London, 15-17 April, 1980.

9 Kubaschewski, O. and Evans, E.L., Metallurgical Thermochemistry, Pergamon, London, 1958.

APPENDIX I

REPORT EXCERPTS FROM REFERENCE 46

(Evans et al., 1979)

Fumes and Gases in the Welding Environment

A Research Report on Fumes and Gases Generated During Welding Operations

Research performed at Battelle-Columbus Laboratories under contract with the American Welding Society and supported by industry contributions

Under the direction of the AWS RESEARCH COMMITTEE ON SAFETY AND HEALTH

Edited by F. Y. Speight, Manager, Safety and Health, and H. C. Campbell, Consultant

AMERICAN WELDING SOCIETY
550 N. LeJeune Road, Miami, Florida 33126

The electrodes used in this investigation were obtained from local commercial sources. Electrodes used for some specific studies (e.g., studies of the fumes produced by electrodes with different diameters) were obtained from one manufacturer.

The electrodes included in this investigation are listed in Appendix A, along with the purposes for which they were used.

Section IIA, Laboratory Test Method

Under the guidance of the AWS Research Committee, a laboratory test method was established to study the fumes associated with arc welding and related processes. Specifically, this method was designed for the laboratory collection of total fume samples in order to determine fume weight as a function of welding time, various electrode characteristics, and procedural variables.

Procedures

Experimental procedures were established to determine the fume generation characteristics of electrodes used in various arc welding processes by gravimetric analyses of fume samples. Samples of the fumes produced by specific electrodes were collected in triplicate to average the inconsistencies of sampling; in some instances, one or two extra samples were collected to obtain additional data or to verify specific results. With appropriate changes to fit the process, the sampling procedures were generally applicable to cutting and spraying as well as arc welding.

After the desired welding conditions were established, the fume samples were collected in accordance with the following procedures:

(1) The filter-prefilter assembly was weighed to 0.1 mg on an analytical balance.

(2) The filter-prefilter assembly was placed in the holder at the apex of the fume collection chamber, the sealing gaskets were installed, and the holder was clamped in place.

(3) The chamber was sealed and the blower that exhausted the fume chamber was turned on. Immediately thereafter, a bead-on-plate weld was made. The welding interval was one-half to one minute, depending on the expected fume generation rate.

(4) With the blower functioning, fumes were collected until the chamber atmosphere was clear.

(5) The filter-prefilter assembly was weighed immediately after its removal from the filter holder to determine the fume weight.

The following were recorded during sampling: (a) filter-prefilter weight before and after sampling, (b) welding conditions, and (c) electrode physical characteristics (diameter, length, and weight of electrode consumed).

To avoid problems caused by the pickup of moisture by the absolute filter, prefilter, or fume sample, welding and sampling were done in a clean room where temperature and humidity could be controlled. Also, glass fiber filters were used because they were nonhygroscopic. Nevertheless, moisture pickup was possible in view of the long periods (15 to 30 minutes) during which fume samples were collected. To examine this possibility, fume samples were collected in accordance with (a) established procedures and (b) procedures in which the filter-prefilter was baked before each weighing operating to remove absorbed moisture. Moisture did not appear to be a problem, because there was essentially no difference in the fume weights. However, the possible effects of moisture pickup on the accuracy of experimental data should be considered if welding and sampling are done in a high humidity area. Additional information on the effect of humidity is given in Part IIE of this report.

Procedures were also established to measure the metal deposition rate during welding. To obtain these data, bead-on-plate welds were deposited on small sections of plate that were weighed before and after welding to determine the amount of metal deposited during the welding interval. In the case of welds made with shielded metal arc or flux cored arc welding electrodes, slag was removed before the weighing operation.

Chamber Evaluation

Studies were conducted to evaluate the performance of the Battelle fume collection chamber and filter system. To provide a common basis for comparing the performance of this chamber with that of equipment designed and used by members of the AWS Research Committee, these studies were undertaken using specific lots of E7018 and E70T-1 electrodes set aside for this purpose. To further insure comparability, the welding conditions used by the subcommittee members for each of the respective electrodes were also used by Battelle; these conditions are shown in Table 2.1A. The data obtained by the AWS Research Committee and by Battelle are presented in Table 2.1B. When the differences in equipment and sampling procedures are considered, the agreement among the data is good.

During the program, the Battelle fume collection chamber and filter system performed well, and consistent results were obtained. In replicate sampling experiments, the fume generation rates varied by only 1 or 2 percent. The variation in calculated quantities (e.g., weight percent of electrode converted to fumes, weight of fumes per weight of deposited metal, etc.) was somewhat greater but generally less than 4 percent. These observations were confirmed by the small standard deviations associated with each group of data.

As indicated, fume samples were collected in triplicate for all of the electrodes evaluated. For any given electrode, these samples were collected one after another under the same welding conditions, and there was little variation in the individual fume sample weights. More variation would be expected if the sampling was made at random and the welding conditions were changed after each fume collection experiment.

Experimental Results

Figures and short tables are used throughout this report to summarize the data and assist in the interpretation of the results. Data on the fume generation characteristics of arc welding electrodes are presented in detailed tabular form in Appendix B. In addition to the fume generation rate for specific electrodes, these sheets contain information on (a) the conditions under which the experimental data were obtained, (b) the melting and metal deposition rates of the electrode, and (c) calculated quantities that relate the amount of fumes produced during welding to the metal deposition rate and other electrode characteristics.

Fume generation rates are expressed in "measured" and "normalized" values. The normalized value provides a means for minimizing the effects of unintentional variations in welding current on fume generation rate. Normalization was accomplished by relating the fume generation rate to the current squared. Figure 2.9 shows the relation of I^2 trend lines and data for two covered electrodes, one cored electrode, and one solid wire electrode. It is apparent that the current-squared normalization will fit a wide variety of fume generation data.

The fume generation rate is most important because it is a direct measure of the amount of the fumes produced during welding under specified conditions. This information can be used effectively by welding engineers, industrial hygienists, ventilation specialists, and others. Of equal importance is the calculated factor "weight of fumes per unit weight of deposited metal," because it can be used to estimate the amount of fumes that will be produced during production welding operations. This factor also provides a convenient means to compare welding processes on a fume-produced to weight-of-deposited-metal basis.

Table 2.1A
Welding conditions for E7018 and E70T-1 electrodes

	E7018		E70T-1	
Parameter	AWS Subcommittee on Sampling	Battelle	AWS Subcommittee on Sampling	Battelle
Current, A	140	135-145	450-470	420-450
Voltage, V	---	23-24	30	30-31
Wire feed rate, in./min (mm/s)	---	---	87.21 (206)	87.00 (205.5)
Welding speed, in./min (mm/s)	5.93 (14)	5.93 (14)	6.77 (16)	6.77 (16)
Shielding gas	---	---	CO_2	CO_2
Gas flow rate, ft^3/h (liters/min)	---	---	19-21 (40-45)	21-24 (45-50)
Electrode stickout, in. (mm)	---	---	32 (1.25)	32-35 (1.25-1.37)
Weld time, s	---	60	---	15 and 30
Electrode polarity	Positive	Postive	Positive	Positive

Table 2.1B
Fume generation characteristics of E7018 and E70T-1 electrodes (AWS Research Committee and Battelle data)

	E7018				E70T-1			
	AWS Subcommittee on Sampling				AWS Subcommittee on Sampling			
Characteristics	A	B	C	Battelle	A	B	C	Battelle
Fume generation rate, g/min	0.50	0.52	0.43	0.51	1.15	1.05	1.27	1.26
Weight percent electrode converted to fumes	1.54	1.79	1.47	1.62	0.75	0.70	0.83	0.85
Melting rate, kg/h (lb/h)	---	---	---	---	---	9.00 (19.8)	9.17 (20.2)	8.90 (19.6)

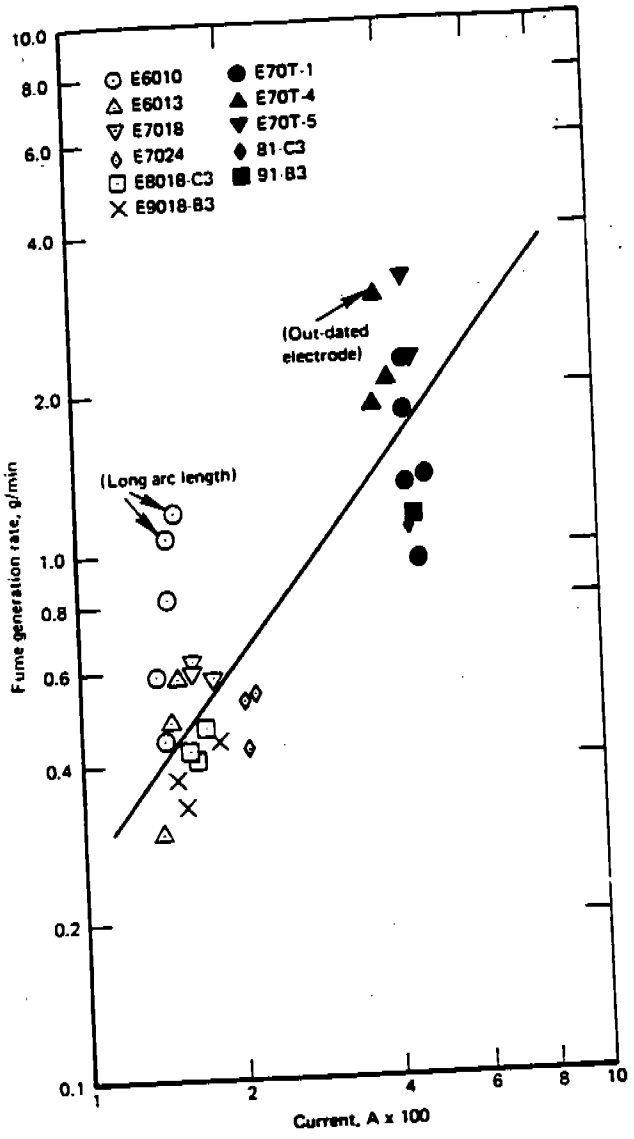

Fig. 2.2—Fume generation rates for covered and flux cored electrodes used for welding carbon and low alloy steels as a function of current

Heile and Hill evaluated the fume generation characteristics of several carbon steel covered electrodes at conventional welding currents, and the resulting data are presented in Fig. 2.4. Kobayashi, et al., investigated electrodes with ilmenite, lime, and lime-titania coverings; data associated with ilmenite coverings are included in this figure. These data also fit the I^2 regression hypothesis reasonably well. In addition, the AWS program data agree well with those developed by the other investigators.

Fume Generation Rate Relative to Electrode Type. The preceding overview of the baseline data has been primarily concerned with (a) the fume generation rates of various classifications of steel covered and flux cored electrodes and (b) an examination of the dependency of fume generation rate on welding current. Grouping of the electrodes in this manner was logical because covered and flux cored electrodes have much in common and because the covering (or flux) as well as the base metal contributes toward the formation of fumes. Data obtained from studies of solid gas metal arc electrodes were not included, because these electrodes do not incorporate a flux and the data could not be compared on an equal basis.

To examine the data obtained for all classifications of electrodes investigated during this program, the results for the following important fume generation characteristics are summarized in Fig. 2.5 and Table 2.2: (a) fume generation rate and (b) ratio of the weight of fume to the weight of deposited metal. Fume generation rate provides an immediate and direct indication of the amount of fumes to which a welder may be exposed. The ratio of the weight of fumes to the weight of deposited metal can be used to compare electrodes or welding processes on a fume exposure basis.

Under the "covered electrode" heading in Fig. 2.5, for example, the "steel" category includes electrodes that are used for welding carbon and low alloy steels: i.e., E6010, E6013, E7018, E7024, E8018 C3, and E9018 B3. The electrodes within any category can be determined from Table 2.2. Data on the fume generation characteristics of individual classifications of electrodes will be reviewed later.

A large quantity of experimental data has been compressed into Fig. 2.5 and its usefulness depends on the care with which it is interpreted. Ranges of fume generation rates and ratios of weight of fume to weight of deposited metal that may be observed when specific base metals are welded with covered, flux cored, and solid electrodes are evident in this figure. However useful this information may appear from the health and safety viewpoint, it must be used cautiously. For example, this figure indicates the fumes were produced at the highest rate when carbon and low alloy steels were welded with flux cored electrodes, and it would appear that problems associated with fumes could be minimized by using covered or solid electrodes. This may or may not be the case, since this conclusion does not consider the effects of the electrode and process variables on fume generation characteristics. When examining these data, the following should be considered:

(1) Fume generation rates are highly dependent on the welding current. Currents for flux cored arc welding were much higher than those used for welding with covered electrodes (Table 2.2). As a result, more fumes were produced during flux cored arc welding. However, since metal deposition rates were higher too, the ratio of weight of fume to weight of deposited metal was lower

for some electrodes during flux cored arc welding than it was when welding was done with certain covered electrodes. The range for this ratio even overlapped a portion of the range associated with gas metal arc welding electrodes which are recognized as low fuming types.

(2) The data in Fig. 2.5 were obtained with electrodes whose diameters were as follows: 4 mm (5/32 in.) for covered electrodes, 2.4 mm (3/32 in.) for flux cored electrodes, and 1.1 mm (0.045 in.) for most of the solid electrodes (a few of the solid electrodes had diameters of 0.8 mm [0.030 in]). Since recommended current ranges are largely based on electrode diameter, fume generation characteristics will change if diameter and current are increased or decreased. As an example, when 6.4 mm (1/4 in.) diameter electrodes were evaluated at currents near 400 A, fume generation rates were about the same as those produced by flux cored electrodes with diameters of 2.4 mm (3/32 in.) when operated at about the same current level.

(3) Other variables (arc length, electrode polarity, etc.) affect fume generation characteristics appreciably. The effects of such variables are not reflected by the data in Fig. 2.5.

Many factors must be considered when the data in Fig. 2.5 are reviewed. Electrodes are selected on the basis of economic and technical considerations (cost, weld metal properties, deposition rate, etc.), and not on the basis of their fume producing propensities. Should

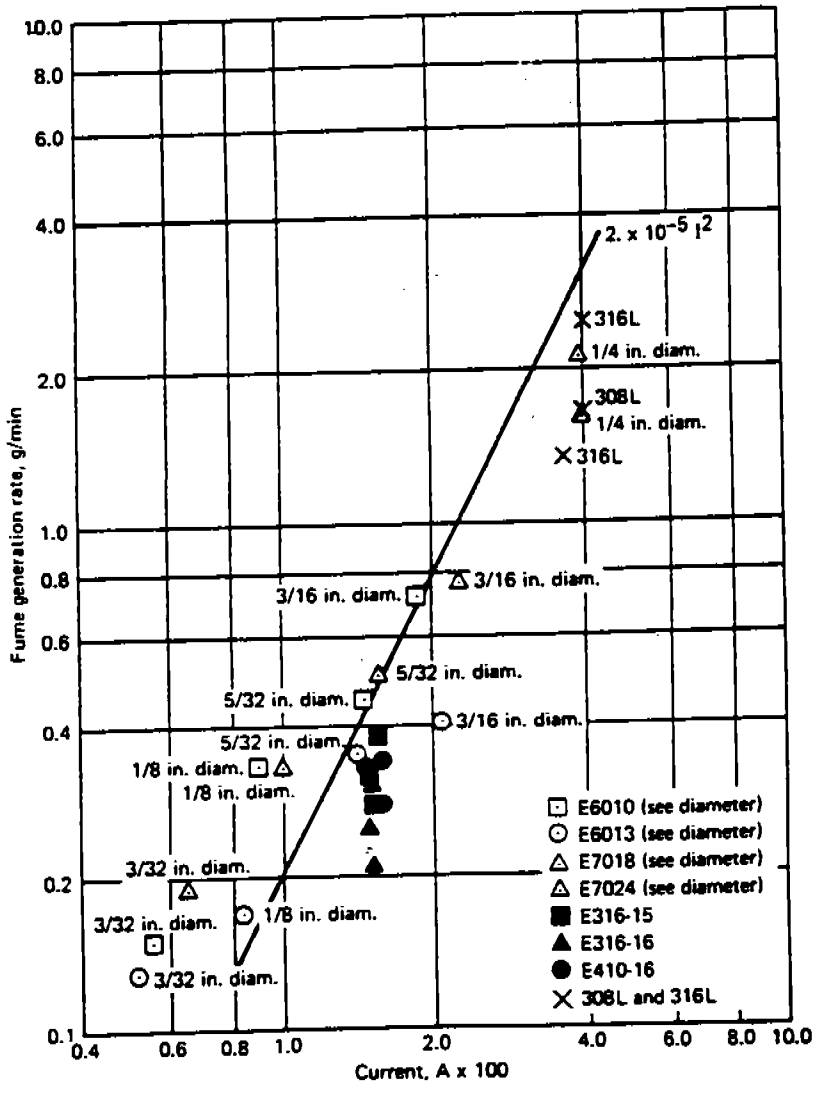

Fig. 2.3—Fume generation rates for carbon and stainless steel covered electrodes as a function of current

the occasion arise to include fuming characteristics among the selection criteria, full use should be made of Table 2.2 (and the more detailed tables in Appendix B) to interpret the data in Fig. 2.5 properly.

Covered and Flux Cored Electrodes

In this section, data obtained at recommended operating conditions are reviewed for covered and flux cored electrodes. These electrodes are considered together because they constitute a metal-flux system, and the amount of fumes produced during welding is dependent upon the flux as well as the metallic part of the electrode.

Covered Electrodes

Fume Generation Characteristics. Data on (a) fume generation rates and (b) ratios of weight of fumes to weight of deposited metal obtained during studies of carbon steel, low alloy steel, stainless steel, nickel, and other high alloy covered electrodes are shown in bar graphs in Fig. 2.6. All of the electrodes were 4 mm (5/32 in.) in diameter and welding was done at current in the mid-to-upper part of the recommended operating range. In most instances, three electrodes made by different producers were evaluated per classification; one electrode per classification was studied in the case of the nickel and other high alloy electrodes. The data upon which this figure is based are shown in Table 2.2; detailed information on welding conditions and fume generation characteristics is contained in Tables B1 through B10.

The trends in fume generation rates and ratios of weight of fumes to weight of deposited metal shown in Fig. 2.6 are in general agreement with those obtained by other investigators (Refs. 2.3 and 2.5). The following data for electrodes with the same diameter as those examined during the AWS program were obtained by Heile and Hill:

Electrode classification	Current, A	Fume generation rate, g/min.	Weight of fume/wgt. of deposited metal, g/kg
E6010	110	0.32	19
E6010	170	0.66	24
E7018	160	0.28	8
E7018	220	0.65	18
E7024	180	0.29	8
E7024	230	0.47	8

At comparable welding currents, these data fell within or near the ranges shown in Fig. 2.6.

The data in Fig. 2.6 must be interpreted carefully because they were obtained by evaluating 4 mm (5/32 in.) diameter electrodes under conditions based on the various

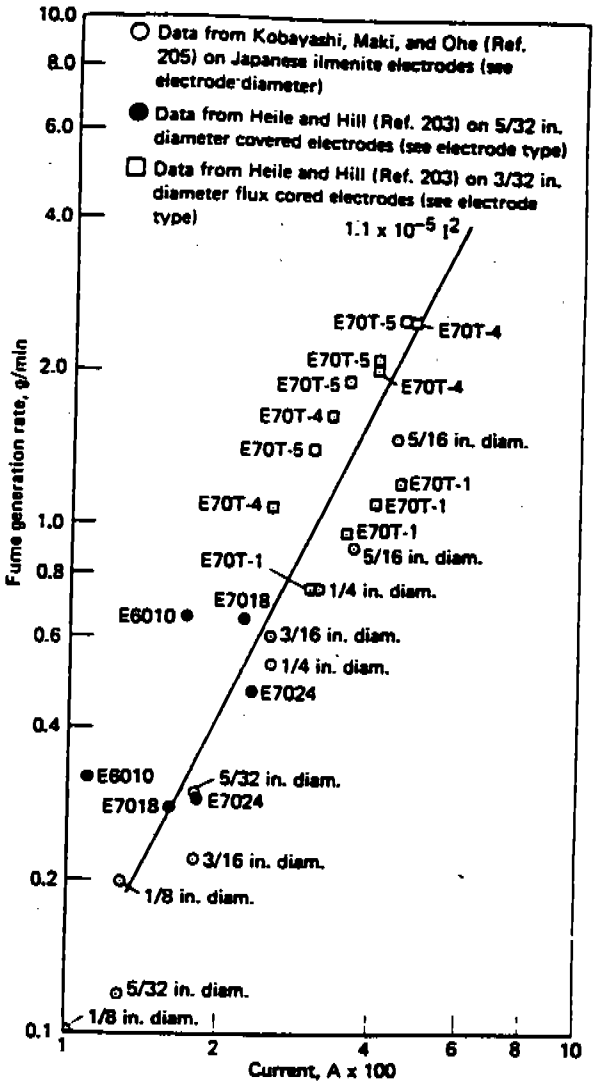

Fig. 2.4—Fume generation rates obtained by other investigators with carbon steel covered and flux cored electrodes as a function of current

manufacturers' recommendations. Data differing from those shown in Fig. 2.6 will be obtained if the electrode diameter or welding conditions are changed.

Fume generation rates and ratios of weight of fume to weight of deposited metal were somewhat higher for E6010 electrodes than for the other covered electrodes, but there was considerable overlapping of the ranges for these quantities. Several carbon and low alloy steel electrodes had fume generation rates that fell within the lower portion of the range associated with E6010 electrodes. It is interesting to note that the fume generation

Table 2.2
Summary of baseline fume generation data for arc welding electrodes

Electrode classification	Number of electrode brands evaluated	Current range, A (nominal)	Average range: Fume generation rate, g/min	Average range: Weight of fumes/weight of deposited metal, g/kg*	Source table-App. B
Shielded metal arc covered electrodes					
Carbon and low alloy steel					
E6010	3	140-150	0.83 (1.20)**	35.85 (54.36)**	B1
E6013	3	145-160	0.31-0.58	14.16-25.75	B2
E7018	3	170-180	0.57-0.60	20.35-21.83	B3
E7024	3	200-230	0.43-0.55	8.92-11.11	B4
E8018 C3	3	160-175	0.43-0.47	15.92-17.82	B5
E9018 B3	3	160-180	0.36-0.46	11.19-14.94	B6
Stainless steel and high alloy					
E316-15	3	150-155	0.28-0.38	8.02-11.08	B7
E316-16	3	145-150	0.21-0.31	6.56-11.92	B8
E410-16	3	145-160	0.28-0.34	11.75-13.97	B9
ENi-CI	1	135	0.37	12.90	B10
ENiCU-2	1	145	0.31	10.08	B10
Inconel 625	1	140-155	0.32	9.24	B10
Haynes C-276	1	130-135	0.37	14.20	B10
Haynes 25	1	135-140	0.26	8.94	B10
Flux cored electrodes					
Carbon and low alloy steel					
E70T-1	5	435-485	0.96-2.27	6.65-17.51	B11
E70T-4	3	370-390	1.86-2.09(2.98)**	12.76-13.83(22.70)**	B12
E70T-5	2	425-450	2.26-3.25	17.87-23.63	B13
81-C3	1	440-445	1.11	8.69	B14
91-B3	1	450	1.15	8.42	B14
Stainless steel					
E308LT-3	1	440-445	1.64	9.11	B15
E316LT-3	2	340-405	1.34-2.48	6.97-12.32	B15
Gas metal arc solid electrodes					
Carbon steel					
E70S-3	3	260-290	0.41-0.46	4.97-5.68	B16
Spray w/Ar-2 O_2	3	260-290	0.41-0.46	4.97-5.68	B18
Spray w/Ar-9 CO_2	3	205-225	0.41-0.49	6.39-8.34	B16,B18
Globular w/CO_2	3	320-330	0.45-0.51	3.09-3.31	B16,B18
Short circuit w/Ar-25 CO_2	3	195-205	0.20-0.25	4.11-4.91	B16,B18
E70S-5					
Spray w/Ar-2 O_2	1	275-290	0.38	5.01	B19
Globular w/CO_2	1	325-345	0.40	2.61	B19
Short circuit w/Ar-25 CO_2	1	210-215	0.24	4.28	B19
Stainless steel and high alloy					
ER316	1	165-175	0.04	0.58	B20
ERNiCu-7	1	250-260	0.16	2.02	B21
Inconel 625	1	190-195	0.06	0.87	B21
Haynes 25	1	200-205	0.08	1.38	B21
Haynes C-276	1	165	0.39	6.98	B21

Table 2.2 (continued)
Summary of baseline fume generation data for arc welding electrodes

Electrode classification	Number of electrode brands evaluated	Current range, A (nominal)	Average range: Fume generation rate, g/min	Average range: Weight of fumes/weight of deposited metal, g/kg**	Source table-App. B
		Aluminum			
ER4043	1	160-165	0.11-0.27	5.6-15.74	B22
ER5356	1	150-165	1.41-1.75(3.59)**	64.94-79.72(164.85)**	B23
		Copper			
ERCu	1	205-210	0.30	4.93	B24
ERCu A1-A2	1	210-215	0.47	8.12	B24

*g/kg ÷ 10 = weight of fumes expressed as a percentage of the deposit weight.

**The data points in parentheses represent data obtained at non-baseline welding conditions (E6010 and ER5356) and with an E70T-4 electrode no longer in production.

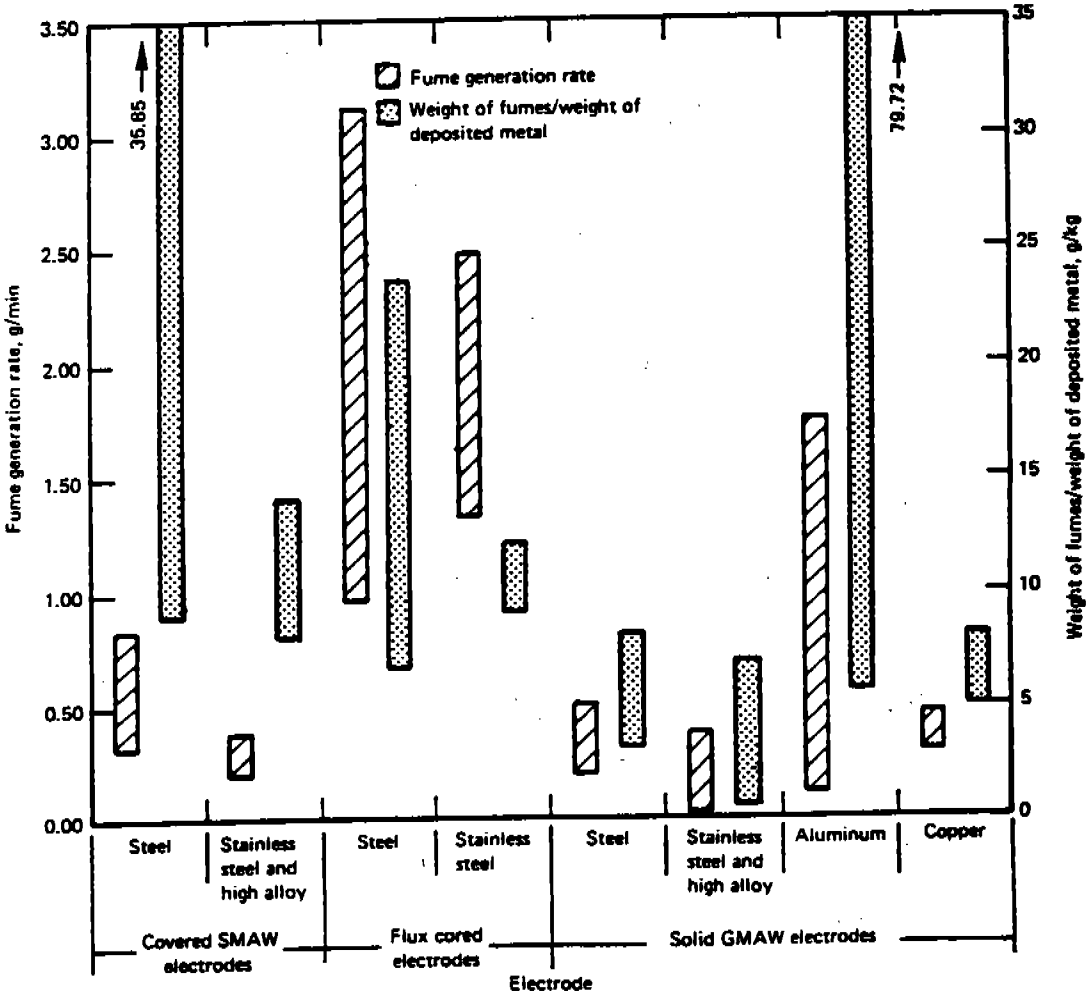

Fig. 2.5—Ranges of fume generation rates and ratios of weight of deposited metal for covered, flux cored, and solid GMAW electrodes

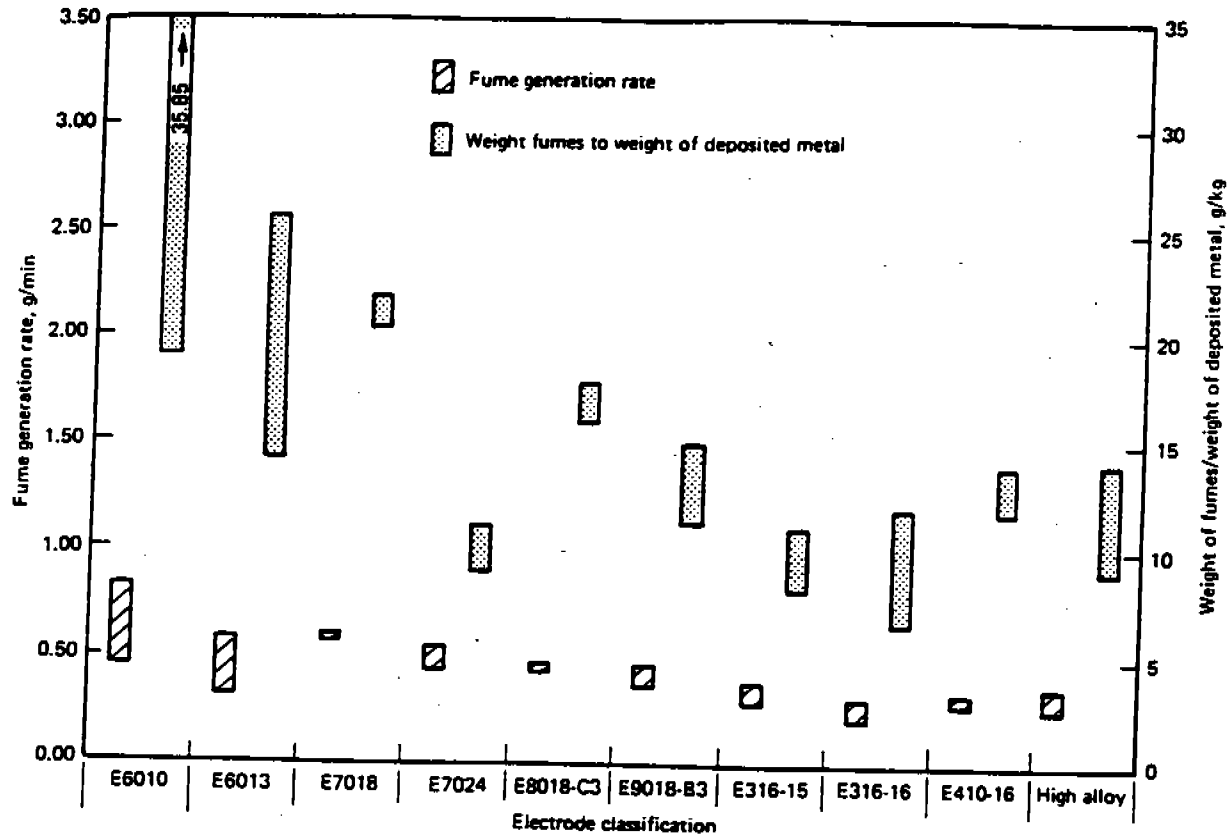

Fig. 2.6—Fume generation rates and ratios of weight of fumes to weight of deposited metal for covered electrodes

rates of the E7024 electrodes were comparable to those of other carbon and low alloy steel electrodes, even though the covering on these electrodes is much thicker than the coverings on the other electrodes. The ratios of weight of fume to weight of deposited metal for E7024 electrodes were lower than those of other electrodes. This results from the combination of a relatively low fume generation rate and the high deposition rate which results from the iron powder (up to 50 percent) in the coverings.

Fume generation rate ranges for stainless steel, nickel, and other high alloy covered electrodes were similar in magnitude; ranges for ratios of weight of fumes to weight of deposited metal generally overlapped one another.

Fume Composition. Studies to determine the complete analysis of the fumes associated with covered (and other types of) electrodes are not common; they can be quite involved and costly and may be unnecessary. Since the composition of the core wire is generally a matter of record, core wire constituents in the fumes can be readily determined by optical emission spectroscopy or atomic absorption procedures. Fume constituents attributable to the electrode coverings are more difficult to determine and a combination of analytical methods may be needed. Optical emission spectroscopy provides a means for identifying most of the constituents in the fumes, since the presence of 70 or more elements can be detected on a semiquantitative base. This method should be supplemented by (a) atomic absorption analysis for more accurately determining elements present in large amounts and (b) wet chemical analysis for determining fluoride contents. X-ray diffraction is useful if there is interest in detecting compounds in the fumes. Such detailed analyses are seldom required; industry is generally concerned only with those fume constituents that have low threshold limit values or are present in large amounts.

Since a large number of electrodes were to be evaluated during this program, the AWS Research Committee agreed that analytical efforts would be limited to the detection of the major elements in the fumes (e.g., iron, manganese, and silicon for carbon steel electrodes) and fluorides. Atomic absorption analysis was used to detect selected elements because the equipment is readily available in industry, is reasonable in cost, and produces accurate results. Wet chemistry was used to detect fluorides. Data on the core wire elements in the fumes

produced by covered (and other) electrodes are presented later in this report (Table 2.21). It is noted that the analytical data do not total 100 percent because these limited studies did not include detection of fume constituents originating from the electrode covering.

Some data on expected fume constituents attributable to the coverings on the electrodes can be obtained from the literature. Compositions of the coverings of representative E6010 (high cellulose-sodium), E6013 (high titania-potassium), and E7016 (low hydrogen-potassium) electrodes have been provided by Smith and Rinehart (Ref. 2.18) and Smith (Ref. 2.19) and are shown in Table 2.3. The E6010 and E6013 electrodes are among the electrodes evaluated during this investigation. E7018 electrodes evaluated during the present program have coverings similar to that of the E7016 electrode except for the presence of iron powder in the E7018 covering. The fumes produced by the electrodes included in Table 2.3 should contain the constituents of the covering and those of the core wire, usually (but not necessarily) in the oxide form of the respective elements.

Examples of complete fume analyses of several Scandinavian electrodes, three of which appear to be low hydrogen electrodes with iron powder additions, are shown in Table 2.4.

Table 2.3
Composition of coverings on representative carbon steel electrodes (Refs. 2.18, 2.19)

Constituent	Covering composition, weight %		
	E6010	E6013	E7016
SiO_2	32.0	25.9	16.0
$TiO_2 + ZrO_2$	18.0	30.6	6.5
Al_2O_3	2.0	5.9	1.0
CaF_2	---	---	27.0
CaO	---	1.6	---
MgO	6.0	2.6	---
Na_2O	8.0	1.1	1.4
K_2O	---	6.7	1.0
CO_2	---	1.7	---
Organics	30.0	17.7	---
Fe	2.0	2.1	---
Mn	7.0	4.8	2.5
$CaCO_3$	---	---	38.0

Table 2.4
Composition of fumes produced by typical Scandinavian covered electrodes (Ref. 220)

Compound	Composition, weight %			
	Electrode 1	Electrode 2	Electrode 3	Electrode 4
SiO_2	7.0	9.5	10.0	30.5
Fe_2O_3	25.5	24.5	36.5	43.5
Al_2O_3	0.6	0.2	<0.1	<0.1
TiO_2	1.1	0.2	0.5	2.2
ZrO_2	---	0.6	---	---
MnO	4.7	7.2	8.2	9.8
ZnO	0.04	0.07	0.09	0.02
CaO	15.9	5.3	0.4	<0.1
MgO	0.1	0.1	1.0	0.1
K_2O	24.4	17.6	17.6	7.2
Na_2O	2.4	17.2	11.0	5.4
Cu	0.03	0.07	0.03	0.06
Pb	0.02	0.02	0.04	0.05
Cr	0.01	0.04	0.01	0.04
Fe	19.8	15.7	17.1	---

In the AWS studies to characterize fumes and fume particles, optical emission spectroscopy was used to determine the constituents in the fumes produced by E7024 and E410-16 covered electrodes. Data on major constituents are shown in Table 2.5.

Flux Cored Electrodes

Fume Generation Characteristics. Ranges of (a) fume generation rates and (b) ratios of weight of fumes to weight of deposited metal for representative carbon steel, low alloy steel, and stainless steel flux cored electrodes are shown in Fig. 2.7. All electrodes were 2.4 mm (3/32 in.) diameter and welding was done at currents in the mid-portion of the manufacturer's recommended operating range. Details on the welding conditions and the experimental results are contained in Tables B11 and B15. Carbon dioxide shielding was used with the E70T-1, E70T-5, 81-C3, and 91-B3 electrodes; the E70T-4 and stainless steel electrodes were self-shielding. The data upon which Fig. 2.7 is based are summarized in Table 2.2; this table should be consulted when this figure is reviewed.

(1) E70T-1 electrodes. The ranges of fume generation and ratios of weight of fumes to weight of deposited metal were broadest for this classification of electrodes. Three of these electrodes were made by the same producer; the other two were made by two different producers. The electrodes made by the same producer were designed for single- or multiple-pass welding, but the core wire and flux composition varied to achieve certain objectives: e.g., the welding of steel with different strength levels, the welding of clean or rusted steel, etc. These special-purpose electrodes defined the upper and lower limits of the ranges in Fig. 2.7. The electrode with the highest fume generation rate contained appreciable amounts of fluorides (Table 2.18); such compounds are known to enhance the production of fumes. The fluoride content of the fumes associated with the electrode having the lowest fume generation rate was very small.

(2) E70T-4 electrodes. A data point outside the indicated ranges for these electrodes is shown in Fig. 2.7. This point represents the fume generation rate for an E70T-4 electrode that was made several years ago and is no longer available on the market. Since another currently available electrode made by the same producer had a much lower fume generation rate, it appears that changes in the flux were made to reduce fume quantities.

(3) E70T-5 electrodes. The highest fume generation rates were encountered with E70T-5 electrodes. This was expected because the E70T-5 electrodes can be used with or without a shielding gas, and the basic type flux contains ingredients that produce large amounts of gas and fumes. Ratios of fume weight to weight of deposited metal were highest for these electrodes also.

Ranges for the fume generation characteristics of other flux cored electrodes overlapped one another in many instances. The experimental results are discussed below.

(1) Low alloy steel electrodes. The fume generation

Table 2.5
Optical emission spectoscopic analysis of fumes produced by two E7024 and one E410-16 covered electrodes

Element	(Oxide)[1]	Composition, weight %		
		E7024(7)[2]	E7024(8)[2]	E410-16(21)[2]
Fe	(Fe_2O_3)	20-30 (28.6-42.9)	20-30 (28.6-42.9)	10-20 (14.3-28.6)
Si	(SiO_2)	10-20 (15.7-31.4)	5-10 (7.8-15.7)	2-3 (3.1-4.6)
K	(K_2O)	8-12 (9.6-14.4)	8-12 (9.6-14.4)	10-20 (12.0-24.0)
Na	(Na_2O)	3-6 (4.0-8.1)	3-6 (4.0-8.1)	4-8 (5.4-10.8)
Mn	(MnO_2)	2-4 (3.2-6.3)	2-4 (3.2-6.3)	1-2 (1.6-3.2)
Ca	(CaO)	0.1 (0.1)	0.05 (0.1)	2-4 (2.8-5.6)
Zn	(Z_nO)	<0.1 (0.1)	<0.1 (0.1)	0.1 (0.1)
Ti	(TiO_2)	0.5 (0.8)	0.3 (0.5)	0.4 (0.7)
Al	(Al_2O_3)	0.1 (0.2)	0.05 (0.1)	0.5 (0.9)
Cr		0.01	0.01	5-10

1. Assuming that elements are completely converted to oxides.
2. The number in parentheses following the electrode designation is the code number identifying the specific electrode.

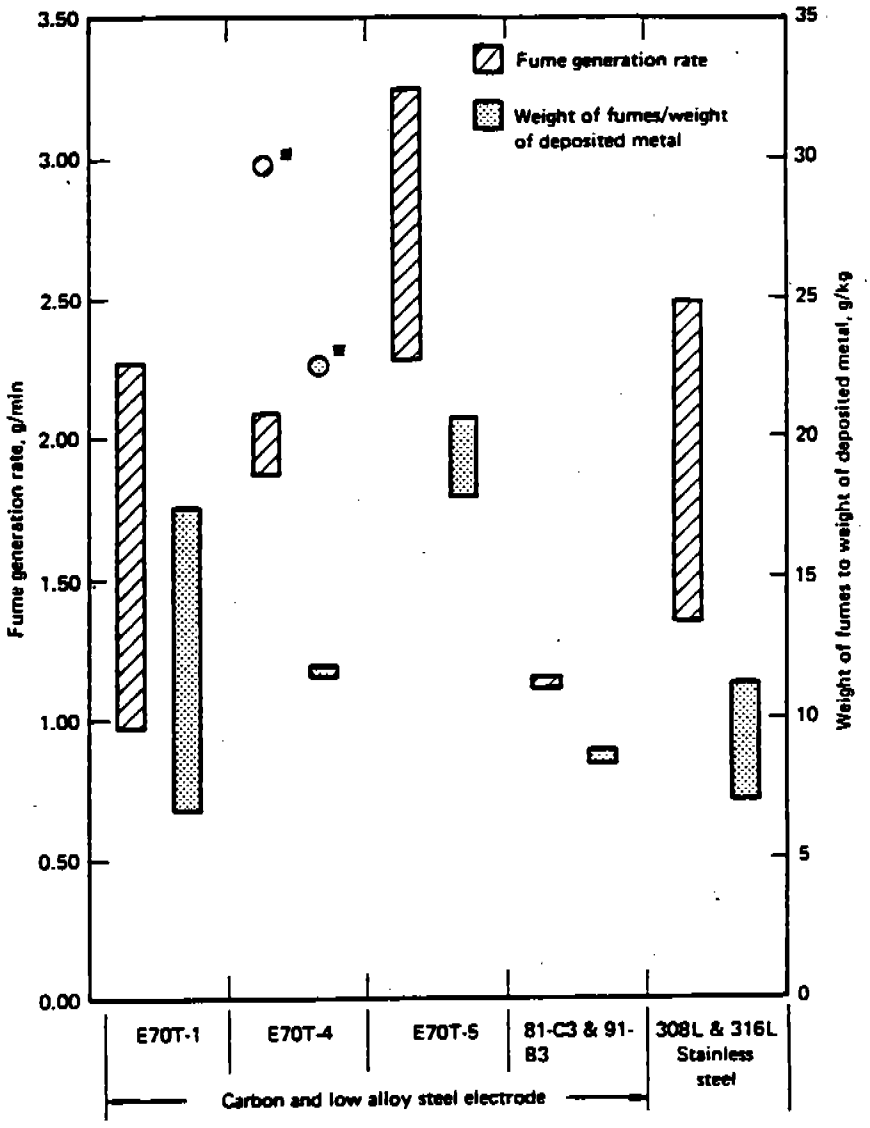

*Data from E70T-4 electrode that is no longer commercially available.

Fig. 2.7—Fume generation rates and ratios of weight of fumes to weight of deposited metal for flux cored electrodes

rates and ratios of weight of fumes to weight of deposited metal for 81-C3 and 91-B3 low alloy steel electrodes were low in comparison with those for carbon steel flux cored electrodes. These results are similar to those observed when these quantities were compared for carbon steel and low alloy steel covered electrodes.

(2) Stainless steel electrodes. The fume generation characteristics of the three self-shielded stainless steel electrodes investigated during this program varied over a wide range. This appears to be a flux-related occurrence. The E308LT-3 electrode and one of the E316LT-3 electrodes were made by the same producer, while the remaining E316LT-3 electrode was made by another producer. The fume generation rates for the electrodes made by the same producer were similar and define the low end of the range shown in Fig. 2.7; this result might be expected because the fluxes used in these electrodes were probably quite similar in composition. However, the fume generation rates and ratios of weight of fumes to weight of deposited metal varied widely for the E316LT-3 electrodes made by two producers. Since the sheath compositions are not likely to differ substantially, this variation must be associated with differences in the flux cores of the respective electrodes.

Table 2.6
Comparison of average fume generation characteristics of 2.4 mm (3/32 in.) diameter E70T-1 flux cored electrodes as a function of shielding gas

Electrode number	Shielding gas[1]	Current, A	Fume generation rate, g/min.	Weight of fumes/ weight of deposited metal, g/kg
E70T-1 (40)[2]	CO_2	475	1.35	10.40
E70T-1 (40)	Ar-25 CO_2	465	1.01	7.78
E70T-1 (42)	CO_2	440	2.27	17.51
E70T-1 (42)	Ar-25 CO_2	445	1.93	14.91

1. Ar-25 CO_2 is a convention used to designate a gas mixture of 25% CO_2, 75% Ar.
2. The number in parentheses after the AWS electrode classification is a code number identifying the specific proprietary electrode.

Table 2.7
Typical flux compositions of the three carbon dioxide shielded flux cored electrode types, percent (Ref. 2.17)

Compound or element	Composition, weight percent		
	Type 1 Titania type (non-basic) flux	Type 2 Lime-titania type (basic or neutral) flux	Type 3 Lime type (basic) flux
SiO_2	21.0	17.8	7.5
Al_2O_2	2.1	4.3	0.5
TiO_2	40.5	9.8	---
ZrO_2	---	6.2	---
CaO	0.7	9.7	3.2
Na_2O	1.6	1.9	---
K_2O	1.4	1.5	0.5
CO_2 (as carbonate)	0.5	---	2.5
C	0.6	0.3	1.1
Fe	20.1	24.7	55.0
Mn	15.8	13.0	7.2
CaF_2	---	18.0	20.5
AWS classification	E70T-1 or E70T-2	E70T-1	E70T-1 or E70T-5

As noted previously, the E70T-1 and E70T-5 electrodes were used with CO_2 shielding. To investigate the premise that fume generation rates can be affected by the type of shielding gas used during welding, the characteristics of two E70T-1 flux cored electrodes were determined with Ar-25 CO_2 shielding. Other than shielding gas, the welding conditions were essentially the same as the baseline conditions. The resulting data are summarized in Table 2.6; additional details are contained in Appendix B (Table B25).

The fume generation rates for each electrode were reduced between 15 and 25 percent when Ar-25 CO_2 shielding was used instead of CO_2. This is because the argon-based shielding gas has a lower oxidation potential than CO_2, and oxidation processes contributing to the formation of fumes at and near the tip of the electrode were decreased as a consequence. The metal deposition rates for these electrodes were unaffected by the type of gas shielding used. Thus, the ratios of weight of fumes to weight of deposited metal were also smaller when Ar-25 CO_2 was used for shielding.

Fume Composition. As in the case of covered electrodes, the composition of fumes produced by flux cored electrodes is determined by composition of the electrode sheath, flux core, and, to a minor extent, by the base metal. Since the composition of the sheath for electrodes within a classification is unlikely to vary much from producer to producer, variations in fume compositions for such electrodes are caused primarily by differences in the flux core ingredients.

To provide an insight into the constituents that may be detected in the fumes associated with welding operations, data on the composition of flux cores and slags associated with representative flux cored electrodes are shown in Tables 2.7 and 2.8 (Ref. 2.17). The compositions of the fluxes used in three CO_2 shielded flux cored electrodes are shown in Table 2.7. Electrodes incorporating these fluxes can be included in one or two AWS classifications; classification criteria are discussed in the article from which these data were taken (Ref. 2.17). The type of flux also determines the classification of self-shielded flux cored electrodes as indicated in Table 2.8.

Table 2.8
Typical flux compositions of the four types of self-shielded flux cored electrodes, percent (Ref. 2.17)

Compound or element	Composition, weight percent			
	Type 1 Fluorspar-aluminum flux	Type 2 Fluorspar-titania flux	Type 3 Fluorspar-lime-titania flux	Type 4 Fluorspar-lime flux
SiO_2	0.5	3.6	4.2	6.9
Al	15.4	1.9	1.4	---
Al_2O_3	---	---	---	0.6
TiO_2	---	20.6	14.7	1.2
CaO	---	---	4.0	3.2
MgO	12.6	4.5	2.2	---
K_2O	0.4	0.6	---	---
Na_2O	0.2	0.1	---	0.6
C	1.2	0.6	0.6	0.3
CO_2 (as carbonate)	0.4	0.6	2.1	1.3
Fe	4.0	50.0	50.5	58.0
Mn	3.0	4.5	2.0	7.9
Ni	---	---	2.4	---
CaF_2	63.5	22.0	15.3	22.0
AWS classification	E70T-4 E60T-7 E60T-8	E70T-3	E70T-6	E70T-5

Most of the flux constituents shown in these tables will be present as elements and compounds in the fumes produced by electrodes incorporating them. They will not be present in the same proportions as in the flux because some constituents are transferred by the arc to the slag and, in some cases, to the weld metal. Elemental compositions of the fumes produced by typical E70T-1, E70T-4, and E70T-5 electrodes are shown in Table 2.9 along with calculated oxide contents (assuming that the elements are converted to oxides (Ref. 2.3). These electrodes were classified as follows: E70T-1, rutile-base; E70T-4, fluorspar-base; and E70T-5, silica-base.

Fume compositions determined by optical emission spectroscopy are shown in Table 2.10 for the E70T-1, E70T-4, and E70T-5 electrodes investigated during this program. These data were acquired during studies to characterize fumes and fume particles. From these data, it appears that the E70T-4 electrodes evaluated by Battelle and by Heile and Hill had fluxes based on similar ingredients (e.g., aluminum and fluorspar). Fluxes for the respective E70T-1 and E70T-5 electrodes differed considerably.

Solid Electrodes

The fume generation characteristics of solid electrodes and rods used for gas metal arc welding and gas tungsten arc welding are reviewed in this section. In comparison with covered and flux cored electrodes, these are low fuming electrodes and rods whose fume generation tendencies are a direct function of the amount of electrode or rod consumed during welding. Other factors which influence the rate at which fumes are produced by the solid electrodes include the type of shielding gas, the metal transfer characteristics of the arc, and the welding conditions.

Gas Metal Arc Electrodes

Fume Generation Characteristics. Ranges for fu generation rates and ratios of weight of fume to wei of deposited metal associated with carbon steel, stainl steel, high alloy, copper, and aluminum gas metal welding electrodes investigated during this program shown in Fig. 2.8. The data upon which these ran are based are summarized in Table 2.2; detailed inform tion on the fume generation characteristics of individ electrodes are contained in Tables B16 to B24 along w the welding conditions.

(1) Steel Electrodes. The results obtained with c bon steel electrodes are reviewed separately from thc obtained with other types of solid electrodes. Caution required in interpreting the data in Fig. 2.8 because the dependency of the fume generation characteristics c welding current and other process variables. The fun generation characteristics of three 1.1 mm (0.045 in E70S-3 electrodes, each made by a different manufa turer, were determined at appropriate current levels i the following transfer modes: spray transfer with Ar-O_2 or Ar-9 CO_2 shielding; globular transfer with CC shielding; and short circuiting transfer with Ar-25 CC shielding. Although the electrodes were made by di ferent producers, there was little variation in composi tion. The thickness of the copper coating on the electrod surface varied from zero to several microinches. A singl E70S-5 electrode was also evaluated in various transfe modes: spray transfer with Ar-2 O_2 shielding; globula transfer with CO_2 shielding; and short circuiting transfe with Ar-25 CO_2 shielding.

Fume generation rates for the three E70S-3 electrode were similar in magnitude during spray transfer weldin with Ar-2 O_2 or AR-9 CO_2 shielding, and durin globular transfer welding with CO_2 shielding. Unde these conditions, the ratios of weight of fumes to weigh of deposited metal varied somewhat because of differ-

Table 2.9
Composition of fumes from flux cored arc welding (Ref. 2.3)

Element	(Oxide)	Composition, weight percent					
		E70T-1		E70T-4		E70T-5	
Fe	(Fe_2O_3)	28	(40.0)	13	(18.6)	23	(32.9)
Mn	(MnO_2)	5	(7.9)	2	(3.2)	4	(6.3)
Si	(SiO_2)	25	(39.3)	4	(6.3)	20	(31.4)
Ca	(CaO)	---		13	(18.2)	8	(11.2)
Ti	(TiO_2)	2	(3.3)	---		---	
Mg	(MgO)	3	(5.0)	9	(14.9)	---	
Al	(Al_2O_3)	---		9	(17.0)	---	
F		7		13		7	

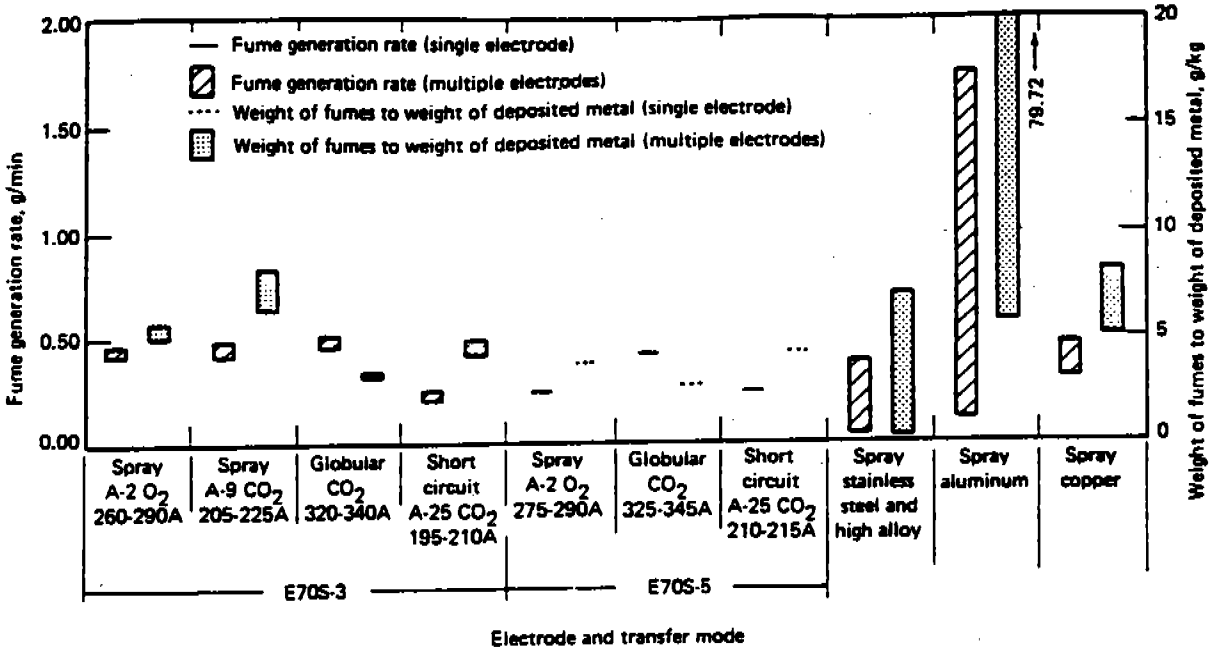

Fig. 2.8—Fume generation rates and ratios of weight of fumes to weight of deposition metal for gas metal arc electrodes

Table 2.10
Optical emission spectroscopic analysis of fumes produced by E70T-1, E70T-4, and E70T-5 flux cored electrodes

Element	(Oxide) [1]	Composition, weight %					
		E70T-1 (42)[2]		E70T-4 (49)[2]		E70T-5 (50)[2]	
Fe	(Fe_2O_3)	30-40	(42.9-57.2)	15-25	(21.4-35.8)	30-40	(42.9-57.2)
Si	(SiO_2)	2-3	(3.1-4.6)	0.1	(0.2)	2-3	(3.1-4.6)
K	(K_2O)	1.0	(1.2)	2.0	(2.4)	4-6	(4.8-7.2)
Na	(Na_2O)	4-6	(5.4-8.1)	0.1	(0.1)	1.0	(1.4)
Mn	(MnO_2)	4-6	(6.3-9.5)	2-3	(3.2-4.7)	4-6	(6.3-9.5)
Ca	(CaO)	0.1	(0.1)	15-25	(21-35)	8-12	(11.2-16.8)
Zn	(ZnO)	0.1	(0.1)	0.1	(0.1)	0.1	(0.1)
Ti	(TiO_2)	0.5	(0.8)	0.01	(0.02)	0.2	(0.3)
Al	(Al_2O_3)	0.4	(0.8)	7-10	(13.2-18.9)	1-2	(1.9-3.8)
Mg	(MgO)	0.02	(0.03)	7-10	(11.6-16.6)	0.2	(0.3)

1. Assuming that elements are completely converted to oxides.
2. The number in parentheses following the electrode designation is the code number identifying the specific electrode.

ences in the metal deposition rates for the respective electrodes. Under short circuiting conditions with Ar-25 CO_2 shielding, fume generation rates were lower than they were with other metal transfer modes and other shielding gases.

The effects of type of shielding gas and mode of metal transfer on fume generation characteristics are not clearly evident from the data in Fig. 2.8 or the tabular data mainly because of the differences in the currents used for welding. If the effects of current are taken into account by normalizing[7] the data to a selected value of current (multiplying the normalized fume generation rate for each electrode by current squared), the effects of shielding gas and metal transfer mode are more readily observed. To facilitate interpreting the data, the average fume generation rates were normalized to a current of 250 A. These data together with the measured rates are shown in Table 2.11.

As indicated in Table 2.11, fumes were produced at the highest rate during spray transfer welding with Ar-9 CO_2 shielding, followed approximately in descending order by spray transfer welding with AR-2 O_2, short cuiting transfer welding with Ar-25 CO_2, and glob transfer welding with CO_2. The effects of shielding on fume generation rates can be best observed by c paring the rates at which fumes were produced du spray transfer welding with Ar-2 O_2 or Ar-9 CO_2 shi ing. When Ar-9 CO_2 was used, the fume generation much higher than when Ar-2 O_2 shielding was used. T reflects the higher oxidation potential of the Ar-9 (shielding gas, and the fume generation rate presuma would increase further if the content of CO_2 in the arg based shielding gas was increased.

The E70S-5 electrode is similar to the E70S-3 electr except that it contains aluminum as well as mangan and silicon as a deoxidizer. If the same welding con tions are used, the fume generation characteristics of t E70S-3 and E70S-5 electrodes should be similar, indeed they were (see Tables B16 through B19).

(2) Other Solid Electrodes. Representative stainle steel, high alloy, copper, and aluminum solid electrode 1.1 mm (0.045 in.) in diameter,[8] were also investigate In each instance, a single electrode per classificatic was evaluated and the welding current was adjusted produce acceptable spray transfer conditions.

(3) High Alloy Electrodes. Five high alloy elec trodes (one stainless steel electrode, three nickel bas electrodes, and one cobalt-base electrode) were invest gated during this program, and all but one had fum generation rates and ratios of weight of fumes to weigh of deposited metal well below those of carbon stee electrodes. This trend was also observed with covere electrodes of the same types. The exception, a nickel base electrode, had fume generation rates approachin

7. In general, fume generation rates for electrodes studied in this and other investigations varied in accordance with current to a power that ranged from greater than one to less than three (current equals I^x where $1 < x < 3$). With current squared accepted as a reasonable power function compromise, a normalized fume generation rate that includes the effect of current on the rate at which fumes are produced can be established. Then, if an electrode is used at one current, it is possible to use the normalized rate (fume generation rate per unit of current squared) and predict the approximate fume generation rate when the electrode is used at a higher or lower rate (provided other welding variables are controlled). Normalized fume generation rates are shown in the tabular data in Appendix B along with measured rates.

8. Because of availability, electrodes with diameters othe than 0.045 in. (1.1 mm) were used in a few instances; such de viations are noted in the tabular data in Appendix B.

Table 2.11
Measured and normalized (Ref. 2.1) fume generation rates for E70S-3 electrodes

Metal transfer mode	Shielding gas	Fume generation rate g/min					
		E70S-3(54)[2]		E70S-3(57)[2]		E70S-3(58)[2]	
		Measured	Normalized	Measured	Normalized	Measured	Normalized
Spray	AR-2 O_2	0.41	0.35	0.46	0.36	0.45	0.35
Spray	AR-9 CO_2	0.41	0.58	0.44	0.62	0.49	0.61
Globular	CO_2	0.51	0.29	0.46	0.28	0.45	0.27
Short circuit	Ar-25 CO_2	0.20	0.33	0.25	0.38	0.24	0.38

1. Fume generation rates normalized to a current of 250 A.

2. The number in parentheses following the electrode designation is the code number identifying the specific electrode.

those of the carbon steel electrodes. It was a small diameter electrode, 0.09 mm (0.035 in.), and the current density was higher than that used with the other electrodes; as a result, arc temperatures were probably higher and more fumes were produced.

(4) Aluminum Electrodes. The aluminum electrodes presented mixed results. The ER4043 electrode produced fumes at low rates and the ratio of weight of fumes to weight of deposited metal was low also. The ER5356 electrode produced fumes at much higher rates than the ER4043 electrode. High fume generation rates were not unexpected, because the ER5356 electrode contains magnesium, a metal that oxidizes easily and has a high vapor pressure. In contrast, the ER4043 electrode contains silicon, an element with a much lower vapor pressure. Using a contact tube-to-work distance of 12.5 mm (0.50 in.), the fume generation rate for the ER5356 electrode was similar to that obtained by Heile and Hill when differences in welding current are taken into account (Ref. 2.3). Much higher fume generation rates were produced at longer contact tube-to-work distances, and there was evidence of lack of shielding of the arc and pool of weld metal. These results point to the need for careful welding torch setup control and good shielding to minimize fumes as well as to insure the production of high quality welded joints.

(5) Copper Electrodes. Fume generation rates and ratios of weight of fumes to weight of deposited metal for an ERCu and an ERCuAl-A2 electrode were comparable in magnitude to those associated with carbon steel electrodes.

Fume Compositions of Gas Metal Arc Electrodes. In contrast to covered and flux cored electrodes, the composition of the fumes produced by gas metal arc welding electrodes is controlled by the composition of the electrode and any coating that might be on the electrode surface. This can be illustrated by considering the composition of the fumes produced by the three E70S-3 electrodes investigated during this study:

	Fume composition, weight percent						
Electrode no.	Fe	(Fe_2O_3)	Mn	(MnO_2)	Si	(SiO_2)	Cu
E70S-3 (54)	63.7	(91.1)	5.3	(8.4)	0.05	(0.1)	0.11
E70S-3 (57)	65.7	(93.9)	3.8	(6.0)	0.79	(1.2)	0.60
E70S-3 (58	62.5	(89.4)	8.5	(13.4)	0.53	(0.8)	1.00

Each of the fume samples contained iron, manganese, silicon, and copper (or their oxides). The amount of copper in the fumes produced by the electrode that was not coated with copper, E70S-3 (54), was higher than expected. Subsequent analyses of short lengths of each electrode from which the copper coating was stripped showed that they all contained a small (0.02 to 0.03) weight percent of copper as a residual element in the electrodes themselves. Apparently, the residual copper in the E70S-3 (54) electrode plus perhaps some copper picked up from contact tube and wire drive was the source of copper in the fumes from this electrode.

Because of its low threshold limit value, there is more concern about the presence of copper fume in the welding environment than about iron oxide fume. Table 2.12 combines data on the baseline fume generation rates of three E70S-3 electrodes with the compositional data on

Table 2.12
Results of studies on copper in the fumes produced by E70S-3 electrodes used for gas metal arc welding

	Electrode		
Characteristic	E70S-3(54)*	E70S-3(57)	E70S-3(58)
Copper coating on electrode			
Thickness, μ in.	0	18	24
weight percent	0	0.19	0.24
Copper content of fumes, weight %	0.11	0.60	1.00
Iron (oxide) content of fumes, weight %	63.7 (91.1)	65.7 (93.9)	62.5 (89.4)
Total fume generation rate, g/min.	0.41	0.46	0.45
Copper fume generation rate, g/min.	0.0004	0.0028	0.0045
Iron (oxide) fume generation rate, g/min.	0.26 (0.37)	0.30 (0.43)	0.28 (0.40)

*The number in parentheses following the electrode designation is a code number identifying the specific electrode.

the fumes. The ACGIH time-weighted average threshold limit value for iron oxide fumes (5 mg/m³) is 25 times as large as that for copper fumes (0.2 mg/m³). However, the results of the experimental studies indicate that the iron oxide fume generation rates for the E70S-3 (54), E70S-3 (57), and E70S-3 (58) electrodes were 925, 154, and 89 times as great, respectively, as the copper fume generation rates. Thus, when welding with these electrodes, the allowable limit for iron oxide fumes would be exceeded long before reaching the limit for copper fumes.

Compositions of the fumes produced by the gas metal arc electrodes used for welding other base metals (stainless steels, nickel base alloys, etc.) are determined by the composition of the respective electrodes.

Gas Tungsten Arc Welding

Fume Generation Characteristics. Two filler rods used for gas tungsten arc welding were also evaluated: a 3.2 mm (1/8 in.) diameter E308L stainless steel wire and a 2.4 mm (3/32 in.) diameter 5356 aluminum alloy wire. The welding conditions are indicated below:

308L Stainless Steel Filler Metal. Welding was done with a torch equipped with a 2.4 mm (3/32 in.) diameter 2 percent thoriated tungsten electrode (AWS EWTh-2). The welding current was 200-215 A (dc), the electrode polarity was negative, and argon was used for shielding.

5356 Aluminum Filler Metal. Welding was done with a torch equipped with a 2.4 mm (3/32 in.) diameter tungsten electrode (AWS EWP). The welding current was 250 A (ac) and argon was used for shielding.

Under these conditions, the fume generation rates were 0.0025 and 0.0065 g/min for the stainless steel and aluminum filler wires, respectively. Such rates are a small fraction of the rates associated with other processes investigated during this program.

Fume Compositions. No analyses were made.

Section IIC. Effects of Process Variables on Fume Generation Rates

While baseline data on the fume generation characteristics of covered, flux cored, and solid electrodes provide a wealth of information that is useful to those concerned with the health and safety of welding personnel, they are by no means the entire story. The term "baseline" itself implies that these data were obtained when the electrodes were used in general accordance with recommended conditions, and questions concerning the effects of the process variables on fume generation characteristics naturally arise. In reviewing the baseline data, reference to the effect of current on these characteristics has been frequently made because it appears to be the dominant variable. Other welding variables also have a bearing on the rate at which fumes are produced during welding. Some of the other variables affecting fume production are

(1) Voltage
(2) Electrode polarity
(3) Shielding gas (flux cored and solid electrod
(4) Contact tube-to-work distance (flux corec solid electrodes)
(5) Metal transfer mode
(6) Electrode characteristics (manufacturer, di ter, core wire composition, covering or composition, etc.).

All of these variables in addition to current and effects on fume generation characteristics will be cussed in this section. It should be noted that the ef of many of these variables are interrelated.

Current Effects

Current is acknowledged to have a major effect on rate at which fumes are produced during welding. In present investigation, current effects were studied w representative covered, flux cored, and solid electro used for welding carbon steels. Trends similar to th observed should be obtained with other classificati of electrodes.

Covered Electrodes. Fume generation rate as a funct of current is shown in Fig. 2.9 for 4 mm (5/32 in.) E6 and E7018 electrodes; the data forming the basis for t figure are contained in Tables B26 and B27. In ea instance, these rates varied nonlinearly with curre Studies to fit the data to a power function indicated t the fume generation rate (FGR) relation to current v different for each type of electrode. For example, regression equations for two of the electrodes were

$$FGR_{E6010} = 0.000011\,I^{2.24} \text{ with } r^2 = 0.93$$
$$FGR_{E7018} = 0.00017\,I^{1.54} \text{ with } r^2 = 0.88$$

The regression lines in the figure are I^2 lines included comparison purposes.

The results obtained are similar to those obtained other investigators. Kobayashi, Maki, and Ohe not that fume generation rates for ilmenite, lime, and lim titania covered electrodes varied with current to powe of 1.17 to 1.74 (Ref. 2.5). Agreement with their resu was good considering differences between domestic a foreign electrodes and differences in fume samplin methods. In work done by Heile and Hill with E6010 ar E7018 electrodes, similar trends in fume generation rat were observed (Ref. 2.3).

Flux Cored Electrodes. The effects of welding curre on fume generation rates for a 2.31 mm (3/32 in.) diame ter E70T-1 electrode using CO_2 shielding are also show in Fig. 2.9; details on the welding conditions and the re sults of this investigation are provided in Table B28 Above 450 A, the fume generation rate increased almo linearly with current; below 450 A, the behavior of th fume generation rate with current was nonlinear. In par ticular, there was a well-defined and reproducible min imum at low current levels that may have been caused b

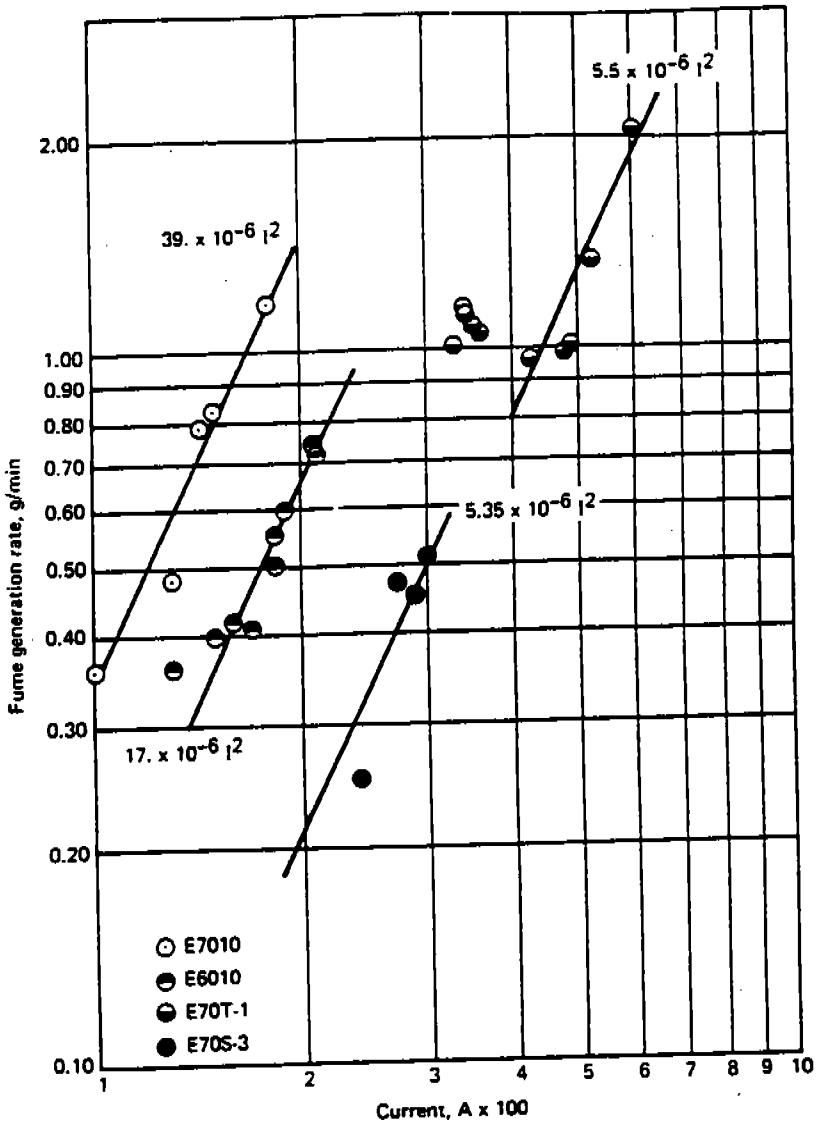

Fig. 2.9—Fume generation rates for selected covered, flux cored, and solid GMAW electrodes as a function of current

changes in arc length, changes in the sizes of globules being transferred across the arc, short-circuiting, etc. Attempts to fit a power function to the data obtained over the entire current range were unsuccessful because of the minimum in the curve at low currents. A reasonable fit with the I^2 line was obtained for data obtained at currents above 425 A. Thus, at currents between 425 and 600 A, there was a strong dependency of fume generation rate on current; at currents below 425 A, the fume generation rate was dependent upon variables other than current. It is emphasized that the indicated relationship between fume generation rate and current is valid only for the data obtained during this study.

A video camera was used to study the arc at currents between 350 and 500 A. At currents around 500 A, the arc was steady and appeared to have a length of about 3.2 mm (1/8 in.). At currents in the 350 A range, the arc was turbulent and its length varied rapidly; at times, the arc was buried. Apparently, the minimum in the curve and the increase in fume generation rate at lower currents were associated with this turbulence and the changes in type of metal transfer.

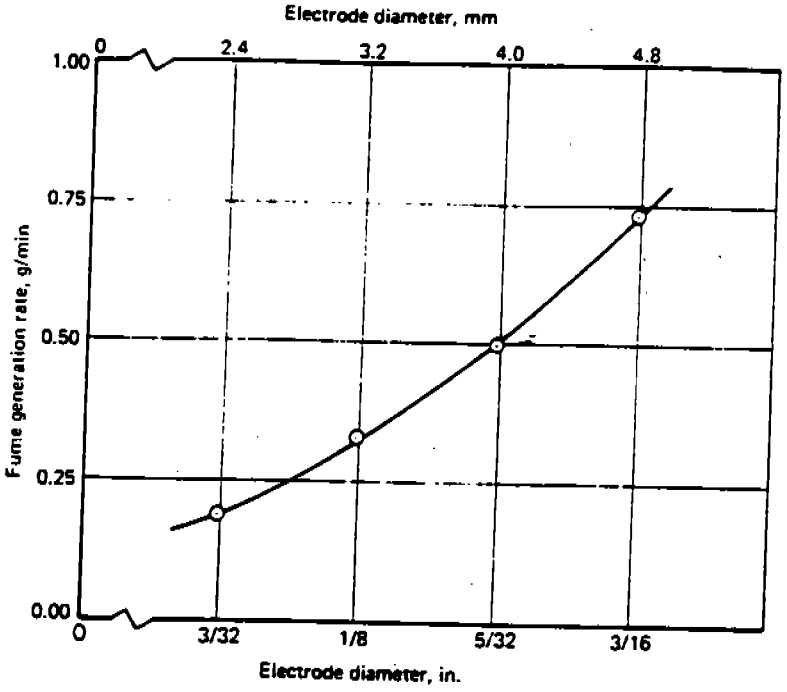

Fig. 2.11–Fume generation rates for E7018 covered electrodes with different diameters at constant current densities

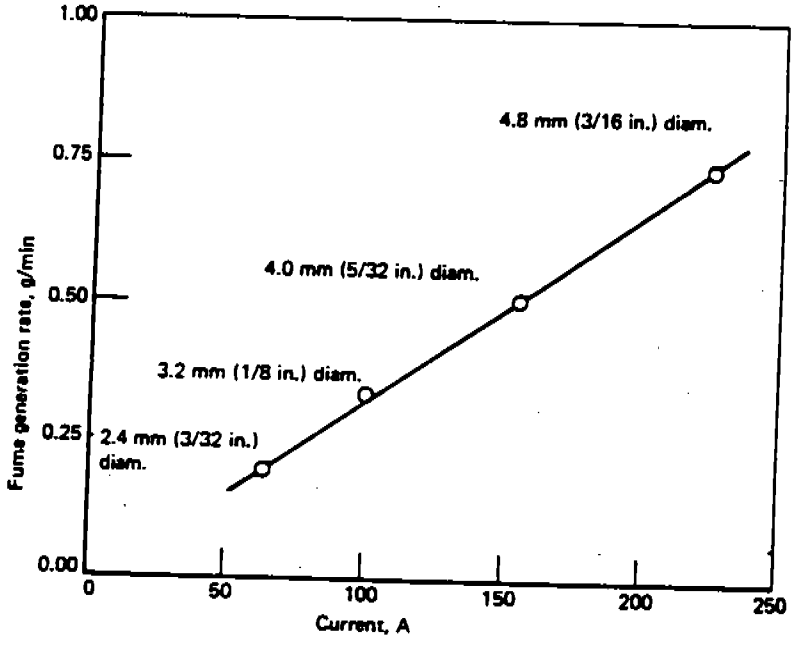

Fig. 2.12–Fume generation rates for E7018 covered electrodes with different diameters as a function of current

of fume generation rate on welding current. With approximately equal current densities in each electrode, the variation of fume generation rate with current was almost linear. Four E6010 and four E6013 electrodes were evaluated in a similar manner and similar results were obtained; these data are shown in Tables B33 and B34 respectively.

Arc Voltage—Arc Length Effects

Arc voltage and arc length are closely related welding parameters: for any given arc length, there is a corresponding value of voltage whose magnitude is determined by the characteristics of the electrode (resistivity, melting rate, etc.) and those of the welding process and power supply. During the investigation, the fume generation characteristics of selected electrodes as a function of voltage (measured across the electrodes) and arc length were studied. Because of the interrelationship between these variables, their effects on the rate at which fumes were produced were similar.

Previously discussed studies to evaluate the fume generation characteristics of a flux cored electrode, E70T-1 (41), were extended to include the effects of voltage. To investigate the dependency of fume generation rate on voltage, welding was done at high and low voltages near the low, middle, and high portions of the current range used for this electrode (330 to 600 amperes). For any given current, the "high" voltage was slightly below that at which the arc became unstable and difficult to control; the "low" voltage was just higher than that at which stubbing of the electrode occurred. The results obtained at the middle and high portions of the current range are shown in Fig. 2.13; tabular data are provided in Table B28. The results showed an increase in voltage was accompanied by an increase in the fume generation rate. Other investigators have reported similar results. In this instance, the effect of voltage was most pronounced at higher current levels.

The effects of arc voltage (or arc length) on the fume generation characteristics of an E6010 covered electrode were also examined. Welding was done at a nominal current of 150 amperes over a voltage range that extended from about 20 to 40 volts. Data on fume generation rates for this electrode are also plotted in Fig. 2.13; complete data on the results of this study are shown in Table B35. Although fumes were produced at different rates by the E6010 and E70T-1 electrodes, the trend toward increasing quantities of fumes at higher voltages was common to both.

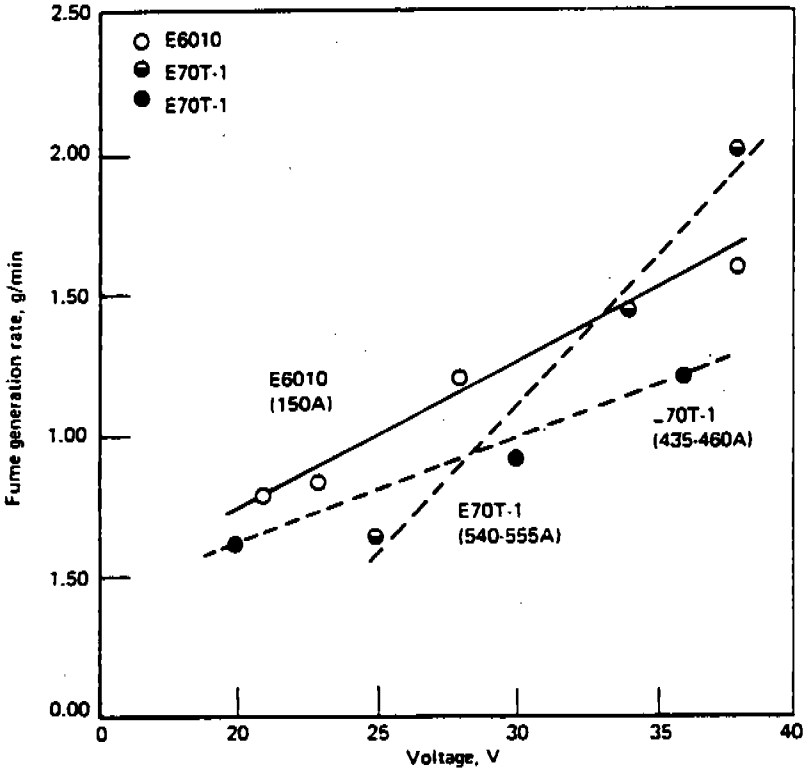

Fig. 2.13—Fume generation rates for an E6010 covered electrode and an E70T-1 flux cored electrode as a function of voltage at selected current levels

Arc length effects were studied with 4 mm (5/32 in.) diameter E6010, E6013, and E7018 electrodes. A video camera connected to a television unit and a video tape recorder were used to display and record arc length; current and voltage were monitored with a strip chart recorder.

Fume samples were obtained when welding was done with each electrode at selected arc lengths. To obtain the desired data, a welding arc was established and the power unit was adjusted to provide current at about 150 amperes. The arc was photographed with the video camera and the result was concurrently displayed on the television screen and stored on video tape for future use. Then, as the welder monitored the screen to maintain as constant an arc length as possible, a bead-on-plate weld was deposited and the fume sample was collected. The welding time was about 30 seconds. This process was repeated for each arc length.

The resulting data were analyzed to determine the effects of arc length on fume generation rates. To accomplish this objective, the data stored on the video tape were displayed on the television screen and the aver arc length over the welding interval was measured fr the plate surface to the electrode tip. It should be e phasized that this was a subjective measurement, cause the arc length varied during welding. Since curr varied also, the fume generation rates were normalizec a current of 150 amperes to provide a common basis comparison. The results of this investigation are su marized in Fig. 2.14; supporting data are provided Table B36.

Fume generation rates increased with increasing length for all of the electrodes included in this inves gation. The slope of the lines relating these variab indicated that arc length had slightly more effect on t rates at which fumes were produced by the E6010 a E6013 electrodes than on the rate at which fumes we produced by the E7018 electrode. The results of th investigation (i.e., the increase in fume generation ra with increasing arc length) are in general agreement wi those observed by Kobayashi, Maki, and Ohe (Ref. 2.5

In a related experiment, the welding current wa

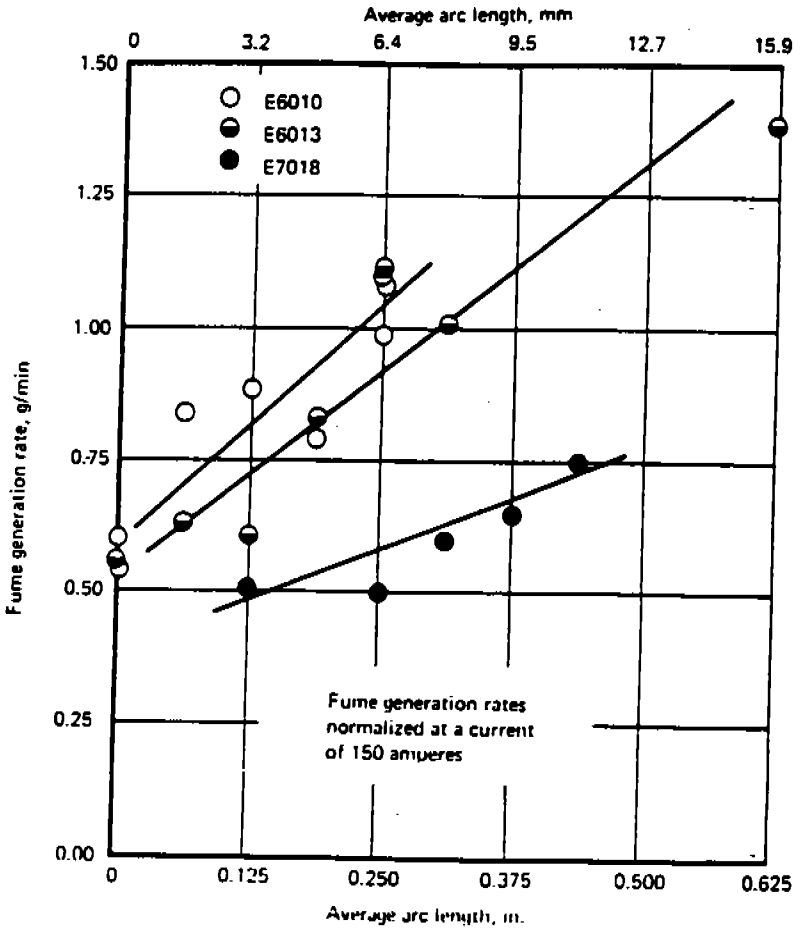

Fig. 2.14—Fume generation rates for selected covered electrodes as a function of arc length

initially established at 150 amperes for an arc length that would normally be used during welding. The current was not adjusted thereafter, but was allowed to vary with different arc lengths. For example, when the arc length was increased, voltage increased and current decreased. Fume samples were collected at selected arc lengths for E6010, E6013, and E7018 electrodes during welding intervals of about 30 seconds. Arc length data were recorded on video tape and analyzed later in the manner described previously. All fume generation rates were normalized to a common current of 150 amperes for comparison purposes. The results were similar to those discussed previously; that is, fume generation rates increased with increasing arc length (see Table B36).

Contact-Tube-To-Work Distance Effects

The distance between the end of the contact tube and the surface of the base plate is a variable that affects the melting and metal deposition rates in flux cored arc welding and gas metal arc welding. Since fume generation rates are closely associated with melting rates, the effects of contact tube-to-work distance were included in this investigation.

The fume generation characteristics of an E70T-1 flux cored electrode as a function of contact tube-to-work distance were determined. Welding was done at two current levels, nominally 450 and 520 amperes, and the contact tube-to-work distance was varied from 19 mm (0.75 in.) to 38 mm (1.50 in.). As the contact tube-to-work distance was varied, the wire feed rate was adjusted to maintain the selected current level. The power supply voltage remained constant during these studies, even though it would be normally increased or decreased with changes in contact tube-to-work distance so that arc length could be controlled.

The following observations are based on an examination of the data presented in Tables B42 and B43 and in Fig. 2.15:

(1) At each current level, there was a gradual increase in metal deposition rate with increasing contact tube-to-work distance (Tables B42 and B43). When the contact tube-to-work distance increases, the wire feed speed must be increased to maintain a constant current level. The increased melting rate is accompanied by a higher deposition rate.

(2) For each current level, the fume generation rate remained essentially constant for each contact tube-to-work distance.

(3) The ratio of weight of fumes to weight of deposited metal decreased gradually with increasing contact tube-to-work distance.

(4) The effect of current on fume generation rate is evident in Fig. 2.15. At 450 amperes, the fume generation rate was about 1 g/min; at 520 amperes, the rate was about 1.3 g/min.

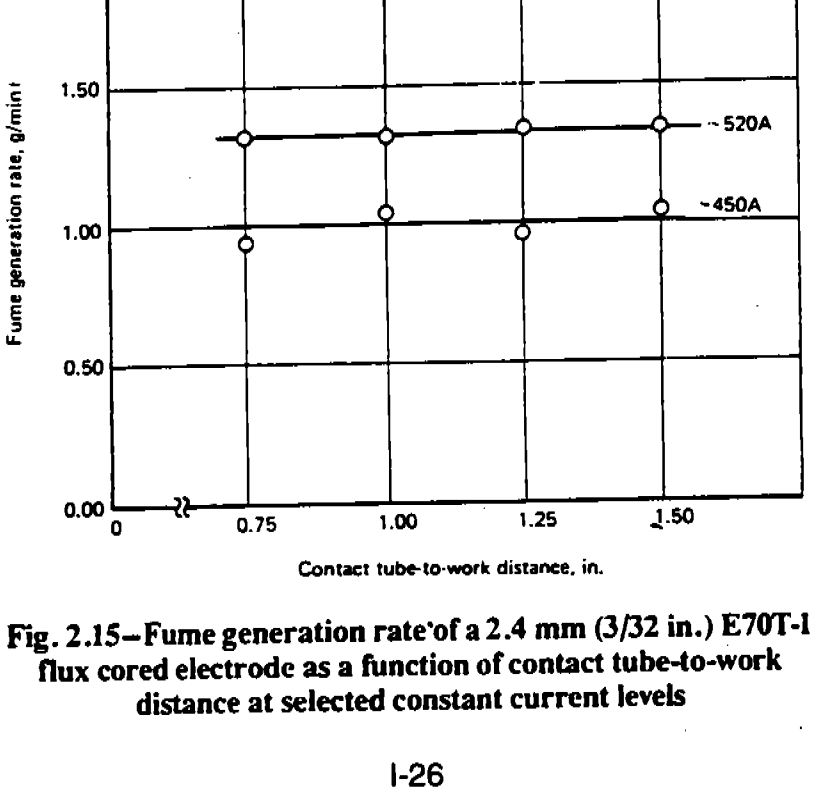

Fig. 2.15—Fume generation rate of a 2.4 mm (3/32 in.) E70T-1 flux cored electrode as a function of contact tube-to-work distance at selected constant current levels

Shielding Gas Effects

The shielding gas is a variable associated with the flux cored and gas metal arc welding processes, and it affects the rate at which fumes are produced during welding and the composition of the fumes. The type of shielding gas also affects the kind of gases to be found in the welding area.

The effects of shielding gases on fume generation rates have already been discussed in the review of the baseline data for flux cored and gas metal arc welding electrodes. These rates were highest when CO_2 or gas mixtures containing CO_2 were used to shield the welding arc.

Since the oxidation potential of the shielding gas affects the rate at which specific elements oxidize as they are vaporized from the tip of the electrode, studies were conducted to determine the effects of shielding gas type on the composition of the fumes produced by E70S-3 gas metal arc electrodes used for welding carbon steels. Each of the three E70S-3 electrodes included in this investigation was evaluated using welding conditions to produce the following transfer modes: (a) spray transfer with Ar-2 O_2 shielding, (b) spray transfer with Ar-9 CO_2 shielding, and (c) globular transfer with CO_2 shielding. The fume samples were collected on cellulose membrane filters and analyzed by atomic absorption procedures. The resulting data plus the calculated weight percentages of e are shown in Table 2.14 and the apparent trend cussed below:

(1) Iron (iron oxide) contents were highe welding was done in the spray transfer mode wi Ar-2 O_2 or Ar-9 CO_2 shielding and lowest when was done in the globular transfer mode with CO_2 s These results are in agreement with those of H Hill (Ref. 2.3).

(2) Manganese (manganese oxide) conten highest when welding was done in either the spra fer mode with Ar-9 CO_2 shielding or in the globul fer mode with CO_2 shielding; this element (or ele oxide) content was lowest when welding was done spray transfer mode with Ar-2 O_2 shielding. He oxidation potential of the shielding gas had a slight on the contents of manganese (manganese oxide) fumes.

(3) Silicon (silicon dioxide) contents were h when welding was done in the globular transfer with an oxidizing gas, CO_2. These results are also in ment with those of Heile and Hill (Ref. 2.3). There w apparent explanation for the low silicon content i fumes produced by the E70S-3(54) and E70S- electrodes.

(4) Copper contents in the fumes appeared to be

Table 2.14
Effects of shielding gas on fume composition

Electrode[1]		Shielding gas	Fume sample weight, g	Composition, weight %						
				Fe	(Fe_2O_3)	Mn	(MnO_2)	Si	(SiO_2)	Cu
E70S-3	(54)	Ar-2 O_2[2]	0.23	61.7	(88.2)	4.6	(7.3)	1.0	(1.6)	0.0
E70S-3	(54)	Ar-9 CO_2	0.55	62.5	(89.4)	6.1	(9.6)	0.5	(0.8)	0.0
E70S-3	(54)	CO_2	0.42	56.3	(80.5)	6.3	(10.0)	2.3	(3.6)	0.1
E70S-3	(57)	Ar-2 O_2[2]	0.32	62.7	(89.7)	4.4	(7.0)	1.1	(1.7)	0.8
E70S-3	(57)	Ar-9 CO_2	0.44	62.2	(88.9)	6.5	(10.3)	0.4	(0.6)	0.70
E70S-3	(57)	CO_2	0.33	55.4	(79.2)	6.8	(10.7)	1.5	(2.4)	1.20
E70S-3	(58)	Ar-2 O_2[2]	0.41	62.1	(88.8)	5.6	(8.8)	1.1	(1.7)	1.29
E70S-3	(58)	Ar-9 CO_2	0.54	62.0	(88.7)	4.6	(7.3)	1.5	(2.4)	0.99
E70S-3	(58)	CO_2	0.40	52.5	(75.1)	5.5	(8.7)	2.5	(3.9)	1.00

1. Welding Conditions:

For spray transfer welding with A-2 O_2 shielding
Electrode No. 54: 35 V; 260-280 A
Electrode No. 57: 35 V; 270-280 A
Electrode No. 58: 34.5 V; 290-300 A

For globular transfer welding with CO_2 shielding
Electrode No. 54: 36 V; 330-340 A
Electrode No. 57: 35 V; 320 A
Electrode No. 58: 32 V; 330 A

For spray transfer welding with A-9 CO_2 shielding
Electrode No. 54: 34.5 V; 210-220 A
Electrode No. 57: 35 V; 205-215 A
Electrode No. 58: 35 V; 215-225 A

2. Average of three analyses.

nental vaporization, condensation, nd oxidation enhanced vaporiza-on.

Additional support for the vaporiza- condensation-oxidation mech- (V-C-O) is also found in the data sented in Table 5 covering GMA ding of aluminum alloys. Because nert shielding, the mechanism for me generation is simply vaporiza- and condensation of elemental aterial. Aluminum 5356 generates re fume because of the additional ntribution of Mg. Note that the Mg ntent of the 5356 fume (Mg/Al = is enriched over that of the wire g Al = 1/16). This results from the that Mg has a considerably higher r pressure in the range of 2000- K and its activity coefficient in ten aluminum is 0.5. In making a mparison of the above data, note that finer wires produce less fume at mparable currents and arc lengths.

The above discussion applies qually well to fume generation in CA and SMA welding. In these rocesses, the fume results from the -C of elemental and lower oxide ies, and the V-C of oxide and ce flux species. As might be ex- ec, the composition of the fume is ngly dependent on flux com- sition since significant quantities of w melting point flux components are ntained in the fume.

V-C-O mechanism advanced to is point is essentially a simple one aving to do with the vapor pres- res and latent heats of vaporiza- n of the constituents present in the m of the consumables and with the izing potential of the shielding if one is used. To first order, these factors determine the amount of a particular constituent appearing in the fume. Obviously, rate controlling steps involving diffusion of the various reactants and products will affect the FFR and composition of the fume as well. A more complete model re- uires consideration of these rate ntrolling factors and the dynamic ture of the metal transfer process luding such factors as residence e of the molten droplet at a par- ticular temperature, degree of sur- face exposed for participation in the aporization process, and the ef- iciency of energy absorption by the surface. These contributions will be considered in turn.

For instance, as observed pre- iously, the higher FFR for CO_2 com- ared with argon-based shield gases believed to be caused by the ater contribution of oxide species ing from the increased oxidizing tial of the CO_2 shielding gas. Additionally, the inability to achieve rapid drop detachment when using CO_2 may further augment the oxide enhancement. With CO_2, the molten drop of metal spends a significant fraction of the total transfer time attached to and wandering about the wire tip. This instability can produce turbulent effects resulting in contamination which, coupled with the long detachment times, can further enhance the vaporization due to oxide species over and above the natural oxidizing potential of the shield gas. The rapid drop detachment obtained in the spray mode using argon-based shield gases does not permit this condition to occur. This fact and the lower oxidizing potential of the argon-based shield gases are sufficient to account for the differences in the mean FFRs.

The problem of instabilities and turbulent effects in FCA and SMA similar to those which exist with CO_2 in GMA is compounded by the presence of extremely volatile flux components. Hence, the FFRs for these processes are substantially higher than for GMA.

In an effort to gain more precise information about how these dynamic effects affect the V-C-O process, it was felt necessary to determine where the vaporization is occurring. Two experiments were performed. The first was to examine fume formation using the GTA process. As stated earlier, no measurable amounts of fume were obtained for all currents between 50 and 450 A using argon shielding. The initial implication is that the molten metal in the weld puddle does not substantially contribute to the fume. The weld puddle is cool relative to the arc. While vaporization is occurring, the partial pressures and hence the contribution to the total fume level is substantially reduced. Adding oxygen to the shielding gas did produce small amounts of fume, supporting the hypothesis of enhanced vaporization due to oxide species.

The second experiment involved the welding of Mg bearing Al plate using the GMA process. Two wire types were employed, type 5356 containing Mg and type 1100 containing no Mg. Referring back to Table 5, Mg was found in the fume when the 5356 wires were used, but no Mg was found when the 1100 wires were used even though Mg was present in the plate in both cases. The conclusion to be drawn, therefore, is that the vaporization of elemental and oxide species is occuring at the wire tip and in the welding arc, but not in the weld puddle to any comparable degree. This is totally consistent with known temperature distributions of the arc.

A feeling for just how the fume evolution is affected by the welding conditions and shielding gas can now be gained by a more critical examination of the behavior of the fume data in CO_2 and argon-based shielding gases exhibited in Figs. 10 and 12.

The CO_2 results are presented in Fig. 12. Two features are apparent. For a given voltage, there is a monotonic increase of fume with current;

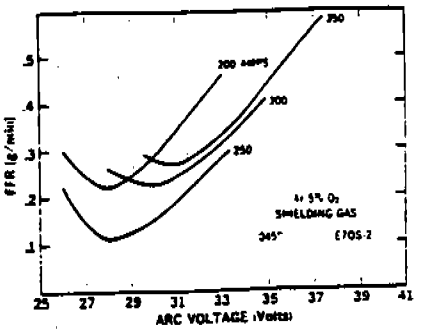

Fig. 10 — The effect of voltage and current on the FFR in GMA welding with argon-5% O_2 shielding gas

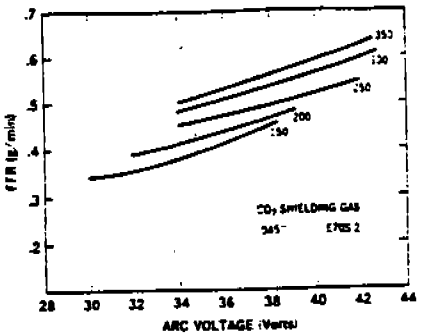

Fig. 12 — The effect of voltage and current on the FFR in GMA welding with CO_2 shielding gas

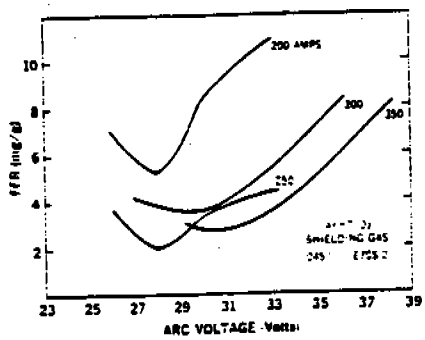

Fig. 11 — Data of Fig. 10 replotted in mg/g

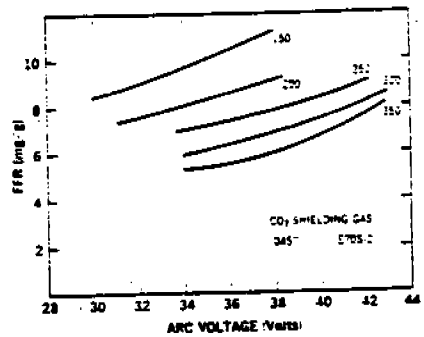

Fig. 13 — Data of Fig. 12 replotted in mg/g

Table 2.15
Summary of data on effects of iron powder on fume generation characteristics of high titania and low hydrogen covered electrodes

Electrode	Covering	Current, A (nominal)	Fume generation rate: Measured, g/min	Fume generation rate: Normalized[1], g/min	Weight of fume/wgt. of deposited metal, g/kg[2]
E6013	High titania	165	0.73	0.81	29.86
E7014	High titania	175	0.72	0.75	23.72
E7024	High titania	210	0.68	0.47	12.13
E7016	Low hydrogen	170	0.50	0.51	20.84
E7018	Low hydrogen	175	0.51	0.50	18.39
E7024	Low hydrogen	230	1.03	0.58	21.27

1. Fume generation rates normalized to 175 A.
2. g/kg ÷ 10 = weight of fume expressed as a percentage of deposit weight.

arc length differences; however, in both instances, the rates decreased with increasing electrode angle by about the same amount.

Welding with covered electrodes is done mostly at large (>60 degree) angles between the electrode and workpiece, so problems with fumes are minimized. It is important to be aware that increased amounts of fumes can be expected when welding is done under confined conditions where the electrode angle might be restricted to small values.

Base Plate Effects. Fume generation characteristics for the covered, flux cored, and solid electrodes investigated during this program were determined with base plates whose composition was similar to that of the core wire or sheath. That is, E6010 and E70T-1 electrodes were evaluated with carbon steel plate, E410-15 electrodes with 400-series stainless steel plate, and so on. Since the base plate has relatively little effect on the production of fumes, the need to match the base plate to the electrode was questioned, particularly with respect to the evaluation of stainless steel electrodes. To resolve this question, fume samples for gravimetric and chemical analyses were collected during the deposition of stainless steel bead-on-plate welds on carbon steel and stainless steel plates. Welding was done with a 4 mm (5/32 in.) diameter E316-16 covered electrode at baseline conditions. The experimental results are discussed below with the aid of Tables 2.16 and 2.17.

(1) As indicated in Table 2.16, fume generation rates and ratios of weight of fumes to weight of deposited metal were unaffected by the type of base metal used during welding. Thus, either carbon steel or stainless steel could be used with equal facility to evaluate stainless steel electrodes in terms of their fume generation rates. Caution in extrapolating these results to other electrodes is advised.

(2) The composition of the fumes did reflect the composition of the base metal upon which the welds were deposited as well as that of the electrode. When the E316-16 electrode was evaluated on stainless steel, the fumes contained higher contents of manganese, nickel, and chromium than when this electrode was used on carbon steel (Table 2.17). The effects of the electrode itself on fume composition can be estimated by examining the composition of the fumes produced when welds were deposited on carbon steel. The difference between the contents of manganese, nickel, and chromium in the sample and in the sample collected when welding was done on stainless steel represents the effects of the stainless steel base plate on fume composition. It was concluded that electrode and base plate should be matched if fume compositions are to be determined.

Diameter Effects with Flux Cored Electrodes. The fume generation characteristics of a 1.6 mm (1/16 in.) diameter E70T-1 electrode were compared to those of a 2.4 mm (3/32 in.) diameter electrode made by the same manufacturer. Welding was done at current levels appropriate for the respective electrodes and CO_2 was used for shielding (Table B41). Data on the "as measured" and "normalized" fume generation rates are presented below.

Electrode	Electrode diam., in. (mm)	Welding current, A	Fume generation rate, g/min. Measured	Normalized
E70T-1 (40)	3/32 (2.4)	480	1.36	1.36
E70T-1 (45)	1/16 (1.6)	330	1.01	2.14

*Fume generation rates normalized to a current of 480 A.

The measured fume generation rate for the small diameter electrode was less than that associated with the larger diameter electrode. However, when the effect of current on this characteristic was taken into account by normalizing the fume generation rates to a common current (480 A),

Table 2.16
Effect of base plate on average fume generation characteristics of 4 mm (5/32 in.) diameter E316-16 covered electrode

Characteristic	Base plate	
	Carbon steel	Stainless steel
Fume generation rate, g/min.	0.24	0.24
Weight of fume/weight of deposited metal, g/kg*	9.96	9.87

*g/kg ÷ 10 = %

Table 2.17
Composition of carbon steel and stainless steel base plate and composition of fume samples

Type	Composition, weight %				
	Fe	Mn	Si	Cr	Ni
		Base plate			
Carbon steel	Bal.	0.68	<0.01	---	---
Stainless steel (Type 304)	Bal.	1.70	0.41	19.43	8.31
		Fumes			
Electrode/base plate					
E316-16/carbon steel	7.85	7.53	<0.01	4.85	1.03
E316-16/stainless steel	8.16	7.80	<0.01	5.60	1.21

in this case), more fumes were produced by the small diameter electrode than by the large diameter one. Fume generation rates are dependent upon the rate at which the electrode is consumed. If two electrodes with different diameters are used at the same current level, the melting rate for the smaller of the two electrodes will be greater in the small diameter electrode. The effect of increased I^2R heating in the smaller electrode probably also contributed to increased melting rate. The effect of I^2R heating on deposition rates was studied by Wilson, Claussen, and Jackson (Ref. 2.22).

Section IID. Analytical Studies

Various analytical methods were used to determine the presence of selected constituents in the fumes produced during arc welding operations. Some of the characteristics of these methods are discussed as follows:

(1) Optical emission spectroscopy yields a wealth of analytical data because 70 or more elements can be detected simultaneously and their content can be estimated on a semiquantitative basis. It is best suited for accurately determining the presence of elements that are present in small amounts. This method is most valuable when the elements in question are present in concentrations of 1 percent or less. If elements are present in large amounts, concentrations are often expressed in percentage ranges, and other techniques (e.g., atomic absorption) must be used to obtain greater accuracy. In the case of welding fumes, optical emission spectroscopy can provide an overview of most of the elements present in the fume sample, regardless of their origin; i.e., from the core wire or sheath, electrode covering or flux, or base plate. This method was used during this program in studies to characterize the nature of welding fumes, and the results have been presented in a previous section of this report. It was not used more extensively because capital equipment costs for optical emission spectroscopy are high, and such equipment is not as readily available in industry as that used with other analytical methods.

(2) Atomic absorption analysis is also capable of determining the presence of about 70 elements, but the concentration of each element must be detected individually. Analytical costs per individual element are not high, but they can be appreciable if the sample contains

Table 2.18

Concentrations of selected constituents in the fumes produced by arc welding electrodes (Analyses by atomic absorption technique)

Electrode	Code	Fume sample weight, g	Concentration, weight percent										
			Fe	Mn	Si	Ni	Cu	Cr	Mo	Al	Mg	F	Other
Covered electrodes													
E6010 (IP)	1	0.49	47.5	3.0	5.7	---	---	---	---	---	---	---	---
E6010 (IP)	2	0.35	49.6	3.4	6.5	---	---	---	---	---	---	---	---
E6010 (IP)	11	0.56	41.6	3.4	3.7	---	---	---	---	---	---	---	---
E6013	4	0.16	61.4	5.1	12.2	---	---	---	---	---	---	---	---
E6013	6	0.08	45.0	5.5	15.0	---	---	---	---	---	---	---	---
E6013	3	0.27	62.2	4.1	11.2	---	---	---	---	---	---	---	---
E7018	5	0.26	26.1	4.5	<0.2	---	---	---	---	---	---	13.1[1]	---
E7018	12	0.30	28.7	4.1	<0.2	---	---	---	---	---	---	14.0[1]	---
E7018	10	0.26	24.2	3.6	<0.2	---	---	---	---	---	---	15.0[1]	---
E7024	7	0.30	30.2	5.3	18.3	---	---	---	---	---	---	---	---
E7024	8	0.31	29.5	5.6	19.7	---	---	---	---	---	---	---	---
E7024[3]	9	0.31	33.3	7.8	13.2	---	---	---	---	---	---	---	---
E6013[3]	34	0.25	41.4	---	---	---	---	---	---	---	---	---	---
E7014[3]	30	0.23	39.0	---	---	---	---	---	---	---	---	---	---
E7024[3]	35	0.27	27.8	---	---	---	---	---	---	---	---	---	---
E7016[3]	29	0.21	32.7	---	---	---	---	---	---	---	---	15.2[1]	---
E7018[3]	36	0.22	27.8	---	---	---	---	---	---	---	---	12.7[1]	---
E7028[3]	32	0.42	38.1	---	---	---	---	---	---	---	---	11.6[1]	---
E8018 C3	14	0.12	45.2	7.2	---	0.3	---	0.1	<0.1	---	---	35.8[1]	---
E9018 B3	17	0.16	21.9	5.9	---	0.1	---	1.6	<0.1	---	---	28.1[1]	---
E316-15	22	0.15	8.4	7.7	---	1.1	---	5.8	<0.1	---	---	---	---
E316-16	20	0.17	10.0	8.8	---	1.5	---	6.5	<0.1	---	---	17.2[1]	---
E410-16	21	0.11	33.1	5.2	---	<0.1	---	---	---	---	---	---	---
ENi-CI	28	0.35	2.5	0.3	---	6.9	<0.1	---	---	---	---	10.0[1]	---
EniCu-2	33	0.31	0.1	2.1	---	4.2	6.2	---	---	---	---	---	---
Inconel 625[7]	62	0.25	0.6	---	---	4.6	0.7	5.9	2.1	---	---	---	---
Haynes C-276[8]	69	0.35	0.3	0.3	---	1.1	---	2.5	0.6	1.0	1.4	5.9[1]	0.1Co-0.1W-2.4Ca-4.9Ti
Haynes 25[8]	70	0.25	---	4.6	---	1.8	---	6.9	---	1.1	0.1	7.7[1]	7.7Co-1.3W-2.4Ca-5.3Ti
Flux cored electrodes													
E70T-1	40	0.53	34.4	7.1	3.7	---	---	---	---	---	---	0.06[2]	---
E70T-1	41	0.60	25.2	13.5	7.5	---	---	---	---	---	---	0.06[2]	---
E70T-1	42	0.91	33.6	9.7	2.2	---	---	---	---	---	---	8.68[2]	---
E70T-1	45	0.51	46.1	12.4	5.2	---	---	---	---	---	---	0.17[2]	---
E70T-1	46	0.63	41.2	6.2	5.4	---	---	---	---	---	---	0.31[2]	---
E70T-1	47	0.89	37.9	6.4	1.0	---	---	---	---	---	---	6.33[2]	---

Table 2.18 (cont.)
Concentrations of selected constituents in the fumes produced by arc welding electrodes
(Analyses by atomic absorption technique)

Electrode	Code	Fume sample weight, g	Concentration, weight percent										
			Fe	Mn	Si	Ni	Cu	Cr	Mo	Al	Mg	F	Other
Flux cored electrodes (cont.)													
E70T-4	48	1.45	11.5	3.3	<0.05	<0.01	---	---	---	---	---	2.73[2]	---
E70T-4	49	0.98	16.2	4.6	<0.05	<0.01	---	---	---	---	---	0.84[2]	---
E70T-4	56	0.95	15.1	1.0	<0.05	<0.01	---	---	---	---	---	1.84[2]	---
E70T-5	44	0.90	26.7	11.3	<0.05	---	---	---	---	---	---	2.63[2]	---
E70T-5	50	0.61	29.2	10.9	0.09	---	---	---	---	---	---	4.80[2]	---
316L	55	0.65	12.4	7.3	0.05	1.06	---	12.5	0.34	---	---	11.5[2]	---
Gas metal arc electrodes													
E70S-3[4]	54	---	63.7	5.3	0.05	---	0.11	---	---	---	---	---	---
E70S-3[4]	54	0.54	61.0	3.6	1.1	---	0.07	---	---	---	---	---	---
E70S-3[4]	54	0.55	60.4	5.0	1.9	---	0.09	---	---	---	---	---	---
E70S-3[5]	54	0.55	62.5	6.1	0.5	---	0.09	---	---	---	---	---	---
E70S-3[6]	54	0.42	56.3	6.3	2.3	---	0.14	---	---	---	---	---	---
E70S-3[4]	57	0.23	65.7	3.8	0.8	---	0.60	---	---	---	---	---	---
E70S-3[4]	57	0.29	61.2	3.5	0.6	---	1.20	---	---	---	---	---	---
E70S-3[5]	57	0.44	61.1	5.8	1.8	---	0.74	---	---	---	---	---	---
E70S-3[6]	57	0.44	62.2	6.5	0.4	---	0.70	---	---	---	---	---	---
E70S-3[4]	58	0.33	52.2	6.8	1.5	---	1.00	---	---	---	---	---	---
E70S-3[4]	58	0.23	62.5	8.5	0.5	---	1.00	---	---	---	---	---	---
E70S-3[4]	58	0.49	60.1	3.4	1.0	---	1.80	---	---	---	---	---	---
E70S-3[5]	58	0.50	63.6	4.8	1.7	---	1.08	---	---	---	---	---	---
E70S-3[6]	58	0.54	62.0	4.6	1.5	---	0.99	---	---	---	---	---	---
E70S-5	59	0.40	55.4	5.5	2.5	---	1.20	---	---	---	---	---	---
ER5356	60	0.11	61.7	5.8	0.93	---	1.75	---	---	---	---	---	---
ER4043	61	1.06	---	---	---	---	---	---	---	---	---	---	---
ERNiCu-7	64	0.10	---	---	1.7	---	---	---	---	38.0	3.8	---	---
Inconel 625[7]	53	0.13	5.0	1.1	0.65	22.1	44.4	<0.01	---	46.2	---	---	---
Haynes C-276[8]	68	0.07	1.9	---	---	27.2	0.69	15.4	2.1	---	---	---	---
Haynes 25[8]	71	0.25	3.6	1.0	---	32.5	---	8.2	16.2	0.4	---	---	3.2W
ERCuA1-A2	75	0.07	---	15.4	---	7.1	---	14.9	---	0.3	---	---	1.0W-33.5 Co
ERCu	76	0.38	---	---	---	---	70.5	---	---	3.4	---	---	---
		0.31	---	---	---	---	66.0	---	---	---	---	---	---

Notes.

1. Total fluorides
2. Water-soluble fluorides
3. These electrodes were used to study the effect of iron powder additions on fume generation rates. Thus, only iron was determined in the analysis
4. Shielding gas: A-2 O_2
5. Shielding gas: A-9 CO_2
6. Shielding gas: CO_2
7. TM, International Nickel Company

E70T-1 electrodes, each of which was made by a different producer. As discussed by Smith (Ref. 2.17), the fluxes of some E70T-1 electrodes contain appreciable amounts of calcium fluoride to form a basic type slag.

Fume Characterization

A study was undertaken to characterize the fumes associated with various welding operations in terms of composition, the presence or absence of crystalline phases, and particle morphology. The fumes produced by electrodes used for shielded metal arc welding (E7024 and E410-16) and flux cored arc welding (E70T-1, E70T-4, and E70T-5) were analyzed for elemental composition by optical emission spectroscopy (OES) and for crystalline phases by x-ray diffraction (XRD). Scanning electron microscopy (SEM) was used to study particle morphology. Semiquantitative results of the OES analysis of the fume samples are shown in Table 2.19.

Optical emission spectroscopy is capable of detecting the presence of 70 or more elements on a semiquantitative basis. Thus, totals of data for the individual fume samples listed in Table 2.19 may approach 100 percent, if the elemental fume constituents are converted to their common oxide forms. In some instances, elemental concentrations are expressed in percentage ranges, if the element is present in large amounts. Another analytical method (atomic absorption, wet chemistry, etc.) must be used to achieve more accuracy. Only one crystalline phase, iron oxide (Fe_3O_4, or magnetite), was detected by XRD in the fumes produced by the covered electrodes; manganese was probably present in this phase also since it can replace iron in the crystal lattice. Crystalline phases containing silicon were not detected. However, since silicon was detected in the fumes produced by the E7024 and E410-16 electrodes, it was probably present as a glassy SiO_2 phase along with potassium and sodium. The x-ray diffraction pattern from the fumes produced by the E410-16 electrode had an extra diffraction line whose presence was attributed to a chromium compound.

In the fumes produced by the flux cored electrodes,

Table 2.19
Elemental composition of fumes produced by various electrodes[1] as determined by optical emission spectroscopy

	Composition, weight percent					
Element	E7024 (7)	E7024 (8)	E410-16 (21)	E70T-1 (42)	E70T-4 (49)	E70T-5 (50)
Fe	20.0-30.0	20.0-30.0	10.0-20.0	30.0-40.0	15.0-25.0	30.0-40.0
Si	10.0-20.0	5.0-10.0	2.0-3.0	2.0-3.0	0.1	2.0-3.0
K	8.0-12.0	8.0-12.0	10.0-20.0	1.0	2.0	4.0-6.0
Na	3.0- 6.0	3.0-6.0	4.0-8.0	4.0-6.0	<0.1	1.0
Mn	2.0-4.0	2.0-4.0	1.0-2.0	4.0-6.0	2.0-3.0	4.0-6.0
Ca	0.1	0.5	2.0-4.0	0.1	15.0-25.0	8.0-12.0
Zn	<0.1	<0.1	0.1	<0.1	<0.1	<0.1
Ti	0.5	0.3	0.4	0.5	<0.01	0.2
Pb	0.2	0.2	0.01	<0.01	0.2	0.02
Al	0.1	0.05	0.5	0.4	7.0-10.0	1.0-2.0
Sn	0.1	0.1	0.2	0.01	<0.01	<0.01
Cr	0.01	0.01	5.0-10.0	0.01	<0.01	<0.01
B	0.01	0.5	0.2	<0.01	<0.01	<0.01
Mg	0.01	0.03	0.3	0.02	7.0-10.0	0.2
Mo	0.005	0.005	0.05	<0.01	<0.01	<0.01
V	0.01	<0.01	0.03	<0.01	<0.01	0.02
Cu	0.05	0.1	0.1	0.1	0.01	0.02
Ni	0.005	0.01	0.05	0.01	<0.01	<0.01
Co	---	<0.01	0.01	<0.01	<0.01	<0.01
Ba	---	<0.01	0.03	0.01	0.05	0.03
Zr	---	---	---	0.1	<0.01	0.03
Sr	---	---	---	<0.01	<0.01	<0.01

1. The number in parentheses following the electrode designation is the code number identifying the specific electrode.

APPENDIX J

REFERENCE 48

(Heile, 1975)

WELDING RESEARCH

SUPPLEMENT TO THE WELDING JOURNAL, JULY 1975

Sponsored by the American Welding Society and the Welding Research Council

Particulate Fume Generation Arc Welding Processes

Mechanisms of particulate emission along with emission rates and composition have been determined for a variety of arc welding processes

BY R. F. HEILE AND D. C. HILL

ABSTRACT. A technical method has been developed that allows a determination of the fume formation rate and fume composition in arc welding processes. This method has been used to characterize particulate emissions in a number of processes: shielded metal arc (SMA), gas metal arc (GMA), flux cored arc (FCA), and gas tungsten arc (GTA) welding, and has permitted a ranking of these processes according to their relative "cleanliness." Of the continuous electrode processes studied, GMA welding with argon-based shielding gas produced the least fumes, while self-shielding FCA welding produced the most. The data indicate that the mechanism of fume formation is one of elemental vaporization-condensation and oxidation enhanced vaporization-condensation of the consumable constituents. A model relating this mechanism to process and process variables is advanced which would allow fume formation rates and composition to be predicted semi-quantitatively given a knowledge of the consumable composition, the volatility of the constituents, the transfer mode, the arc temperature and stability as determined by the welding parameters and shield gas, and the oxidizing potential of the shield gas. Based on the results, methods of fume control are indicated which can serve as a supplement to ventilation.

R. F. HEILE is Senior Research Physicist and D. C. HILL is Group Leader, Linde Research Department, Linde Division, Union Carbide Corporation, Tarrytown, New York 10591.

Introduction

Although numerous studies of the generation of smoke and fume in arc welding have been made (Ref. 1), the mechanism and character of the fume formation have not been extensively investigated or reported. It is now recognized that variations in sampling techniques, electrode compositions, and welding parameters all have a major impact on the results of fume experiments. As a result, care must be exercised in interpreting the existing literature. Recently, a proposed technique for measurement of fume generation in arc welding has been published (Ref. 2). Unfortunately, little statistical evidence for the accuracy and reproducibility of this technique was advanced.

The purposes of this study are to provide fume generation comparisons among different arc welding processes, to understand the mechanism of fume formation, and to supply the information necessary for choice of a welding process when ventilation considerations are important.

Method for Particulate Sampling

General

A critical aspect of particulate sampling is the technique itself. Various sampling techniques have been employed by other investigators (Ref. 1). Many of these techniques collect all of the evolved fume. In so doing, oftentimes unrealistic conditions are imposed on the particular welding process. We chose, instead, to use a modified stack sampling technique which would minimally disturb the welding process and at the same time allow a carefully controlled sample to be taken at a predetermined rate. This section briefly describes the technique and discusses the accuracy and reproducibility of the results.

Experimental Technique

A schematic of the stack sampling system employed in this work is shown in Fig. 1. A duct was placed coaxially over a stationary welding torch. Welds were made on a rotating workpiece. The gas flow rate of the duct was set to allow collection of most all the fume, yet not so fast as to disturb the shielding gas. The duct velocity was measured using an inclined manometer. A probe, connected to a filter and a sampling pump, was inserted in the duct. The velocity in the probe was adjusted to match the duct velocity. By maintaining isokinetic sampling conditions, it is possible to relate the size of the sample collected to the total fume evolution without having to collect all of the fume.

This technique is applicable over a range of duct velocities, i.e., sampling rates for a constant sampling time. This is especially important in sampling emissions where the saturation time of the filter is short. Without control over the sampling rate in such situations, the results would be subject to transient effects related to short sampling times. This technique eliminates those problems.

The basic procedure followed for taking a sample was to establish isokinetic sampling conditions and then, before actually beginning the sample, to choose the welding parameters. Sampling was begun after the arc was struck and steady-state conditions established. The duration of the sampling period depended upon the fume formation rate and the filter capacity. The importance of the sampling period is discussed in greater detail in the section below.

Two types of filters were employed, glass fiber filters and triacetate filters. The glass fiber filters were used principally to determine the fume generation rates, and the triacetate filters were used to collect fume for chemical analysis. Typical sampling times were 2 minutes for the glass fiber filters and 30 seconds for the triacetate filters.

An optical viewing system attached to the welding station permitted a simple measurement of arc length.

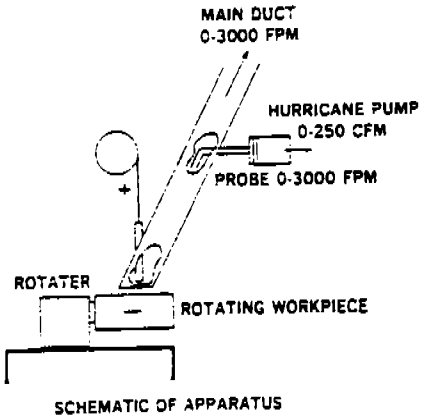

Fig. 1 — Schematic diagram of fume sampling apparatus

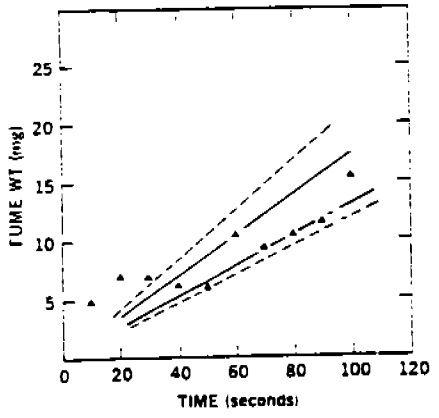

Fig. 2 — Variations and collection efficiencies for several filters as a function of time

Reproducibility and Variations

The purpose of sampling is, of course, to arrive at a fume formation rate (FFR) and a fume composition which can be assigned to a given welding process. It is obvious that the generation rate will depend upon voltage and current as well as the process and that the fume generation rate must be expressed as a function of these or related parameters. It is not so obvious how sensitive fume formation is to such things as work travel speed and variations in the plates on which the welds are made or, for that matter, to the sampling procedure itself.

In order to assess the accuracy of these experiments and to determine what parameters are needed to specify FFRs unambiguously, a two-fold investigation was undertaken. This included an investigation of the dependence of fume formation on voltage, current, work travel speed, and plate variations and an investigation of sources of error associated directly with the sampling technique.

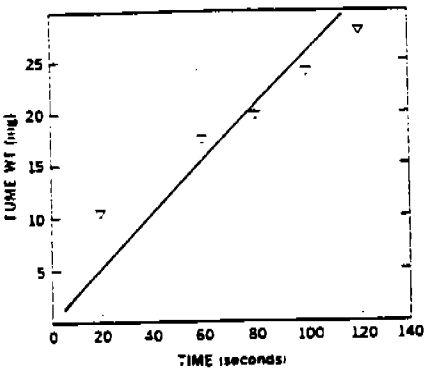

Fig. 3 — Collection linearity of a single filter as a function of time

Although there is some evidence of a variation in fume formation for different plates, the effect can be minimized, as far as relative measurements are concerned, by collecting a given series of weld data on the same plate. In absolute terms, the variation is a source of error on the order of a percent or two. Such an error is insignificant when compared to other sources yet to be discussed.

Work travel speed can also be omitted in the specification of FFRs. Increasing the travel speed by a factor of two produces a 5% decrease in the formation rate. Small variations in work travel speed from nominal values have, therefore, no significant effect. The observed variation is also not great enough to warrant specifying travel speed when stating the fume formation rates.

Depending on the shield gas, voltage and current are by far the most important factors among the welding parameters. For argon-based shielding gas, a 1 to 5% variation in voltage for a fixed current can produce changes in the FFR of as much as 20%. By way of contrast, the sensitivity of the FFR to changes in the voltage and current is far less for CO_2 shielding gases. In terms of reproducibility of the results, one must exercise great care in maintaining the voltage and current settings when welding with the argon-based shielding gases. In this regard, the ability to measure the arc length is exceedingly useful.

From the above information, it was expected that the FFRs would be reproducible to within 10%, yet statistical fluctuations of as high as 40% were observed. The large standard deviations that resulted tended to reduce the statistically meaningful information which could be extracted from the data. As a result, the sampling method was explored as the source of the problem. The sensitivity of the fume generation rate to the fume collection rate was examined. Different fume collection rates produced statistically consistent FFRs as long as isokinetic sampling conditions were maintained. However, an investigation of the sensitivity of the FFR to the sampling period revealed that the problem resided in variations in the stopping power of the filters. This data is presented in Figs. 2 and 3. In Fig. 2, ten welds were made at a constant sampling rate. All conditions were held constant except for the sampling period which was increased by 10 seconds for each successive weld. In principle, all the points should be on a straight line passing through the origin. The slope of this line is proportional to the FFR. Instead of a straight line, a wide scatter was observed as Fig. 2 demonstrates.

In addition to the data, there are four lines drawn in Fig. 2. The outer lines represent the worst case slopes for all the data points. There is a factor of six difference between them. The inner lines are the worst case slopes for the data where the sampling period was greater than or equal to one minute. The longer sampling period tends to reduce the variations in the filters. In this case, the slopes are within 40% of one another. It should be remembered that these are worst case slopes. The accuracy can be further improved by making a least squares fit and limiting the sampling periods to one minute or greater. This results in an overall statistical accuracy of approximately 20% for the absolute measurements of the FFRs cited in this report.

The behavior of individual pieces of filter paper was also examined as a function of time. The same piece of filter paper was successively exposed for constant time increments and weighed after each increment. These results are plotted in Fig. 3. In this case, the points lie on a straight line, as expected, although there appears to be a nonlinearity during the initial few seconds of sampling. This does not present a problem since the information can be drawn from the linear portion of the curve. Equally important is that over typical sampling periods of one or two minutes, no saturation of the filter was observed. In fact, no saturation was observed even with sampling periods as long as four minutes for many welding processes.

To summarize, therefore, absolute measurements of the FFRs are subject to large variations. Voltage and current must be precisely determined and maintained. Plate variations and work travel speed, although factors, do not result in significant variations. Differences from filter to filter account for the largest and least controllable variation. As a result, FFRs can be conveniently determined within no more than 20%. Greater accuracies are possible but are not required for the purpose of the comparisons made in this article.

Table 1 — Fume Sampling in SMA Welding

Class	Electrode Brand	Diam	Current	Voltage	Polarity	Fume formation rate g/min	mg/g
6010	A	5/32	110	29	RP	.32	19
6010	A	5/32	170	31	RP	.66	24
6012	B	5/32	108	20	SP	.12	7
6012	B	5/32	190	21	SP	.25	9
7018	B	5/32	160	22	RP	.28	8
7018	B	5/32	220	26	RP	.65	16
7024	C	5/32	180	32	RP	.29	8
7024	C	5/32	230	36	RP	.47	8
7024	C	5/32	180	30	SP	.29	7
7024	C	5/32	250	37	SP	.50	9
7024	D	3/16	230	36	RP	.54	9
7024	D	3/16	250	36	RP	.58	9
7024	C	3/16	250	34	RP	.39	7
7024	C	3/16	220	32	RP	.31	7
7024	D	3/16	230	30	SP	.50	9
7024	D	3/16	250	32	SP	.56	9
7024	C	3/16	230	32	SP	.48	9
7024	C	3/16	250	34	SP	.68	13
308-16	E	5/32	160	23	RP	.25	10
308-16	E	5/32	210	28	RP	.51	16

Particulate Data by Process

General

Firm limits exist for both the time weighted and excursion levels of solid materials dispersed in air. These limits are rather arbitrary, although some toxicological data exist to support them. They are deficient in that they fail to recognize that variations in crystallographic structure, particle size, and chemical activity are important in influencing the interaction of such materials with the human system. We have studied fume generation in several arc welding processes: shielded metal arc (SMA), flux cored arc (FCA), gas metal arc (GMA), and gas tungsten arc (GTA) welding. Fume generation is measured in two ways: g of fume/min of arc time and mg of fume/g of metal deposited. These formalisms (g/min and mg/g) express the relative "cleanliness" of a process on real time and real completion rate bases.

FFR measurements were made on 200 × 250 mm fiberglass filters using the techniques described in the previous section. Samples for compositional analysis were made on triacetate filters and analyzed using atomic absorption spectrophotometry and x-ray fluorescence techniques. A limited amount of size distribution data has been taken.

SMA Welding

Only electrodes for the welding of ferrous materials were studied. These electrodes include those of the cellulosic type, rutile type, rutile-iron powder type, and low hydrogen type. Both dcsp and dcrp were studied wherever possible. A constant current type power supply was used. Results are briefly summarized in Table 1.

The FFR data (mg/g) is plotted against current in Fig. 4 for 5/32 in. electrodes. Data reduced from Refs. 2, 3, and 4 are also included. Note that the data fall into three bands. The lowest FFRs are associated with rutile and rutile-iron powder type electrodes. Higher rates are found for low hydrogen type electrodes, probably due to the presence of CaF_2 in the flux. Cellulosic electrodes have the highest rates.

Variations in rates accompanying polarity changes are best understood by variations in arc voltages due to the polarity change.

No chemical analyses were performed on SMA welding fume. It is expected that the principal difference between fume from rutile, rutile-iron powder electrodes, and from low hydrogen electrodes will be the presence of CaF_2.

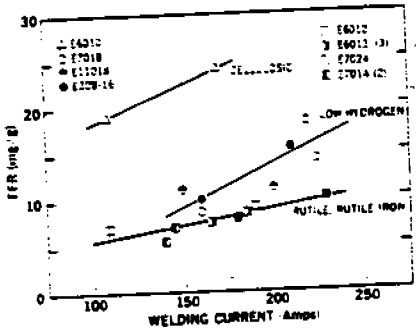

Fig. 4 — Comparison of FFRs for several SMA electrodes

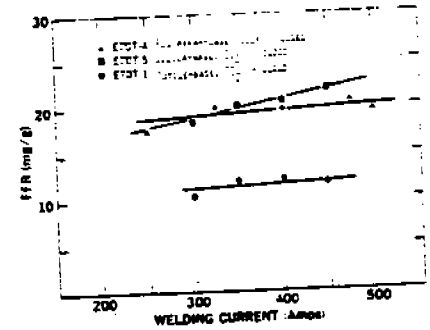

Fig. 5 — Comparison of FFRs in FCA welding for three electrodes

FCA Welding

Three types of flux cored electrodes were studied: CO_2 shielded,

Table 2 — Fume Sampling in FCA Welding

Electrode Designation	Brand	Current	Voltage	Shielding gas	Fume formation rate g/min	mg/g
E70T-1 Rutile-base	D	300	28	CO_2	.75	11
		350	30		.96	12
		400	31		1.10	12
		450	32		1.20	11
E70T-5 Silica-base	E	300	28	CO_2	1.40	18
		350	29		1.90	20
		400	30		2.10	21
		450	31		2.50	22
E70T-4 Fluorspar-base	B	250	29	None	1.08	18
		325	30		1.62	20
		400	31		2.00	20
		475	32		2.50	20

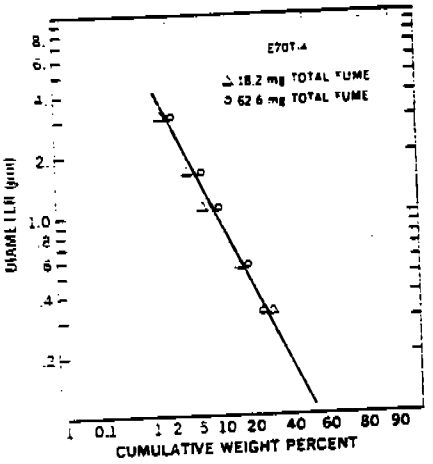

Fig. 6 — Particle size distribution by weight percent in FCA welding

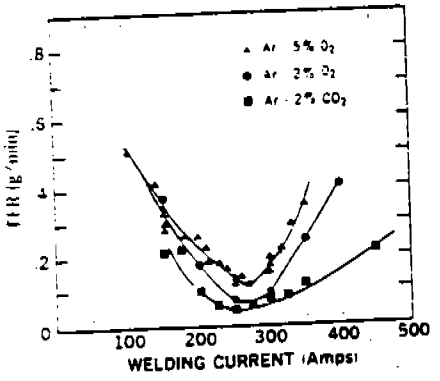

Fig. 7 — Comparison of FFRs in GMA welding using argon-based shield gases

silica-base (E70T-5); CO_2 shielded, rutile-base (E70T-1); selfshielded, fluorspar-base (E70T-4). A constant potential type power supply was used. The results of the fume generation studies are shown in Table 2.

Figure 5 shows a combined plot of /g versus current for the data. ..ere is an appreciable difference in FFR between selfshielded, fluorspar-base and CO_2 shielded, rutile-base electrodes. A similar difference is noted between CO_2 shielded, silica-base and CO_2 shielded, rutile-base electrodes. These differences are primarily due to variations in arc stability and CaF_2 content.

Table 3 shows the comparative and absolute variations in fume composition for the three types of electrodes. Note that the rather large variation in fume composition results from differences in the flux compositions.

Variations in welding parameters dic not seem to have a significant effect on FFR. Voltage increases did not produce FFR increases in any way comparable with those found in SMA welding.

Particle size distribution data were taken using an inertial separation system. The results of two of the studies with the selfshielded, fluorspar-base electrode are shown in Fig. 6. The plot shows the cumulative weight percent of fume due to particles larger than any diameter. The weight distribution is log-normal. The mean particle size by weight calculated from this data is 0.12μm.

GMA Welding

Particulate data were gathered in GMA welding with a variety of wire compositions, wire sizes, and shielding gases over a broad range of welding conditions. General considerations on reproducibility and technique were discussed in previous sections of this article. This section covers additional work on ferrous materials and aluminum alloys.

Ferrous Materials

Effect of Shielding Gas on FFR. Treating first the effect of shielding gas, reference is made to Figs. 7 and 8. Figure 7 shows the FFR plotted against current for argon-base shielding gases. The wire diameter was 0.045 in. and the welding voltage was 28 V. Note the presence of a well defined minimum in the 250-300 A range for each of the shielding gases. Figure 8 plots FFR versus current for CO_2 and Ar-25% CO_2. For these gases FFR is a monotonic function of current. Note that significant, reproducible departures from the Ar-25% CO_2 curve occur at 300 and 400 A.

A comparison of these figures reveals that considerably more fume is produced when welding with CO_2 shielding compared with argon-based shielding. The explanation of this effect involves consideration of the oxidizing nature of the shield gas and of the mode of metal transfer.

The dependence of the FFR on the oxidation potential of the shield gas was examined by measuring the FFR as a function of the oxygen content of an argon-based shielding gas. These results are shown in Fig. 9 for O_2 additions of up to 40%. Note that the FFR is approximately equal to $(\%O_2)^{3/4}$. Since oxygen is present as atomic oxygen in the arc to a certain extent, it is possible that the dependence would be greater than $(\%O_2)^{1/2}$. Thus the exponent $^3/_4$ is reasonable.

Effect of Welding Parameters and Wire Size on FFR. The existence of the minimum in FFR noted above for argon-based shielding gases was explored further as a function of welding parameters. Figure 10 shows constant current plots as a function of arc voltage for FFR (g/min). In all cases, arc length increased for increasing arc voltage. Note that the minimum FFR occurs at 28 V, 250 A. If mg/g is used as a criterion instead, a similar observation is made. Fig. 11. The minimum correlates with the transition from globular to spray transfer. This minumum is thought to result from the establishment of a stable spray arc at a minimum voltage.

Similar plots for CO_2 shielding gas are shown in Figs. 12 and 13. Note the absence of any minima. This observation reinforces the hypothesis that the transfer mode affects the FFR.

Figure 14 shows the effect of wire diameter on FFR in Ar-5%O_2.

Fume Composition and Particle Size Distributions. Fume composition was measured for a number of welding conditions. Data may be found in Table 4. For the most part, as measured by weight percent, the composition of the fume is constant. The most significant exception to this is that the fume silicon contents generated in argon shielding gas are significantly less than those produced with oxygen bearing argon-based gases and substantially less than CO_2.

Particle size analysis of the fume produced using argon-based shielding gases and CO_2 shielding gases was attempted. However, when argon-based shielding was used, no fume could be collected on the upper

stages of the sorter. Electron micrographs revealed fume particle sizes on the order of 0.005 to 0.1 microns. These particle sizes are much smaller [illegible] for any other welding process [illegible] explains the null result with the [illegible]er. A visual comparison of particle [illegible]s is presented in Fig. 15.

The particle size distribution measurements for CO_2 shielding gas were made at 300 A, 34 V. The results are plotted in Fig. 16. An extrapolated mean particle diameter of 0.03 micron, considerably smaller than for FCA welding, is determined from this data.

Aluminum Alloys

FFRs and fume compositions were determined for 1100 and 5356 alloys welded in argon. Typical FFRs (g/min) and fume compositions are given in Table 5.

It is interesting to note the decrease in FFR with increasing current. This observation is similar to that observed in GMA spray arc welding of steel over a certain range of current and voltage. A precise understanding of this effect is lacking at this time.

GTA Welding

Fume formation in GTA welding of steel using 3 mm and 5 mm thoriated tungsten electrodes with argon shielding gas was studied. The FFRs for all currents between 50 and 450 A were essentially zero.

Discussion of Results and Probable Mechanisms

In addition to supplying comparative data among different arc welding processes, it was believed that the FFRs and the composition of the welding fume could help to identify the mechanism of fume formation.

Consider first free elemental vaporization as a source of fume. The partial pressures of Mn, Si, and Fe above molten steel with the composition of the E70S-2 electrode are plotted as a function of temperature in Fig. 17. Two things are apparent. Free vaporization can account for the increase in fume with arc temperature, but based on this mechanism alone there should be but negligible silicon in the fume compared with Mn and Fe. Since this is not the case, other mechanisms must contribute.

The notable difference in fume composition between weldments made in argon-based gases and CO_2 is the silicon content of the fume. The same difference, although somewhat smaller in magnitude, exists between fume produced with Ar-2%O_2 and Ar-5%O_2. This suggests that oxidation may be important in producing fume containing silicon. The supporting data, drawn from Table 4, are indicated below:

Current, A	% Si for shielding gases of: Ar	Ar-2% O_2	Ar-5% O_2	Ar-25% CO_2	CO_2
250	2	5	14	—	25
300	1	7	14	17	27
360	4	10	14	—	—

Table 3 — Fume Composition in FCA Welding [a]

	E70T-1 %	E70T-4 %	E70T-5 %
Fe	28	13	23
Mn	5	2	4
	25	4	20
	—	13	8
	2	—	—
	2	—	—
Mg	3	9	—
Al	—	9	—
F	7	13	7

	E70T-1 mg	E70T-4 mg	E70T-5 mg
F	2.1	1.8	3.3
Mn	.4	.3	.6
	1.8	.5	2.9
	—	1.8	1.1
	.2	—	—
Mg	.2	1.2	—
Al	—	1.2	—
F	.5	1.8	1.0

[a] E70T-1, rutile base flux, CO_2 gas shielding; E70T-4, fluorspar base flux, no gas shielding; E70T-5, silica base flux, CO_2 gas shielding.

Table 4 — Fume Formation Composition in GMA Welding of Ferrous Materials

Shield gas	Current	Voltage	FFR mg/min	Mn %	Si %	Fe %	O %	Mn mg/min	Si mg/min	Fe mg/min
Argon	250	29	35	4	2	63	31	1	1	22
	300	31	25	4	1	46	49	1	0	12
	350	35	98	5	4	52	39	5	4	51
Ar-2%O_2	150	28	257	6	3	52	39	15	8	134
	200	28	147	8	7	51	34	12	10	75
	250	28	37	8	5	70	16	3	2	26
	300	29	56	9	7	63	22	5	4	35
	350	31	115	9	10	50	31	10	11	58
	400	34	162	11	10	53	26	18	16	86
Ar-5% O_2	100	28	557	5	6	49	40	29	33	273
	150	28	299	5	7	50	37	16	21	150
	200	28	257	6	9	50	35	16	22	129
	250	28	140	7	14	43	36	10	20	60
	300	28	162	6	14	47	33	10	23	76
	300	28	169	5	14	41	40	9	23	70
	80	20	110	9	11	56	24	10	12	62
	120	20	140	9	14	51	26	13	20	71
	200	20	162	9	18	52	21	15	29	84
Ar-25% CO_2	100	23	120	9	17	63	12	11	20	75
	150	27	210	6	17	50	27	13	35	105
	300	35	367	8	17	52	23	29	62	191
CO_2	130	27	198	7	30	43	20	13	59	86
	150	30	264	5	24	45	25	14	63	120
	180	30	321	7	26	47	21	22	83	150
	200	30	279	7	26	45	22	19	73	126
	250	30	449	7	25	48	20	31	112	216
	300	30	455	8	27	47	18	36	125	214
	140	22	198	7	32	43	18	14	63	85

Much work has been done studying the properties of SiO. Silicon monoxide is a gas at all temperatures of interest, 1500-3000 K. It is often formed when insufficient oxygen is available to form continuous SiO_2 layers over silicon-bearing liquids. It has a high vapor pressure. The reaction of interest is:

$$Si + \tfrac{1}{2} O_2 \rightarrow SiO, \text{ or} \quad (1)$$
$$Si + CO_2 \rightarrow CO + SiO \quad (2)$$

The standard free energy of each of these reactions may be calculated from thermodynamic data (Refs. 5, 6). Consider Equation (1) for the E70S-2 electrode composition, $a_{Si} = 3.35 \times 10^{-5}$; the partial pressure of SiO (P_{SiO}) as a function of temperature is:

Temp. (K)	Partial pressure P_{SiO} (atm) for P_{O_2} (atm) = .01	.02	.05
2000	.097	.137	.217
2500	.023	.033	.051
3000	.009	.013	.020

Obviously, since the reaction is controlled by $(P_{O_2})^{\frac{1}{2}}$, the ratio of P_{SiO} at any temperature in equilibrium with Ar-5%O_2 to that in equilibrium with Ar-2%O_2 is $(5/2)^{\frac{1}{2}}$ or 1.58. If equilibrium thermodynamics can tell us anything about the relative fume formation, then we should measure this increase in silicon in our fume samples. The actual ratios, at each set of welding currents, for silicon emission from Table 4 are:

Current, (A)	Si (5% O_2) / Si (2% O_2)
150	2.6
200	2.2
250	10.0
300	5.7

Interpretation of these results is uncertain because of possible variations in arc behavior; however, it is apparent that the generation of silicon-bearing fume is dependent on oxidation potential. If we now perform the calculations for Equation (2) and assume that the stoichiometry of the reaction as written applies, we find:

Temp. (K)	P_{SiO} (atm)
2000	.290
2500	.508
3000	.672

Thus, we would expect significant increases in the rate of silicon emission, when CO_2 is present in the shielding gas, as great as an order of magnitude. It is not reasonable to compare data taken in Ar-2%O_2, Ar-5%O_2, and CO_2 except under conditions of globular transfer. The only data points are at 150 A, and caution must be used because the arc lengths vary significantly. Data from Table 4 show:

$$Si(CO_2)/Si(5\%O_2)/Si(2\%O_2) = 7.9/2.6/1.0$$

Further comparisons are not justified. If we solve Equation (2) with $P_{CO_2} = .25$, for Ar-25%CO_2 we obtain:

Temp. (K)	P_{SiO} (atm)
2000	.123
2500	.185
3000	.216

Silicon emission should now be roughly the same as it is for Ar-2%O_2 and Ar-5%O_2 in the temperature range 2000-2500 K. The data of Table 4 agree with these calculations.

What then of vaporization of FeO and MnO as contributors to fume generation? The calculations for FeO are tabulated below, for three partial pressures of oxygen:

Temp. (K)	P_{FeO} (atm) for P_{O_2} (atm) = .01	.02	.05
2000	.003	.005	.007
2500	.039	.055	.087
3000	.204	.288	.456

The calculations in CO_2 yield:

Temp. K	P_{FeO} (atm) for P_{CO_2} (atm) = .25	1.0
2000	.003	.007
2500	.054	.115
3000	.198	.567

Changing from Ar-5%O_2 to CO_2 does not alter the FeO contribution significantly. The same is true for changing from Ar-2%O_2 to Ar-25%CO_2. The data agree with these calculations. For the temperature and ranges of Mn activity of interest, no significant amounts of MnO form.

Based on the above, it can be understood why fume generation is significantly less in the GMA welding process when argon-based shielding gases are employed than when CO_2 is used, and why there is a suppression of the silicon content of the fume. Both of these facts support the hypothesis that fume generation is the sum of elemental vaporization and oxide vaporization. It is felt that the Mn component comes strictly from elemental vaporization, the Si component from SIO formation, and the Fe component from elemental plus FeO vaporization. FFRs with argon-based shielding gas are lower because there is no enhanced vaporization due to oxide species as the data drawn from Table 4 indicate:

Current, A	FFR (g/min) Ar	2% O_2	5% O_2	25% CO_2	CO_2
250	35	37	140	—	449
300	25	56	162	367	455
350	98	115	—	—	—

The mechanism of fume formation appears to be, therefore, one of ele-

Table 5 — Fume Formation Rate and Composition in GMA Welding of Aluminum Alloys

Alloy	Diam	Current	Voltage	FFR (g/min)	Fume composition % Al	% Mg
5356	.045	150	24	1.10	45	5
5356	.045	200	25	.95	46	6
5356	.045	250	27	.85	47	8
5356	.045	300	28	.70	40	11
1100	.035	130	23	.70	50	0
1100	.035	210	26	.60	50	0

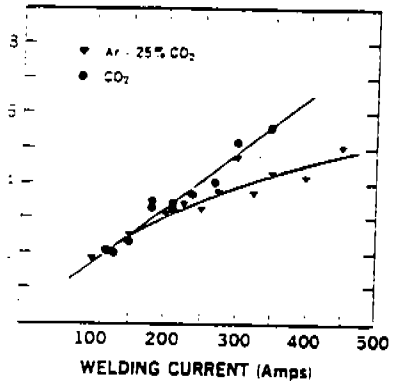

Comparison of FFRs in GMA ...ing using shield gases containing ...e than 25% CO_2

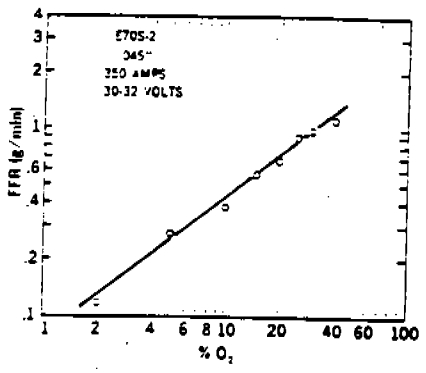

Fig. 9 — The effect of oxidizing potential on the FFR in GMA welding

mental vaporization, condensation, and oxidation enhanced vaporization.

Additional support for the vaporization-condensation-oxidation mechanism (V-C-O) is also found in the data presented in Table 5 covering GMA welding of aluminum alloys. Because of inert shielding, the mechanism for fume generation is simply vaporization and condensation of elemental material. Aluminum 5356 generates more fume because of the additional contribution of Mg. Note that the Mg content of the 5356 fume (Mg/Al = 1/8) is enriched over that of the wire (Mg/Al = 1/16). This results from the fact that Mg has a considerably higher vapor pressure in the range of 2000-3000 K and its activity coefficient in molten aluminum is 0.5. In making a comparison of the above data, note that finer wires produce less fume at comparable currents and arc lengths. The above discussion applies equally well to fume generation in FCA and SMA welding. In these processes, the fume results from the V-C-O of elemental and lower oxide species, and the V-C of oxide and surface flux species. As might be expected, the composition of the fume is strongly dependent on flux composition since significant quantities of low melting point flux components are contained in the fume.

The V-C-O mechanism advanced to this point is essentially a simple one having to do with the vapor pressures and latent heats of vaporization of the constituents present in the form of the consumables and with the oxidizing potential of the shielding gas if one is used. To first order, these factors determine the amount of a particular constituent appearing in the fume. Obviously, rate controlling steps involving diffusion of the various reactants and products will affect the FFR and composition of the fume as well. A more complete model requires consideration of these rate controlling factors and the dynamic nature of the metal transfer process including such factors as residence time of the molten droplet at a particular temperature, degree of surface exposed for participation in the vaporization process, and the efficiency of energy absorption by the surface. These contributions will be considered in turn.

For instance, as observed previously, the higher FFR for CO_2 compared with argon-based shield gases believed to be caused by the greater contribution of oxide species resulting from the increased oxidizing potential of the CO_2 shielding gas. Additionally, the inability to achieve rapid drop detachment when using CO_2 may further augment the oxide enhancement. With CO_2, the molten drop of metal spends a significant fraction of the total transfer time attached to and wandering about the wire tip. This instability can produce turbulent effects resulting in contamination which, coupled with the long detachment times, can further enhance the vaporization due to oxide species over and above the natural oxidizing potential of the shield gas. The rapid drop detachment obtained in the spray mode using argon-based shield gases does not permit this condition to occur. This fact and the lower oxidizing potential of the argon-based shield gases are sufficient to account for the differences in the mean FFRs.

The problem of instabilities and turbulent effects in FCA and SMA similar to those which exist with CO_2 in GMA is compounded by the presence of extremely volatile flux components. Hence, the FFRs for these processes are substantially higher than for GMA.

In an effort to gain more precise information about how these dynamic effects affect the V-C-O process, it was felt necessary to determine where the vaporization is occurring. Two experiments were performed. The first was to examine fume formation using the GTA process. As stated earlier, no measurable amounts of fume were obtained for all currents between 50 and 450 A using argon shielding. The initial implication is that the molten metal in the weld puddle does not substantially contribute to the fume. The weld puddle is cool relative to the arc. While vaporization is occurring, the partial pressures and hence the contribution to the total fume level is substantially reduced. Adding oxygen to the shielding gas did produce small amounts of fume, supporting the hypothesis of enhanced vaporization due to oxide species.

The second experiment involved the welding of Mg bearing Al plate using the GMA process. Two wire types were employed, type 5356 containing Mg and type 1100 containing no Mg. Referring back to Table 5, Mg was found in the fume when the 5356 wires were used, but no Mg was found when the 1100 wires were used even though Mg was present in the plate in both cases. The conclusion to be drawn, therefore, is that the vaporization of elemental and oxide species is occuring at the wire tip and in the welding arc, but not in the weld puddle to any comparable degree. This is totally consistent with known temperature distributions of the arc.

A feeling for just how the fume evolution is affected by the welding conditions and shielding gas can now be gained by a more critical examination of the behavior of the fume data in CO_2 and argon-based shielding gases exhibited in Figs. 10 and 12.

The CO_2 results are presented in Fig. 12. Two features are apparent. For a given voltage, there is a monotonic increase of fume with current;

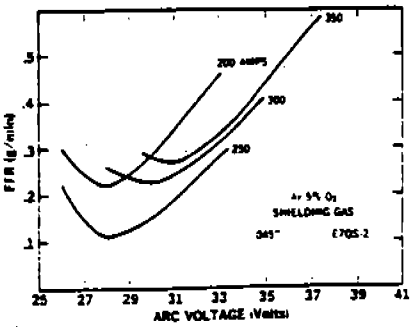

Fig. 10 — The effect of voltage and current on the FFR in GMA welding with argon-5% O_2 shielding gas

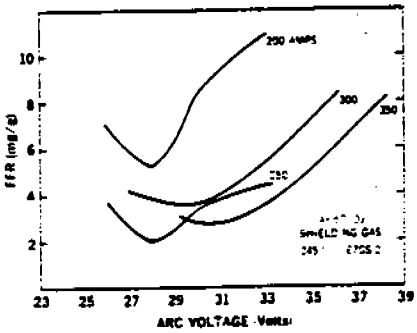

Fig. 11 — Data of Fig. 10 replotted in mg/g

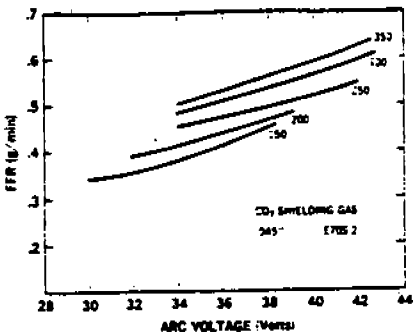

Fig. 12 — The effect of voltage and current on the FFR in GMA welding with CO_2 shielding gas

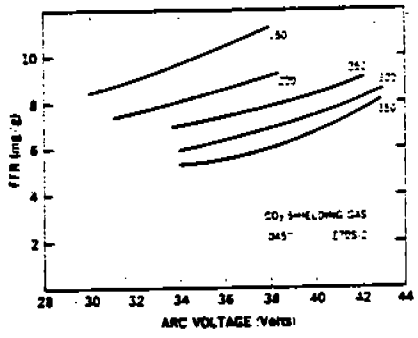

Fig. 13 — Data of Fig. 12 replotted in mg/g

APPENDIX K

REPORT EXCERPTS FROM REFERENCE 50

(Battelle-Columbus Lab, 1973)

THE WELDING ENVIRONMENT

A Research Report on Fumes and Gases
Generated During Welding Operations

Research performed at Battelle-Columbus Laboratories
under contract with the American Welding Society and
supported by industry contributions

Under the direction of the AWS Technical Activities Committee's
Task Group on Welding Fume Research

Edited by the AWS Technical Department
Jay Bland, Technical Director

AMERICAN WELDING SOCIETY
2501 NW 7th Street
Miami, Florida 33125

1973

bon steel is welded with the CO_2-metal-arc process using a copper-coated solid electrode, the following contaminants will (or may) be present in significant amounts in the welding fumes and gases:

Fumes	Gases
Fe_2O_3	CO
MnO_x	CO_2
SiO_2	NO_x
Cu	O_3

In this case, optical emission spectroscopy would be used to determine the elemental concentrations of iron, manganese, silicon, and copper since all of these elements are expected to be present in significant quantities. The concentrations of carbon dioxide and nitrogen oxides would be determined by gas mass spectroscopy; another technique, such as the Saltzman method, would be used to detect the presence of nitrogen dioxide if this information were needed. Gas chromatography would be used to determine the concentration of carbon monoxide. Procedures for detecting the presence of ozone in welding fumes require more research to develop a reliable method.

It should be recognized that the spectrograph contains information on concentrations of elements other than those listed in the example. Therefore, the entire spectrograph should be examined for unsuspected elements that may be present in hygienically significant amounts.

Wet chemical methods can also be used to detect the presence of specific elements and compounds in welding fumes and gases. Such methods can be readily mastered, and they produce accurate results at low costs during routine use. If multiple wet chemical analyses must be made for several elements, the total cost may exceed that of a spectrographic analysis. Also, the use of wet chemical methods does not permit the detection of unexpected potentially hazardous elements.

It has been suggested that the hygienic hazards associated with a particular welding operation could be determined by analyzing the fumes and gases for a single element. This suggestion would be valid if the proportions of the fume constituents remained constant, regardless of the welding conditions. Such is not the case, however. For example, in work conducted by Thrysin, the amount of iron oxide produced during welding with a specific low-hydrogen electrode varied nonlinearly from about 38 to 43% as the welding current was increased from 400 to 800 A.[10] Changes in the proportions of other fume constituents varied also. Similar results were observed during other work conducted at Battelle-Columbus.

TOTAL FUME STUDIES

OBJECTIVE

The objective of this task was to select and evaluate methods to measure the total quantity of fumes produced during welding with E11018, E70S-3, E70T-1, E70T-4, and EM12K electrodes, and determine the distribution of fume particles according to size for the same welding electrodes.

Data on fume quantities and fume generation rates are important for these reasons:

(1) The fume generation rate can be used to indicate the buildup of potentially hazardous fumes associated with the use of a particular electrode.
(2) The fume generation rate can be used to predict ventilation requirements.
(3) Total fume data can be used in product development activities.

The classification of fume particles according to size is important from the hygienic standpoint because the quantity of fumes that is retained in the human respiratory system and the depth in the system to which they penetrate are largely functions of particle size. Data on fume particle sizes are also important in the selection of ventilating equipment and devices (scrubbers, precipitators, etc.) to remove or collect fumes from the atmosphere surrounding welding operations.

PROCEDURES

Total Fume Measurements

During studies to measure total fume quantities, welding was done in a partially closed chamber. An absolute filter plus prefilters were used to collect the fumes produced by E11018, E70S-3, E70T-1, and E70T-4 electrodes; prefilters were not required during the collection of fumes produced by the two submerged arc welding electrodes, EM12K.

The fume samples were collected in triplicate at each of two representative welding current levels. Triplicate samples were obtained to permit averaging of the data in order to minimize scatter attributable to minor variations in the welding or sampling procedures. The welding conditions are shown in Table 2.9.*

*It should be noted that two tests were conducted with the EM12K electrode designated as No. 1 to determine if the method of applying the flux (that is, before or during welding) influenced the amount of fumes produced during welding. Since the flux deposition method did not significantly affect the fume generation rate, only one test was conducted with the EM12K No. 2 electrode. A higher welding current was used for this test than those conducted with the other submerged arc welding electrode to determine if the fume quantities would be increased appreciably.

TABLE 2.9. WELDING CONDITIONS FOR TOTAL FUME STUDIES

Electrode	Electrode Diameter, in.	Current, A (Nominal)	Voltage, V	Shielding Gas	Wire Feed Rate, ipm (Average)	Contact-to-Work, in.	Welding Time, s
E11018	3/16	150	20-30	N/A[1]	N/A	N/A	90-100
		200	20-35	N/A	N/A	N/A	115-118
E70S-3	0.045	250	30-31	CO_2	428	3/4	110-120
		300	29-30	CO_2	607	3/4	110-120
E70T-1	3/32	400	31-32	CO_2	142	1	30
		500	30-31	CO_2	186	1	30
E70T-4	3/32	400	31-32	None	140	1	30
		500	30-31	None	220	1	30
EM12K No. 1[2]	3/32	400	32-33	None	84	1-1/4	120
		500	31-32	None	138	1-1/4	120
EM12K No. 1[3]	3/32	400	32-33	None	92	1-1/4	120
		500	31-32	None	145	1-1/4	120
EM12K No. 2[2]	3/32	500	31-32	None	144	1-1/4	120
		600	29-31	None	193	1-1/4	120

(1) N/A: not applicable
(2) Flux poured on plate before welding
(3) Flux poured on plate during welding

The fume samples were collected in accordance with the procedures outlined earlier.

The data obtained during these studies (fume weight, weight of filler metal consumed, and sampling time) permitted calculation of the fume generation rate, and the weight of electrode converted to fumes. For comparison purposes, the fume generation rates were normalized on a per-minute basis. In calculating the weight of electrode converted to fumes, the total electrode weight (metal weight plus flux or covering weight) was used because the amount of fumes produced during welding is dependent on the flux or covering and the metallic portion of the electrode. Repeated measurements indicated that the flux in the E70T-1 and E70T-4 electrodes used in this program accounted for 14 and 15% of the electrode weight, respectively; the covering of the E11018 electrode amounted to about 30% of the electrode weight.

Fume Particle Size Classification

A cascade impactor was used to classify the fume particles according to size. The manner in which particle classification is accomplished with this equipment has been discussed previously.

The particle size distribution was determined on a weight basis in accordance with the procedures outlined earlier. To insure that sufficient fumes would be available for collection near the inlet, the cascade impactor was placed inside the welding chamber that was used for total fume measurements; the impactor inlet was located about 16 in. above and 8 in. to the side of the arc. The operating vacuum for the impactor was provided by a small pump.

Two particle size analyses of the fumes produced by each of the E11018, E70S-3, E70T-1, and E70T-4 electrodes were made with the cascade impactor; the conditions for the analyses of fumes produced by one electrode differed only in the length of the welding or sampling period or both. Only one analysis of the fumes produced by each of the EM12K electrodes was made, because the quantity of fumes evolved during submerged arc welding was insignificant, unless the arc broke through the flux cover.

The welding and sampling conditions for each particle size analysis are shown in Table 2.10.

RESULTS AND DISCUSSION

Total Fume Measurements

The results of these fume studies are summarized in Table 2.11. For easy comparison, the fume generation

TABLE 2.10. WELDING CONDITIONS FOR FUME PARTICLE SIZE ANALYSIS

Electrode	Electrode Diameter, in.	Current, A (Nominal)	Voltage, V	Shielding Gas	Wire Feed Rate, ipm	Contact-to-Work, in.	Welding Time, s	Sampling Time, s(1)
E11018	3/16	150	20-30	N/A(2)	N/A	N/A	45	105
		150	20-30	N/A	N/A	N/A	45	150
E70S-3	0.045	250	30-31	CO_2	450	3/4	60	240
		250	30-31	CO_2	450	3/4	60	180
E70T-1	3/32	500	30-31	CO_2	170	1	30	90
		500	30-31	CO_2	170	1	60	180
E70T-4	3/32	500	30-31	None	216	1	60	180
		500	30-31	None	216	1	30	90
EM12K No. 1	3/32	600	29-30	None	180	1-1/4	180	180
EM12K No. 2	3/32	600	29-30	None	185	1-1/4	150	150

(1) Sampling was conducted during the welding cycle and for selected times thereafter to determine if the results were affected by the length of the sampling cycle.

(2) N/A - Not applicable.

rate and the weight of electrode converted to fumes are also plotted as bar graphs in Figs. 2.5 and 2.6. In each case, data for the submerged arc welding electrodes are shown separately, because the quantity of fumes produced by these electrodes was very small in comparison with that produced by shielded metal-arc and gas metal-arc welding electrodes.

The equipment and procedures used in this investigation produced consistent results within experimental limits. For example, at a current of 400 A, the weights of three fume samples collected during 30 s of welding with the E70T-1 electrode were 0.3997, 0.4059, and 0.3939 g. The mean fume weight was 0.3998 g and the standard deviation from this value was 0.0060 g.

Fume Generation Rate. Fumes were generated at the highest rate by the two flux cored arc-welding electrodes. The fume generation rates of the E11018 and E70S-3 electrodes were comparable. Fumes were produced at insignificant rates by the submerged arc welding electrodes, regardless of whether the flux was poured in the joint area before or during welding. However, in cases where the arc broke the cover momentarily, the fume generation rate increased sharply. For example, at a welding current of 500 A, the rate at which fumes were produced by one of the EM12K electrodes increased from 4.2 mg/min to 15.2 mg/min, even though the arc was unshielded for only a few seconds.

An examination of the data contained in Table 2.11 indicates some ambiguities. With few exceptions (E70S-3 fumes and the fumes from one of the EM12K electrodes), fumes were produced at increased rates when the arc current level was increased. Other investigators have also noted an increase in the quantity of fumes produced as a function of increased welding current. For example, Thrysin reported that 1.5 g of fumes were produced at an arc current of 240 A; at 350 A, 2.1 g of fumes were produced.[10] During an investigation of the fumes associated with gas (CO_2) metal-arc welding, Erman, et al., observed that the fume generation rate increased from 0.35 to 0.84 g per min at welding currents of 190 and 300 A, respectively.[11] However, in other work where the fume generation rates for several electrodes were determined over a wide range of welding currents, the variation in fume generation rate appeared to be more complex than a simple dependence on welding current (Fig. 2.7). The fume generation rates of electrodes used for flux cored arc welding (E70T-1 and E70T-4) increased to a maximum with increasing arc current and then de-

TABLE 2.11. SUMMARY OF DATA ON [illegible]AL FUME MEASUREMENTS

Electrode (AWS Designation)	Current, A (Nominal)	Fume Generation Rate, g/min(1) Average	Fume Generation Rate, g/min(1) Std. Dev.	Weight of Electrode Converted to Fumes, % Average	Weight of Electrode Converted to Fumes, % Std. Dev.	Remarks
E11018	150	0.3770	0.0103	1.110	0.052	
	200	0.4390	0.0055	1.110	0.014	Arc interrupted; average values based on two samples
E70S-3	250	0.4150	0.0273	0.475	0.011	Arc interrupted; average values based on two samples
	300	0.2570	0.0304	0.212	0.013	
E70T-1	400	0.7996	0.0120	0.776	0.012	
	500	0.8994	0.0300	0.670	0.017	
E70T-4	400	2.0310	0.0187	1.990	0.021	
	500	2.5106	0.2310	1.550	0.168	
EM12K(2) No. 1	400	0.0310	0.0016	0.0041	0.0020	Arc broke cover; average values based on two samples
	500	0.0042	0.0010	0.0034	0.0007	
EM12K(3) No. 1	400	0.0012	0.0007	0.0015	0.0011	
	500	0.0029	0.0009	0.0022	0.0007	
EM12K(2) No. 2	500	0.00166	0.0005	0.0014	0.0002	
	600	0.00029	0.00004	0.00016	0.00002	Arc broke cover; average values based on two samples

(1) Average values based on three samples

(2) Flux poured on plate before welding

(3) Flux poured on plate during welding

(4) Electrode weight is equal to sum of metal weight plus flux (or electrode covering) weight.

creased. The opposite variation in fume generation rate was observed for an electrode used for gas (CO_2) metal-arc welding.

It is believed that the rate at which fumes are generated is largely dependent on the stability of the welding arc and its metal-transfer characteristics. The fume generation rate could also be affected by process variables other than arc current such as arc voltage, electrode stick-out, shielding gas type and gas flow rate. More work on the fundamental nature of fumes and the mechanics of fume generation is needed to explain the observations made during this program.

Electrode Conversion to Fumes. The E70T-4 electrode produced the most fumes per unit weight of electrode consumed, followed in decreasing order by the E11018, E70T-1, E70S-3, and EM12K electrodes.

As in the case of the fume generation rate, the effect of the welding current on the amount of the electrode that was converted to fumes is not clearly evident from the data shown in Fig. 2.6. At the current levels investigated during this program, a decrease in this parameter usually occurred when the welding current was increased. However, this relationship was not consistent when the welding current was varied over a wide range (Fig. 2.8). The amount of the E70T-4 electrode that was converted to fumes increased to a maximum and then decreased as the welding current was increased; the opposite behavior was observed for the E70S-3 electrode. The most consistent dependence of this parameter on current was noted when the E70T-1 electrode was used for welding. The amount of electrode converted to fumes is affected by the same parameters as the fume generation rate.

Fume Particle Size Classification

The results of the studies to classify fume particles according to size are shown in Tables 2.12 through 2.16. With few exceptions, the fume particles produced during welding were smaller than 1.0 μm in size. These results are in substantial agreement with those obtained by other investigators.[12, 13]

On the average, the particles in the fumes produced by the E11018 electrode were larger than those associated with the electrodes used for gas metal-arc and submerged arc welding. A sizeable proportion of the E11018 fume particles had sizes of 1.0 to 2.0 μm while the particle sizes of fumes produced with other

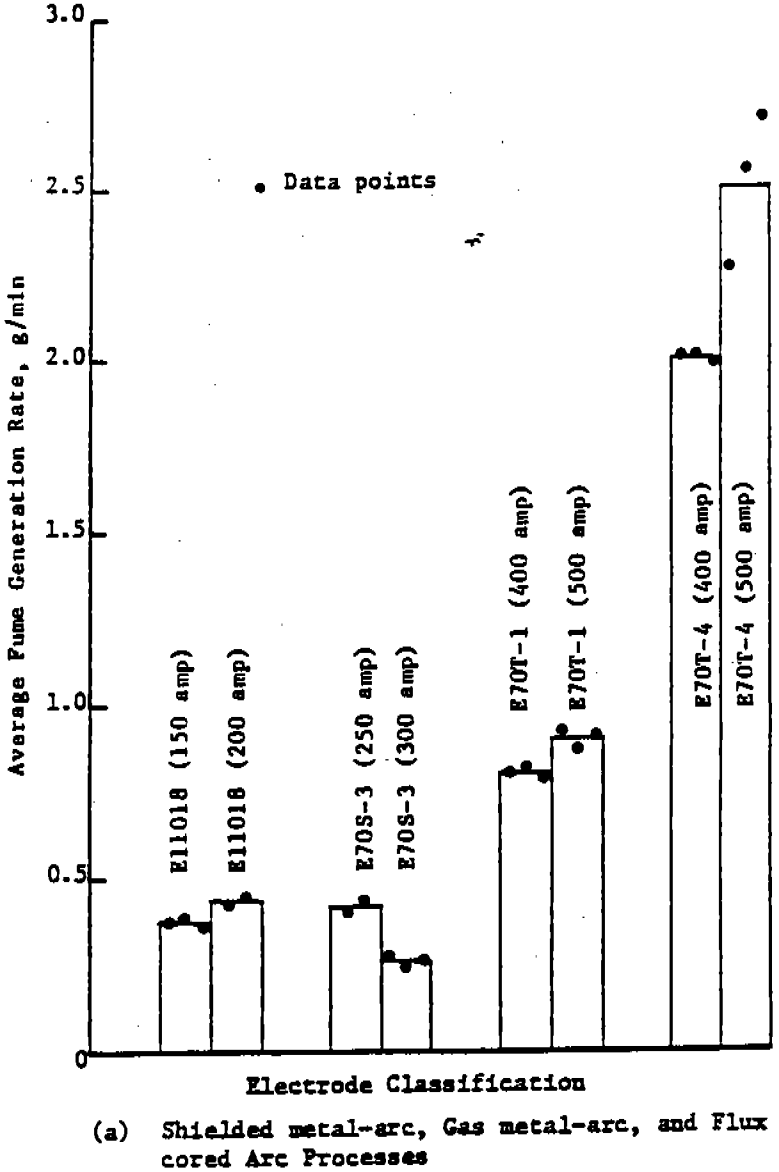

(a) Shielded metal-arc, Gas metal-arc, and Flux cored Arc Processes

Fig. 2.5—Fume generation rate as a function of electrode classification and current.

electrodes were 1.0 μm or less. It is believed that the presence of these large particles can be attributed to arc instability during shielded metal-arc welding and to the agglomeration (or coagulation) characteristics of the fumes. These same factors could also account in part for the large amount of fumes collected during the second test with the E11018 electrode. Some increase in fume weight over that collected during the first test with this electrode was expected because the sampling period was lengthened; however, the magnitude of the increase was unexpected.

A relatively short welding period had to be used in classifying the fume particles produced by the E70T-4 electrode to prevent overloading the cascade impactor. Because of the high fume generation rate associated with this electrode, wall losses (that is, some fume particles collected on the inner walls of the impactor instead of on the impactor filters) occurred at longer

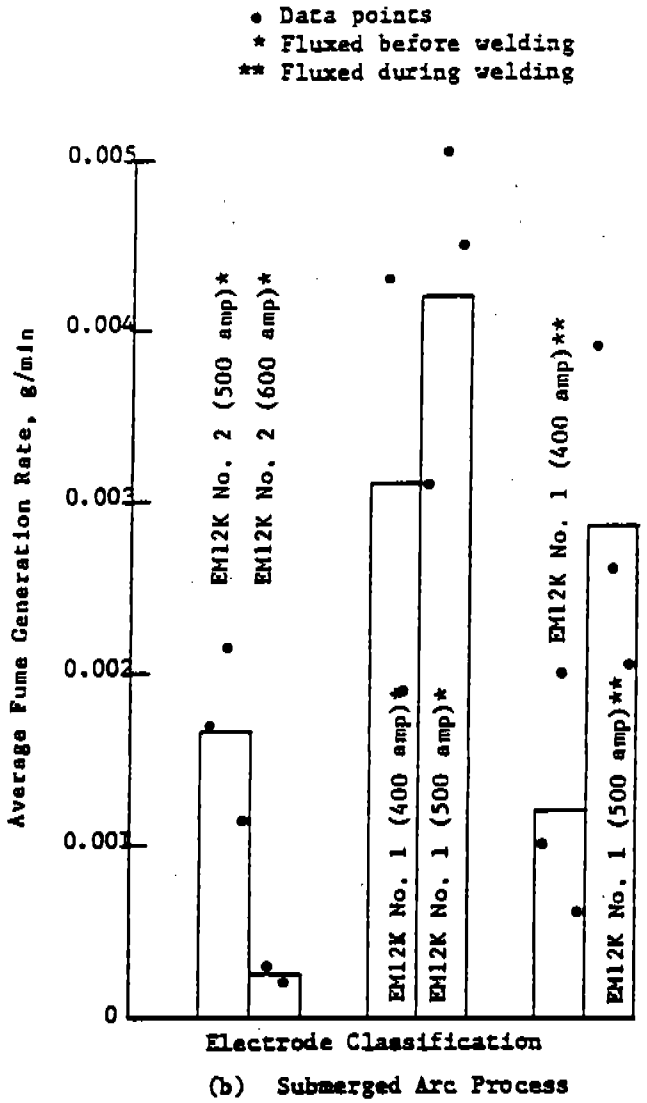

(b) Submerged Arc Process

Fig. 2.5—(Continued). (Note change in vertical scale.)

welding times, and a valid classification of the fume particles was not possible.

CONCLUSIONS

The equipment and procedures used to determine the total quantities of fumes produced as a function of welding current and welding time and to classify fume particles according to size have produced reasonable results with electrodes used for shielded metal-arc, gas metal-arc, flux cored arc, and submerged arc welding. As a result, the use of such techniques or their equivalent by industry is recommended.

The importance of the fume generation rate can be judged by considering the fume concentrations that will exist in a closed area unless adequate ventilation is provided. For example, if iron oxide fumes are being generated at the rate of 1 g/min in an unventilated room with a volume of 10,000 cu ft (283.2 m^3), the total fume concentration will exceed the threshold limit value for iron oxide (10 mg/m^3) in less than 3 min, if it is assumed that the fumes diffuse uniformly throughout the room. Such is not the case, of course, since fume particles are subject to gravitational forces and the effects of air currents. For a room of this size the publication, "Safety in Welding and Cutting," (ANSI Standard Z49.1-1967) recommends that general

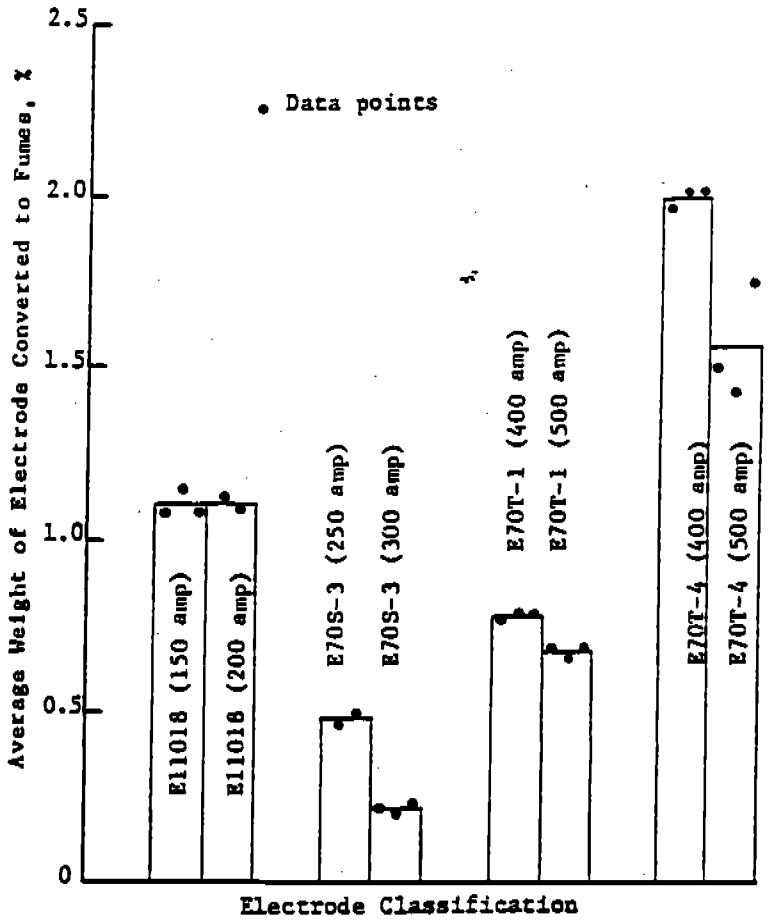

(a) Shielded Metal-Arc, Gas Metal-Arc, and Flux Cored Arc Processes

Fig. 2.6—Weight of electrode converted to fumes as a function of electrode classification and current.

ventilation at 2000 cfm be provided for each welder unless local exhaust hoods are available. This may or may not be adequate depending on the electrode being used and the rate at which fumes are being generated.

The hazards that may be associated with welding operations could be minimized if information were available on the rate at which fumes are generated by particular electrodes. It is not known if the fume generation rate is characteristic of a class of electrodes or if it is different for various electrodes of the same class. In the case of bare, solid electrodes (for example, E70S-3), it is believed that the fume generation rate and other fume characteristics should be similar for all electrodes corresponding to a single classification, regardless of the producer. Such is not expected to be the case for covered and flux cored electrodes because of differences in the compositions of the covering or flux.

With the exception of the fumes associated with the E11018 electrode, the particle sizes of fumes produced during welding were smaller than 1.0 μm in size (some particles in E11018 fumes had sizes of 1.0 to 2.0 μm). Since the sizes of welding fume particles are well within the range where maximum retention in the lower parts of the human respiratory system occurs,[14 to 18] it appears that further efforts to classify particles according to size or shape is not needed. Instead, such efforts should be directed toward minimizing the fumes in the welding area.

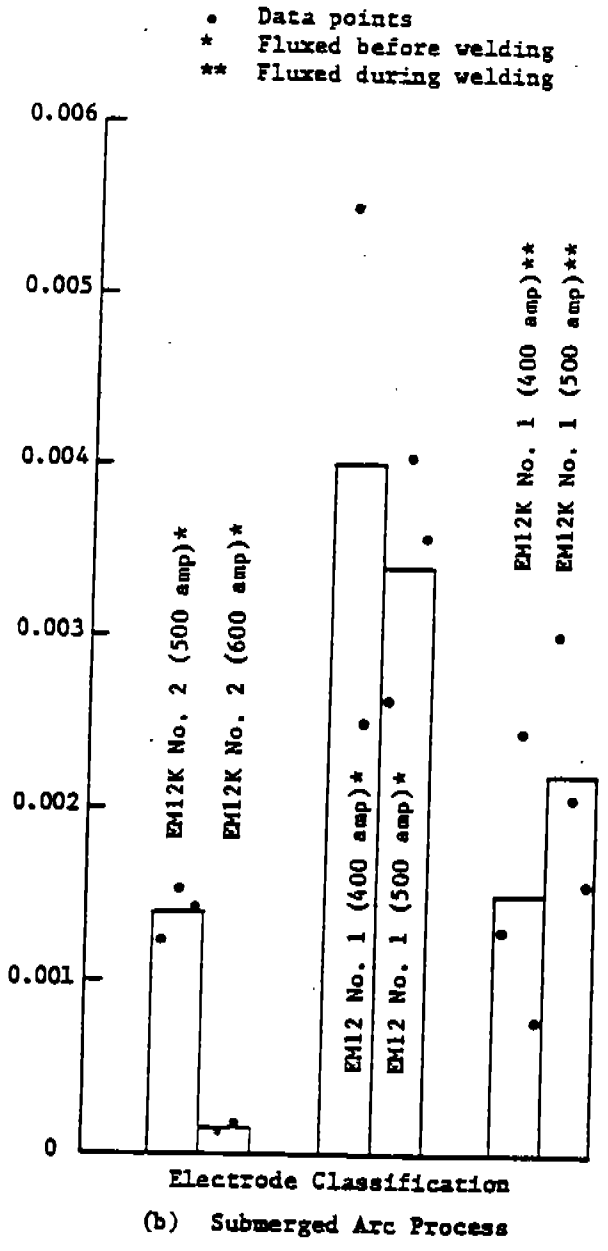

(b) Submerged Arc Process

Fig. 2.6—(Continued). (Note change in vertical scale.)

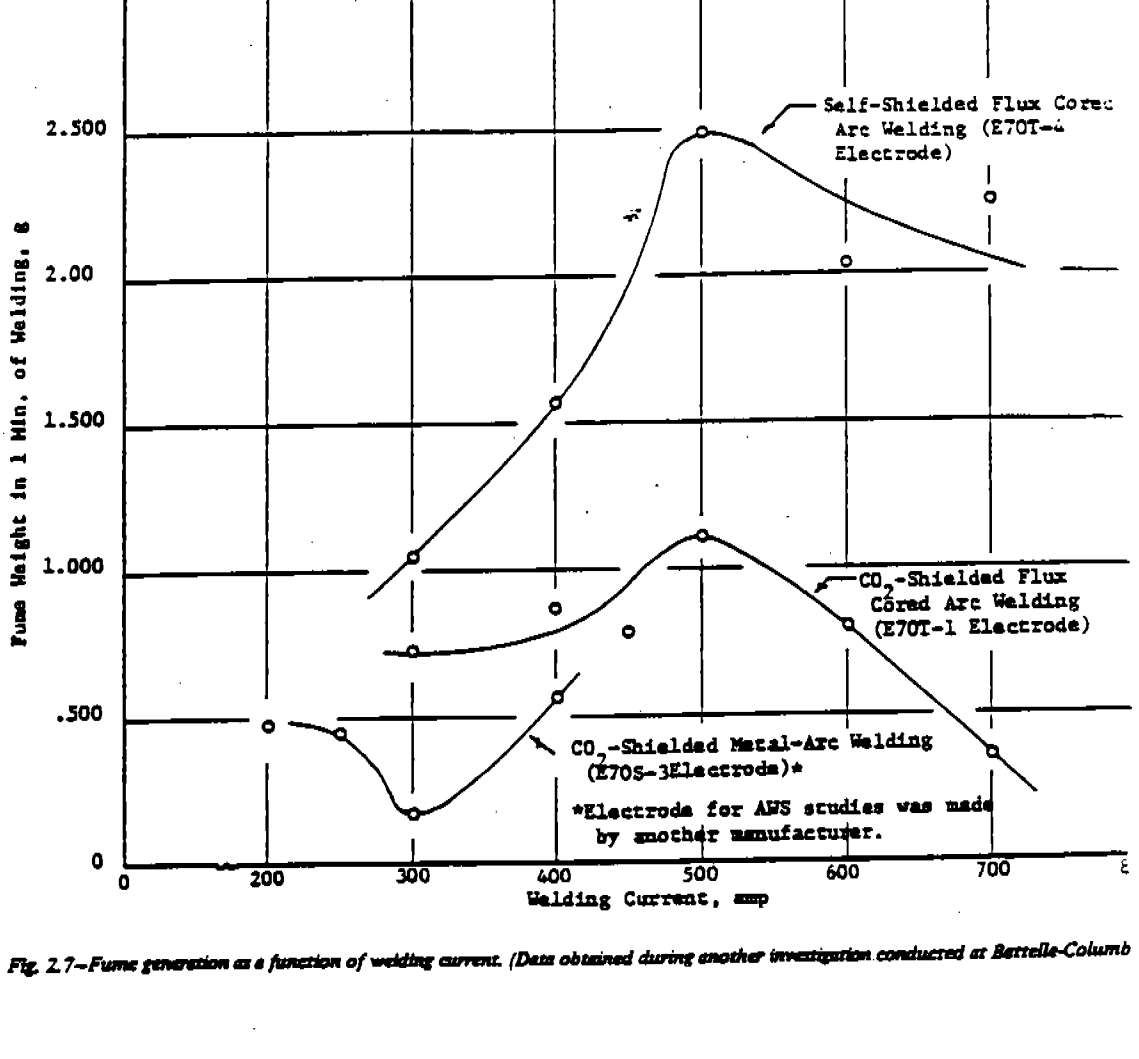

Fig. 2.7—Fume generation as a function of welding current. (Data obtained during another investigation conducted at Battelle-Columb

TABLE 2.12. CASCADE IMPACTOR PARTICLE-SIZE ANALYSIS OF E11018 WELDING FUMES

Impactor Stage No.	Jet Cutoff, μ	Run No. 1(1) Fume Wt. mg	Fume Wt. %	Cumulative Wt., %	Run No. 2(2) Fume Wt. mg	Fume Wt. %	Cumulative Wt., %
1	16	—	—	—	—	—	—
2	8	—	—	—	—	—	—
3	4	—	—	—	—	—	—
4	2	—	—	—	—	—	—
5	1	0.2	13.3	100.0	5.2	61.9	100.0
6	0.5	0.5	33.3	86.7	2.3	27.4	38.1
7	0.25	0.7	46.7	53.4	0.7	8.3	10.7
-	<0.25	0.1	6.7	6.7	0.2	2.4	2.4

(1) Welding current: 150 A; welding time: 45 s; sampling time: 105 s (45 s during welding +60 s after welding).

(2) Welding current: 150 A; welding time: 45 s; sampling time: 150 s (45 s during welding +105 s after welding).

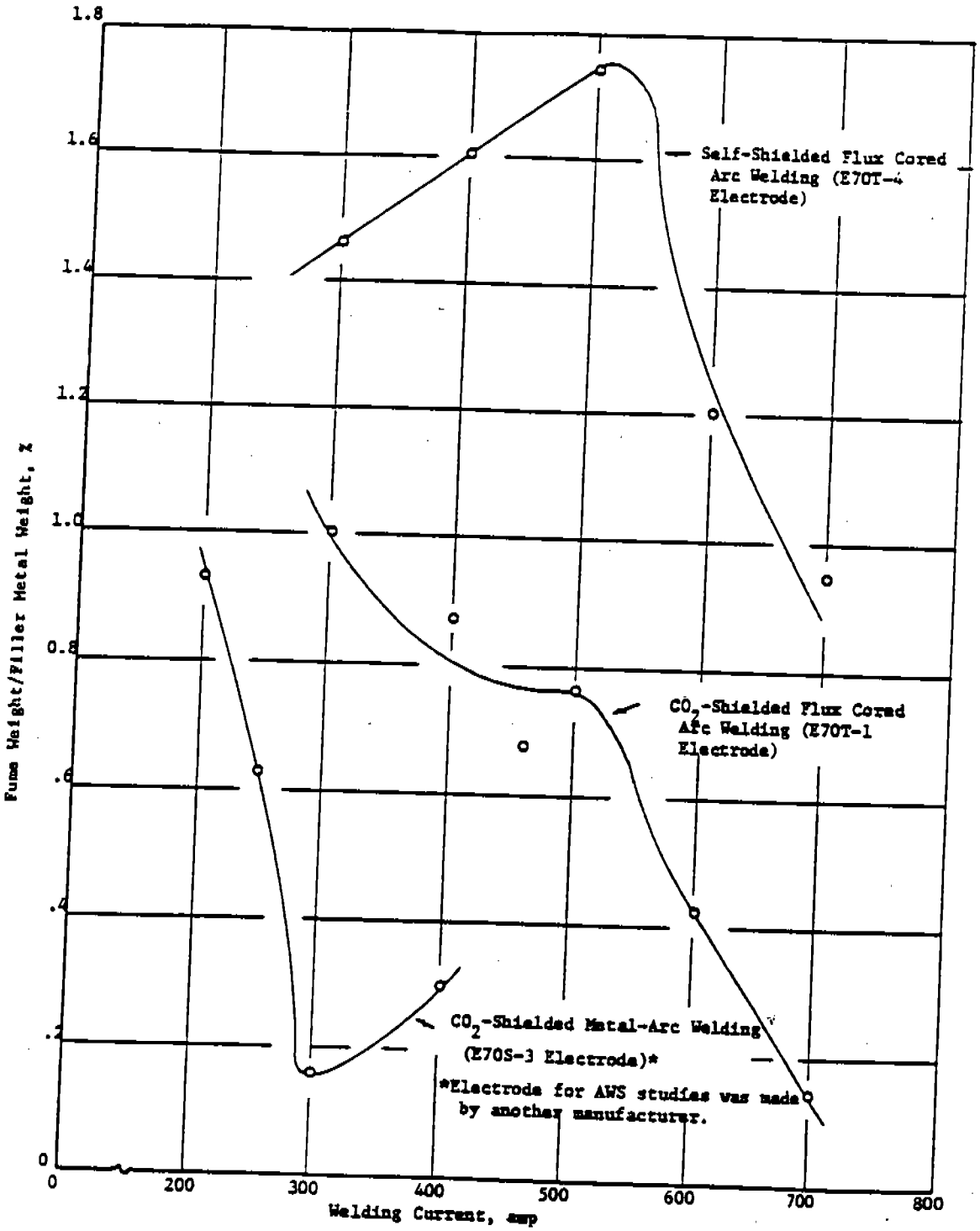

Fig. 2.8—Amount of filler metal converted to fumes vs. welding current. (Data obtained during another investigation conducted at Battelle-Columbus).

TABLE 2.13. CASCADE IMPACTOR PARTICLE-SIZE ANALYSIS OF E70S-3 WELDING FUMES

Impactor Stage No.	Impactor Jet Cutoff, μm	Run No. 1(1) Fume mg	Run No. 1(1) Wt. %	Run No. 1(1) Cumulative Wt., %	Run No. 2(2) Fume mg	Run No. 2(2) Wt. %	Run No. 2(2) Cumulative Wt., %
1	16	--	--	--	--	--	--
2	8	--	--	--	--	--	--
3	4	--	--	--	--	--	--
4	2	--	--	--	--	--	--
5	1	--	--	--	--	--	--
6	0.5	0.8	57.2	100	0.1	8.3	100.0
7	0.25	0.4	28.6	42.9	0.6	50.0	91.7
-	<0.25	0.2	14.3	14.3	0.5	41.7	41.7

(1) Welding current: 250 A; welding time: 60 s; sampling time: 240 s (60 s during welding +180 s after welding).

(2) Welding current: 250 A; welding time: 60 s; sampling time: 180 s (60 s during welding +120 s after welding).

TABLE 2.14. CASCADE IMPACTOR PARTICLE-SIZE ANALYSIS OF E70T-1 WELDING FUMES

Impactor Stage No.	Impactor Jet Cutoff, μm	Run No. 1(1) Fume mg	Run No. 1(1) Wt. %	Run No. 1(1) Cumulative Wt., %	Run No. 2(2) Fume mg	Run No. 2(2) Wt. %	Run No. 2(2) Cumulative Wt., %
1	16	--	--	--	--	--	--
2	8	--	--	--	--	--	--
3	4	--	--	--	--	--	--
4	2	--	--	--	--	--	--
5	1	--	--	--	--	--	--
6	0.5	0.2	25	100	0.2	22.2	99.9
7	0.25	0.4	50	75	0.4	44.4	77.7
-	<0.25	0.2	25	25	0.3	33.3	33.3

(1) Welding current: 500 A; welding time: 30 s; sampling time: 90 s (30 s during welding +60 s after welding).

(2) Welding current: 500 A; welding time: 60 s; sampling time: 180 s (60 s during welding +120 s after welding).

TABLE 2.15. CASCADE IMPACTOR PARTICLE-SIZE ANALYSIS OF E70T-4 WELDING FUMES

Impactor Stage No.	Impactor Jet Cutoff, μm	Run No. 1(1) Fume mg	Run No. 1(1) Wt. %	Run No. 1(1) Cumulative Wt., %	Run No. 2(2) Fume mg	Run No. 2(2) Wt. %	Run No. 2(2) Cumulative Wt., %
1	16				--	--	--
2	8				--	--	--
3	4				--	--	--
4	2	(impactor overloaded)			--	--	--
5	1				0.2	1.9	99.9
6	0.5				6.1	58.1	98.0
7	0.25				1.8	17.1	39.9
-	<0.25				2.4	22.8	22.8

(1) Welding current: 300 A; welding time: 60 s; sampling time: 80 s (60 s during welding +120 s after welding).

(2) Welding current: 300 A; welding time: 30 s; sampling time: 90 s (30 s during welding +60 s after welding).

TABLE 2.16. CASCADE IMPACTOR PARTICLE-SIZE ANALYSIS OF EMI2K WELDING FUMES

Impactor Stage No.	Jet Cutoff, μm	EM12K No. 1(1) Fume wt., %	EM12K No. 1(1) Wt., %	EM12K No. 1(1) Cumulative wt., %	EM12K No. 2(2) Fume wt., %	EM12K No. 2(2) Wt., %	EM12K No. 2(2) Cumulative wt., %
1	16	--	--	--	--	--	--
2	8	--	--	--	--	--	--
3	4	--	--	--	--	--	--
4	2	--	--	--	--	--	--
5	1	--	--	--	--	--	--
6	0.5	--	--	--	--	--	--
7	0.25	Discoloration			Discoloration		
-	<0.25	0.1	100	100	0.1	100	100

(1) Welding current: 600 A; welding time: 150 s; sampling time: 150 s during welding.

(2) Welding current: 600 A; welding time: 180 s; sampling time: 180 s during welding.

FUME MEASUREMENTS IN THE HELMET REGION

OBJECTIVE

This task was undertaken to evaluate methods for determining the concentrations of fumes to which the welder is subjected during welding. Fume samples were collected outside and inside the welder's helmet while he was welding, and fume concentrations were calculated for comparison with established threshold limit values.

PROCEDURES

The fumes produced by E11018, E70S-3, and E70T-1 electrodes were collected on cellulosic membrane filters using equipment and procedures discussed earlier. Welding was done in the flat position; that is, the position in which the welder is subjected to maximum fume concentrations. The welding area was an open and unventilated room with an approximate volume of 2200 ft^3 (62.4 m^3); the fumes were exhausted from the room after each experimental test.

As mentioned earlier, equipment was incorporated in the fume sampling train to measure the volume of fume-laden air that passed through the filter (Fig. 2.3). This volume is required to calculate fume concentrations. To insure a relatively constant position for the sampling device, the filter holder was mounted in a hole that was drilled in the welder's helmet at a location immediately in front of his mouth and nose. Depending on the data required, the holder was mounted inside or outside the helmet (Fig. 2.4).

The welding conditions for these studies were identical to those used for the studies to evaluate analytical techniques (Table 2.3). The gun used for gas metal-arc welding with solid or flux cored filler wires was held manually, and efforts were made to maintain a constant arc length during welding. The same procedures were used for shielded metal-arc welding. During welding, the welder assumed a position that was comfortable for him; another welder might have used a slightly different position.

RESULTS AND DISCUSSION

Fume samples, in duplicate, were collected outside and inside the welder's helmet during the welding of steel with E11018, E70S-3, and E70T-1 electrodes.* The results of these studies are shown in Tables 2.17 through 2.20. A summary of the data collected is shown in Table 2.17 along with the total fume concentrations in front of and behind the welder's

*Fume concentration is defined as a ratio of the weight of fumes collected on the filter to the volume of fume-laden air passing through the filter. For direct comparison with established threshold limit values, fume concentrations are expressed as mg/m^3.

APPENDIX L

REPORT EXCERPTS FROM REFERENCE 51

(IT Corporation, 1992)

DEVELOPMENT OF ENVIRONMENTAL RELEASE ESTIMATES FOR WELDING OPERATIONS

by

IT Corporation
11499 Chester Road
Cincinnati, Ohio 45246

Contract No. 68-C9-0036
Work Assignment No. 2-54
JTN 803812-16-2

U.S. ENVIRONMENTAL PROTECTION AGENCY
RISK REDUCTION ENGINEERING LABORATORY
26 WEST MARTIN LUTHER KING DRIVE
CINCINNATI, OHIO 45268

1992

These metals are reportable under SARA Title III, Section 313, and could be expected from these types of welding operations. Based on the analysis of these samples and the weights of all materials used, emission release factors were developed for fume and slag generated during welding operations. These emission factors can be used to estimate releases to the air and off-site transfers.

TABLE 1. TYPES OF ELECTRODES USED IN FUME TESTS

AWS[a] Class	Type of electrode
E308LSi	Solid electrode
E70S-3	Solid electrode
E70S-6	Solid electrode
E70T-1	Flux-cored electrode
E71T-1	Flux-cored electrode
E6010	Manual
E6011	Manual
E6013	Manual
E308-16	Manual
E7018	Manual

[a] American Welding Society.

The procedures used to develop these data are described in this report. Section 2 describes the sampling procedures. Section 3 presents an overview of the quality of the data generated. Section 4 describes the results of the study. Conclusions are presented in Section 5.

SECTION 4

RESULTS OF WELDING TEST

This section discusses the results of the welding tests and the fate of electrodes during welding. As an electrode is consumed, most of it is deposited onto the base metal. The remainder is either emitted to the air as fume or is deposited onto the weld in the form of slag. Slag is then chipped or brushed from the weld and disposed of as solid waste. The quantity of fume and slag generated for each class of electrode tested is given in Subsections 4.1 and 4.2. Because the steel plates were extremely heavy in comparison with the weight of the weld, the quantity deposited onto the base metal could not be accurately determined; thus, a complete mass balance was infeasible.

4.1 Airborne Emission Results

On the basis of procedures outlined in Section 2 of this report, emission factors were determined for the quantity of fume generated per weight of welding electrode used. Table 5 presents the average weight of fume generated per weight of electrode consumed for the classes of electrodes investigated in this study as well as values extracted from Draft 5 of "Guidelines to Cover SARA Requirements Section 313" (November 20, 1989),[1] denoted as Reference 1.

As shown in Table 5, the weight of fume generated per weight of electrode consumed varied from 0.54 lb/100 lb of electrode for E308LSi to 3.84 lb/100 lb of electrode for E6011. Manual electrodes generally emitted more fume than flux-cored electrodes, which in turn emitted more fume than did solid electrodes.

The experimental values either fell within the range given in Reference 1 or were slightly higher. Experimental values for E308-16, E6010, and E70S-3 electrodes were higher than the range given in Reference 1.

TABLE 5. FUME GENERATED PER AMOUNT OF ELECTRODE USED (lb fume/100 lb electrode consumed)

Electrode class	Type of electrode	Ratio	Reference 1
E70S-3	Solid electrode	0.86	0.20-0.80
E70S-6	Solid electrode	0.79	NA[a]
E308LSi	Solid electrode	0.54	NA
E70T-1	Flux-cored electrode	0.87	0.40-1.1
E71T-1	Flux-cored electrode	1.2	NA
E6010(A)	Manual electrode	2.27	1.0-2.0
E6010(B)	Manual electrode	2.05	1.0-2.0
E6011	Manual electrode	3.84	NA
E6013	Manual electrode	1.36	NA
E308-16	Manual electrode	0.64	0.30-0.60
E7018	Manual electrode	1.57	1.5-2.0

[a] NA = Not available.

Reference 1 did not give details of the welding conditions used. As mentioned in Section 2, all of the tests in this study were performed at the manufacturer's recommended conditions. Detailed operating conditions for each test are given in Appendix B. In all cases, a ½-inch-thick Type A36 steel plate was used for welding.

Shielding gas having a flow rate of 0.67 ft^3/min was used for all flux-cored and solid-wire electrodes. A 98 percent argon/2 percent oxygen mixture was used with Electrode ER308LSi, and carbon dioxide was used with the remainder of the electrodes. A DC600 power supply was used with all of these electrodes. An automatic wire feeder (shown in Figure 2) fed the wire at a constant rate of 275 inches per minute for E308LSi, E70T-1, and E70T-2 electrodes, and 450 inches per minute for E70S-6 and E70S-3 electrodes. The electrode angle was set at a 10-degree lag for all solid-wire and flux-cored welding. The electrical extension (distance between the tip of the electrode and the plate) was set at 3/4 inch for E70S-3, E70S-6, E71T-1, and ER308LSi electrodes and 1 inch for E70T-1. The plate was set to make a weld at a rate of 14 inches per minute. The voltage for all tests was set between 23 and 31 volts, and the current was between 250 and 425 amperes.

A TIG350 power supply (shown in Figure 2) was used with the manual electrodes. Manual electrodes have no electrical extension, but are dragged along the surface of the plate. Although the voltage varies slightly during manual welding, an

experienced welder can hold it constant. The voltage read from the power source was watched carefully during each test to ensure it was constant. The voltage for each electrode is given in Appendix B. The current for all of the manual tests was kept constant at the recommended conditions. For all electrodes, the current was in the range of 130 to 180 amps.

These emission factors should suffice for most uses of the studied electrodes. In the event that the welding conditions are vastly different from the manufacturer's recommended conditions, information concerning the effects of operating conditions for different types of electrodes may be obtained from studies compiled in "Fumes and Gases in the Welding Environment." The quantity of fume generated varies directly as a function of the applied voltage and current for all classes of electrodes, though this function may vary for each electrode.[2] Other variables that may impact the quantity of fume generated include the diameter of the electrode, the presence of iron powder, types of shielding gas used, and the presence of fluorides.

For manual (covered) electrodes, the ratio of fume weight to weight of electrode consumed and fume generation rate (FGR) depend on the diameter of the electrode and the composition of the coverings (e.g., presence of iron powder). Fume generation rate (grams per minute) is defined as the amount of fume generated per unit of time. Measured FGRs and ratios of fume weight to weight of electrode consumed for a small-diameter electrode have been found to be less than those of a larger-diameter electrode.[3] It is important to keep in mind that all tests were performed at the manufacturer's recommended conditions. If both small- and large-diameter electrodes are operated at the same conditions (i.e., voltage and current), this would not be the case. Higher voltage and current settings are always recommended for a larger-diameter electrode. If a smaller-diameter electrode were operated at the same current as a larger-diameter electrode, it would have a higher current density (current/unit volume) than the latter electrode. This would then cause the smaller-diameter electrode to generate a higher value for the ratio of fume weight to weight of electrode consumed. The presence of iron powder in the covering of the electrode reduces fume generation rates and the ratio of fume weight to electrode weight consumed.[3]

The fume generation characteristics of flux-cored electrodes are influenced by the diameter of the electrode, the shielding gas used during welding, and the presence of fluorides. If the electrodes are operated at the commercially recommended conditions, as the diameter of flux-cored electrodes is increased, the FGR and ratio of fume weight to electrode weight consumed also increase.[4] Fume generation characteristics can be affected by the type of shielding gas used during welding. An argon-based shielding gas (Ar-XCO_2, where X is an integer) yields lower values for the fume generation characteristics than pure carbon dioxide because the argon-based shielding gas has a lower oxidation potential. Therefore, oxidation processes contributing to fume generation around the tip of the electrode are reduced.[5] Fluorides also may be present in the flux core, which increases fume production.

When electrodes are used at the recommended conditions, fume generation characteristics of solid electrodes depend directly upon the quantity of electrode consumed during welding, as well as the type of shielding gas. The shielding gas has the same effect on solid electrodes as it does for flux-cored electrodes.

Table 6 presents the results of the metals analyses of the welding fume samples. It contains the concentrations expressed in average percent of metal in fume. Laboratory analyses are presented in Appendix C. It should be noted that because the fume was only analyzed for Section 313 metals, the summation of the percentages in Table 6 will not be 100 percent. The remaining percentage will consist primarily of iron with a small amount of silicone.

In general, the composition of the fume generated by manual electrodes reflects the composition of the electrode and the base metal upon which the weld is placed. Estimates of fume compositions could be made for different classes of covered electrodes if the base plate and electrode are matched (electrode is used on the recommended base plate).[6] If this is not the case, fume composition cannot be estimated.

The fume composition of flux-cored electrodes depends on the compositions of the electrode sheath, the flux core, and, to a lesser extent, the base metal. Because the composition of the electrode sheath differs little among manufacturers, variations in

the composition of the fume for this type of electrode result from differences in the composition in the flux core.[7] For the purpose of estimating emissions, if no fume composition data are available for a given electrode class, the electrode class that most nearly has the same electrode (flux core) composition should be chosen.

TABLE 6. METAL CONCENTRATION IN FUME OF COMMONLY USED ELECTRODES (percent of total fume)

Electrode class	Aluminum	Barium	Chromium	Cobalt	Copper	Manganese	Nickel	Vanadium	Zinc
E70S-3	0.069	0.011	0.020	0.0017	0.65	6.7	0.0072	0.00076	0.094
E70S-6	0.060	0.0030	0.015	0.0029	0.44	10.4	0.014	0.00099	0.078
E308LSi	0.077	0.0014	6.0	0.0071	0.50	6.4	3.4	0.012	0.042
E70T-1	0.11	0.0018	0.013	0.0022	0.016	9.0	0.0058	0.0045	0.065
E71T-1	0.042	0.0026	0.014	0.0029	0.048	8.1	0.0040	0.0057	0.086
E6010(A)	0.043	0.0012	0.018	0.0023	0.26	3.9	0.026	0.0031	0.022
E6010(B)	0.018	0.00088	0.011	0.0035	0.033	4.4	0.0080	0.0023	0.036
E6011	0.016	0.0012	0.012	0.0025	0.014	2.6	0.014	0.0038	0.016
E6013	0.18	0.00097	0.030	0.0030	0.16	4.1	0.018	0.012	12
E308-16	0.78	0.0062	6.2	0.0078	0.10	3.8	0.82	0.019	0.087
E7018	1.3	0.042	0.024	0.0016	0.072	3.9	0.012	0.00070	0.12

The compositions of the electrode and any coating on the surface of the electrode are the only factors contributing to the composition of the fume generated during the welding with solid electrodes.[8] Thus, fume compositions can be estimated for classes of solid electrodes for which no fume composition data exist.

A comparison was made between the results obtained from these analyses and data in "Fumes and Gases in the Welding Environment"[9] (denoted as Reference 9). A second set of results was extracted from Draft 5 of "Guidelines to Cover SARA Requirements Section 313" (November 20, 1989)[1] (denoted as Reference 1). These results (Table 7) were expressed as percent of metal in fume. In general, the relative percent differences between values generated in this study and those found in Reference 9 are acceptable. Comparison of the values from this study with the range of values found in Reference 1 indicates general agreement on the composition of the

welding fume and metal concentrations. No data are available for comparison of some of the fume components.

TABLE 7. PERCENT METAL IN FUME

Electrode class	Metal	This study	Reference 9	Reference 1	RPD[a]
E70S-3	Mn	6.7	5.3	6.5-9.0	23
	Cu	0.65	0.7	0.20-0.60	7.4
E70S-6	Mn	10.4	No data	No data	NA[b]
E308LSi	Mn	6.4	No data	No data	NA
	Cu	3.4	No data	No data	NA
	Cr	6.0	No data	No data	NA
E70T-1	Mn	9.0	9.2	7.5-10.5	2.2
E71T-1	Mn	8.1	No data	No data	NA
E6010(A)	Mn	3.9	3.2	3.0-4.0	20
E6010(B)	Mn	4.4	3.2	3.0-4.0	32
E6011	Mn	2.6	No data	No data	NA
E6013	Mn	4.1	4.9	No data	18
E308-16	Mn	3.8	No data	3.0-4.0	NA
	Cu	0.10	No data	No data	NA
	Cr	6.2	No data	5.5-6.5	NA
	Ni	0.82	No data	0.25-0.75	NA
E7018	Mn	3.9	4.1	3.0-5.0	5.0
	Al	1.3	No data	No data	NA

[a] RPD = Relative percent difference between this study and Reference 9.

[b] NA = Not available.

Average chemical-specific emission factors for the electrode classes studied are presented in Table 8. A chemical-specific emission factor is the estimate of the number of pounds of a particular chemical (in this case, metal) released in the form of fume per a given weight of welding electrode consumed. This factor depends on the class of the welding electrode because it is the product of the ratio of weight of fume generated to weight of electrode consumed and the concentration of the chemical in the fume from that electrode. The values are expressed in units of pounds per ton of electrode consumed and are based on total weight of fume (i.e., weight of fume on glass-fiber filter plus weight of fume on wipe cloth).

TABLE 8. AVERAGE CHEMICAL-SPECIFIC EMISSION FACTORS (FUME)
(pounds of metal in fume per ton of electrode consumed)

Electrode class	Aluminum	Barium	Chromium	Cobalt	Copper	Manganese	Nickel	Vanadium	Zinc
E70S-3	0.012	0.0019	0.0034	0.00029	0.11	1.2	0.0012	0.0013	0.016
E70S-6	0.0094	0.00047	0.0023	0.00045	0.069	1.6	0.0022	0.00015	0.012
E308LSi	0.0083	0.00015	0.65	0.00077	0.054	0.69	0.37	0.0013	0.0045
E70T-1	0.019	0.00034	0.0022	0.00038	0.0028	1.56	0.0010	0.00077	0.011
E71T-1	0.010	0.00062	0.0034	0.00070	0.0012	1.9	0.00096	0.0014	0.021
E6010(A)	0.020	0.00054	0.0082	0.0010	0.12	1.8	0.012	0.0014	0.010
E6010(B)	0.0074	0.00036	0.0045	0.0014	0.014	1.8	0.0033	0.00094	0.015
E6011	0.012	0.00092	0.0092	0.0019	0.011	2.0	0.011	0.0029	0.012
E6013	0.049	0.00026	0.0082	0.00082	0.044	1.1	0.0049	0.0033	3.3
E308-16	0.10	0.00079	0.79	0.0010	0.013	0.49	0.10	0.0024	0.011
E7018	0.41	0.013	0.0075	0.00050	0.023	1.2	0.0038	0.00022	0.038

Table 9 presents the composition of the electrodes according to the material safety data sheets (MSDS). Although aluminum, barium, cobalt, and vanadium are reportable metals under Section 313, none of these metals was listed on the MSDSs. Therefore, they are present at levels below de minimis for each metal and would not be reportable under Section 313. This explains why these metals are present at relatively low levels in the fume. For all of the electrodes except E308-16, manganese is reportable, which explains the higher concentrations of manganese in the fume. The highest chromium and nickel fume concentrations were found in E308LSi and E308-16 electrodes, which were the only electrodes that contained reportable quantities of this metal. The highest zinc levels were found in E6013 and E7018, as expected considering the electrode composition. Although a higher metal concentration in electrodes indicates a higher metal concentration in the fume, no direct relationship appears to exist between the levels in the fume and those in the electrode.

4.2 Slag Release Results

In addition to releases to air during welding operations, many classes of electrodes generate a solid waste (slag) that must also be considered during the development of release estimates under Section 313. Table 10 presents the ratios of the

APPENDIX M

EXAMPLE HAND CALCULATION FOR PARTICULATE EMISSION FACTOR DEVELOPMENT

HAND CALCULATIONS

PROCESS	ELECTRODE	REFERENCE	# OF TESTS	PARTICULATE EMISSION (g/Kg ELECTRODE)	NICKEL (Ni) % COMPOSITION OF FUME
SMAW	E6010	1	3	15.0	4.7
SMAW	E6010	2	8	11.4	6.1

FOR AVERAGE PARTICULATE EMISSION FACTOR –

$$\text{Avg. PARTICULATE EMISSION FACTOR} = \frac{(3 \times 15.0\ g/Kg) + (8 \times 11.4\ g/Kg)}{(3+8)}$$

$$= 12.4\ g/Kg$$

FOR HAPS EMISSION FACTOR –

$$\text{Ni Avg \% COMPOSITION} = \frac{(3 \times 4.7) + (8 \times 6.1)}{(3+8)} = 5.7$$

$$\text{AVG EMISSION FACTOR FOR Ni} = \left(\begin{array}{c}\text{AVG EMISSION FACTOR} \\ \text{FOR TOTAL PARTICULATE}\end{array}\right) \times \left(\begin{array}{c}\text{AVERAGE \% of Ni} \\ \text{as FUME}\end{array}\right)$$

$$= 12.4\ g/Kg \times 5.7/100$$

$$= 0.707\ g \text{ of Ni} / Kg \text{ of ELECTRODE}$$

$$\text{AVG. EMISSION FACTOR FOR Ni} = 7.07 \times 10^{1}\ g/Kg \text{ of ELECTRODE}$$